SYSTEMS BIOLOGY APPROACH FOR TARGETED THERAPY OF LIVER CANCER
PI3K/AKT/MTOR PATHWAY INHIBITORS: AN ALLY OR RIVAL FOR SORAFENIB

A THESIS SUBMITTED TO
THE DEPARTMENT OF MOLECULAR BIOLOGY AND GENETICS
AND THE GRADUATE SCHOOL OF ENGINEERING AND
SCIENCE OF BILKENT UNIVERSITY
IN PARTIAL FULFILLMENT OF THE REQUIREMENTS FOR
THE DEGREE OF DOCTOR OF PHILOSOPHY

BY
TÜLİN ERŞAHİN
AUGUST 2014

I certify that I have read this thesis and that in my opinion it is fully adequate, in scope and in quality, as a thesis for the degree of Doctor of Philosophy.

_____

Assoc. Prof. Dr. Rengül Çetin-Atalay

I certify that I have read this thesis and that in my opinion it is fully adequate, in scope and in quality, as a thesis for the degree of Doctor of Philosophy.

_____

Prof. Dr. Mehmet Öztürk

I certify that I have read this thesis and that in my opinion it is fully adequate, in scope and in quality, as a thesis for the degree of Doctor of Philosophy.

_____

Assoc. Prof. Dr. Işık Yuluğ

I certify that I have read this thesis and that in my opinion it is fully adequate, in scope and in quality, as a thesis for the degree of Doctor of Philosophy.

_____

Assist. Prof. Dr. Özgür Şahin

I certify that I have read this thesis and that in my opinion it is fully adequate, in scope and in quality, as a thesis for the degree of Doctor of Philosophy.

_____

Assoc. Prof. Dr. Batu Erman

Approved for the Graduate School of Engineering and Science

_____

Director of Graduate School of Engineering and Science
Prof. Dr. Levent Onural

ABSTRACT

SYSTEMS BIOLOGY APPROACH FOR TARGETED THERAPY OF LIVER CANCER
PI3K/AKT/MTOR PATHWAY INHIBITORS: AN ALLY OR RIVAL FOR SORAFENIB

Tülin Erşahin
Ph.D. in Molecular Biology and Genetics
Supervisor: Assoc. Prof. Dr. Rengül ÇETİN-ATALAY
August 2014, 146 Pages

Hepatocellular carcinoma (HCC) is one of the leading causes of cancer-related mortality worldwide. It is the second most frequent cause of cancer death in men, and the sixth in women due to its aggressive behavior and resistance to conventional therapies. Sorafenib (Nexavar, BAY43-9006), a multi-kinase inhibitor with anti-angiogenic functions, is the only FDA-approved molecular-targeted agent for the treatment of patients with advanced HCC. Yet, Sorafenib shows limited overall survival benefit associated with resistance and tumor recurrence. Current mono-target- or single pathway-centric drug designs are not sufficient for effective therapy of advanced HCC. Negative results of clinical trials on targeted therapies for advanced HCC are due to clinical heterogeneity, complexity of cirrhotic background and interconnected regulation of cancer hallmarks through compensatory signaling pathways with redundant functions. Secretion of growth factors, pro-inflammatory and immune-suppressive cytokines and chemokines in the tumor microenvironment and consequent activation of tumor-promoting signaling cascades confer resistance to Sorafenib treatment. RAF/MEK/ERK and PI3K/AKT/mTOR are the major tumor-promoting signaling pathways with regulatory functions in all hallmarks of HCC. They have redundant functions and inhibition of one pathway can stimulate compensatory signaling from the other pathway. Since Sorafenib targets angiogenic

VEGFR and PDGFR kinases and RAF/MEK/ERK signaling, the primary mechanism of resistance to Sorafenib and tumor recurrence in HCC patients emerges to be the compensatory signaling from the PI3K/AKT pathway. Therefore, we anticipated that combined treatment with Sorafenib and PI3K/AKT inhibitors could reverse drug resistance in HCC.

In this study, we analyzed the synergistic effects of Sorafenib and PI3K/AKT inhibitors on HCC cell growth and migration, determined possible mechanisms underlying synergistic mechanism of action by transcriptome analysis, and further showed that combination therapy leads to tumor regression in PTEN-deficient HCC xenografts *in vivo*. We showed that PTEN-deficient HCC cells with constitutively active PI3K/AKT signaling depend on the alpha isoform of PI3K (p110-α) for survival and co-targeting these cells with the isoform specific PI3K inhibitor (PI3Ki-α, PIK-75) overcomes resistance to Sorafenib. Indeed, while dual-targeting of PTEN-deficient HCC cells with Sorafenib and PI3Ki-α results in synergistic growth inhibition, dual-targeting these cells with Sorafenib and a beta isoform specific inhibitor of PI3K (PI3Ki-β, TGX-221) leads to an antagonistic increase in tumor growth compared to single treatment with Sorafenib, since inhibiting p110-β promotes compensatory signaling from p110-α.

We also investigated the cytotoxic effects of inhibiting Akt kinase by using an Akt2 isoform-specific inhibitor (Akti-2) and a general Akt inhibitor targeting both isoforms (Akti-1,2). Akti-1,2 and Akti-2 did not induce anti-growth or pro-apoptotic mechanisms, but they were highly effective in reducing migration. Akt2 isoform is specifically overexpressed in HCC, and is correlated with its progression. Moreover, the Akt2 isoform-specific role of Akt kinase on migration has been demonstrated in breast cancer, and depletion of AKT2, but not AKT1, was shown to promote regression of PTEN-deficient prostate cancer xenografts. Based on these findings, we predicted a prominent role of Akt2 in PTEN-deficient HCC cells and examined the therapeutic efficacy of combined treatment of Sorafenib and Akti-2 *in vivo* in athymic mice bearing Mahlavu tumor xenografts. After 3 weeks of treatment, tumor growth was reduced significantly in all tested groups (Sorafenib, Akti-2 and Combination) compared to the control group. Substantial intra-tumoral necrosis

produced a temporary increase in tumor size but resulted in significant reduction in tumor weight ($p<0.001$) in combination-treated mice compared to Sorafenib-treated mice and further produced tumor regressions.

In this study, we showed cytotoxic activity of a new PI3K α isoform specific kinase inhibitor (PI3Ki-α / PIK-75) at 0.1 μM that acts synergistically with Sorafenib *in vitro*, determined the predominant role of PI3K isoform p110α in PTEN-deficient HCC cells, and revealed synergistic anti-tumor effect of combining Sorafenib with a new Akt isoform 2 specific kinase inhibitor (Akti-2) *in vitro* and *in vivo*.

ÖZET

KARACİĞER KANSERİ TEDAVİSİNE SİSTEM BİYOLOJİSİ YAKLAŞIMI
PI3K/AKT/MTOR SİNYAL YOLAĞI İNHİBİTÖRLERİ: SORAFENİB`E MÜTTEFİK VEYA RAKİP

Tülin Erşahin
Moleküler Biyoloji ve Genetik Doktorasi
Tez Yöneticisi: Assoc. Prof. Dr. Rengül ÇETİN-ATALAY
Ağustos 2014, 146 Sayfa

Hepatosellüler kanser (HCC) dünyada kanser nedenli ölümlerin başlıca nedenlerindendir. Agresif doğası ve geleneksel terapilere dirençli olması nedeniyle erkeklerde ikinci kadınlarda ise altıncı en sık görülen kanser ölümü sebebidir. Sorafenib (Nexavar, BAY43-9006), anti-anjiyojenik özelliler taşıyan çoklu-kinaz inhibitörü, FDA tarafından ileri düzey HCC hastalarının tedavisi için onaylanan tek moleküler-hedefli ajandır. Lakin, Sorafenib sınırlı sağkalım avantajı sağlamakta, direnç ve tümör nüksü gözlemlenmektedir. Güncel tek-hedefli veya tek sinyal yolağı merkezli ilaç tasarımları ileri düzeydeki HCC tedavisi için yeterli değildir. İleri düzeydeki HCC tedavisine yönelik klinik çalışmaların olumsuz sonuçları klinik heterojenite, sirozlu doku ve birbirini kompanse edebilen sinyal yolakların kanser karakteristik özelliklerini sağlamadaki örtüşen fonksiyonlarıdır.

Tümör ortamında salgılanan büyüme faktörleri, pro-inflamatuar ve immün-baskılayıcı sitokinlerin ve kemokinlerin tümör arttırıcı sinyal yolaklaını aktive etmesi Sorafenib tedavisine karşı direnç kazandırır. Raf/MEK/ERK ve PI3K/AKT/mTOR başlıca tümör destekleyici sinyal yolaklarıdır ve kanserin karakteristik özelliklerini düzenleyici fonksiyonları vardır. Birbiriyle örtüşen işlevleri vardır ve bir yolun inhibisyonu diğer telafi edici yolu uyarabilir. Sorafenib anjiyojenik VEGFR ve

PDGFR kinazları ve RAF/MEK/ERK sinyalizasyonunu hedeflediği için, Sorafenib'e direncin ve HCC hastalarında tümör nüksünün ana mekanizmasının PI3K/Akt yolağının telafi edici etkisi olduğu düşünülmektedir. Bu nedenle, Sorafenib ve PI3K/Akt inhibitörleri ile kombine tedavinin HCC`de ilaç direncini önleyebileceğini düşünmekteyiz.

Bu çalışmada, Sorafenib ve PI3K/Akt inhibitörünün hücre büyümesi ve migrasyon üzerindeki sinerjistik etkisini analiz ettik ve sinerjistik etkinin altında yatan olası mekanizmaları transkriptom analizi ile belirledik. Ayrıca, bu kombinasyon tedavisinin PTEN-eksikli HCC tümör xenograftlarında gerilemeye yol açtığını *in vivo* olarak gösterdik. PTEN-eksikliği nedeniyle sürekli aktif PI3K/Akt sinyali olan HCC hücrelerinin hayatta kalmalarının PI3K`in alfa izoformuna bağlı olduğunu ve izoforma özel PI3K inhibitörünün (PI3Ki-α, PIK-75) Sorafenib`e olan direnci yenebileceğini gösterdik. PTEN-eksikliği olan HCC hücrelerinde Sorafenib ve PI3Ki-α uygulaması sinerjistik büyüme inhibisyonuna yol açarken, Sorafenib ve PI3K`in beta izoformuna specifik inhibitörü (PI3Ki-β, TGA-221), alfa izoformu üzerinden gelen sinyalin artması nedeniyle antagonistik hücre büyümesine neden olmuştur.

Ayrıca, Akt2 izoformuna spesifik Akt inhibitörü (Akti-2) ve her iki izoformu da hedef alan genel Akt inhibitörü (Akti-1, 2) kullanılarak Akt kinazın inhibe etmenin sitotoksik etkileri araştırıldı. Akti-1, 2 ve Akti-2 büyüme karşıtı ya da apoptoz sağlayıcı mekanizmaları uyarmamış fakat migrasyonu azaltmada oldukça etkili olmuştur. Özellikle Akt2 izoformu HCC`de aşırı eksprese edilir ve HCC`nin ilerlemesi ile ilişkilidir. Ayrıca, meme kanserinde spesifik olarak Akt2 izoformunun migrasyon üzerindeki etkisi gösterilmiş olup, Akt1`in değil ama Akt2`nin azalmasının PTEN eksikliği olan prostat kanseri ksenograftlarının gerilemesini teşvik ettiği gözlemlenmiştir.

Bu bulgulara dayanarak, PTEN eksikliği olan HCC hücrelerinde Akt2`nin rolü öngörülerek, Mahlavu tümör ksenograftları taşıyan atimik farede *in vivo* olarak Sorafenib ve Akti-2`nin kombine tedavisinin terapötik etkinliği incelenmiştir.

3 haftalık tedavinin ardından, test edilen tüm gruplarda (Sorafenib, Akti-2 ve kombinasyon) tümör büyümesi kontrol grubuna kıyasla, önemli ölçüde azaltılmıştır.

İntra-tümör nekrozu tümör boyutunda geçici bir artış yaratsa da Sorafenib ile tedavi

edilen fareler ile karşılaştırıldığında kombinasyon ile tedavi edilmiş farelerde tümör ağırlığı anlamlı derecede azalırken aynı zamanda tümörde gerileme görüldü ($p < 0.001$).

Bu çalışmada 0.1 μM dozda sitotoksik aktivitesi olan yeni bir PI3K α izoformu spesifik kinaz inhibitörünün (PI3Ki-α / PIK-75) *in vitro* deneylerde Sorafenib ile sinerjistik olarak hareket ettiğini, PTEN eksikliği olan HCC hücrelerinde PI3K p110α izoformunun baskın rol aldığını, ve yeni bir Akt 2 izoformu spesifik kinaz inhibitörünün (Akti-2) Sorafenib ile birlikte kullanıldığında Sorafenib`in tekli kullanımına kıyasla anti-tümör etkiyi arttırdığını *in vitro* ve *in vivo* olarak gösterdik.

ACKNOWLEDGEMENTS

First of all, I would like to express my gratitude to my supervisor, Assoc. Prof. Dr. Rengül Çetin-Atalay, for her guidance, support, motivation and enthusiasm. She has been a great mentor with her endless patience and encouraging comments.

I would like to thank Prof. Dr. Mehmet Öztürk for his guidance and valuable suggestions throughout this project. I would like to thank all past and present members of MBG family members, especially Assist. Prof. Özlen Konu, Assist. Prof. Özgür Şahin, Assoc. Prof. Işık Yuluğ, Prof. Ihsan Gürsel, Assoc. Prof. Can Akçalı, Assist. Prof. Ali Güre and Prof. Tayfun Özçelik for sharing their knowledge and experience. Many thanks to all MBG family members for their friendship, great working atmosphere and technical support.

I would also like to thank Prof. Volkan Atalay, Prof. Luca Neri and Assist. Prof. Aybar Acar for their valuable contributions to our collaborative projects.

I am grateful to my group members İrem Durmaz, Deniz Cansen Yıldırım, Ece Akhan and Damla Gözen for their great friendship and support not only during my research studies but also outside the lab.

I was delighted to interact with Füsun Elvan, Sevim Baran, Abdullah Ünnü, Bilge Kılıçoğlu, Gamze Aykut and Yıldız Karabacak during my research at Bilkent University.

Last but not least, I would like to thank my family for their moral support and patience.

This project was supported by TÜBİTAK.

TABLE OF CONTENTS

LIST OF TABLES

LIST OF FIGURES

ABBREVIATIONS

ACTB	b-actin
AFB1	AflotoxinB1
AFP	Alpha-feto Protein
AMPK	AMP-activated protein kinase
Ang-2	Angiopoietin-2
APC	Antigen-presenting cell
ASK1	Apoptosis-signal-regulating kinase 1
BAD	BCL2-associated agonist of cell death
BMP	Bone Morphogenetic Protein
bp	Base Pairs
BSA	Bovine Serum Albumin
cDNA	Complementary DNA
CDK	Cyclin Dependent Kinase
CO2	Carbon Dioxide
Cq	Quantitative Cycle
ddH2O	Double Distilled Water
DMEM	Dulbecco's Modified Eagle's Medium
DMSO	Dimethyl Sulphoxide
DNA	Deoxyribonucleic Acid
dNTP	Deoxyribonucleotide Triphosphate
DUSP	Dual-specificity MAP kinase phosphatases
EDTA	Ethylenediaminetetraacetic Acid
EMT	Epithelial-Mesenchymal Transition
EtBr	Ethidium Bromide
FACS	Fluorescence-activated cell sorting
FBS	Fetal Bovine Serum
FGF	Fibroblast growth factor

FOXO1	forkhead box O1
g	Gram
GITR	glucocorticoid-induced tumor necrosis factor receptor
GAPDH	Glyceraldehyde-3-phosphate Dehydrogenase
GO	Gene Ontology
GPCR	G protein-coupled receptor
GSK3β	Glycogen Synthase Kinase 3-beta
HBV	Hepatitis B Virus
HBX	Hepatitis B virus X protein
HCC	Hepatocellular Carcinoma
HCV	Hepatitis C Virus
HGF	Hepatocyte Growth Factor
HNF	Hepatocyte nuclear factor
HRR	homologous replication repair
hTERT	human Telomerase Reverse Transcriptase
hTR	human telomerase RNA
IC50	Inhibitory Concentration 50
ICOS	inducible T cell co-stimulator
IL	Interleukin
JNK	c-JUN N-terminal kinase
kDa	kilo Dalton
LOH	Loss of Heterozygosity
MAPK	Mitogen Activated Protein Kinase
MESH	Medical Subject Headings
mg	Milligram
µg	Microgram
MRI	Magnetic resonance imaging
mRNA	Messenger RNA
mTOR	Mammalian target of rapamycin
µl	Microliter
NEAA	Non-essential Amino Acid

NF-κB	nuclear factor-κB
nm	Nanometer
NK	Natural killer cell
Oligo(dT)	Oligodeoxythymidylic Acid
PARP	Poly ADP-ribosyl polymerase
PBS	Phosphate Buffered Saline
PBS-T	Phosphate Buffered Saline with Tween-20
PCR	Polymearase chain reaction
PDGF	platelet-derived growth factor
PI3K	Phosphatidylinositol 3-kinase
PTEN	Phosphatase and tensin homologue
qRT-PCR	Quantitative Reverse Transcription PCR
Rb	Retinoblastoma Protein
RNA	Ribonucleic acid
ROC	Receiver Operating Characteristic
RT-CES	Real-time cell electronic sensing
RTK	Receptor tyrosine kinase
SDS	Sodium Dodecyl Sulfate
SRB	Sulphorhodamine B
TAE	Tris-Acetate-EDTA Buffer
TAM	Tumor-associated macrophage
TBS	Tris Buffered Saline
TBS-T	Tris Buffered Saline with Tween-20
TGF-β	Transforming growth factor-beta
TIGAR	TP53-induced glycolysis and apoptosis regulator
TNF	Tumor Necrosis Factor
Treg	Regulatory T cell
Tris	Tris (hydroxymethyl)-methylamine
VEGF	Vascular endothelial growth factor

CHAPTER 1. INTRODUCTION

1.1. Hepatocellular Carcinoma

Primary liver cancer is one of the leading causes of cancer-related mortality worldwide (Jemal, Bray, & Ferlay, 2011). 748,300 new liver cancer cases and 695,900 cancer deaths were reported in 2008 (Ferlay et al., 2010). Hepatocellular carcinoma (HCC) is the major histological subtype of primary liver cancers, accounting for about 80% of all liver cancer cases (Perz, Armstrong, Farrington, Hutin, & Bell, 2006).

The major risk factors for HCC are hepatitis B virus (HBV) and hepatitis C virus (HCV) infections, alcohol consumption, and aflatoxin B1 exposure. HBV DNA integrates into the host genome, while HCV RNA induces oxidative stress and pro-inflammatory response. Alcohol and aflatoxins also lead to hepatic injury (Aston, Watt, Morton, Tanner, & Evans, 2000; Eckers, Reimann, & Klotz, 2009; Jung et al., 2000; Kedderis, 1996; Ozcelik, Ozaras, Gurel, Uzun, & Aydin, 2003). Development of HCC is a multistep process, where hepatic injury first leads to chronic liver disease and then continuous inflammation results in cycles of cell death and hepatocyte regeneration. The increase in the proliferating fraction of hepatocytes and subsequent expansion of dysplastic nodules along with telomerase reactivation, and increased genomic instability is followed by malignant transformation (Figure 1.1) (Farazi & DePinho, 2006). Acquisition of the malignant phenotype is achieved by inactivation of tumor suppressors, activation of oncogenes and an increase in growth factor signaling. Tumor-promoting inflammation and metabolic alterations also favor the uncontrolled growth of hepatocytes as the cancer advances. The highly malignant state associated with stemness markers is maintained by the acquisition of invasive, metastatic and angiogenic capabilities.

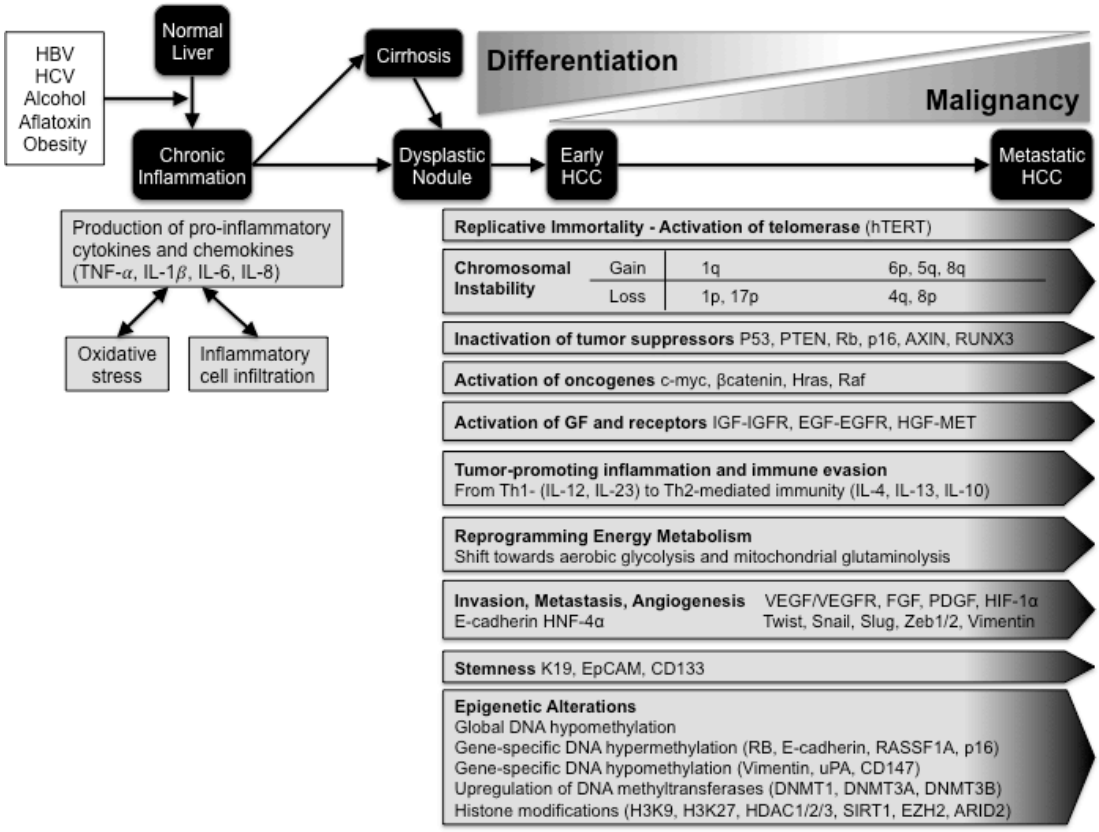

Figure 1.1: Multi-step progression of Hepatocarcinoma. Development of HCC is a multistep process, where injured hepatocytes promote chronic inflammation leading to hepatocyte death and regeneration. The subsequent expansion of dysplastic nodules, telomerase reactivation, increased genomic instability, inactivation of tumor suppressors, activation of oncogenes and increase in growth factor signaling initiates HCC. Chromosomal instability and somatic mutations that favor the uncontrolled growth of HCC cells accumulate as malignancy of carcinoma increases. Acquisition of the malignant phenotype is supported by tumor-promoting inflammation, capability to evade immune destruction and metabolic alterations that allow continued growth and survival of cancer cells. Onset of invasion, metastasis and angiogenesis capabilities promotes progression of carcinoma to the highly malignant metastatic state associated with stemness markers. Molecular alterations throughout the malignant transformation of HCC are regulated both in genetic and epigenetic levels.

Patients with HCC are often diagnosed at advanced stage, where chemotherapy is the only treatment option. Sorafenib (Nexavar, BAY43-9006), a multi-kinase inhibitor, is the only FDA-approved molecular-targeted agent for the

treatment of patients with advanced HCC (Cheng et al., 2012; Raoul et al., 2012; Wilhelm et al., 2006). Sorafenib inhibits Raf, VEGFR, and PDGFR kinases, and thereby suppresses cell proliferation and angiogenesis. In phase III randomized controlled trials, Sorafenib showed an overall survival benefit of only three months (Cheng et al., 2009; Llovet, Di Bisceglie, et al., 2008). Besides, resistance to Sorafenib and tumor recurrence occurs at a high rate. The highly heterogenic character of HCC necessitates a molecular level classification for effective diagnosis and personalized treatment options (El-Serag, 2011; J.-S. Lee, Kim, Park, & Mills, 2011).

Sequencing of the liver cancer genome and comprehensive analyses of large-scale omics data (genomics, transcriptomics, methylomics, metabolomics) revealed multiple critical genes and pathways associated with hepatocarcinogenesis, which can be potential therapeutic targets in HCC (Table 1.1) (Fujimoto et al., 2012; Han, 2012; Nakagawa & Shibata, 2013; Totoki et al., 2011; Woo et al., 2009).

Table 1.1: Molecular Alterations of Critical Genes in HCC

Cellular Process	**Molecule**	**Alteration in HCC**	**Acquired Capability**
Growth factor signaling	EGF / EGFR	Up-regulation	Sustaining proliferative signaling
	HGF / MET	Up-regulation	
	IGF / IGFR	Overexpression	Resisting cell death
	VEGF / VEGFR	Up-regulation	Inducing angiogenesis
	PDGF / PDGFR	Up-regulation	
	FGF / FGFR	Up-regulation	
Cell Cycle Regulation	TP53	Inactivating mutation / LOH	Sustaining proliferative signaling Evading growth suppressors
	RB1	Inactivating mutation / LOH	
	c-myc	Overexpression	
	p16 (CDKN2A)	Inactivating mutation / Hypermethylation	
	Cyclin D1	Overexpression	
	IRF2	Inactivating mutation	
Ras/RAF pathway	RAS	Activating mutation	Sustaining proliferative signaling Evading growth suppressors Inducing angiogenesis
	RPS6KA3	Inactivating mutation	

			Activating invasion and metastasis
PI3K/AKT pathway	PI3K-alpha (PIK3CA)	Activating mutation	Sustaining proliferative signaling Evading growth suppressors Inducing angiogenesis Activating Invasion and Metastasis Reprogramming energy metabolism
	PTEN	Inactivating mutation / LOH	
	AKT	Constitutive activation	
	mTORC1	Up-regulation	
JAK/Stat pathway	Stat	Constitutive activation	Tumor-promoting inflammation
	SOCS1,SOCS3	Down-regulation	
NF-κB pathway	NF-κB	Constitutive activation	Sustaining proliferative signaling Resisting cell death Tumor-promoting inflammation
Wnt/*β*-catenin pathway	β-catenin (CTNNB1)	Activating mutation / Overexpression	Sustaining proliferative signaling Tumor-promoting inflammation
	AXIN1, AXIN2	Inactivating mutation / LOH	
	APC	Inactivating mutation	
Hedgehog pathway	SHH	Overexpression	Reprogramming energy metabolism
	SMO	Overexpression	
	HHIP	LOH, hypermethylation	
Histone modification	DNMT1, 3A, 3B	Up-regulation	Sustaining proliferative signaling Evading growth suppressors
	EZH2	Overexpression	
	ARID1, ARID2	Inactivating mutation	
Apoptosis	Fas	Down-regulation	Resisting cell death
	FasL	Up-regulation	
	DR5	Down-regulation	
Angiogenesis	Angiopoietin	Up-regulation	Inducing angiogenesis
	Tie-2	Up-regulation	
Immunity	Glypican-3	Up-regulation	Evading immune destruction

1.2. Current targeted therapeutics for HCC

The multi-kinase inhibitor Sorafenib (Nexavar, BAY43-9006) is the only approved systemic therapy for patients with advanced HCC so far (Cheng et al., 2009; Llovet, Ricci, et al., 2008). Sorafenib targets angiogenesis and proliferation by

inhibiting Raf, VEGFR, and PDGFR kinases. However, systematic mechanism of action of Sorafenib is still poorly understood due to its capacity to inhibit multiple other targets. Limited overall survival benefit, acquired resistance and tumor recurrence in HCC patients treated with Sorafenib accelerated research on molecular targeted therapies (Table 1.2).

Angiogenesis is the most extensively targeted characteristic of HCC. Nevertheless, none of the anti-angiogenic tyrosine kinase inhibitors under clinical trials showed higher efficacy than Sorafenib so far. Following the failure of subsequent clinical trials with anti-angiogenic agents, therapeutic approach for advanced HCC shifted towards oncogenic signaling pathways (Bergers & Hanahan, 2008; He & Goldenberg, 2013). However, agents targeting EGFR, IGFR, MEK, c-Met, TGF-β, STAT3 and mTOR have not shown improvement in overall survival compared to Sorafenib (Y.-C. Shen et al., 2013; Wörns & Galle, 2014).

Consequently, new therapeutic designs started to use combinations of targeted agents. Ongoing clinical studies mostly involve multi-targeting of a single pathway (vertical inhibition) or two alternative pathways (horizontal inhibition) alone or in combination with Sorafenib. Compensatory up-regulation of pro-angiogenic signals upon Sorafenib treatment or continuing signaling from untargeted growth/survival pathways can be major mechanisms of acquired resistance to Sorafenib and tumor recurrence. Nonetheless, combination of Sorafenib with other anti-angiogenic (Brivanib etc.) or anti-proliferative (Erlotinib etc.) agents could not provide median survival advantage compared to Sorafenib alone. The failure of clinical trials highlights the requirement of new network-based combinational therapies.

Table 1.2: Clinical trials of molecular targeted agents for the treatment of advanced HCC

Therapeutic agent	Target Molecule(s)	Target Cellular Process	Phase	Trial Number
AMG386	Angiopoietin	Angiogenesis	II	NCT00872014
Axitinib	VEGFR, PDGFR	Angiogenesis	II	NCT01210495

Bevacizumab	VEGF	Angiogenesis	II	NCT00867321
Brivanib	VEGFR, PDGFR, FGFR	Angiogenesis	III	NCT00858871
Dovitinib	VEGFR, PDGFR, FGFR	Angiogenesis	II	NCT01232296
Lenvatinib	VEGFR, PDGFR, FGFR, RET, KIT	Angiogenesis	III	NCT01761266
Linifanib	VEGFR, PDGFR	Angiogenesis	III	NCT01009593
Nintedanib	VEGFR, PDGFR, FGFR	Angiogenesis	I	NCT01594125
Orantinib	VEGFR, PDGFR, FGFR	Angiogenesis	I / II	NCT00784290
Ramucirumab	VEGFR2	Angiogenesis	III	NCT01140347
Regorafenib	VEGFR, RET, KIT, PDGFR, RAF-1, BRAF, BRAFV600E, FGFR1, FGFR2, TIE2, DDR2, Trk2A, Eph2A	Angiogenesis	III	NCT01774344
Sunitinib	VEGFR, PDGFR, KIT, RET, Flt-3	Angiogenesis	III	NCT00361309
Vandetanib	VEGFR, EGFR	Angiogenesis	II	NCT00508001
PD-0332991	CDK 4/6	Growth	II	NCT01356628
Erlotinib	EGFR	EGFR signaling	II	NCT00881751
BIIB022	IGF-1R	IGF signaling	I	NCT00956436
Cixutumumab	IGF-1R	IGF signaling	II	NCT00906373
MEDI-573	IGF-1, IGF-2	IGF signaling	I	NCT01498952
OSI-906	IGF-1R, IR	IGF signaling	II	NCT01101906
AZD8055	mTOR	mTOR signaling	I	NCT00999882
Everolimus	mTOR	mTOR signaling	III	NCT01035229
Sirolimus	mTOR	mTOR signaling	II / III	NCT00328770
Temsirolimus	mTOR	mTOR signaling	II	NCT01687673
Selumetinib	MEK	MEK signaling	II	NCT00604721
INC280	c-Met	HGF/MET signaling	II	NCT01737827
Tivantinib	c-Met	HGF/MET signaling	III	NCT01755767
Mapatumumab	TRAIL-R1	Apoptosis	II	NCT01258608

CT-011	PD-1	Immunity	II	NCT00966251
GC33	Glypican 3	Immunity	II	NCT01507168
MK2206	AKT	AKT signaling	II	NCT01239355
LY2157299	TGFβ	TGFβ signaling	II	NCT01246986
OPB-31121	STAT 3	STAT signaling	I / II	NCT01406574

1.3. Molecular Hallmarks of HCC

HCC drive from initially quiescent hepatocytes, whose growth is tightly controlled. Hepatic injury leads to chronic liver disease, where hepatocytes gain several growth-promoting characteristics to become tumorigenic. During progression from chronic liver disease to HCC, tumorigenic cells acquire phenotypic hallmarks of cancer and eventually become malignant.

Six core and two emerging cancer hallmark capabilities have been suggested by Hanahan and Weinberg: sustaining proliferative signaling, evading growth suppressors, resisting cell death, enabling replicative immortality, inducing angiogenesis, and activating invasion and metastasis, along with deregulating cellular energetics, and avoiding immune destruction (Hanahan & Weinberg, 2011). Acquisition of these capabilities is facilitated by two enabling characteristics: genome instability and tumor-promoting inflammation. Recent advances in sequencing and molecular profiling of HCC emphasize its intra-tumoral heterogeneity and uncover how molecular alterations promote hallmark capabilities of cancers and favor tumor progression (Figure 1.2). Therapeutic agents used in clinical trials mostly target individual tumor-promoting processes such as angiogenesis and growth factor signaling (Table 1.2). So far, none of the targeted agents have shown enhanced therapeutic benefit compared to Sorafenib. The failure of clinical trials emphasizes the requirement of combinational therapies that can increase overall survival and prevent resistance and tumor recurrence in HCC patients by simultaneous targeting of all hallmark capabilities.

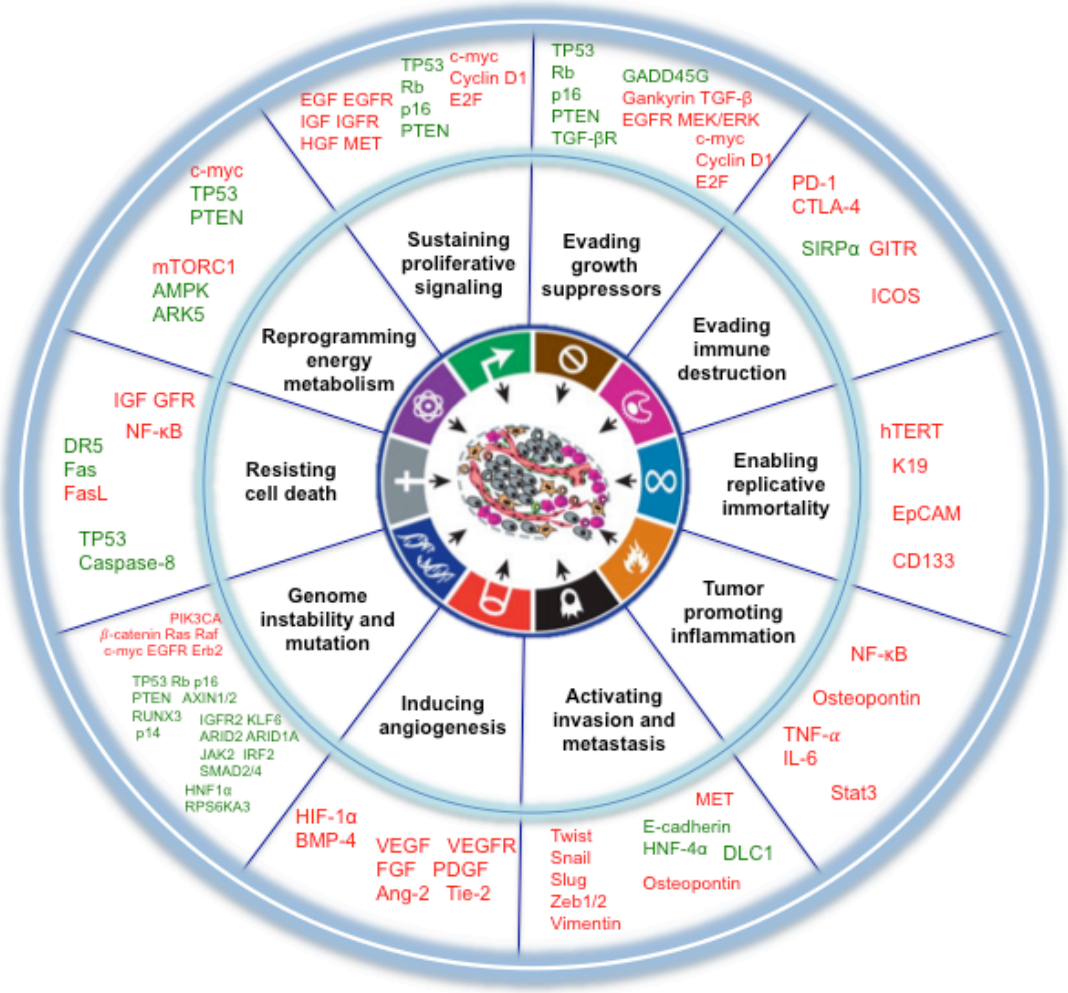

Figure 1.2: Molecular Hallmarks of Hepatocellular Carcinoma. Molecular alterations promote hallmark capabilities through either activation/expression/up-regulation (red) or inactivation/loss/down-regulation (green). (Modified from Hanahan & Weinberg, 2011 with copyright permission).

1.4. PI3K/AKT signaling-mediated acquisition of cancer hallmark capabilities during hepatocarcinogenesis

Recent advances in large-scale molecular profiling of HCC revealed the role of PI3K/Akt/mTOR signaling in the acquisition of all cancer hallmark capabilities (Figure 1.3). The phosphatidylinositol 3-kinase (PI3K) / AKT / mammalian target of rapamycin (mTOR) signaling pathway is one of the most frequently activated signaling pathways in cancer and regulates a broad spectrum of cellular mechanisms

including survival, proliferation, growth and metabolism (Figure 1.4) (Engelman, 2009; Fruman & Rommel, 2014; Manning & Cantley, 2007).

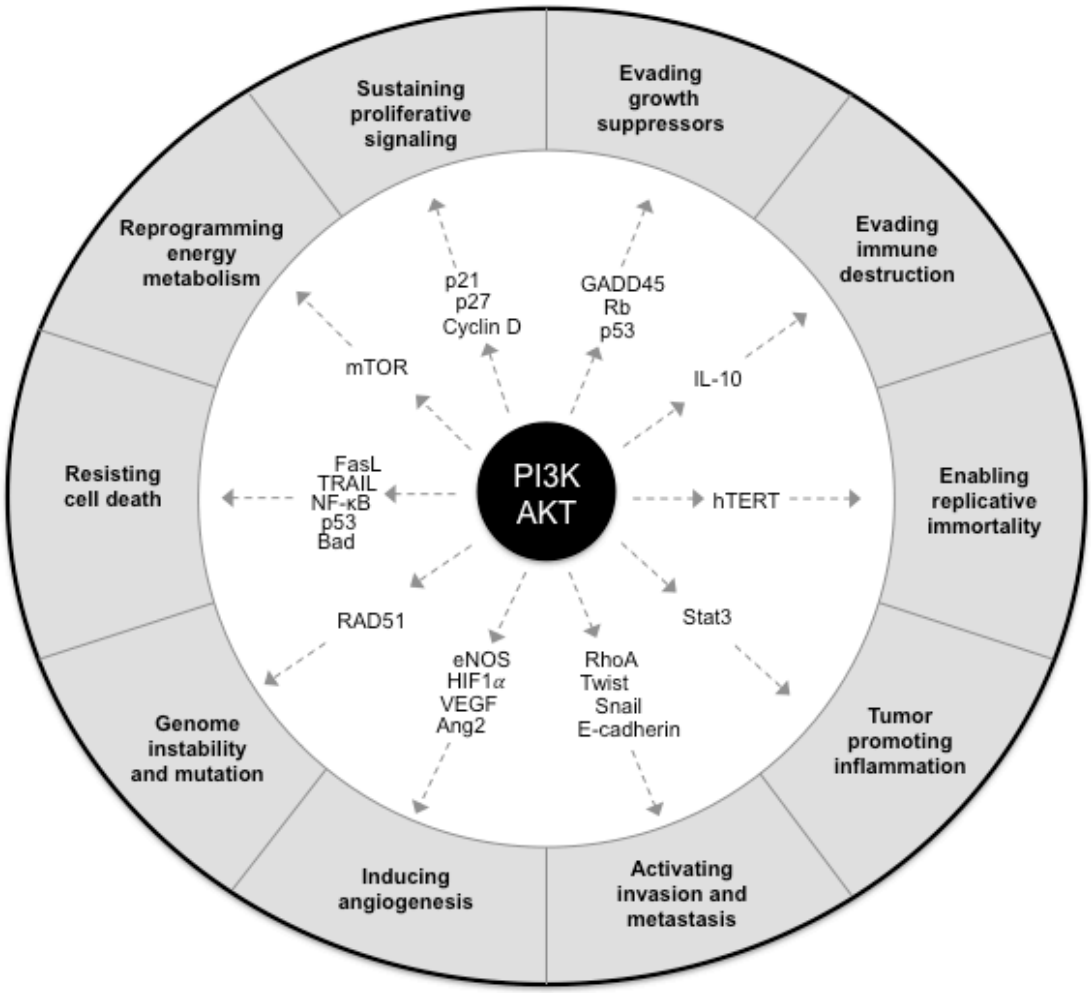

Figure 1.3: PI3K/AKT signaling-mediated acquisition of cancer hallmark capabilities in HCC. PI3K/AKT signaling is involved in the regulation of all cancer hallmark capabilities. Major downstream proteins of PI3K/AKT pathway that are regulated to maintain tumor-promoting characteristics are demonstrated. Mechanisms of regulation are explained in text.

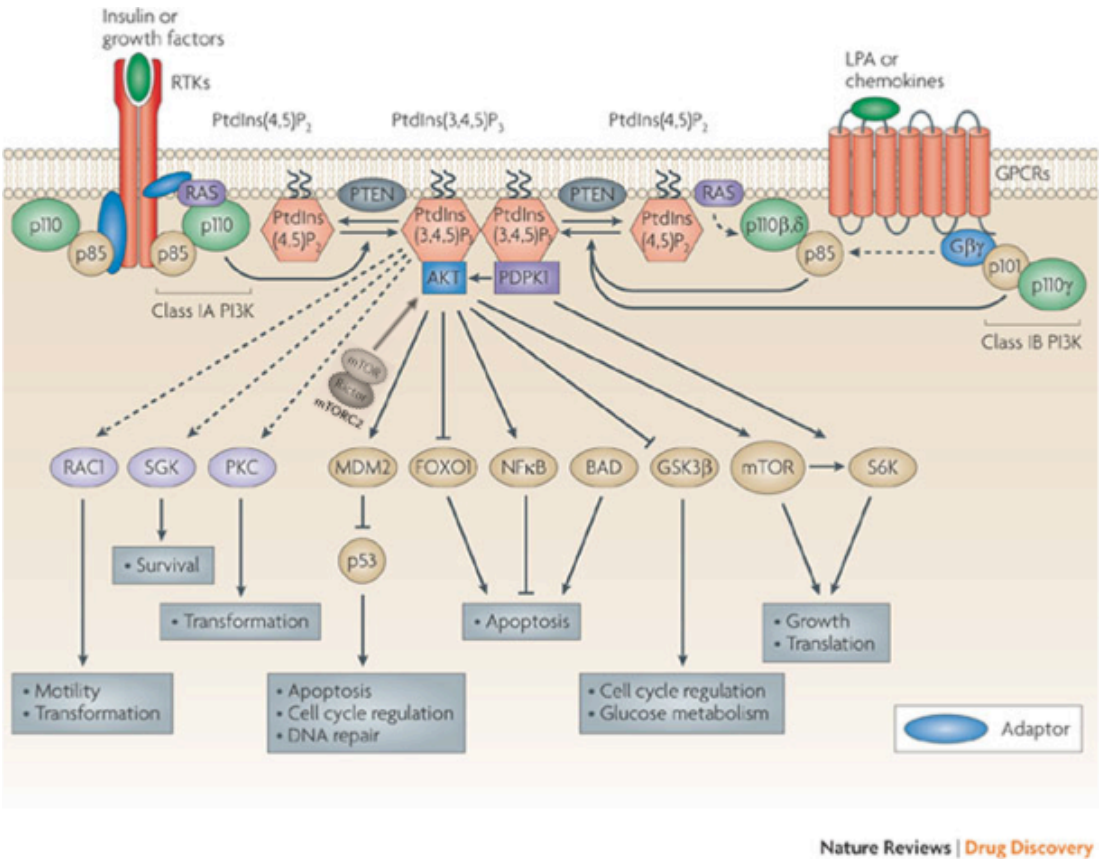

Figure 1.4: PI3K/Akt/mTOR signaling pathway. Growth factor-stimulated activation of receptor tyrosine kinases (RTKs) leads to activation of class IA phosphoinositide 3-kinases (PI3Ks), which converts phosphatidylinositol-4,5-bisphosphate (PtdIns(4,5)P2) to phosphatidylinositol-3,4,5-trisphosphate (PtdIns(3,4,5)P3) at the membrane, recruiting AKT kinase. PDPK1 and mTORC2 phosphorylate and activate AKT, which regulates a broad range of downstream proteins and cellular processes. Activation of Akt is antagonized by PTEN (phosphatase and tensin homologue). (Modified from Liu, Cheng, Roberts, & Zhao, 2009 with copyright permission).

PI3Ks are grouped into three classes based on their structures and substrate specificities (Vanhaesebroeck, Guillermet-Guibert, Graupera, & Bilanges, 2010). The most commonly studied PI3Ks in cancer are the class I enzymes, which are heterodimers of the p110 catalytic subunit and the p85 regulatory subunit. There are four catalytic isoforms of with different functions. The PI3K isoform p110α (encoded by *PIK3CA*) is the major effector kinase downstream of receptor tyrosine kinases (RTKs) and the RAS oncogene. PI3K signaling mostly depends on p110α in

cancers with oncogenic alterations in RTK, RAS or PIK3CA and regulates proliferation, growth, metabolism and angiogenesis. The PI3K isoform p110β, encoded by *PIK3CB*, is regulated mostly by G protein-coupled receptors (GPCRs) and has critical functions in inflammatory cells (Figure 1.5) (Liu et al., 2009). p110γ and p110δ also mediate inflammation and p110δ controls adaptive immunity, but their roles in cancer development and progression are not well-defined.

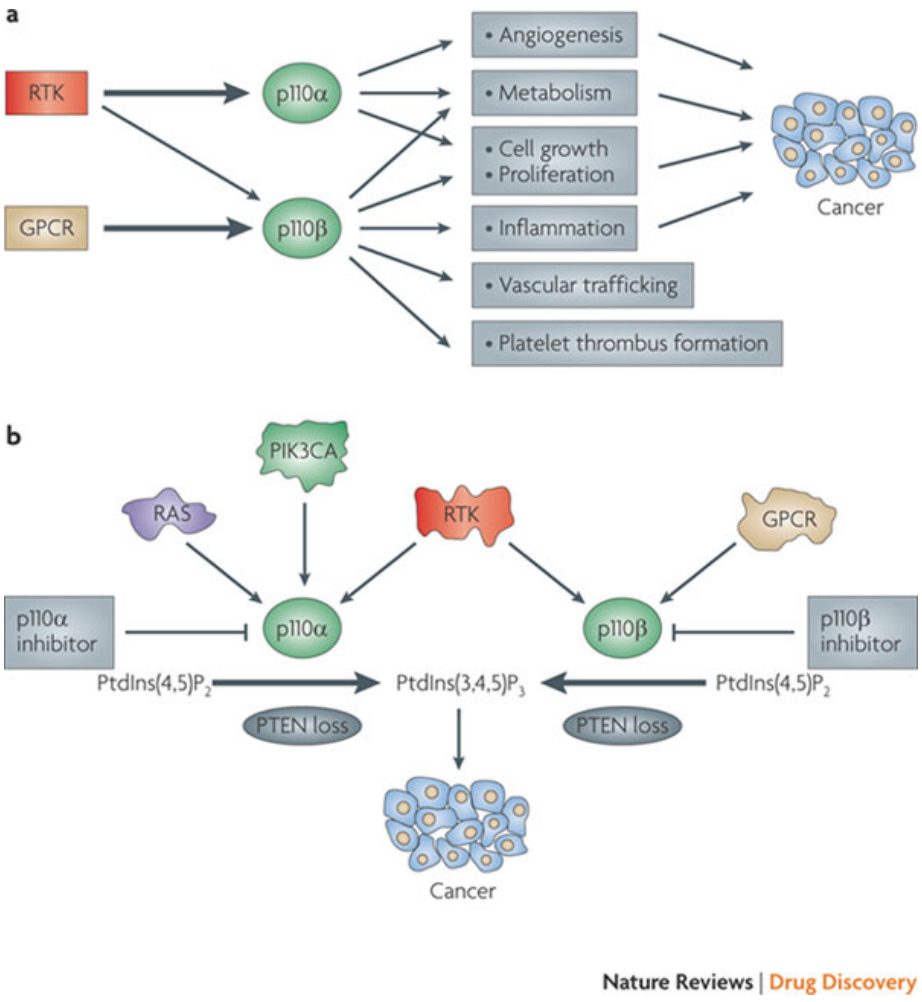

Figure 1.5: Isoform-specific PI3K signaling. A) Differential roles of p110α and p110β are indicated. **B)** Inactivation of either p110α or p110β can counteract loss of PTEN tumor suppressor (Berenjeno et al., 2012). In PTEN-deficient tumors, differences in PI3K-isoform (p110α or p110β) dependence can be explained by the upstream activation mechanisms. PTEN-loss can confer dependence on p110α isoform upon input signaling from receptor tyrosine kinases (RTKs) or RAS and on p110 β isoform when signals are from G protein-coupled receptors (GPCRs) (Jia, Roberts, & Zhao, 2009). (from Liu et al., 2009 with copyright permission)

The PI3K/AKT/mTOR signaling pathway is constitutively hyper-activated in HCC, through inactivating mutations or loss of heterozygosity (LOH) of PTEN, activating mutations of PIK3CA or a disrupted negative-feedback loop from mTOR (Bae et al., 2007; Buontempo et al., 2011; Engelman, 2009; Fujiwara et al., 2000; Kawamura et al., 1999; Yao et al., 1999). Upon growth factor induced activation of receptor tyrosine kinases (RTKs), PI3Ks convert phosphatidylinositol-4,5-bisphosphate (PtdIns(4,5)P2) (PIP2) to phosphatidylinositol-3,4,5-trisphosphate (PtdIns(3,4,5)P3) (PIP3) at the cell membrane. Conversion of PIP2 to PIP3 provides docking sites for 3-phosphoinositide-dependent kinases, PDK1 and mTORC2 (PDK2), which in turn phosphorylate the Akt serine/threonine kinase at Thr308 and Ser473, respectively and result in its activation. Activation of Akt is antagonized by PTEN (phosphatase and tensin homologue), which dephosphorylates PIP3.

Active Akt phosphorylates several proteins, including glycogen synthase kinase 3 (GSK3α/β), forkhead box O transcription factors (FOXO), MDM2, BCL2-associated agonist of cell death (BAD), BCL2-interacting mediator of cell death (BIM), tuberous sclerosis 2 (TSC2), and NF-κB, thereby regulating cell survival, proliferation, protein synthesis and metabolism (Manning & Cantley, 2007; Camillo Porta, Paglino, & Mosca, 2014). AKT-mediated phosphorylation of TSC2 and subsequent activation of RHEB activates mTORC1 kinase. Active mTORC1 stimulates protein translation through 4E-BP1 and P70S6K. During insufficiency of energy and nutrients, mTOR activity is down-regulated in order to reduce biosynthesis. Moreover, when mTOR is bound to Rictor in the mTORC2 complex, instead of mTORC1, mTOR functions as a PDK2 and phosphorylates AKT.

Knockout studies of Akt isoforms revealed isoform-specific functions of Akt (Chin & Toker, 2009; Gonzalez & McGraw, 2009). Loss of Akt1 caused growth retardation, increased apoptosis, defective ischemia and VEGF-induced angiogenesis in mice (Ackah et al., 2005; W. S. Chen et al., 2001; Cho, Thorvaldsen, Chu, Feng, & Birnbaum, 2001). Loss of Akt2 impaired glucose utilization and developed a type 2 diabetes-like phenotype in mice (Cho, Mu, et al., 2001; Dummler et al., 2006; Garofalo et al., 2003). Akt3 knockout mice exhibited impaired brain development but contribution of Akt3 in cancer development has not been identified (Tschopp et al., 2005). Overexpression of AKT2 was frequently observed in HCC (21 cases (38%)), while AKT1 was only moderately expressed (Xu et al., 2004). Increased

Akt2 expression was shown to correlate with the progression of HCC. Moreover, a recent study showed that PTEN-deficient prostate tumors depend on AKT2 for maintenance and survival (Chin, Yuan, Balk, & Toker, 2014). Depletion of AKT2, but not AKT1, promoted regression of PTEN-deficient prostate cancer xenografts.

Several small molecule inhibitors targeting the PI3K/AKT/mTOR pathway are currently in clinical development, including PI3K inhibitors, isoform-specific PI3K inhibitors, mTOR inhibitors, dual PI3K/mTOR inhibitors, and AKT inhibitors (Figure 1.6). Although most existing ATP-competitive small-molecule AKT inhibitors target all three Akt isoforms (Akt1, Akt2, Akt3) non-selectively, recent studies on isoform-specific functions of Akt suggest that isoform-specific targeted agents might show enhanced efficacy.

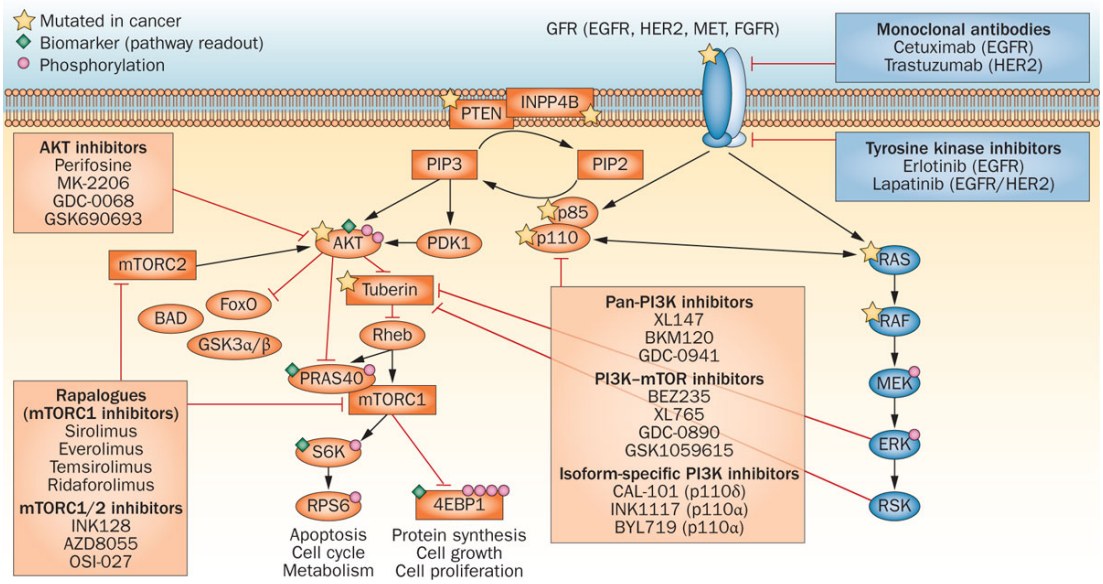

Figure 1.6: Targeting PI3K/AKT signaling. Clinical phase inhibitors that target key nodes of PI3K/Akt/mTOR pathway. (from Rodon, Dienstmann, Serra, & Tabernero, 2013 with copyright permission)

1.5. Genome Instability and Mutations

Chronic inflammation in the liver is associated with high levels of oxidative stress that can cause severe DNA damage and hence increase genomic instability (Ha, Shin, Feitelson, & Yu, 2010). DNA damage leads to hyper-activation of PARP (poly ADP-ribose polymerase), which is the key regulator of cell death during inflammation-related oxidative stress (Bai & Virág, 2012; Nomura et al., 2000;

Shimizu et al., 2004). PARP1 is over-expressed in HCC tumors compared to normal liver and is essential for base excision repair (BER) (Audeh et al., 2010; Bryant et al., 2005; Farmer et al., 2005; Fong et al., 2009).

While the defects in one DNA repair pathway create genomic instability that favors the progression of cancer, the cancer cell meanwhile becomes dependent on the compensatory repair mechanisms for its survival. Therefore, tumors with dysfunctional homologous replication repair (HRR), due to either BRCA1/BRCA2 mutations or deficiency in other HRR components, including RAD51, RAD54, ATR, ATM, CHK1 and CHK2, are sensitive to PARP inhibition (Drew et al., 2011; McCabe et al., 2006; Williamson et al., 2010). This vulnerability can be exploited in HCC by dual-targeting of PARP and PI3K, since inhibitors of PI3K impair HRR by increasing DNA damage and reducing RAD51 focus formation (Juvekar et al., 2012; Kimbung et al., 2012).

Moreover, the tumor suppressor phosphatase and tensin homolog (PTEN), which suppresses PI3K/AKT signaling, is a major guardian of genomic stability in addition to its role in cell growth, survival and energy metabolism (Song, Salmena, & Pandolfi, 2012). Nuclear PTEN maintains chromosomal stability through physical interaction with centromeres and control of DNA repair (Shen et al., 2007). The inactivating mutations or deletions of PTEN are observed in many tumors, including HCC (Bae et al., 2007; Buontempo et al., 2011; Fujiwara et al., 2000; Kawamura et al., 1999; Yao et al., 1999). Loss of PTEN disrupts PI3K pathway mediated Rad51 expression and leads to HRR dysfunction and PARP inhibitor sensitivity (Dedes et al., 2010; McEllin et al., 2010; Mendes-Pereira et al., 2009; Shen et al., 2007).

1.6. Sustaining Proliferative Signaling and Evading Growth Suppressors

Cell cycle progression and sustained proliferation of HCC cells are achieved by inactivation of p53, Rb, and p16, overexpression of c-myc and Cyclin D1, and overexpression of E2F family members. Enhanced stimulation of growth factor receptors EGFR, IGFR and MET leads to constitutive activation of proliferative signaling, especially through Ras/Raf/MEK/ERK and PI3K/AKT/mTOR pathways (Boyault et al., 2007; Challen, Guo, Collier, Cavanagh, & Bassendine, 1992; Hwang et al., 2004; Takada & Koike, 1989; Tsuda et al., 1989; Xu et al., 2013). AKT

promotes cell proliferation and growth primarily through activation of mTORC1, which activates 4E-BP1 and P70S6K and initiates protein translation. Moreover, active Akt signaling suppresses FOXO transcriptional activity, induces Cyclin D, inhibits p21, p27 and GADD45G (Growth arrest and DNA damage 45G), and thereby contributes to cell cycle progression (Manning & Cantley, 2007). Additionally, PI3K/AKT-mediated up-regulation of the oncoprotein Gankyrin mediates degradation of the tumor suppressor proteins Rb and p53 and thereby accelerates cell cycle progression in HCC (Dong et al., 2011).

PI3K/AKT contributes to evasion of growth-inhibitory signals not only by inactivating Rb and p53, but also through converting tumor-suppressing signal of TGF-β/SMAD to a tumor-promoting signal. Transforming growth factor-beta (TGF-β) signaling has a growth suppressive role in the early stages of HCC, whereas in the late stages, down-regulation of TGF-β receptors and up-regulation of EGFR and Raf/MEK/ERK pathways confer resistance to TGF-β signaling-mediated growth inhibition (Bierie & Moses, 2006; Caja et al., 2009; Caja, Sancho, Bertran, & Fabregat, 2011; Mazzocca et al., 2010; Sugano et al., 2003; van Zijl et al., 2009; Yamazaki, Masugi, & Sakamoto, 2011). Indeed, TGF-β-induced AKT activation leads to inactivation of GSK-3β, and consequent accumulation of epithelial repressors Snail, Slug and Twist results in the suppression of E-Cadherin and subsequently promotes epithelial–mesenchymal transition (EMT), invasion, and metastasis (Lamouille, Xu, & Derynck, 2014; Zhang, Zhou, & Dijke, 2013).

1.7. Resisting Cell Death

HCC cells can resist apoptotic cell death by up-regulating anti-apoptotic factors (Bcl-2, Bcl-xL, Mcl-1, IAP) and down-regulating pro-apoptotic factors (Bax, Bim, Puma) through dysregulation of PI3K/AKT, Raf/MEK/ERK and NF-κB signaling (Fabregat, Roncero, & Fernández, 2007). Loss of p53 activity is the best known strategy to circumvent DNA damage response and inhibit apoptotic stimuli (Honda et al., 1998; Hussain, Schwank, Staib, Wang, & Harris, 2007). Hence, inhibitory signaling through PI3K/AKT/MDM2/p53 axis is critical in HCC cells with hyperactive Akt pathway. PI3K/AKT signaling, suppresses PUMA through inhibiting p53. Deficiency of pro-apoptotic BH3-only protein Puma (p53 up-

regulated modulator of apoptosis) protects cells from cell death (Villunger et al., 2003; J. Yu & Zhang, 2008). Sorafenib is known to activate PUMA through GSK3β and NF-κB to suppress growth and induce apoptosis (Dudgeon et al., 2012). Indeed, resistance to Sorafenib-mediated apoptosis was shown to correlate with PUMA down-regulation (Sonntag, Gassler, Bangen, Trautwein, & Liedtke, 2014). Furthermore, PI3K/Akt pathway protects hepatocytes from TNF-alpha- and Fas-mediated apoptosis by suppressing the expression of their ligands TRAIL and FasL and further activating anti-apoptotic NK-κB pathway (Deng et al., 2010; Hatano & Brenner, 2001; Imose et al., 2003; Ladu et al., 2008). PI3K/Akt pathway also confers resistance to c-Myc-driven apoptosis by increasing expression of E2F family members (Deng et al., 2010; Hatano & Brenner, 2001; Imose et al., 2003; Ladu et al., 2008).

1.8. Enabling Replicative Immortality

Telomere shortening in dysplastic nodules is an early event in multistep hepatocarcinogenesis that induces chromosomal instability in hepatocytes. During transition from dysplasia to early HCC, reactivation of telomerase maintains telomere length and replicative immortality (Oh et al., 2003, 2008; Plentz et al., 2004; Yildiz et al., 2013). High telomerase activity and long telomeres in advanced HCC is associated with aggressive behavior and poor prognosis (Hu et al., 2011; Toh et al., 2013). Human telomerase reverse transcriptase (hTERT) is composed of a catalytic subunit (TERT) and an RNA component (hTR). RNAi gene therapies targeting hTERT or hTR effectively down-regulate telomerase activity and suppress the growth of HCC cells (Hu et al., 2011; Liu, Zhu, Li, Zhao, & Li, 2008). The catalytic subunit, TERT, interacts with the 90 kDa heat shock protein (HSP90) and Akt. Phosphorylation of TERT by Akt promotes its nuclear localization, and thereby enhances telomerase activity (Haendeler, Hoffmann, Rahman, Zeiher, & Dimmeler, 2003; Kang, Kwon, Kwon, & Do, 1999).

1.9. Inducing Angiogenesis and Activating Invasion and Metastasis

HCC is a highly vascularized cancer and the up-regulation of angiogenic factors and receptors including vascular endothelial growth factor (VEGF), VEGF receptors (VEGFR-1, VEGFR-2), fibroblast growth factors (FGF), platelet-derived growth factor (PDGF), angiopoietin-2 (Ang-2) and Tie-2 are associated with aggressiveness and poor prognosis of HCC (Campbell et al., 2007; Chiang et al., 2008; Li, Tang, Zhou, Lui, & Ye, 1998; Mitsuhashi et al., 2003; Ng et al., 2001; Pang & Poon, 2006; Poon et al., 2004; Shimamura et al., 2000).

Hypoxia, which occurs during fibrosis, cirrhosis and malignant transformation of HCC, enhances proliferation, angiogenesis and metastasis (Wu et al., 2012). Sorafenib-resistant HCC exhibit increased intra-tumoral hypoxia compared to Sorafenib-sensitive HCCs and HCCs before treatment (Liang et al., 2013). Hypoxia induced by sustained Sorafenib treatment confers resistance to Sorafenib through activation of Hypoxia induced factor 1 alpha (HIF-1α) and NF-κB. Under hypoxic conditions, signaling through PI3K/AKT/HIF-1α promotes hepatocyte EMT, which is associated with enhanced metastatic potential and poor prognosis in HCC (Copple, 2010; Liu et al., 2010; Yan et al., 2009). Moreover, signaling from PI3K, particularly α isoform, regulates migration of endothelial cells through RhoA (Graupera & Potente, 2013; Graupera et al., 2008). Angiopoietin (Ang)/Tie vascular signaling activates PI3K/Akt pathway. In turn, active AKT signaling through FOXO induces Ang-2 expression and promotes vascular remodeling (Augustin, Koh, Thurston, & Alitalo, 2009; Graupera & Potente, 2013; Potente et al., 2005). Furthermore, Akt increases expression of VEGF through HIF-1α and facilitates VEGF-mediated angiogenesis and endothelial nitric oxide synthase (eNOS)-mediated vascular remodeling and angiogenesis (Manning & Cantley, 2007).

Disappointingly, results of anti-angiogenic therapies showed that anti-angiogenic agents induce intra-tumoral hypoxia, which in turn, promotes invasion and metastasis (Bergers & Hanahan, 2008). Invasion and metastasis are associated with chemoresistance and recurrence in patients with advanced HCC. Epithelial-mesenchymal transition (EMT), which involves up-regulation of Twist, Snail, Slug, Zeb1/2, and Vimentin, and down-regulation of E-cadherin and hepatocyte nuclear factor (HNF)-4α, is critical for triggering invasion and metastasis of HCC and

correlate with poor prognosis in liver cancer (Lamouille et al., 2014; Lee et al., 2006; Niu et al., 2007; van Zijl et al., 2009; Yang et al., 2009).

EMT-inducing transcription factors Twist, Snail and Zeb1 are highly expressed in HCC through PI3K/AKT signaling and facilitate invasion and metastasis of HCC (Lee et al., 2006; Matsuo et al., 2009; Yang et al., 2009). Different isoforms of Akt have distinct effects on migration, invasion and metastasis. Isoform-specific roles of Akt are more extensively studied in breast cancer (Figure 1.7). Akt1 suppresses migration by inhibiting ERK and TSC2, inducing degradation of NFAT and down-regulating genes involved in invasion and metastasis of breast cancer cells (Chin & Toker, 2011). On the contrary, Akt2 up-regulates integrins and promotes migration.

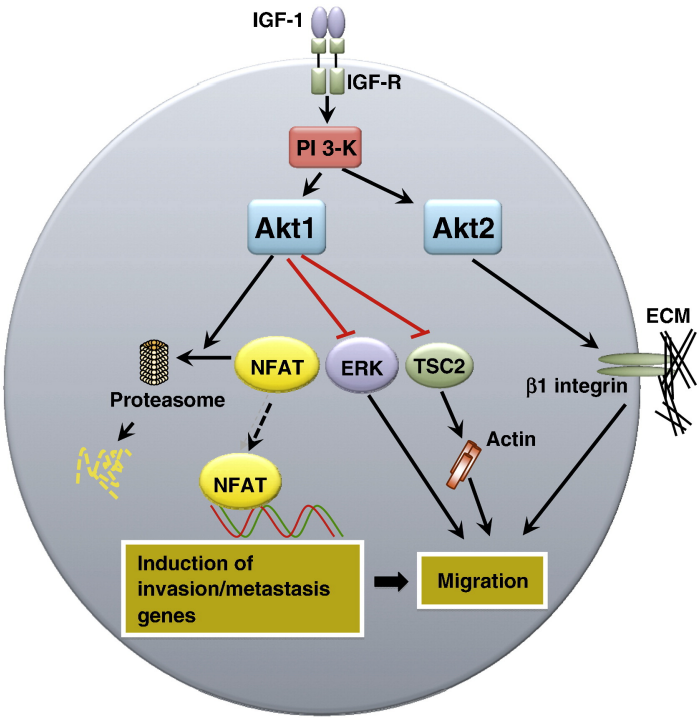

Figure 1.7: Isoform-specific role of Akt on migration, invasion and metastasis in breast cancer. In breast cancer cells, Akt1 suppresses cell migration through inducing degradation of NFAT or blocking activity of ERK and TSC2, whereas Akt2 enhances migration by up-regulating integrins (from Chin & Toker, 2009 with copyright permission).

1.10. Reprogramming Energy Metabolism

Recent transcriptomics and metabolomics studies revealed that HCC has lower levels of glucose and other metabolites involved in energy production compared to healthy liver (Beyoğlu et al., 2013). Cancer cells reprogram their energy metabolism to maintain high rates of aerobic glycolysis for ATP generation, known as the Warburg effect, and use glutamine to provide intermediates of the tricarboxylic acid (TCA) cycle (Cantor & Sabatini, 2012; Sun & Denko, 2014; Warburg, 1956). Alterations in metabolism related enzymes are frequent in cancers including HCC (Teicher, Linehan, & Helman, 2012). 28 metabolites and 169 genes involved in energy metabolism were found to be correlated with aggressive HCC (Budhu et al., 2013). Metabolic reprogramming is regulated by PI3K/AKT/mTOR pathway, especially through PTEN, HIF-1α, p53 and TSC2 (Elstrom et al., 2004; Levine & Puzio-Kuter, 2010).

Hyper-active PI3K/Akt/mTOR and paracrine Hedgehog signaling in malignant hepatocytes promote metabolic changes that favor aerobic glycolysis during tumorigenesis (Chan et al., 2012; Elstrom et al., 2004). For instance, up-regulation of the endoplasmic reticulum enzyme ENTPD5 in PTEN-null cells exhibiting hyper-active Akt causes increased protein translation, promotes ATP consumption, and favors aerobic glycolysis through a compensatory increase in glucose flux (Fang et al., 2010; Z. Shen, Huang, Fang, & Wang, 2011).

Low cellular energy levels activate AMP-activated protein kinases (AMPKs) and LKB1/AMPK signaling pathway suppresses mTORC1 activity to restore energy homeostasis by reducing biosynthesis and promoting catabolism (Guertin & Sabatini, 2007; Hanahan & Weinberg, 2011; Xu, Ye, Araki, & Ahmed, 2012). In healthy cells, activation of AMPK by the tumor suppressor p53 stimulates oxidative phosphorylation and reduces the rate of glycolysis through the up-regulation of TP53-induced glycolysis and apoptosis regulator (TIGAR) (Bensaad et al., 2006; Budanov & Karin, 2008). In HCC, deregulation of AMPK leads to metabolic reprogramming towards aerobic glycolysis to provide enough ATP for the continuous growth of cancer cells and is correlated with aggressiveness and poor prognosis in HCC patients (Zheng et al., 2013).

1.11. Tumor-promoting inflammation and Evading Immune Destruction

Injured hepatocytes promote chronic inflammation leading to a cycle of hepatocyte death and compensatory proliferation. Necrotic hepatocytes stimulate release of pro-inflammatory cytokine interleukin-6 (IL-6) from Kupffer cells, leading to recruitment of macrophages (Sakurai et al., 2008). Macrophages activate JAK/STAT signaling and constitutive activation of STAT3 mediates tumor-promoting inflammation and suppresses anti-tumor immune responses (Yu, Pardoll, & Jove, 2009). Elevated levels of IL-6 and constitutively activated STAT3 are frequent in HCC patients and blocking STAT3 can effectively alter cytokine profile of the immunosuppressive tumor microenvironment and enhance natural killer (NK) cell cytotoxicity (Calvisi et al., 2006; Li et al., 2006; Liu, Fuchs, Li, & Lin, 2010; Niwa et al., 2005; Porta et al., 2008; Rebouissou et al., 2009; Sun, Sui, Zhang, Tian, & Zhang, 2013; Trikha, Corringham, Klein, & Rossi, 2003; Yoshikawa et al., 2001).

Recent studies identified crosstalk between PI3K and STAT3 (Vogt & Hart, 2011). HCV-induced STAT3 activation is dependent on the PI3K/AKT pathway (Tacke, Tosello-Trampont, Nguyen, Mullins, & Hahn, 2011). PI3K/Akt signaling through GSK3 increases production of the immunosuppressive cytokine Interleukin-10 (IL-10) and regulates TLR-mediated production of pro- and anti-inflammatory cytokines (Antoniv & Ivashkiv, 2011; Martin, Rehani, Jope, & Michalek, 2005). PI3K/AKT signaling through mTOR induces the production of pro-inflammatory cytokines and regulates the activation of antigen-presenting cells (APCs), effector T cells and regulatory T cells (Tregs) (Thomson, Turnquist, & Raimondi, 2009). Tumor-infiltrating Tregs are critical for immune evasion in HCC, since they suppress tumor-specific CD4+ T cell responses. Tregs are characterized by up-regulated expression of GITR (glucocorticoid-induced tumor necrosis factor receptor) and ICOS (inducible T cell co-stimulator) (Pedroza-Gonzalez et al., 2013). These receptors activate PI3K/Akt signaling, suggesting a role for PI3K/Akt in immune escape (Noh et al., 2009). Another escape mechanism from phagocyte-mediated immune destruction in HCC involves CD47–SIRPα (signal regulatory protein α) interaction between tumor cells and macrophages (Pan et al., 2013). SIRPα prevents activation of Akt and NF-κB in tumor-associated macrophages (TAMs). In order to increase the capacity of macrophages for migration, survival, and pro-inflammatory cytokine production, tumor-derived factors down-regulate expression of SIRPα on

TAMs, relieving inhibitory signal on Akt pathway, and hence contribute to the progression of HCC.

In chronic HCV patients, natural killer (NK) cells have reduced cytotoxicity (Brenndörfer & Sällberg, 2012). Yet, treatment with Sorafenib not only targets malignant cells but also suppresses proliferation and activation of NK cells (Zhang et al., 2013). Consequently, reduced cytotoxicity of NK cells renders HCC patients more susceptive to tumor growth and metastasis. Therefore, there is an urgent need to develop new therapeutic agents with less severe off-target effects or design optimal combinational treatments of Sorafenib with immunotherapeutic agents that activate NK cells.

1.12. Large scale drug transcriptomics

Hepatocarcinogenesis develops through acquisition of multiple genetic, epigenetic, and molecular alterations that are regulated by complex interconnected signaling networks (Figure 1.1, Table 1.1). Current mono-target- or single pathway-centric drug designs are not sufficient for effective targeting of this highly heterogeneous and aggressive cancer. Not only should genetic backgrounds, feedback loops and pathway redundancies be considered for each individual subtype of HCC, but also off-targets of drugs should be foreseen to prevent chemoresistance and recurrence.

Integration of omics data with network-centered computational biology offers a systems-level perspective on mechanism of action of critical proteins and uncovers the crosstalk among pathways. Global understanding of the interplay between drug targets provides a rational basis for multi-target drug development and discovery of optimal combinations of targeted therapeutics.

There are many approved or clinical phase drugs with known targets for various kinds of diseases, including cancer. Although these drugs are developed to interact with specific targets, most of them activate or inhibit off-targets (unexpected targets) and consequently manipulate more biological processes and pathways than anticipated (Yang et al., 2011). Effective bench-to-clinic translational research, which integrates omics data with systems biology, will identify primary therapeutic targets, secondary or off-targets, compensatory signaling and drug resistance

mechanisms. Following this perspective, new approaches such as drug combination and drug repositioning have emerged (Harrold, Ramanathan, & Mager, 2013; Wu, Wang, & Chen, 2013). Drug repositioning (drug repurposing) is the process of revealing new roles of existing drugs and is currently the most outstanding approach in drug discovery and development for personalized medicine (Li & Jones, 2012; Shim & Liu, 2014). These analyses have great potential to identify previously unrecognized drug targets and improve single drug repositioning or drug combination strategies of new and existing therapeutic agents with enhanced efficacy and minimized side effects. Therefore, we analyzed drug transcriptomics from a network-based perspective searching for optimal drug combination partners for Sorafenib.

CHAPTER 2. OBJECTIVES AND RATIONALE

Hepatocellular carcinoma (HCC) is one of the leading causes of cancer-related mortality worldwide (Ferlay et al., 2010; Jemal et al., 2011). Patients with HCC are often diagnosed at advanced stage, where chemotherapy is the only treatment option. Sorafenib (Nexavar, BAY43-9006), a multi-kinase inhibitor, is the only FDA-approved molecular-targeted agent for the treatment of patients with advanced HCC (Cheng et al., 2012; Raoul et al., 2012; Wilhelm et al., 2006). None of the therapeutic agents under clinical trials showed an improvement in overall survival compared to Sorafenib so far (Shen et al., 2013; Wörns & Galle, 2014). Systematic mechanism of action of Sorafenib is still poorly understood due to its wide-range of targets.

HCC patients treated with Sorafenib showed limited overall survival benefit, acquired resistance and tumor recurrence. Compensatory up-regulation of proliferator and angiogenic signals upon Sorafenib treatment is anticipated to be the major mechanisms of acquired resistance to Sorafenib and tumor recurrence. Sorafenib primarily inhibits Raf, VEGFR, and PDGFR kinases, and thereby targets cell proliferation and angiogenesis. Yet, signaling from VEGFR, PDGFR kinases and Ras protein through Raf/MEK/ERK is not the only pathway with tumor-promoting functions. Cancer cells can up-regulate existing alternative/parallel pathways to compensate for the inhibited pathway. Indeed, the phosphatidylinositol 3-kinase (PI3K) / AKT / mammalian target of rapamycin (mTOR) signaling pathway is an alternative pathway that can be induced with the same up-stream elements and can transmit signal to mostly overlapping downstream effectors. Moreover, PI3K/AKT/mTOR pathway is constitutively activated in HCC and correlates with aggressiveness and poor prognosis (Bae et al., 2007; Buontempo et al., 2011; Engelman, 2009; Fujiwara et al., 2000; Kawamura et al., 1999; Yao et al., 1999).

We analyzed small molecule inhibitors targeting the PI3K/AKT/mTOR pathway, including pan-PI3K inhibitors, isoform-specific PI3K inhibitors, mTOR inhibitors, dual PI3K/mTOR inhibitors, and isoform-specific or non-specific AKT inhibitors with a network-based therapeutic perspective. We aimed to find potential PI3K/AKT/mTOR inhibitors to be used in the clinic and to increase efficacy of Sorafenib by combinational treatments. We searched for the most effective PI3K/AKT/mTOR inhibitors that can reduce tumor growth alone or in combination

with Sorafenib *in vitro* and *in vivo* and further revealed their mechanism of action via network-based drug transcriptomics.

Figure 2.1: Objective of this study.

CHAPTER 3. MATERIALS AND METHODS

3.1. MATERIALS

3.1.1. Cell culture reagents and materials

Dulbecco's modified Eagle's medium (DMEM), Roswell Park Memorial Institute (RPMI) 1640 medium, penicillin/streptomycin, trypsin-EDTA, fetal bovine serum (FBS) and L-glutamine were from GIBCO (Invitrogen, Carlsbad, CA, USA). Cell culture flasks, petri dishes, plates, cryovials were from Corning Life Sciences Incorporated (USA). Serological pipettes and sealed-cap polycarbonate centrifuge tubes were from Costar Corporation (Cambridge, UK).

3.1.2. Kinase inhibitors

Multi-kinase inhibitor Sorafenib (BAY 43-9006, Nexavar) targets angiogenic VEGFR/PDGFR kinases and RAF/MEK/ERK pathway. Experimental pan-PI3K inhibitors LY294002 and Wortmannin target all isoforms of PI3K. ZSTK474 is also a novel PI3K inhibitor that targets all isoforms. PIK-75 (PI3Ki-α) and TGX-221 (PI3Ki-β) are isoform specific inhibitors of PI3K that target p110α and p110β, respectively. PI-103 is a dual PI3K/mTOR inhibitor. Rapamycin is an inhibitor of mTORC1. Akt inhibitor viii (Akti-1,2) is an inhibitor of Akt1 and Akt2 isoforms and Akt xii (Akti-2) is a selective inhibitor of Akt2 isoform.

Table 3.1: Kinase inhibitors used in this study

Inhibitor	Target	PubChem CID	Catalog #	Molecular Formula	Structure
Sorafenib (BAY 43-9006)	**B-Raf VEGFR**	216239	Biovision 1594	$C_{21}H_{16}ClF_3N_4O_3$	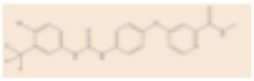
ZSTK474	**PI3K**	11647372	Selleck Chemicals S1072	$C_{19}H_{21}F_2N_7O_2$	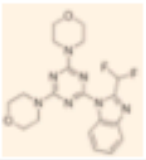
PI-103	**PI3K mTOR**	9884685	Calbiochem 528100	$C_{19}H_{16}N_4O_3$	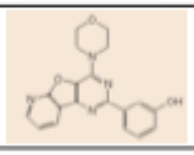
PI3Ki-α (PI3K alpha Inhibitor VIII) (PIK-75)	**p110α isoform of PI3K**	42622917	Calbiochem 528116	$C_{16}H_{19}BrClN_5O_6S$	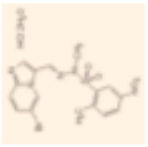
PI3Ki-β (PI 3-Kβ Inhibitor VI) (TGX-221)	**p110β isoform of PI3K**	9907093	Calbiochem 528113	$C_{21}H_{24}N_4O_2$	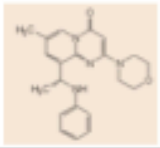
Akti-2 (Akt Inhibitor XII, Isozyme-Selective, Akti-2)	**Akt2**	25020796	Calbiochem 124029	$C_{39}H_{39}N_7O_2 \cdot 3HCl$ ($C_{78}H_{78}N_{14}O_4$)	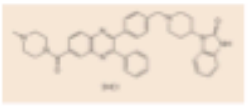
Akti-1,2 (Akt Inhibitor VIII, Isozyme-Selective, Akti-1/2)	**Akt1 Akt2**	10196499	Calbiochem 124018	$C_{34}H_{29}N_7O$	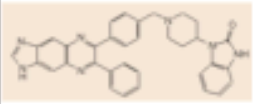
LY294002	**PI3K**	3973	Calbiochem 440202	$C_{19}H_{17}NO_3$	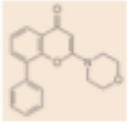
Wortmannin	**PI3K**	312145	Calbiochem 681675	$C_{23}H_{24}O_8$	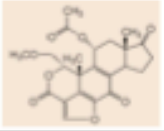
Rapamycin	**mTORC1**	5284616	Calbiochem 523210	$C_{51}H_{79}NO_{13}$	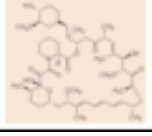

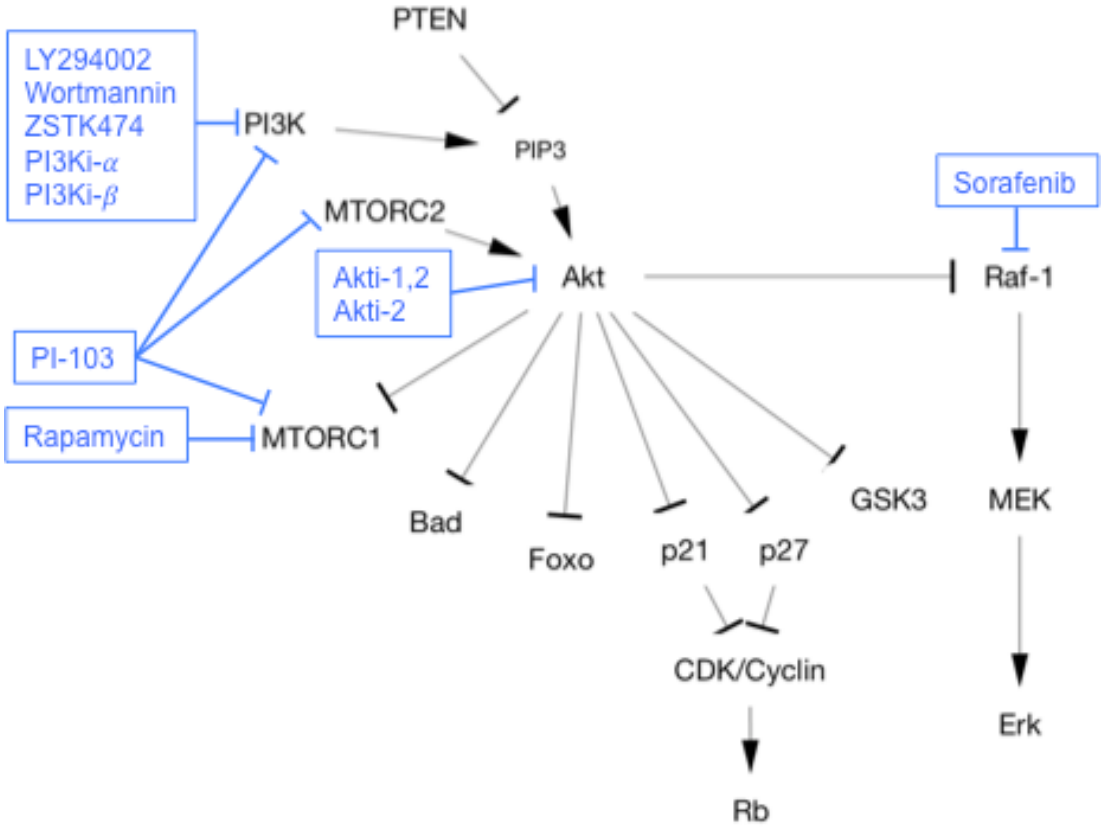

Figure 3.1: Schematic representation of kinase inhibitors and their targets

3.1.3. Sulforhodamine B (SRB) and Real-time cell electronic sensing (RT-CES) cytotoxicity assay reagents

Trichloroacetic acid (TCA) was from Merck (Darmstadt, Germany). Sulforhodamine B (SRB) sodium salt was from Sigma Aldrich (St. Louis, MO, USA). Tris was from Amresco (USA). The RTCA (Real-Time Cell Analyzer) SP (Single Plate) Instrument and E-Plate 96 were from Roche Applied Sciences (Mannheim, Germany). ELISA reader was from Beckman Instruments (CA, USA). CloneFill Instrument for solution distribution into 96-well plates was from Genetix (Hampshire, UK).

3.1.4. RNA extraction, cDNA synthesis and polymerase chain reaction (PCR) reagents

Total RNA isolation kit Nucleospin RNA II was from Macherey-Nagel (Duren, Germany). RevertAid First Strand cDNA synthesis kit and Polymerase Chain Reaction (PCR) reagents; 10X Taq DNA Polymerase Buffer (+$(NH_4)_2SO_4$, -$MgCl_2$), Taq DNA Polymerase, 2 mM dNTP, 25 mM $MgCl_2$, were from Fermentas (Leon-Rot, Germany). DyNAmo HS SYBR Green qPCR Kit for quantitative PCR reactions was purchased from Finnzymes (Finland). NanoDrop ND-1000 spectrophotometer used for nucleic acid concentration measurements was from Thermo Fisher Scientific (Wilmington, DE, USA). Semi-quantitative PCR machine was Techne TC-512. iCycler iQ real-time RT-PCR machine was from Bio-Rad.

3.1.5. Oligonucleotides

All primers used in this study were synthesized by İONTEK (Istanbul, Turkey). The list of primers is given in Table 3.2.

Table 3.2: Primer list

Gene	Primer	Oligo sequence (5'→3')	Amplicon size (bp)
AARS	sense	CCAGTGGCAGAAGGATGAAT	206
	antisense	GCTTCAAGGCTTCATTCAGG	
ACTB	sense	GGACTTCGAGCAAGAGATGG	234
	antisense	AGCACTGTGTTGGCGTACAG	
CFL1	sense	GTGCTCTTCTGCCTGAGTGA	247
	antisense	TCTTCTTGATGGCGTCCTTG	
EEF2	sense	AACGGCAAGTTCAGCAAGTC	182
	antisense	TTGTCCTTGTCCTCGCTGTC	
GAPDH	sense	GGCTGAGAACGGGAAGCTTGTCAT	272
	antisense	CAGCCTTCTCCATGGTGGTGAAGA	
GSTO1	sense	TCGATCCGCATCTACAGCAT	271
	antisense	TTCCAGAACTGGCACCAGAC	
H2AFZ	sense	GTGCGACGAAGGAGTAGGTG	176
	antisense	CTCTGCGGTGAGGTACTCCA	
HBXIP	sense	GCAGCACTTGGAAGACACAA	294
	antisense	TCCTATGACAGGCTGCTGAA	
RPL30	sense	CCTAAGGCAGGAAGATGGTG	171
	antisense	GGCAGTTGTTAGCGAGAATG	
RPL41	sense	AAGATGAGGCAGAGGTCCAA	248
	antisense	TCCAGAATGTCACAGGTCCA	
RPL7	sense	AAGGTGTTGCAGCTTCTTCG	164

	antisense	TTGCCATAACCACGCTTGTA	
RPN2	sense	GCTCTCGCATAATCGCTACC	289
	antisense	CCGGTTGTCACCTTCAACTT	
RPS10	sense	CGCAGAGATGTTGATGCCTA	162
	antisense	AGAGACTGCATGGCCTTCAT	
RPS17	sense	CAACGACTTCCACACGAACA	210
	antisense	ATCTCCTGATCCAAGGCTGA	
RPS3A	sense	CCGATGGTTACTTGCTTCGT	193
	antisense	CCAATGCTGTCTGGAATCAAT	
SOD1	sense	AGGCTGTACCAGTGCAGGTC	193
	antisense	ATGATGCAATGGTCTCCTGA	
TPT1	sense	ATGAATCCAGATGGCATGGT	167
	antisense	TGTGGATGACAAGCAGAAGC	

3.1.6. Agarose gel electrophoresis, photography and spectrophotometer

Electrophoresis grade agarose (Basica Le) was from Prona (Spain). 1kb and 100bp DNA ladders and 6x gel loading buffer were from Fermentas (Leon-Rot, Germany). Horizontal electrophoresis equipment was from Thermo Scientific (Wilmington, USA). Power supplies Power-PAC200 and Power-PAC300 were from Bio Rad Laboratories (CA, USA). The Chemi-Capt software for image acquisition was from Vilber Lourmat (France).

3.1.7. Protein gel electrophoresis, autoradiography and spectrophotometer

NuPAGE pre-cast 10% and 12% Bis-Tris mini gels, MOPS and MES running buffers, transfer buffer, 4X sample loading buffer, 10X sample reducing agent, antioxidant and electrophoresis and transfer equipments were from Invitrogen. SMO671 prestained protein ladder was from Fermentas (Leon-Rot, Germany). Phosphatase inhibitor cocktail (PhosStop) and Protease inhibitor cocktail tablet (complete EDTA free) were from Roche Applied Sciences. ECL-Plus Western blot detection kit and nitrocellulose membrane (0.2µm) were from Amersham GE Healthcare Life Sciences (Buckinghamshire, UK). Bradford reagent was from Sigma Aldrich (St. Louis, MO, USA). Beckman Spectrophotometer Du640 was purchased from Beckman Instruments Inc. (CA. USA). Ponceau S was from Applichem Biochemica (Darmstadt, Germany). 3MM filter paper was from Whatman

International Ltd. (Madison, USA). The films used for autoradiography were from Kodak. The films were developed with Hyperprocessor (Amersham, UK).

3.1.8. Antibodies

Sources, and working dilutions of all primary antibodies used in this study are listed in Table 3.3. Working dilutions indicated in the table are for 2 hours incubation at room temperature.

Table 3.3: Antibody list

Antibody	Company	Cat. No.	Working Dilution
PI3K p110 alpha	Cell Signaling	4249S	1:500 in 5%BSA-0.1%TBS-T
PI3K p110 beta	Cell Signaling	3011S	1:500 in 5%BSA-0.1%TBS-T
PTEN	Cell Signaling	9552	1:300 in 5%BSA-0.2%TBS-T
p-Akt (Ser 473)	Cell Signaling	9271L	1:100 in 5%BSA-0.1%TBS-T
Akt	Cell Signaling	9272	1:300 in 5%BSA-0.2%TBS-T
p-ERK 1/2 (Thr 202/Tyr 204)	Santa Cruz	sc-16982	1:200 in 5%BSA-0.1%TBS-T
ERK 1/2 (MK1)	Santa Cruz	sc-135900	1:200 in 5%BSA-0.1%TBS-T
Phospho-GSK3-a/ß (Ser21/9)	Cell Signaling	9331L	1:200 in 5%BSA-0.1%TBS-T
GSK3-a/ß	Santa Cruz	sc-7291	1:500 in 5%BSA-0.1%TBS-T
a-Phospho-FoxO1 (Ser256) FKHR	Cell Signaling	9461S	1:200 in 5%BSA-0.1%TBS-T
Phospho-Rb (Ser807/811)	Cell Signaling	9308S	1:200 in 5%BSA-0.1%TBS-T
Rb	BD Biosciences	554136	1:300 in 5%BSA-0.2%TBS-T
Phospho-Bad (Ser136)	Cell Signaling	9295	1:200 in 5%BSA-0.1%TBS-T
Bad	Cell Signaling	9292	1:300 in 5%BSA-0.2%TBS-T
PARP-1 (46D11)	Cell Signaling	9532	1:200 in 5%BSA-0.1%TBS-T
p21	Calbiochem	OP64	1:200 in 5%milk-0.1%TBS-T
cyclin D1 (HD11)	Santa Cruz	sc246	1:200 in 5%milk-0.1%TBS-T
Actin (I-19)	Santa Cruz	sc1616	1:200 in 5%milk-0.1%TBS-T

3.1.9. Cell cycle distribution analysis with flow cytometry

RNaseA was from Fermentas (Leon-Rot, Germany). Propidium iodide was from Sigma Aldrich (St. Louis, MO, USA). FACSCalibur Flow Cytometer and CellQuest software were from Becton Dickinson (BD Biosciences, San Jose, CA).

3.1.10. Immunofluorescence staining reagents

Fluorescent mounting medium was from Dako (Denmark). Hoechst stain was from Sigma Aldrich (St. Louis, MO, USA).

3.1.11. General reagents

Most of the laboratory chemicals, including Haematoxylin, Ethanol and Methanol were from Sigma Aldrich (St. Louis, MO, USA). X-Gal was from Fermentas (Leon-Rot, Germany). Dimethyl sulfoxide (DMSO) was from AppliChem Biochemica (Darmstadt, Germany).

3.2. SOLUTIONS AND MEDIA

3.2.1. Cell culture solutions

DMEM complete medium:	10% Fetal bovine serum (FBS), 1% penicillin/streptomycin, 1% non-essential amino acid. Stored at 4^{o}C.
RPMI complete medium:	10% Fetal bovine serum (FBS), 1% penicillin/streptomycin, 1% non-essential amino acid, 1% L-Glutamine. Stored at 4^{o}C.
10X Phosphate buffered saline (PBS):	80 g NaCl, 2 g KCl, 14.4 g Na_2HPO_4, 2.4 g KH_2PO_4 in 1L ddH_2O. atoclaved. pH of 10X buffer=6.8 When diluted to 1X working concentration pH=7.4.
Starvation medium:	Same as the complete medium but has 1% Fetal bovine serum (FBS) instead of 10%. Stored at 4^{o}C.
Freezing Medium:	20% FBS, 7% DMSO, 73% complete medium

3.2.2. Reconstitution of kinase inhibitors

Kinase inhibitors are solubilized in dimethyl sulfoxide (DMSO). Stock solutions (ranging from 10mM to 40mM) are prepared based on their solubility in DMSO. Solubilized inhibitors are stored at -20°C. For all the experiments with drug-treated cells, solvent (DMSO)-treated cells are used as controls.

3.2.3 Sulphorhodamine B assay solutions

SRB stain solution:	0.04gr SRB stain in 10ml 1% acetic acid solution.
10% TCA solution:	100% TCA diluted into 10% in cold ddH_2O.
10mM TrisBase:	0.6gr Tris was dissolved in 1L cold ddH_2O.

3.2.4. Electrophoresis buffers

50x Tris Acetate EDTA (TAE):	242 g Tris base, 37.2 g EDTA, 57.1 ml glacial acetic acid, in 1L ddH_2O. pH=8.5. Stir to dissolve. Dilute with ddH_2O for 1X working solution.
Ethidium bromide:	10 mg/mL in water (stock solution), 1 µg/mL (working solution)
2% Agarose gel:	2 g agarose in 100 ml TAE buffer. Boiled, 1 µg/µL etidium bromide added, swirled, poured onto gel casting apparatus.
DEPC-treated water:	0.1% Diethylpyrocarbonate (DEPC) (v/v) solubilized in ddH_2O overnight under the hood in a loosely plugged bottle. Then autoclaved.

3.2.5. Microarray reagents

All reagents used for the microarray experiments (GeneChip Human Genome U133 Plus 2, One-Cycle cDNA synthesis kit, IVT labeling kit, Poly-A exogenous positive controls) were purchased from Affymetrix.

3.2.6. Western blotting reagents

NP-40 lysis buffer:	150 mM NaCl, 50 mM TrisHCl (pH 8), 1% NP-40, 0.1% SDS, 1x protease inhibitor cocktail, 1x phosphatase inhibitor cocktail in ddH_2O.
10X Tris buffered saline (TBS):	12.2 g Trisma base, 87.8 g NaCl in 1 liter ddH_2O. pH 7.6.
TBS-Tween (TBS-T):	0.1% Tween-20 in 1x TBS.
Ponceau S:	0.1% (w/v) Ponceau, 5 % (v/v) acetic acid in ddH_2O.
Blocking solution:	5% (w/v) non-fat dry milk or bovine serum albumin (BSA) in 0.1% TBS-T.

3.2.7. Cell cycle distribution analysis solutions

Propidium Iodide staining solution:	50 mg/mL propidium iodide, 0.1 mg/mL RNase A and 0.05% TritonX-100 in PBS.

3.2.8. Immunofluorescence solutions

Hoechst-33258 stock solution:	300µg/ml Hoechst-33258 dissolved in ddH_2O. Stored at $+4^oC$ in dark.
Hoechst-33258 working solution:	1µg/ml Hoechst-33258 diluted from 300µg/ml stock in 1x PBS.
Blocking solution	3% BSA, 0.1% Triton-X in PBS.

4% paraformaldehyde:	4 g paraformaldehyde, in 100 ml PBS, Stirred 4 hours at 58°C, pH 7.4. Stored at -20°C in dark.

3.3. METHODS

3.3.1 Cell culture methods

14 HCC cell lines (Huh7, HepG2, Hep3B, Hep3B-TR, Hep40, PLC/PRF/5, FOCUS, Mahlavu, Snu182, Snu387, Snu398, Snu423, Snu449, Snu475) were used in this study. Snu cell lines were cultured in RPMI-1640 medium and the rest of the cell lines were cultured in DMEM medium, both supplemented with 10% fetal bovine serum (FBS), 1% penicillin/streptomycin (P/S) and 1% non-essential amino acids (NEA). All cell lines were incubated in humidified 37 °C incubators with 5% CO_2.

3.3.1.1 Growth and sub-culturing of cells

Cells were passaged regularly when they reached 70–80% confluency. Briefly, the old medium was aspirated, cells were washed twice with PBS. After aspirating the PBS, trypsin-EDTA solution was applied on to the cells (500µl for 100mm dish). When the adherent cells started to detach from the surface of the dish, they were collected in fresh medium (at least of 4ml so that the FBS inside the medium can inactivate the trypsin) and mixed thoroughly with serological pipettes to prevent aggregates and cell clumps. Cells were re-seeded on new culture dishes with fresh medium. The new dishes were moved back and forth and left to right gently in order to allow the cells to be distributed evenly and without any clumps. Sub-culturing ratios for the used HCC cell lines were between 1:4 – 1:10 depending on the growth rate and cell size. Media, PBS, trypsin-EDTA and NEA were stored at +4ºC. FBS stock solutions were stored at -20ºC, thawed at 4ºC, heat-inactivated at 56ºC for 30 minutes, then aliquoted into sterile 50 ml falcons and stored at -20ºC. P/S and L-Glutamine were stored at -20ºC. All solutions and media were warmed to 37ºC in water bath prior to use. For the experiments with a defined number of cells, the trypsinized cells were collected in falcons and after a thorough mixing, 10µl of cell

suspension was applied to both sides of the haemocytometer and the cells were counted. The number of cells counted in the defined area of the haemocytometer was multiplied with 10^4 to get the number of cells in 1 ml of the cell suspension.

3.3.1.2. Cryopreservation of cells

Cells that were in their exponential growth phase, at approximately 60% confluency, were washed, trypsinized, collected in fresh medium and centrifuged at 1500 rpm for 5 minutes. The supernatant was aspirated and the pellet was resuspended in freezing medium (20% FBS, 7% DMSO, 73% complete medium). 1ml of the cell suspension was transferred into a cryovial. More than 5 vials were prepared especially from the early passaged cells to prevent over-passaging. Cryovials were placed at -20ºC for 1 hour, then kept in -80ºC overnight and finally transferred into liquid nitrogen tanks for long term storage.

3.3.1.3. Thawing of frozen cells

One vial of the frozen cell line was taken out from the nitrogen tank or -80^0C and put into 37^{o}C waterbath for 1-2 minutes so that the cell solution starts to thaw. Before the cells were completely thawed, while they were still icy, the cell suspension was transferred into a 15ml falcon with 5ml medium and centrifuged at 1500rpm for 3 minutes, to remove the DMSO that was present in the freezing medium. The supernatant was aspirated, pellet was resuspended in 10ml complete medium and transferred into a 100mm culture dish. The dish was moved back and forth and left to right gently in order to allow the cell suspension to be distributed evenly. Cells were incubated overnight at a 37ºC humidified incubator with 5% CO_2. The next day, culture mediums were replaced with fresh complete mediums.

3.3.2. Sulforhodamine B (SRB) cytotoxicity assay

Huh7 (2000cell/well) and Mahlavu (1000cell/well) cell lines were seeded into 96-well plates in 150µl of medium/well. Next day, medium was discarded and 150µl of new complete medium was applied to each well. Extra 150µl medium was added

into the first wells of the dilution series. Then, the starting highest concentration desired for each drug was applied to the corresponding wells.

$$Stock\ Conc\ (mM) \times Volume\ (\mu l) = Final\ Conc\ (\mu M) \times Final\ Volume\ (300\mu l)$$

$$20\ mM \times 0.6\ \mu l = 40\ \mu M \times 300\ \mu l$$

In order to use only 1 common DMSO control for 5 different drugs, the stock concentrations of the inhibitors were prepared such that for the first wells of each dilution series the volume added (0.6µl) into the final volume (300µl) was the same. With a multichannel pipette adjusted to 150µl, 2-fold dilution series were done until the last concentration. Each drug treatment was performed in triplicates. Dilutions were done from the ends of the plate to the middle, so that the highest concentrations were always at the far end and the lowest concentrations were close to DMSO control. In this study, all drugs except one were solubilized in DMSO. Therefore, DMSO was used as control. For Akti-2 inhibitor, which was soluble in water, non-treated cells were used as control. One of the plates was not treated but instead fixed at the time of treatment, so that the initial cell density before drug treatment can be obtained. The other plates were fixed at the desired times (24h, 48h, 72h). For the fixation process, the media was discarded, wells were washed once with PBS, 50µl of 10% cold TCA was applied to each well. The plates were incubated with TCA at +4oC in dark for 1 hour. After 1 hour TCA was discarded, wells were washed with ddH_2O 4 times and the plates were air-dried at room temperature. Finally, 50µl of 0.4% sulphorhodamine B (SRB) solution in 1%acetic acid was applied to each well and the plates were incubated for 10min in dark at room temperature. After the incubation, excess dye was washed off with 1% acetic acid until no dye comes out of the wells (4 or 5 washes). The plates were air-dried at room temperature. Finally, 200µl of 10mM cold Tris-Base was applied o each well to solubilize SRB. Then, the absorbance was measured at 515nm with Elisa reader. OD values were analyzed to determine the effect of each drug on cell proliferation as compared to control.

Formulas for IC50 calculation in Excel:

$$\%inhibiton = (1-(AVERAGE(OD_{Drug})/AVERAGE(OD_{DMSO})))*100$$

$$y\text{-}int = INDEX(LINEST(J6:O6,LN(J5:O5),TRUE,FALSE),2)$$

$$slope = INDEX(LINEST(J6:O6,LN(J5:O5),TRUE,TRUE),1)$$

$$R2 = INDEX(LINEST(J6:O6,LN(J5:O5),TRUE,TRUE),3)$$

$$IC50 = EXP((50 - y\text{-}int)/slope)$$

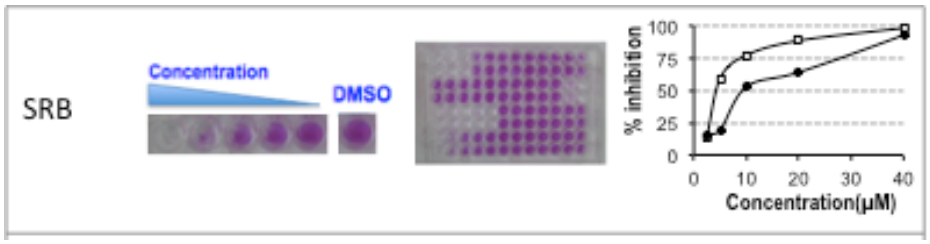

Figure 3.2: Schematic representation of SRB assay.

3.3.3. Real-time cell electronic sensing (RT-CES) system for cell growth and cytotoxicity analysis

50µl complete medium was added to each well of the E-Plate 96. Background reading (1 min) was done to eliminate background noise and to check that data can be collected from each well. Huh7 (2000cell/well) and Mahlavu (1000cell/well) cell lines were seeded into 96-well plates in 100µl of medium/well. Proliferation was monitored and cell index (CI) data was collected every 30 min for 24 h. Next day, medium was discarded and 150 µl fresh medium was added to each well. Inhibitors with indicated concentrations were applied as it was done for the SRB assay. CI values were taken every 10 min for 4 h to get the fast drug response and then every 30 min to obtain the long-term drug response. Impedance measurements that were displayed as Cell Index (CI) values reflect cell growth. When the cells adhere to electrodes on the bottom of the wells, CI values increase in parallel to the cell growth due to the insulating properties of the cell membrane. As the number of cells covering the electrodes increases the electrical impedance (Z) increases ($Z_0 = 0 \rightarrow Z = Z_{cell}$). The effect of the inhibitors on cell growth was calculated compared to DMSO control (CI_{Drug}/CI_{DMSO}).

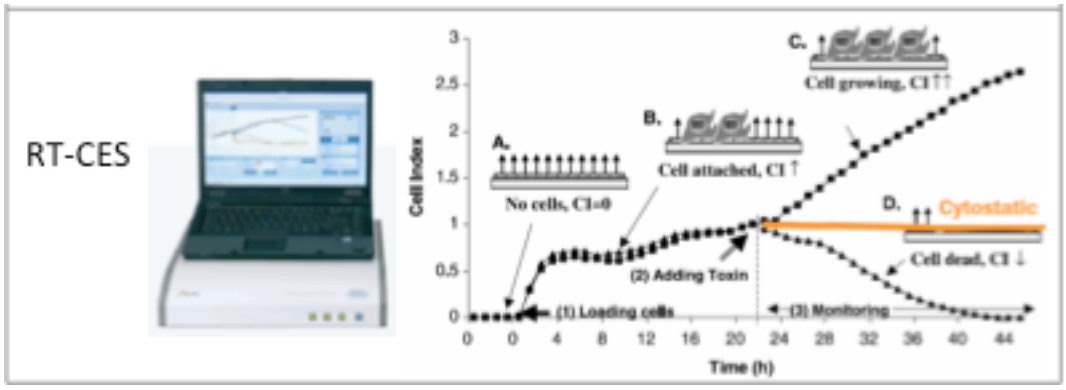

Figure 3.3: Schematic representation of RTCES system.

3.3.4. RNA extraction and cDNA synthesis

Total RNA was isolated with NucleoSpin RNA II Kit (Macherey-Nagel) according to the manufacturer's protocol (MN, Duren, Germany) with small modifications such as 30min of DNA digestion instead of 15min and 2-step elution with 20µl water instead of one elution with 60µl. RNA concentration was measured with NanoDrop and A260/A280, A260/A230 ratios were checked for RNA quality and purity. First-strand cDNA synthesis was carried out from 2 µg of total RNA using Oligo(dT)18 primers with the RevertAid First Strand cDNA synthesis kit (Fermentas). cDNAs were stored at -20°C. In order to check for genomic DNA contamination, RT (-) cDNA samples were also synthesized from total RNA, where no reverse transcriptase enzyme was added in the reaction, so that any amplification with this control cDNA would indicate genomic DNA contamination.

For microarray experiments, quality of extracted RNA was assessed with Agilent 2100 bioanalyzer using RNA 6000 Nano Kit, which reports an RNA Integrity Number (RIN) as a measure of quality. RIN value of 1 represents the most degraded and 10 represents the most intact RNA. RNAs having RIN values higher than 9 were used in microarray experiments.

3.3.5. Primer design for expression analysis with semi-quantitative and quantitative real-time RT-PCR

The sequences of the genes of interest were obtained from NCBI (National Center for Biotechnology Information) website at: http://www.ncbi.nlm.nih.gov/, and UCSC (University of California, Santa Cruz) Genome Bioinformatics website at: http://genome.ucsc.edu/. Primers were designed using the Primer3 online web tool, provided by Steve Rozen and Helen J. Skaletsky (2000) at the website: http://frodo.wi.mit.edu/primer3/. The designed primer pairs were checked to confirm that they amplify only the desired specific region using the *in silico* PCR online tool of UCSC Genome Bioinformatics website. Primers with a length of 18-22bp were designed to amplify the genes of interest so that they are long enough for adequate specificity and short enough to bind easily to the template at the annealing temperature. Primers were designed to have a GC% of 40%-60% and a melting temperature of around 60°C. Difference between the melting temperatures of forward

and reverse primers were set to be no greater than 1ºC. Repeats and runs of the same nucleotide more then 3bp and hairpins and primer dimers were avoided. Primers were specifically designed for the particular gene of interest so that they do not amplify a different region, and this was further confirmed with BLAST analysis. Moreover, forward and reverse primers were positioned on different exons of the gene of interest, so that if the primer pair amplifies a longer product than expected, this would indicate genomic DNA contamination. All primers used for gene expression analysis are listed in Table 3.2.

3.3.6. Expression analysis with semi-quantitative RT-PCR

Before continuing with gene expression analysis, the housekeeping gene GAPDH was amplified to rule out any possible genomic DNA contamination and to normalize the cDNA amounts to be used during further analysis. GAPDH primers were designed to amplify a 151 bp fragment from cDNA, and a 250 bp fragment from genomic DNA if any genomic DNA contamination is present. GAPDH RT-PCR was performed with 1 µl of each sample and the products were run on an agarose gel. By comparing the band intensities using the Molecular Analyst software, the cDNA amount to be used from each sample was determined. All the other RT-PCRs were performed with these determined cDNA amounts. GAPDH RT-PCR was done with 20 cycles. The optimum cycle number for each semi-quantitative RT-PCR reaction was determined by setting up multiple PCR reactions with different cycle numbers to achieve the minimum cycle number that allows the visualization of the desired product to prevent erronous results due to possible saturation of the bands at high cycle numbers. PCR conditions for gene expression analysis were an initial denaturation step at 95°C for 5 min; a loop cycle of 95°C for 30 sec, at Tm (mostly 60^0C) for 30 sec, at 72^0C for 30sec; and a final extension at 72°C for 10 minutes.

3.3.7. Expression analysis with quantitative RT-PCR

Primer efficiency was calculated by running a qPCR reaction with a 10-fold cDNA dilution series for each primer set in triplicate. The cycle where the fluorescence of the sample exceeds a threshold level, termed quantification cycle (Cq) value, was determined by the BioRad iCycler software. A standard curve (Cq vs

log of starting quantity) was plotted and efficiency of each primer pair was calculated using the linear regression slope of the dilution series with the equation:

$E = 10(-1/slope)$ for 10-fold dilutions.

Real-time quantitative PCR assays were performed in triplicate for each candidate gene using 1µl of 1:100 diluted cDNA template. The following program was used: Initial denaturation at 95 °C 15 min amplification for 45 cycles (95°C 15 s followed by 57°C 30 s and 72°C 30 s), and final extension at 72°C 10 min. Melting curve analysis was done to confirm the amplicon size and to check the presence of any primer-dimer or genomic DNA amplification.

Cq values generated by BioRad iCycler system were transformed into quantities (relative expression values) according to Vandesompele et al. (Vandesompele et al., 2002). Relative expression (amplification) values were calculated with the equation:

$Relative\ Expression = E(-\Delta Cq).$

Relative expression levels between two samples were calculated with the equation:

$R = (E_{target})\Delta Cq_{target}(control\text{-}sample) / (E_{ref})\ \Delta Cq_{ref}(control\text{-}sample)$

, where E_{target} and E_{ref} represent the primer efficiencies for target and reference genes, respectively.

3.3.8. Agarose gel electrophoresis of PCR products

Agarose was completely dissolved in TAE buffer in microwave. 1 µg/µL ethidium bromide was added, swirled, and the buffer was poured onto gel casting apparatus. PCR products that were mixed with 6X loading buffer were loaded onto gels. According to the size of the expected product either a 100 bp ladder or a 1 kb ladder was used. The gel was run at 100-120 V at room temperature until the fragments were separated. Bands were visualized under UV transillumination.

3.3.9. Expression Analysis with Affymetrix

cDNA and eventually cRNA were synthesized from the high quality RNA samples (RIN above 9) using the One-Cycle cDNA Synthesis Kit from Affymetrix.

cRNA (~5µg) from each clone was hybridized to Affymetrix HGU133Plus2 Chips. Signals from the chips were exported as .CEL files. Raw .CEL files were processed using 'R' software. Bioconductor Packages such as Biobase, affy, genefilter, simpleaffy, AnnotationDbi, annotate, affyQCReport, affyPLM, and limma were used for quality control, preprocessing and differential gene expression in R.

Quality of arrays was checked using the simpleaffy or the affyQCReport package. For quality control, RNA degradation plots (probe vs mean intensity), boxplots and histograms for probe intensity distribution analysis (log intensity vs density), RLE (Relative Log Expression) plots and NUSE (Normalized Unscaled Standard Error) plots were drawn and % presence of probes, 3'/5' ratios for GAPDH and Actin were compared. Hierarchical clustering and principal component analysis (PCA) were performed to check correlation between replicate arrays.

Robust Multi-array Average (RMA) was used for data normalization and computation of expression values. Boxplots, histograms, RLE and NUSE plots were drawn again ensure successful normalization. Differentially expressed genes were identified by performing t-tests with function rowttests() from package "limma". Results were exported with function write.table().

3.3.10. Identification of optimal reference genes for microarray normalization

Gene expression data were downloaded from the NCBI Gene Expression Omnibus (NCBI-GEO) database [5] and were mean-normalized. A rank value was assigned for each gene in each sample using percentile ranking. The average change in the rank of each gene in each GEO dataset (GDS) was calculated as the ratio of the standard deviation to the mean and was used as a measure of coefficient of variation (CV). To account for genes having CV values only for a subset of the available GDSs, a new expression stability measure, $Ratio_t(Gi)$, was introduced. $Ratio_t(Gi)$ is the ratio of GDSs, in which a gene has CV less than t. However, since a gene that is present in only a single GEO dataset but has a small enough CV value can get a perfect $Ratio_t(Gi)$, the percentage of datasets in which that gene is present (percentage of occurrence PO(Gi)) was introduced as a new parameter to adjust $Ratio_t(Gi)$.

As result of testing various CV thresholds of t=0.5, t=0.1, t=0.05, and t=0.01 and minimum PO values of PO=75%, 50%, 25% and 5% to analyze normalized gene expression values, CV was used to set a classifier with fixed PO and $Ratio_t$ values at 75% and 0.90 respectively. Specificity and sensitivity of the classifier was demonstrated by plotting receiver-operating characteristic (ROC) curves. Since candidate reference genes are anticipated to have lower CV and higher $Ratio_t$(Gi) than that of randomly selected genes, the classifier was tested by comparing a previously published reference gene dataset of 566 housekeeping genes by Eisenberg et al. to five different randomly selected sets of non-housekeeping genes having the same mean rank distribution (Eisenberg & Levanon, 2003). The ratio distribution ($Ratio_t$) of housekeeping genes was significantly different than that of randomly selected non-housekeeping gene sets ($p<0.0001$), supporting steady expression of the tested housekeeping genes across different experiment sets compared to randomly selected gene sets.

3.3.11. Signal transduction score flow algorithm

Raw expression data from microarray was normalized by Robust Multi-array Average (RMA). Normalized and log2-transformed gene expression values were provided as the input score of each gene. Next, the rank score of each gene was computed based on fold change ratios between experiments (treated versus control). If *r(x)* indicates the order of the score *x* when all the scores are sorted in ascending order, and *TS* is the total number of scores, then the rank of *x, R(x)* is calculated as: $R(x) = r(x) / TS$. Score of each gene was assigned to its node (protein) in signaling pathway. Nodes transmitted their scores to their first downstream neighbour node and signal flowed through edges connecting the nodes (regulatory relationship: activation or inhibition). The initial score of the node (protein) was partitioned to the interacting edges based on the weights of the interacting neighborhood nodes' raw data score (Figure 3.4). Sum of the incoming edge score and the initial score of the node itself provided the final score of the node. Score partitioning was based on protein concentrations, where raw data scores were used as the stoichiometric concentrations of the node. Activator edges passed positive values and inhibitory edges passed negative values on the interacting nodes. A modified breadth-first search (BFS) algorithm was applied to simulate the effect of negative and positive

feedback loops. The algorithm was iterated 10–15 times over the entire cyclic graph until the convergence of gene node scores was attained. Score flow algorithm traversed the signaling pathway until a pre-defined biological target response was reached. The score flow calculation algorithm is publicly available as a Cytoscape plug-in (Isik, Ersahin, Atalay, Aykanat, & Cetin-Atalay, 2012).

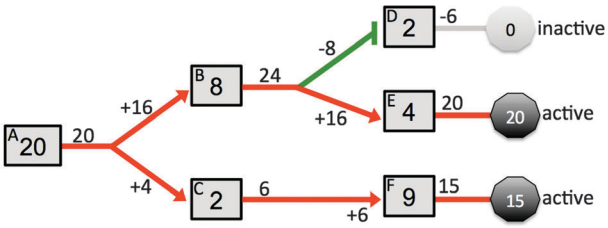

Figure 3.4: Schematic representation of signal transduction score flow algorithm Raw data scores are given in square protein nodes. Protein A transforms its score to Proteins B and C based on their weights (raw data scores of proteins B and C). The 8/10 fraction of the score of A (20) is partitioned to B and the 2/10 fraction to C. The new scores of proteins B and C become 24 (8 + 16) and 6 (2 +4) respectively. Then, protein B partitions its new score to proteins D and E based on their weights. Since, the interaction between proteins B and D is of inhibitory type, score is transferred with a negative value (from Isik et al., 2012 with copyright permission).

3.3.12. Crude total protein extraction from cultured cells

Huh7 (250,000 cell in 100mm dish), HepG2 (250,000 cell in 100mm dish) and Mahlavu (100,000 cell in 100mm dish) cell lines were cultured into 100mm dishes. Next day, medium was aspirated and the cells were washed twice with PBS. 6ml of new complete medium with the kinase inhibitor or DMSO control was given to the cells. All kinase inhibitors were used at a concentration of 10µM, except PI3Kalpha inhibitor and Rapamycin, which were used at 0.1µM concentrations. Cells were collected after 72 hours and changes in protein levels were analyzed with western blot. When collecting the cells, first the medium containing the swimming apoptotic cells was transferred into a 15ml falcon. Then the possible remaining but detached cells were collected with PBS and transferred to the same falcon. The adherent cells were then trypsinized and collected with new complete medium and

combined with the swimming cells in the same falcon. Since trypsin can disrupt membrane proteins, for the analysis of E-cadherin, cells were not trypsinized but instead, at this step ice-cold PBS was applied to the adherent cells in the dish and the cells were scraped using rubber scrapers. The scraped cells were collected into the falcon containing the swimming cells. Then, for both the trypsinized and scraped cells, cell suspensions in the falcons were centrifuged at 1600rpm for 10min +4°C. Supernatant was discarded and cells were resuspended in 5ml ice-cold PBS and centrifuged at 1600rpm for 10min +4°C. The supernatant was discarded and cell pellets were either lysed immediately for the following western blot analysis or frozen in liquid nitrogen and stored in -80°C. Cell pellets were lysed in twice their volume of lysis buffer (150mM NaCl, 50mM Tris-HCl pH=7.6, 1% NP40, 0.1% SDS, 1x Protease inhibitor cocktail and 1x PhosStop) by vortexing every 5 min and incubating on ice for 30 min. If the lysate was viscous after this 30 min of incubation, samples were sonicated to shear DNA. Then the lysates were centrifuged at 13000rpm for 20 minutes at +4ºC and the supernatant containing total protein was transferred into new eppendorphs and stored at -20ºC.

3.3.13. Western Botting

Protein concentrations of the cell lysates were measured by the conventional Bradford assay using a spectrophotometer at 595 nm. Bovine serum albumin (BSA) protein of known concentrations was used as reference for standard curve formation. Sample protein concentrations were normalized with respect to the standard curve. 2µl of sample was used for Bradford assay and to calibrate the spectrophotometer, lysis buffer was used as blank.

	Blank	BSA Standards from 1mg/ml stock					
BSA (µl)	0	1	2	4	8	16	32
ddH_2O (µl)	100	99	98	96	92	84	68
Bradford (µl)	900	900	900	900	900	900	900

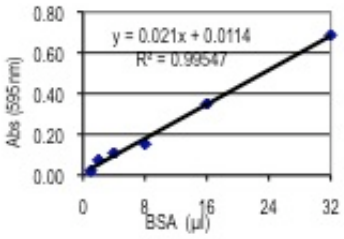

Protein samples were prepared by mixing equal amounts of cell lysates (25 – 40 µg protein) with 4x NuPAGE loading dye and 10X sample reducing agent (or 25mM DTT) in ddH_2O in a total volume of 12µl for 15-well gels and 25µl for 10-well gels. The samples were heated at 70ºC for 10 min for denaturation and put on ice for 1 min. Then the samples were spinned down for 3 sec and were loaded into the gel. 10%, 12% or 4-12% Bis-Tris gels were used depending on the protein of interest. MOPS running buffer was used for high kDa proteins (PARP, E-cadherin, Rb, etc.) and MES running buffer was used for low kDa proteins (p21, Caspase 3, etc). 10% methanol was added to the transfer buffer before use. NuPAGE NOVEX pre-cast gel system was used for electrophoresis and transfer following the manufacturer's protocol. Electrophoresis was carried out for 1.5 to 3 hours depending on the protein of interest and transfer was done at 30V for 90 min for all proteins. The gels were transferred to HyBond ECL nitrocellulose membranes. After transfer, the membranes were stained with Ponceau S for 1 min to control whether the transfer was successful. Ponceau S was washed off with ddH_2O and the membrane was incubated in blocking solution (%5 milk powder in 1xTBS-T(0.1%tween)) on shaker overnight at +4°C. Then, the membrane was probed with primary antibody for 2 hours at room temperature or overnight at +4°C depending on the antibody. Unbound antibodies were washed off extensively for 30 min (5 min, 10 min, 10 min, 5 min) with 1xTBS-T(0.1%tween). Afterwards, the membrane was incubated with the secondary antibodies conjugated with horse-radish peroxidase (HRP) for 1 hour at room temperature. Membrane was washed again for 30 min. Finally, chemiluminescent detection was performed by using ECL+ western blot detection kit from Amersham, according to the manufacturer's protocol. X-ray films were exposed to the emitted chemiluminescence for different exposure times depending on the antibody (30 sec – 20 min).

3.3.14. Cell cycle distribution analysis with flow cytometry

Huh7 (250,000 cell in 100mm dish), HepG2 (250,000 cell in 100mm dish) and Mahlavu (100,000 cell in 100mm dish) cell lines were cultured into 100mm dishes. Next day, medium was aspirated and the cells were washed twice with PBS. 6ml of new complete medium with the kinase inhibitor or DMSO control was given to the cells. All kinase inhibitors were used at a concentration of 10µM, except

PI3Kalpha inhibitor and Rapamycin, which were used at 0.1µM concentrations. Cells were collected at 72h and changes in cell cycle distribution were analyzed with flow cytometry. When collecting the cells, first the medium containing the swimming apoptotic cells was transferred into a 15ml falcon tube. Then the possible remaining but detached cells were collected with PBS and transferred to the same falcon tube. The adherent cells were then trypsinized and collected with new complete medium and combined with the swimming cells in the same falcon. The cell suspensions in the falcon tubes were centrifuged at 1600rpm for 10min +4°C. Supernatant was discarded and cells were resuspended in 5ml ice-cold PBS and centrifuged at 1600rpm for 10min +4°C. The supernatant was discarded and cell pellets were resuspended in 1ml ice-cold PBS and fixed by dropwise addition of 2.5ml 100% EtOH (obtaining a final concentration of 70% ethanol) while vortexing at the same time to prevent cells to form aggregates. The samples were either incubated at +4^{o}C for 30 min before continuing with PI staining or they were stored at this step at +4^{o}C for up to 2 weeks. The cell pellet was resuspended in 500µl Propidium iodide (PI) staining solution (50µg/ml PI (from 1mg/ml stock), 0.1mg/ml RNaseA (from 10mg/ml stock), 0.05% Tritron-X-100 (from 100% stock) in cold PBS) and incubated 40min at 37^{o}C in dark. After the incubation, 3ml PBS was added onto the samples and the samples were centrifuged at 1500rpm for 5min, +4^{o}C. Supernatant was discarded and pellet was transferred to polystyrene tubes with 500 mL PBS and analyzed with FACSCalibur Flow Cytometer (BD Biosciences). Cell cycle distribution and apoptotic cells were assessed by analyzing the proportion of cells in the G1, S, and G2/M fractions and sub-G1 respectively, using the Cell Quest 3.2 software.

3.3.15. Wound Healing

In the wound-healing assay, a wound was made in the middle of a confluent cell monolayer and the migration of cells to this area was assessed by taking photos at different time points and calculating the wound closure with respect to the initial wound width. Since the wounds were done by hand with a 30µl tip, the width of the wounds can differ from area to area. To assure that photos taken at different time points were from the exact same location inside a well, bottom of 12-well plates were marked by drawing vertical straight lines into the middle of each column and the

photos were taken from left and right sides of this mark. Cells were seeded in 1ml complete medium into 12-well plates. Next day, a horizontal wound was made into the middle of each well by scratching the bottom of the well with a 30µl tip. To remove the detached cells from the scratched area, the medium was aspirated and the cell layers were washed twice with PBS. Immediately, the time-zero photos of the wounds were taken to note the initial wound width. 1 ml of new starvation medium (containing 1% FBS instead of 10% so that migration will be promoted rather than proliferation) with the kinase inhibitor or DMSO control was given to the cells. All kinase inhibitors were used at a concentration of 10µM, except PI3Kalpha inhibitor and Rapamycin, which were used at 0.1µM concentrations. Photos of the wounds were taken after 24h and 48h. The sizes of the wounds were calculated at all time points. At least 12 different wound distances were noted for each condition at each time point and the averages were taken to construct graphs.

3.3.16. Immunofluorescence

Huh7 (90,000 cell/well) and Mahlavu (30,000 cell/well) cell lines were seeded in 2ml complete medium on autoclaved sterile coverslips placed into 6-well plates. Next day, medium was aspirated and the cells were washed twice with PBS. 1.5ml of new complete medium with the kinase inhibitor or DMSO control was given to the cells. All kinase inhibitors were used at a concentration of 10µM, except PI3Kalpha inhibitor and Rapamycin, which were used at 0.1µM concentrations. After 72h of incubation, cells were washed twice with cold PBS and fixed and permeabilized with 100% ice-cold methanol for 10 min. Methanol was discarded and the cells were washed once with cold PBS. (If the cells were fixed with paraformaldehyde, then they were permeabilized with 100% ice-cold methanol.) After fixation, cells were blocked in 1 ml blocking solution (3% BSA in PBS-T(0.1%)) for 1h on shaker at room temperature. Coverslips were then probed with primary antibody in appropriate dilution for 2h at room temperature. Coverslips were then washed 3 times with PBS-T for 5 min, and then either appropriate FITC-conjugated or AlexaFluor secondary antibody was applied for 1h at room temperature. All steps after the addition of secondary antibody were performed in dark. Cells were washed 3 times with PBS-T for 5 min and counterstained with 1µg/ml Hoechst dye (250µl/well) at dark for 5 min. Then, Hoechst was discarded,

cells were washed once with ddH_2O briefly and then they were de-stained in ddH_2O for 10 min. Excess water was removed from the coverslips by tissue paper, and they were mounted onto slides containing DAKO Fluorescent Mounting Medium. Stained cells were examined under fluorescence microscope (ZEISS) and pictures were captured in a digital ZEISS AxioCam MRc5 camera.

3.3.17. *In vivo* tumor xenografts

Mahlavu cells ($10x10^6$ cells) were injected subcutaneously in nude mice. Mice were randomly divided into four groups: control (simple syrup), Sorafenib (30 mg/kg), Akti-2 (7.5 mg/kg) and combination (30 mg/kg Sorafenib plus 7.5 mg/kg Akti-2). There were 5 animals per group, except Akti-2, which had 4 animals. Treatments were initiated when tumors reached an average volume of 150 mm^3. Drugs were administered by oral gavage 5 days a week for 3 weeks. Tumor volumes were measured twice a week. After 3 weeks of treatment, animals were anesthetized and tumors were visualized by MR imaging. Tumors were excised and their weights were recorded.

CHAPTER 4. RESULTS

4.1. Differential PTEN expression and AKT phosphorylation in HCC cell lines

Inactivating mutations of the tumor suppressor gene Phosphatase and tensin homolog (PTEN), which is a negative regulator of PI3K/Akt survival pathway, are frequently observed in HCC (Bae et al., 2007; Buontempo et al., 2011; Fujiwara et al., 2000; Kawamura et al., 1999; Yao et al., 1999). Decreased PTEN expression is correlated with increased tumor grade, advanced disease stage and reduced overall survival in patients with HCC (Hu et al., 2003). Aberrant mTOR signaling is also frequent in HCC and is associated with IGF pathway activation, EGF up-regulation, and PTEN dysregulation (Villanueva et al., 2008).

Therefore, we initially analyzed expression and activity status of the PI3K/Akt pathway. Total Akt protein levels were the same in all HCC cell lines. Loss of PTEN protein expression in Mahlavu and Snu475 poorly-differentiated aggressive HCC cell lines were associated with hyper-phosphorylation of Akt (Figure 4.1).

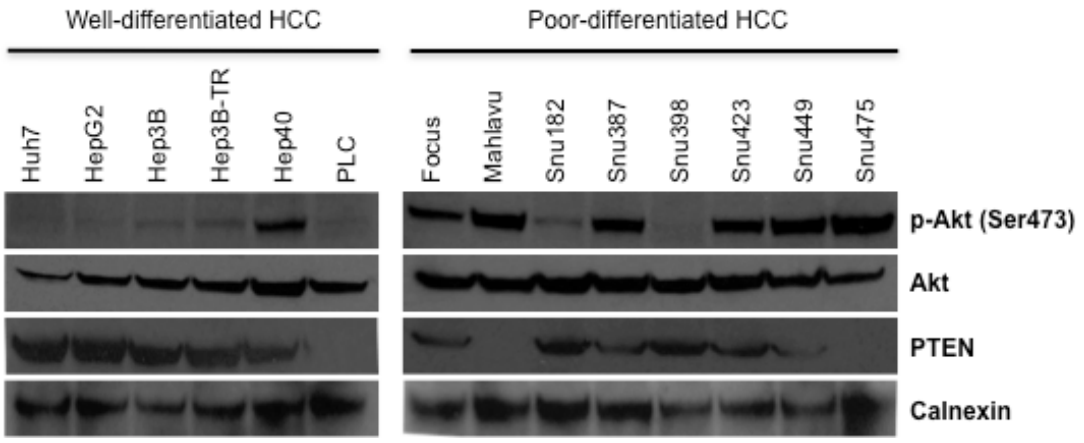

Figure 4.1: Expression of PTEN and activating phosphorylation of Akt in HCC cell lines. Whole-cell lysates (40 μg) were analyzed by Western blotting.

Next, we examined mRNA level expression of PTEN and showed that gene fragment within exons 4 and 5 is lost in the Mahlavu cell line. Akt-specific

phosphorylation of downstream proteins GSK3*α*/*β* and Bad in the absence of PTEN showed that loss of PTEN results in hyper-phosphorylation and hyper-activation of Akt as seen by Akt-specific phosphorylation of downstream proteins GSK3*α*/*β* and Bad (Figure 4.2.B,C). Although the phosphorylation of Bad on Ser136 and GSK3*α*/*β* on Ser21/9 residues are Akt-specific, we also performed kinase activity assay with exogenous GSK3*α*/*β* to validate Akt-specific activity (Figure 4.2.D).

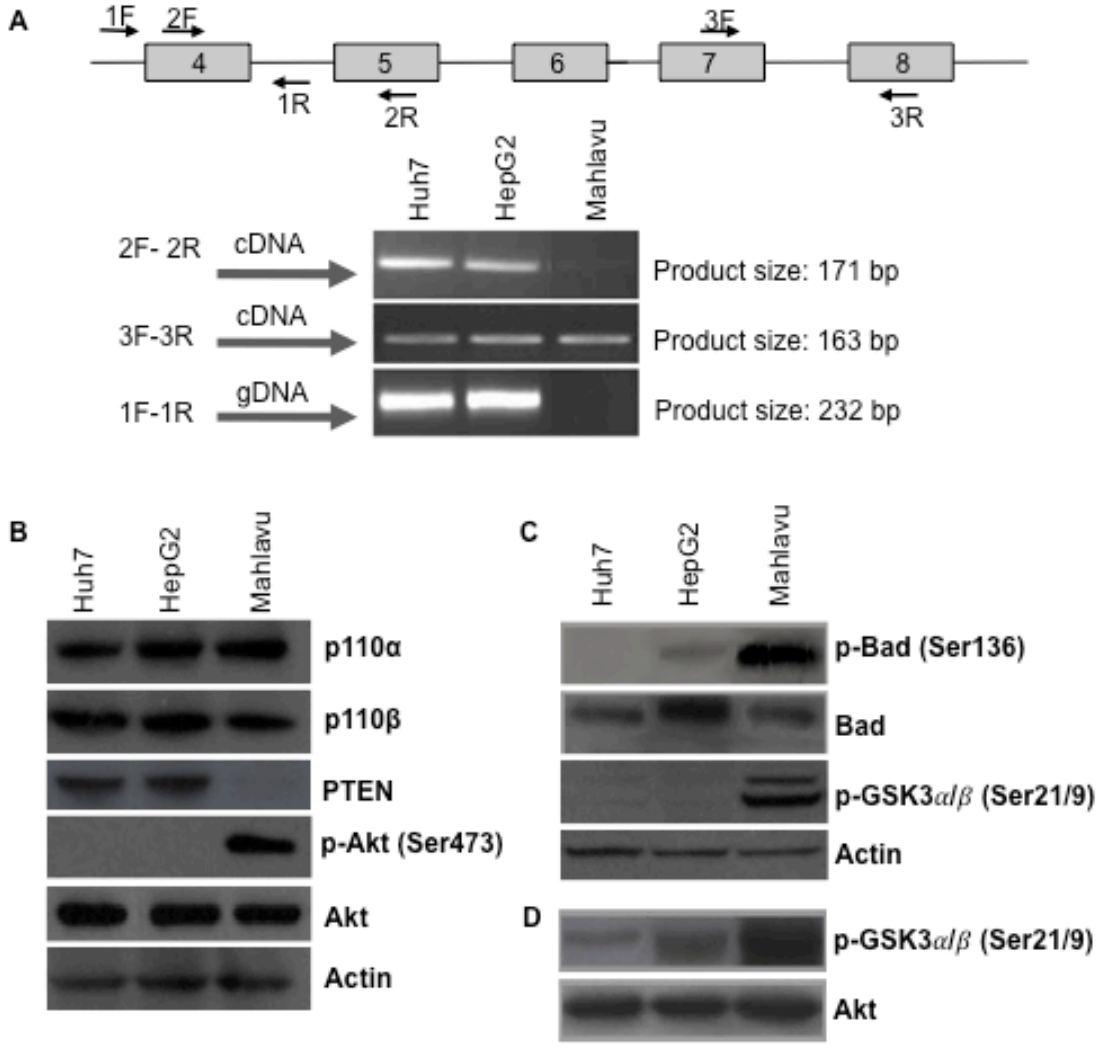

Figure 4.2: Differential expression of PTEN and subsequent activity of Akt in HCC cell lines. A) PCR analysis of the PTEN gene in HCC cell lines. The gene fragment within exons 4 and 5 is lost in Mahlavu cell line. B) Whole-cell lysates (40 μg) were analyzed by Western blotting. Loss of PTEN results in hyper-phosphorylation of Akt. C) Hyper-phosphorylated Akt hyper-actively phosphorylates its downstream targets Bad and GSK3*α*/*β*. D) Kinase assay on exogenous GSK3*α*/*β*.

4.2. Response of HCC cell lines to PI3K/AKT pathway inhibition

4.2.1. Cytotoxic activity analysis of classic PI3K/AKT pathway inhibitors

We analyzed the cytotoxic activity of two pan-PI3K inhibitors (LY294002, Wortmannin) and one Akt inhibitor (Akti-1/2) in Huh7 and Mahlavu cell lines using Sulforhodamine B (SRB) assay, as described in the methods section. All inhibitors caused growth inhibition, even after 24 hours of exposure (Figure 4.3). However, their cytotoxic effect was transient, since remaining cells resumed growing in the presence of these inhibitors. For instance, although the highest dose of Wortmannin (50 μM) caused 60% growth inhibition at 24 hours, inhibition was lowered to 30% after 96 hours. Lower doses resisted growth inhibition completely. We showed that these inhibitors can target growth of HCC cells but cannot establish complete blockage. Calculation of IC50 values for each time point showed that the required concentration of inhibitor to suppress growth and induce cytotoxicity increases with time (Table 4.1).

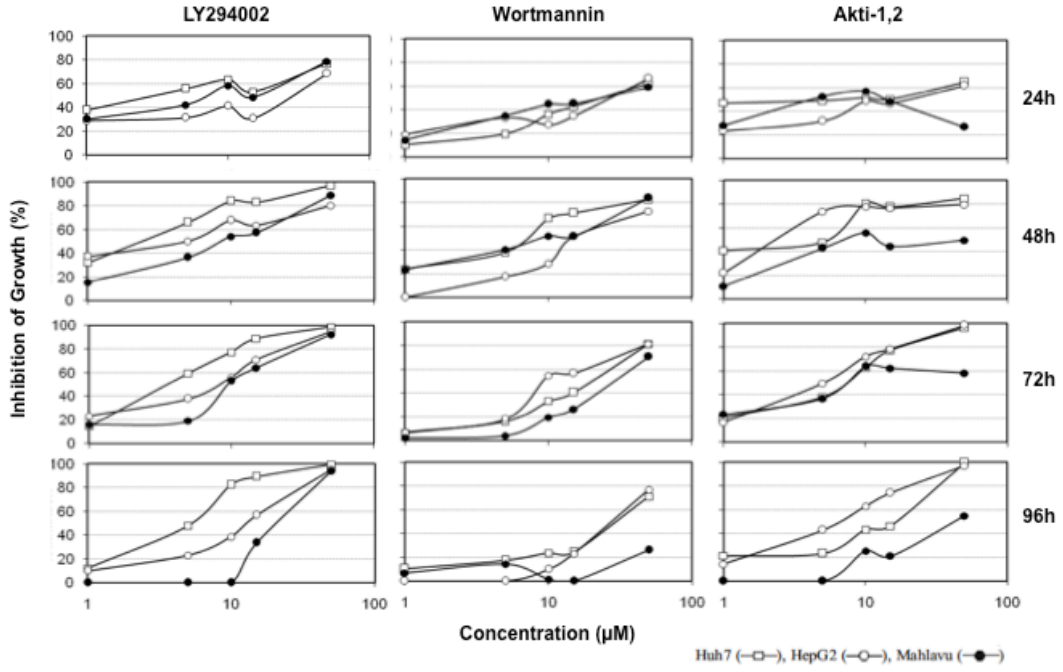

Figure 4.3: Inhibitory effects of LY294002, Wortmannin and Akti-1,2 on HCC cell growth. % inhibition of cell growth after 24, 48,72 and 96 hours of treatment

with the indicated inhibitors. SRB was performed in quadruplets with different concentrations (50 μM, 15 μM, 10 μM, 5 μM, 1 μM)

Table 4.1: Time-dependent IC50 values, calculated based on SRB

		Huh7	HepG2	Mahlavu
LY294002	24h	4.0 μM	25.0 μM	7.0 μM
	48h	2.2 μM	3.4 μM	8.0 μM
	72h	3.8 μM	5.8 μM	8.7 μM
	96h	4.2 μM	10.5 μM	24.0 μM
Wortmannin	24h	26.0 μM	29.0 μM	20.0 μM
	48h	5.5 μM	18.9 μM	8.1 μM
	72h	17.8 μM	11.3 μM	36.9 μM
	96h	36.1 μM	37.6 μM	> 50 μM
Akti-1,2	24h	4.5 μM	18.0 μM	10.0 μM
	48h	2.3 μM	2.7 μM	21.1 μM
	72h	5.3 μM	4.5 μM	9.0 μM
	96h	9.8 μM	5.6 μM	69.4 μM

4.2.2. Apoptotic cell death caused by classic PI3K/AKT pathway inhibitors

After showing the growth-inhibitory function of kinase inhibitors, we examined their role in the induction of apoptotic cell death. Inhibitors were used at their IC50 (concentration causing 50% inhibition) values calculated from the growth inhibition graphs, as explained in methods section (LY294002 (Huh7: 4 μM, HepG2:

25 µM, Mahlavu: 7 µM), Wortmannin (Huh7: 26 µM, HepG2: 29 µM, Mahlavu: 20 µM), Akti-1,2 (Huh7: 4.5 µM, HepG2: 18 µM, Mahlavu: 10 µM). Cells were treated with the indicated inhibitors for 24 hours and their pro-apoptotic effect was assessed by Poly ADP-ribosyl polymerase (PARP) cleavage analysis using western blot. All inhibitors induced typical PARP cleavage from 113 kDa to 89 and 24 kDa fragments by caspase-3 during apoptosis (Figure 4.4.A) (Soldani & Scovassi, 2002). Pro-apoptotic effect of kinase inhibitors was further validated by Hoechst staining, which shows morphological features of apoptosis, i.e. chromatin condensation and fragmented nuclei (Figure 4.4.B). We showed that inhibition of PI3K/AKT signaling with well-known kinase inhibitors disrupts growth of HCC cells and induces cell death independent of Akt activation status.

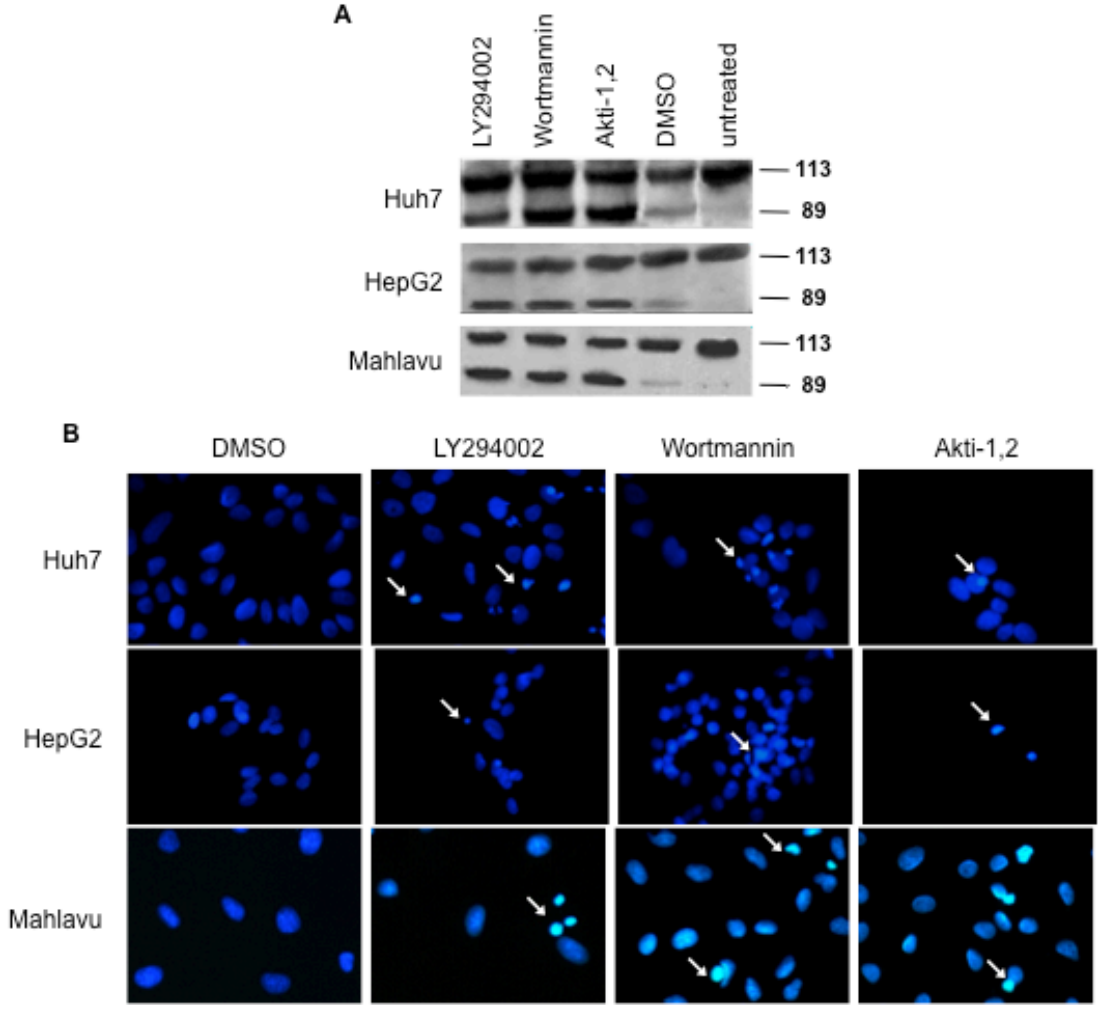

Figure 4.4: Induction of apoptosis in HCC cells upon treatment with LY294002, Wortmannin and Akti-1,2 for 24 hours at their IC50s. A) Western blot analysis of

PARP cleavage. B) Immunofluorescence analysis of Hoechst-stained apoptotic cells. White arrows indicate apoptotic cells.

4.3. Expression and activity of critical components of PI3K/AKT/mTOR and RAF/MEK/ERK signaling pathways

We selected the well-differentiated (epithelial-like, less malignant) Huh7 cell line with intact PTEN and the poor-differentiated (mesenchymal-like, highly malignant) Mahlavu with PTEN loss for our further experiments. Initially, we demonstrated PI3K/AKT and MEK/ERK signaling status in these cell lines (Figure 4.5). Not only Akt, but also Erk kinase is hyper-active in the aggressive Mahlavu cell line. Active Akt phosphorylates and thereby inhibits the FoxO1 transcription factor, and promotes cell cycle progression through Rb.

Figure 4.5: Expression and activity of PI3K/AKT/mTOR and RAF/MEK/ERK signaling pathways in selected HCC cell lines.

4.4. Cytotoxic activity analysis of PI3K/AKT signaling pathway inhibitors

We analyzed the cytotoxic activity of PI3K/AKT signaling pathway inhibitors in Huh7 and Mahlavu cell lines using the SRB assay, and calculated their IC50 values at 72 hours of incubation (Table 4.2). In addition to SRB, we used RTCES assay to monitor real-time, dynamic changes in cell growth in inhibitor-treated Huh7 (Figure 4.6) and Mahlavu cells (Figure 4.7) and calculated their IC50 values at 72 hours of incubation (Table 4.3).

Table 4.2: IC50 values at 72 hours, calculated based on SRB

	Huh7	**Mahlavu**
Sorafenib	8.0 μM	6.6 μM
LY294002	3.8 μM	8.7 μM
Wortmannin	17.8 μM	36.9 μM
ZSTK474	6.6 μM	6.7 μM
PI-103	4.0 μM	1.7 μM
Rapamycin	0.1 μM	0.1 μM
PI3Ki-α	<0.3 μM	<0.3 μM
PI3Ki-β	>40.0 μM	>40.0 μM
Akti-1,2	5.3 μM	9.0 μM
Akti-2	22.7 μM	13.8 μM

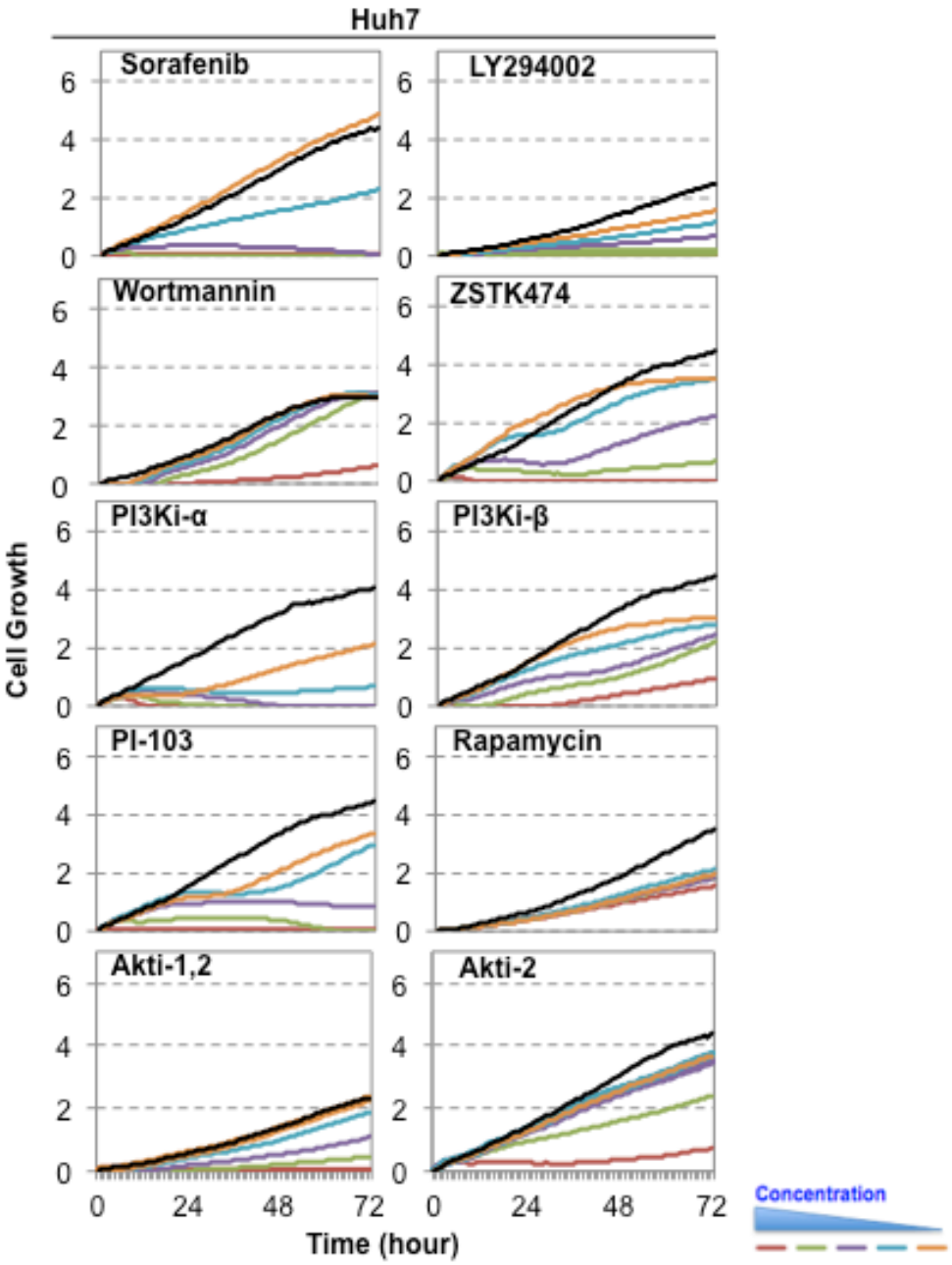

Figure 4.6: Real-time cell growth analysis of kinase inhibitors in Huh7 cells. Huh7 cells were treated with the indicated kinase inhibitors for 72 hours. Black line represents control cells treated with DMSO. Dose curves are color-coded, red representing the highest dose and orange representing the lowest for each inhibitor. Best dose ranges of each inhibitor were selected to demonstrate dose-dependent cytotoxicity.

Sorafenib, PI3Ki-β, Akti-2, Akti-1,2, LY294002: 40μM, 20μM, 10μM, 5μM, 2.5μM

ZSTK474, PI-103: 20μM, 10μM, 5μM, 2.5μM, 1.25μM

PI3Ki-α: 1μM, 0.5μM, 0.25μM, 0.125μM, 0.0625μM

Rapamycin: 6.4μM, 1.6μM, 0.4μM, 0.1μM, 0.025μM

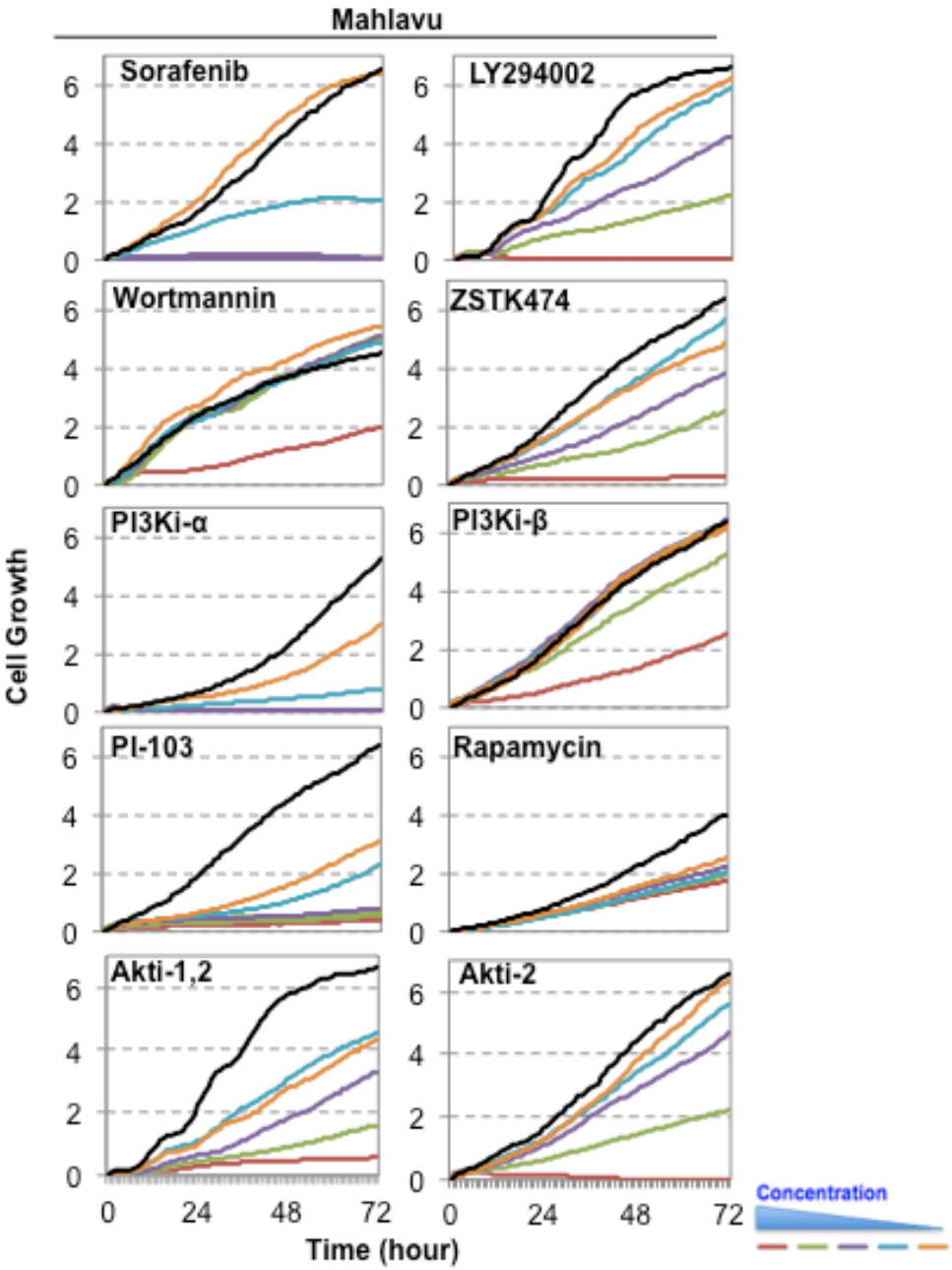

Figure 4.7: Real-time cell growth analysis of kinase inhibitors in Mahlavu cells. Mahlavu cells were treated with the indicated kinase inhibitors for 72 hours. Black line represents control cells treated with DMSO. Dose curves are color-coded, red representing the highest dose and orange representing the lowest for each inhibitor. Best dose ranges of each inhibitor were selected to demonstrate dose-dependent cytotoxicity.

Sorafenib, PI3Ki-β, Akti-2, Akti-1,2, LY294002: 40μM, 20μM, 10μM, 5μM, 2.5μM

ZSTK474, PI-103: 20μM, 10μM, 5μM, 2.5μM, 1.25μM

PI3Ki-α: 1μM, 0.5μM, 0.25μM, 0.125μM, 0.0625μM

Rapamycin: 6.4μM, 1.6μM, 0.4μM, 0.1μM, 0.025μM

Table 4.3: IC50 values at 72 hours, calculated based on RTCES

	Huh7	**Mahlavu**
Sorafenib	10 μM	10 μM
LY294002	10 μM	10 μM
Wortmannin	10 μM	10 μM
ZSTK474	10 μM	8 μM
PI-103	12 μM	10 μM
Rapamycin	0.1 μM	0.1 μM
PI3Ki-α	0.1 μM	0.1 μM
PI3Ki-β	10 μM	15 μM
Akti-1,2	10 μM	10 μM
Akti-2	10 μM	8 μM

Differences in the calculated IC50 values based on SRB and RTCES can be explained with regard to the underlying principle of the assays. SRB assay measures protein content of attached cells and uses the amount of protein-bound SRB to estimate the number of adherent alive cells. RTCES, on the other hand, uses the area occupied by cells in the plate to estimate the number of adherent alive cells. Both assays have their own advantages and disadvantages. For instance, SRB can biasedly estimate lower IC50 in cells treated with drugs that can inhibit protein synthesis, such as PI-103. Likewise, RTCES can biasedly estimate higher IC50 in cells treated with drugs that cause vacuolization. Therefore, we treated cells with various concentrations of drugs and analyzed their morphology under light microscope (Figure 4.8). Finally we decided to use the concentrations given in Table 4.4 for our further experiments.

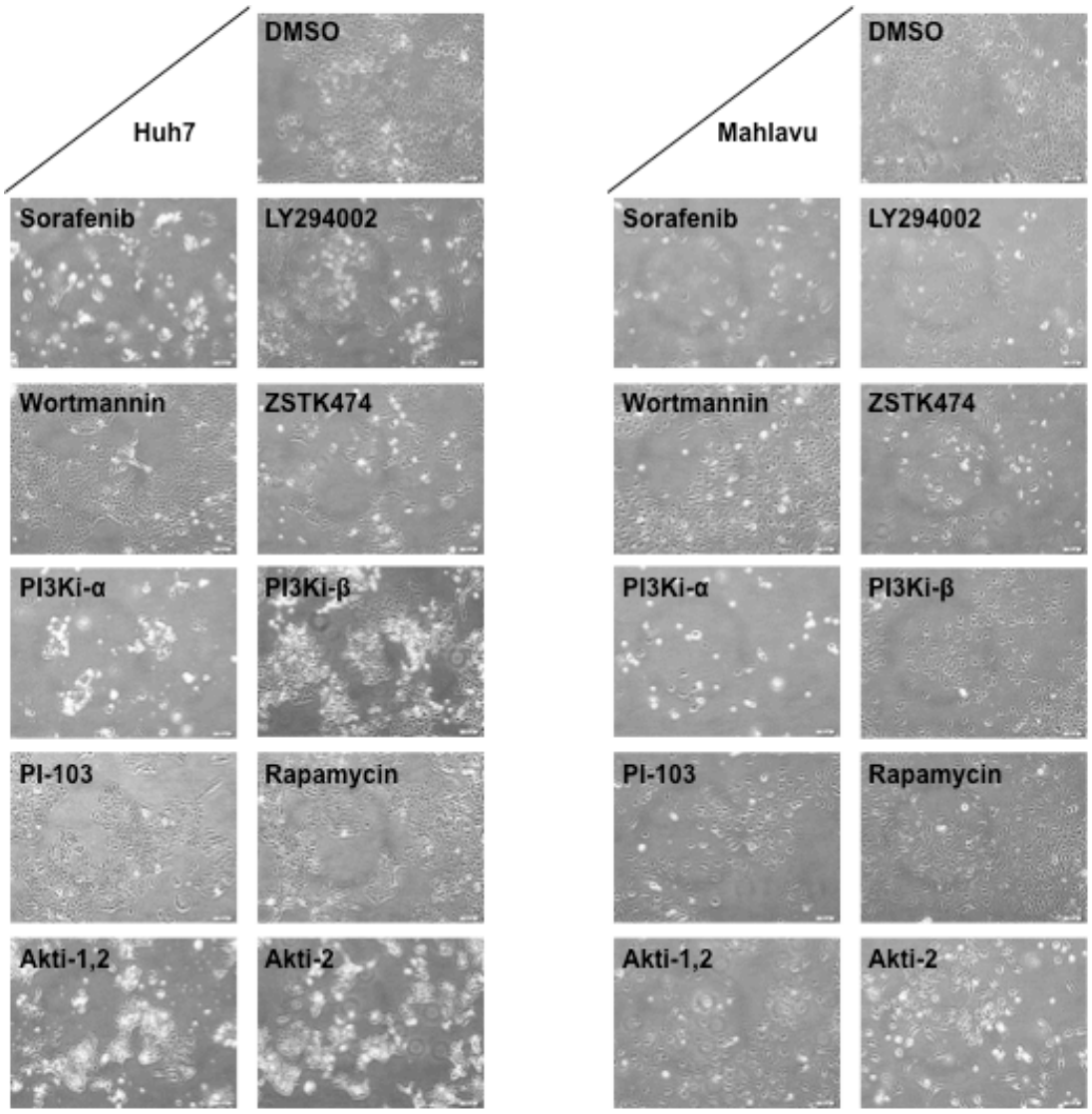

Figure 4.8: Light microscope images of HCC cells treated with inhibitors at concentrations given in Table 4.4.

Table 4.4: Concentration of each inhibitor chosen for our experiments

Inhibitor	Concentration
Sorafenib	10 μM
LY294002	10 μM
Wortmannin	10 μM
ZSTK474	10 μM
PI-103	10 μM
Rapamycin	0.1 μM
PI3Ki-α	0.1 μM
PI3Ki-β	10 μM
Akti-1,2	10 μM
Akti-2	10 μM

4.5. Effect of PI3K/AKT signaling pathway inhibitors on cell cycle

First of all, we analyzed the effect of all inhibitors on viability and cell cycle progression in HCC cells. Cells were treated with concentration indicated in Table 4.4, and were incubated for 72 hours. Propidium iodide, which intercalates into double-stranded DNA, was used to evaluate cell viability and DNA content in flow cytometric cell cycle analysis. Distribution of viable cells in G1, S and G2/M phases of cell cycles, and the percentage of apoptotic cells represented by the sub-G1 population were analyzed. None of the inhibitors had significant effect on the cell cycle distribution of cells. Treatment with Sorafenib and PI3Ki-α resulted in enhanced sub-G1 population, indicating induction of apoptosis in both cell lines (Figure 4.9). Sorafenib was more effective in Huh7 cells, while PI3Ki-α was more

effective in Mahlavu cell lines, which depend on PTEN-loss mediated hyper-active PI3K signaling.

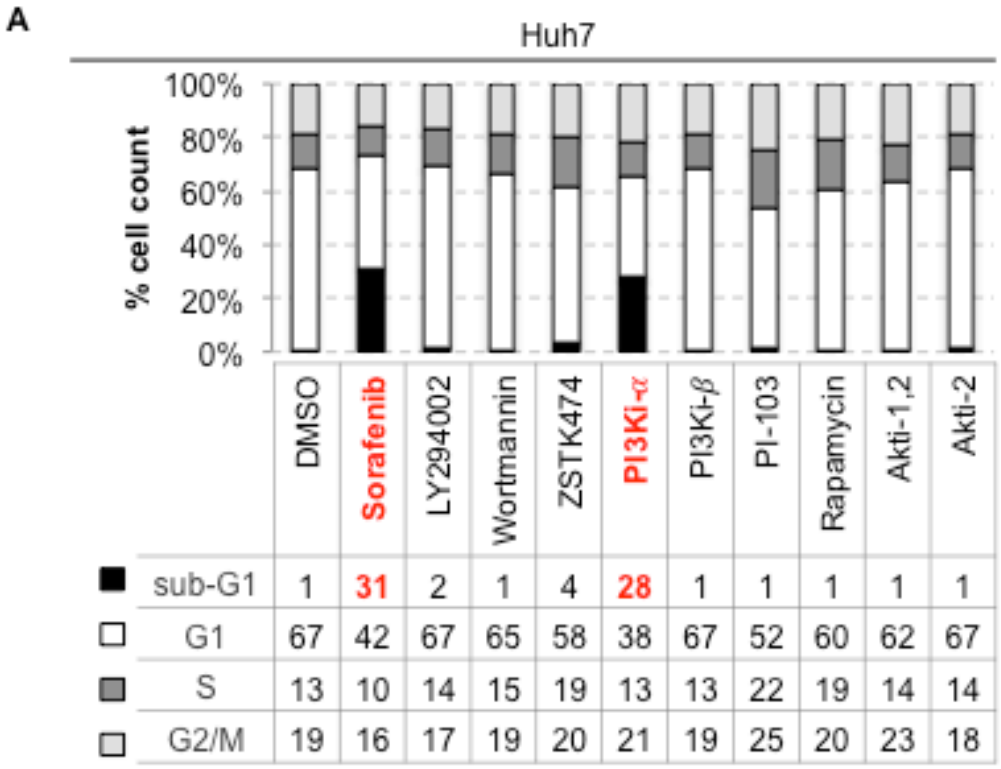

Figure 4.9: Flow Cytometric Analysis of Cellular DNA Content. Sub-G1 population represents apoptotic cells.

4.6. Effect of PI3K/AKT signaling pathway inhibitors on migration

In addition to cell survival and proliferation, PI3K/AKT/mTOR and Raf/MEK/ERK pathways are known to regulate migration of cells. Since the inhibitors, except Sorafenib and PI3Ki-α, did not affect cell cycle progression and viability of HCC cells, we examined their role in migration. We performed a wound-healing assay (scratch assay), and took pictures immediately after the scratch was made, after 24 hours and after 48 hours to show the migration of cells to the wounded area. Wound closure percentage after 48 hours was calculated to show the migratory capacity of cells in the presence of kinase inhibitors in Huh7 (Figure 4.10) and Mahlavu (Figure 4.11) cell lines. Wortmannin and Rapamycin could not reduce migration of Mahlavu cells, but they were able to affect Huh7 cells. Sorafenib, PI3Ki-α, Akti-1,2 and Akti-2 reduced migration significantly ($p<0.001$) in both Huh7 and Mahlavu.

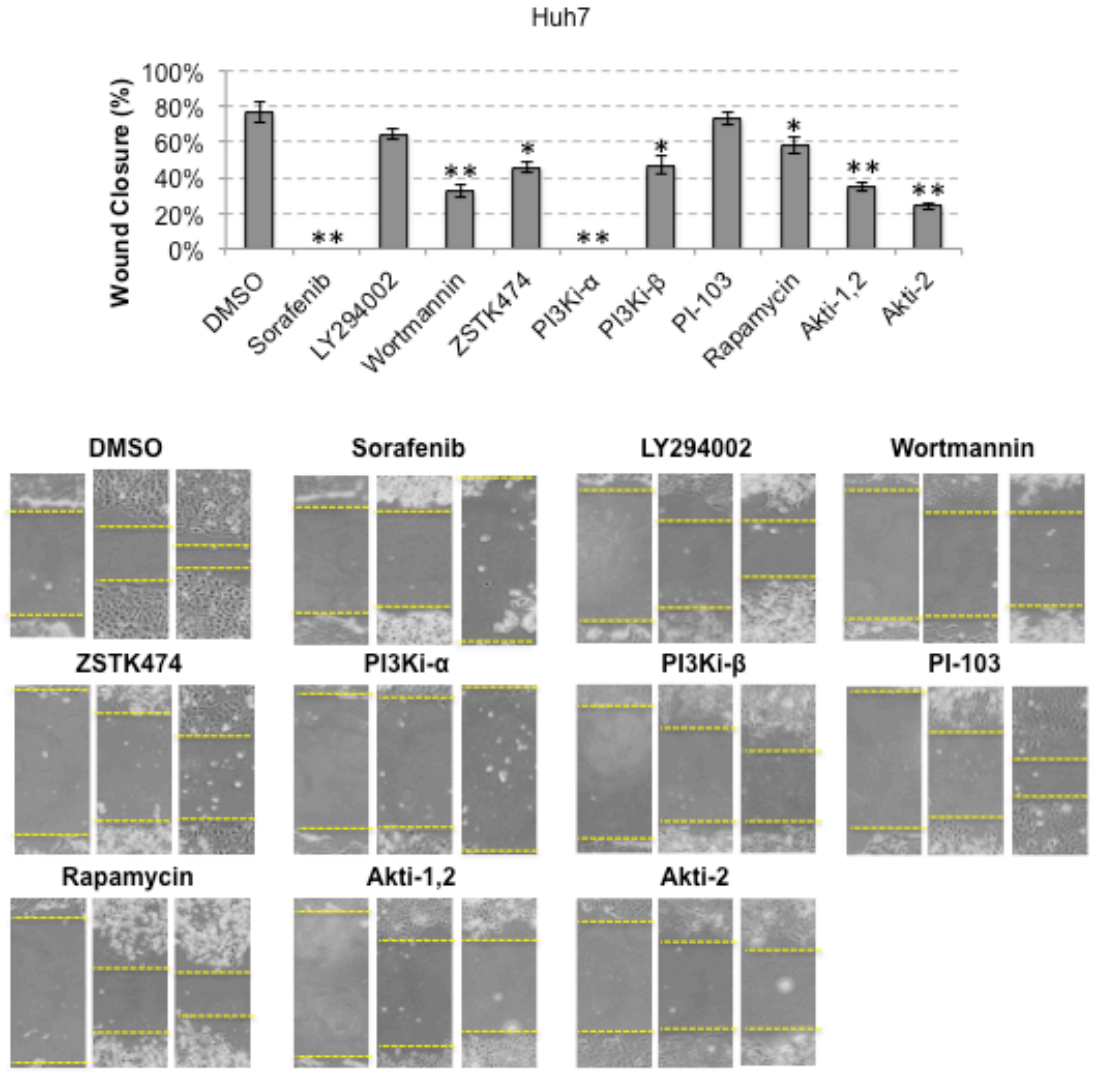

Figure 4.10: Effect of kinase inhibitors on migration of Huh7 cells. Wound closure percentage after 48 hours of incubation with the indicated kinase inhibitors represents the effect of inhibitors on migration. Pictures were taken at 3 time points: immediately after the scratch was made, after 24 hours and after 48 hours. Statistically significant differences in migration compared to DMSO controls were represented (**: p<0.001, *: p<0.01).

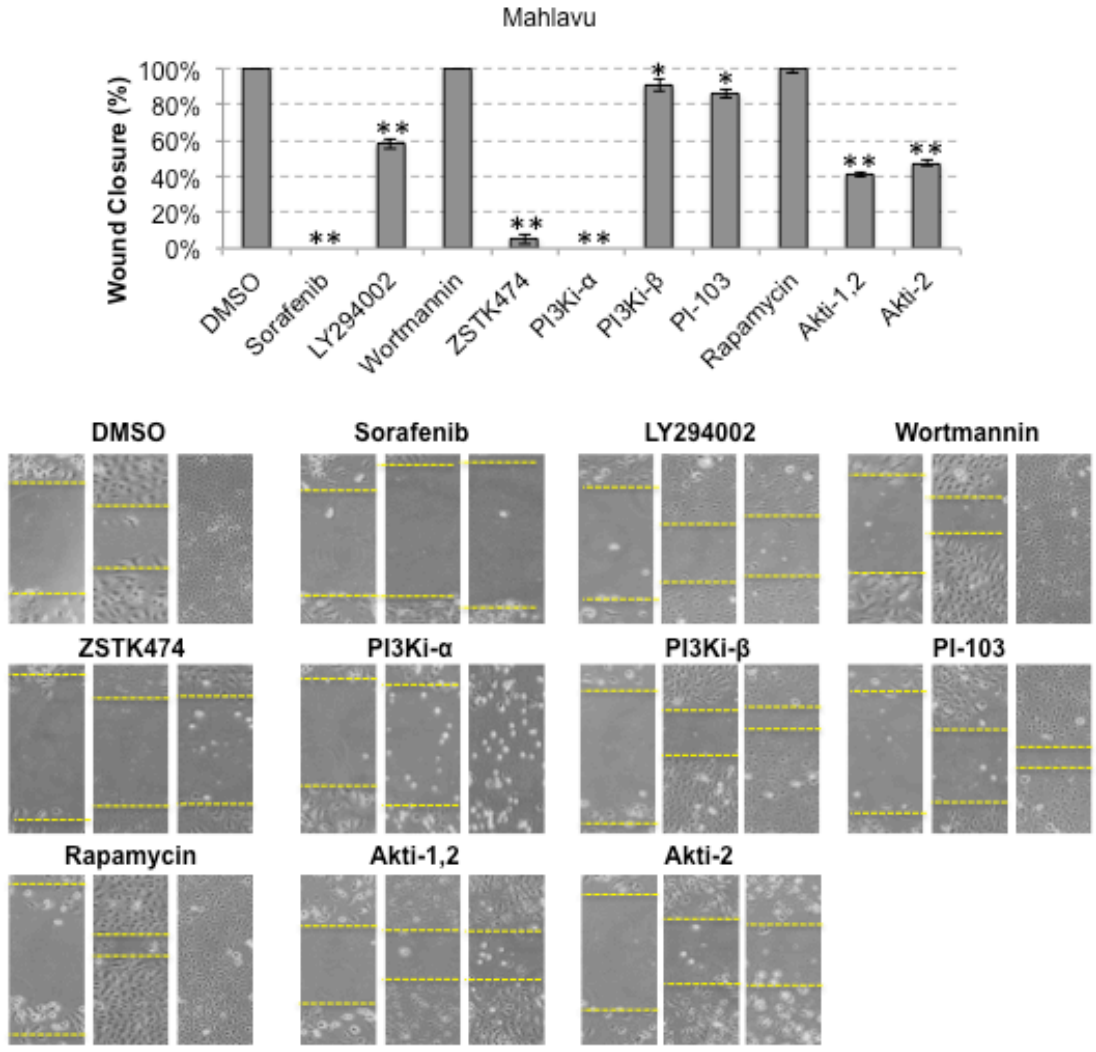

Figure 4.11: Effect of kinase inhibitors on migration of Mahlavu cells. Wound closure percentage after 48 hours of incubation with the indicated kinase inhibitors represents the effect of inhibitors on migration. Pictures were taken at 3 time points: immediately after the scratch was made, after 24 hours and after 48 hours. Statistically significant differences in migration compared to DMSO controls were represented (**: p<0.001, *: p<0.01).

4.7. Effect of PI3K/AKT signaling pathway inhibitors on apoptosis

PI3K/AKT/mTOR and Raf/MEK/ERK signaling pathways maintain cell survival, proliferation and migration. All kinase inhibitors in this study showed cytotoxic anti-proliferative activity at various doses ranging from 40μM to 0.1μM. Analysis of their cytotoxic mechanism of actions at clinically relevant doses (10μM at most) revealed anti-migratory effects of Akti-1,2 and Akti-2 and pro-apoptotic roles of Sorafenib and PI3Ki-*α*. We further examined the effect of kinase inhibitors on apoptotic cell death and showed caspase-mediated PARP cleavage in cells treated with Sorafenib and PI3Ki-*α*, as an indicator of apoptosis (Figure 4.12.A) (Soldani & Scovassi, 2002). Apoptotic cell death in both Huh7 and Mahlavu cells were associated with cytochrome c release from mitochondria, which is necessary to activate pro-apoptotic caspase cascade (Goldstein, Waterhouse, Juin, Evan, & Green, 2000). Pro-apoptotic effect of kinase inhibitors was further validated by Hoechst staining, which shows morphological features of apoptosis, i.e. chromatin condensation and fragmented nuclei (Figure 4.12.B).

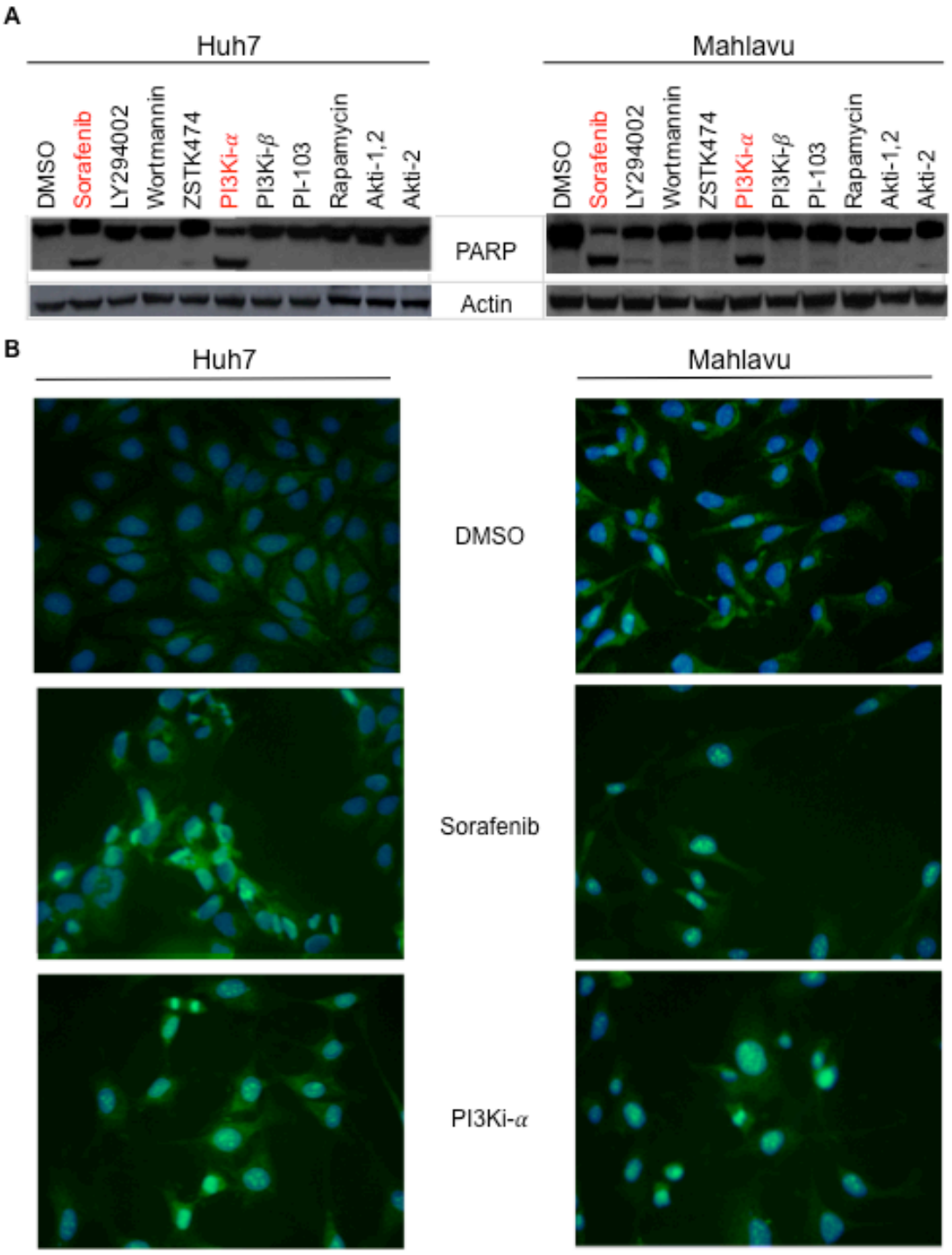

Figure 4.12: Effect of kinase inhibitors on apoptotic cell death. A) PARP cleavage analysis with Western blot using 25µg whole cell lysates. Cells were treated with the indicated inhibitors for 72 hours. B) Immunofluorescence analysis of Cytochrome c (green) and Hoechst (blue) staining. Cells were treated with the indicated inhibitors for 48 hours.

4.8. Combinational treatment of most potential PI3K/AKT signaling pathway inhibitors with Sorafenib

4.8.1 Synergistic cytotoxicity analysis

PI3Ki-α, Akti-1,2 and Akti-2 were the most promising drug candidates in our 9 PI3K/AKT/mTOR pathway kinase inhibitor panel. We showed that Sorafenib and PI3Ki-α effectively inhibits growth and induces apoptosis in Huh7 and Mahlavu cell lines. PI3Ki-α is effective even at very low doses (0.1μM). Although Akti-1,2 and Akti-2 did not induce significant anti-growth or pro-apoptotic mechanisms at 10μM concentration, they were highly effective in reducing migration in both cell lines. Therefore, we addressed the effectiveness of a combined treatment of Sorafenib with PI3Ki-α, Akti-1,2 and Akti-2. We compared growth of Sorafenib-treated cells and combination-treated cells with the RTCES assay.

Co-treatment of Sorafenib and PI3Ki-α resulted in synergistic growth inhibition in both cell lines. Both PI3Ki-α and PI3Ki-β showed synergistic growth inhibition in Huh7 (Figure 4.13). However, only co-treatment with PI3Ki-α led to synergistic growth inhibition in the Mahlavu cell line (Figure 4.14). Interestingly, combined treatment of Sorafenib with PI3Ki-β exhibited an antagonistic effect and promoted cell growth. Co-targeting Raf with Sorafenib and alpha-isoform of PI3K with PI3Ki-α simultaneously can inhibit growth completely in Mahlavu cells. Yet, co-targeting Raf with Sorafenib and beta-isoform of PI3K (p110β) with PI3Ki-β probably intensifies signaling from the alpha isoform (p110α) and promotes growth. Indeed, Mahlavu cells are more sensitive to co-treatment of Sorafenib and PI3Ki-α than Huh7 cells. Collectively, these findings suggest that PTEN-loss induced constitutively active PI3K/Akt signaling in Mahlavu cells depend primarily on the alpha isoform (p110α).

We have shown that Akti-1 and Akti-2 cause growth inhibition and reduce migration but cannot induce apoptosis when used at 10μM. Interestingly, co-treatment of Sorafenib and either Akti-1 or Akti-2 resulted in synergistic growth inhibition in both cell lines (Figures 4.15 and 4.16). These results highlight the therapeutic potential of combining Sorafenib with PI3Ki-α, Akti-1,2 or Akti-2 for the treatment of HCC (Figure 4.17).

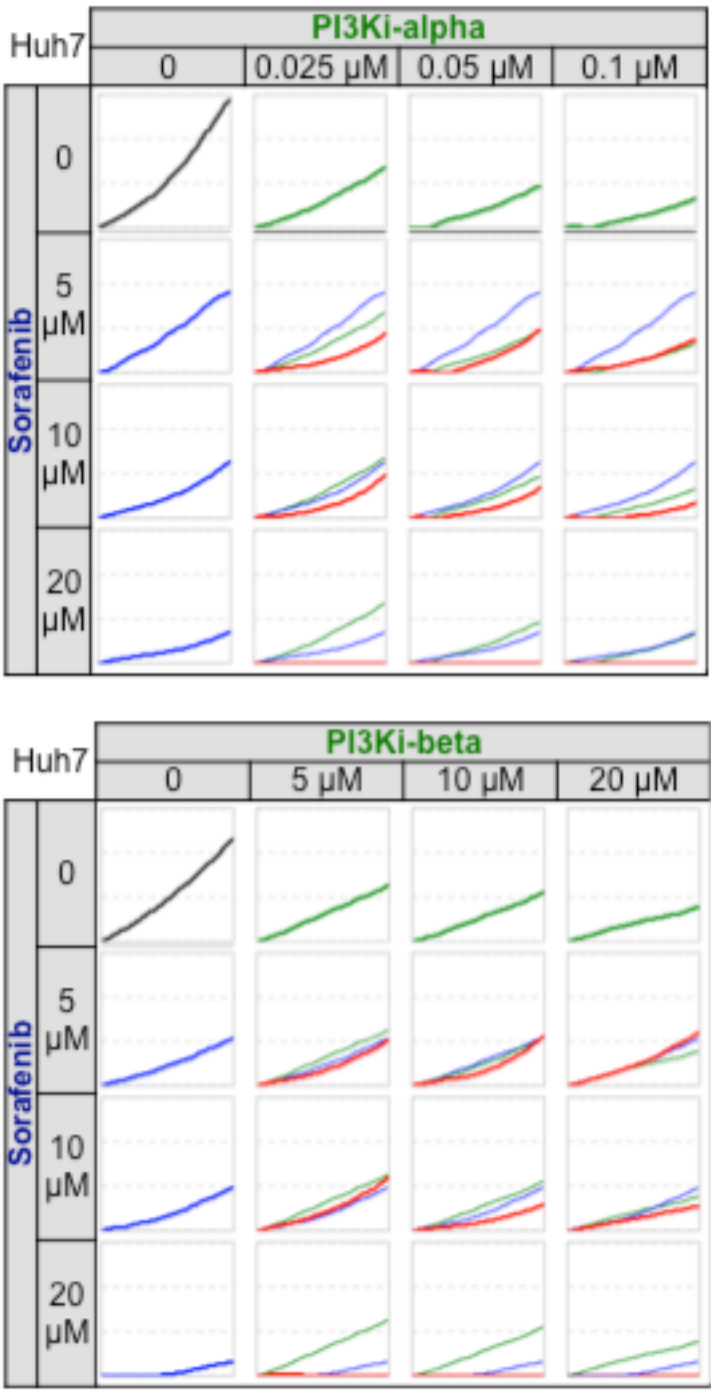

Figure 4.13: Real-time cell growth analysis of Huh7 cells targeted with isoform-specific PI3K kinase inhibitors in combination with Sorafenib. Huh7 cells were treated with the indicated kinase inhibitors for 72 hours. RTCES-based cell growth values (y-axis) were plotted against time (x-axis). Black line represents control cells treated with DMSO. Growth of Sorafenib treated cells are represented in blue and PI3K inhibitor treated cells are in green. Red plot represents the growth of cells treated with both Sorafenib and PI3K inhibitor in combination.

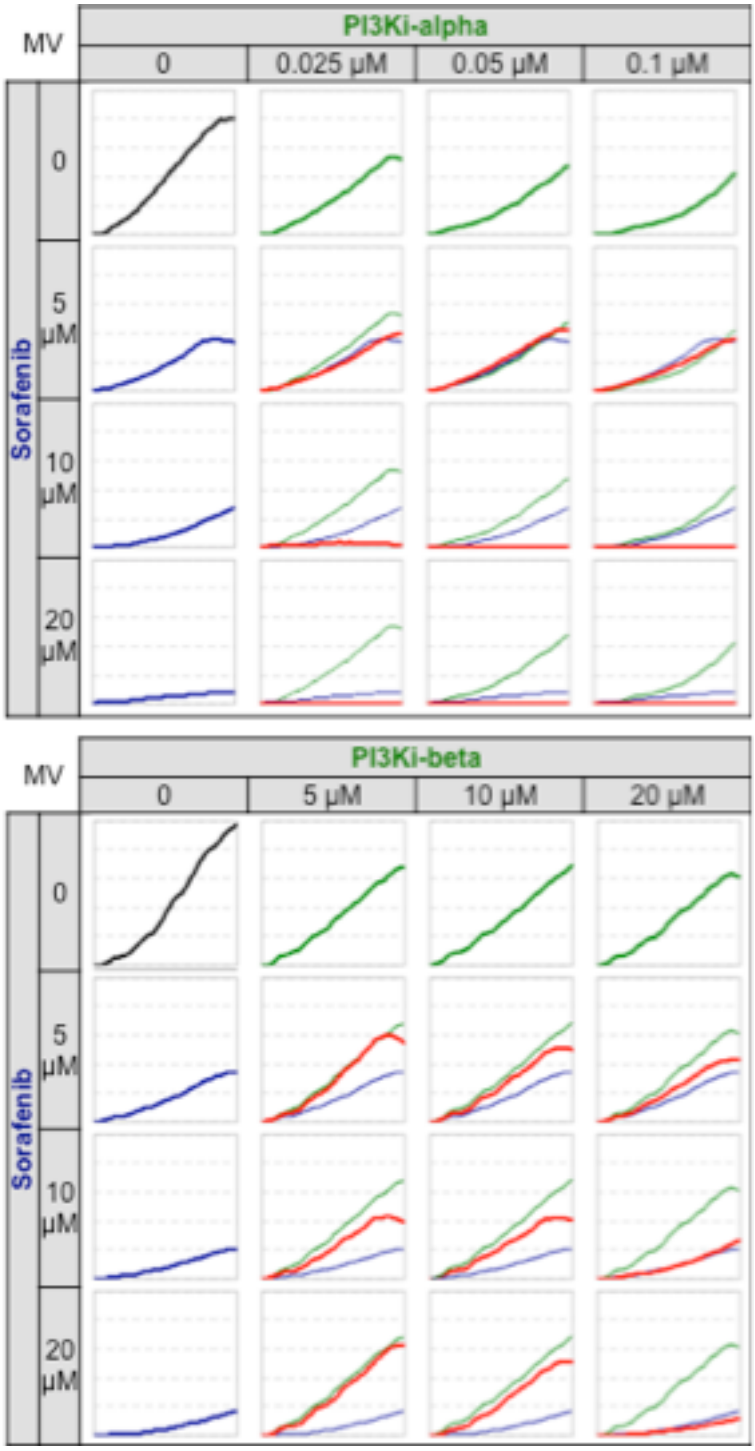

Figure 4.14: Real-time cell growth analysis of Mahlavu cells targeted with isoform-specific PI3K kinase inhibitors in combination with Sorafenib. Huh7 cells were treated with the indicated kinase inhibitors for 72 hours. RTCES-based cell growth values (y-axis) were plotted against time (x-axis). Black line represents control cells treated with DMSO. Growth of Sorafenib treated cells are represented in

blue and PI3K inhibitor treated cells are in green. Red plot represents the growth of cells treated with both Sorafenib and PI3K inhibitor in combination.

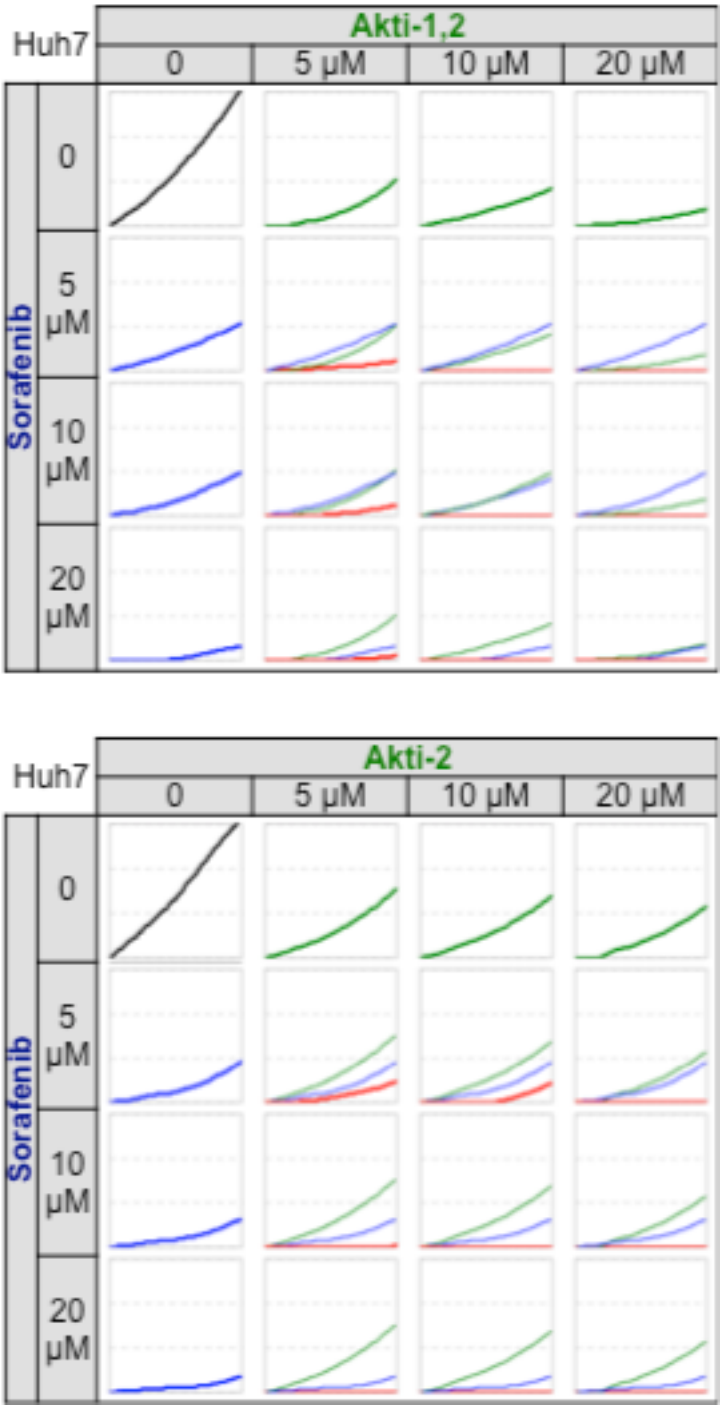

Figure 4.15: Real-time cell growth analysis of Huh7 cells targeted with isoform-specific Akt inhibitors in combination with Sorafenib. Huh7 cells were treated with the indicated kinase inhibitors for 72 hours. RTCES-based cell growth values (y-axis) were plotted against time (x-axis). Black line represents control cells treated with DMSO. Growth of Sorafenib treated cells are represented in blue and Akt

inhibitor treated cells are in green. Red plot represents the growth of cells treated with both Sorafenib and Akt inhibitor in combination.

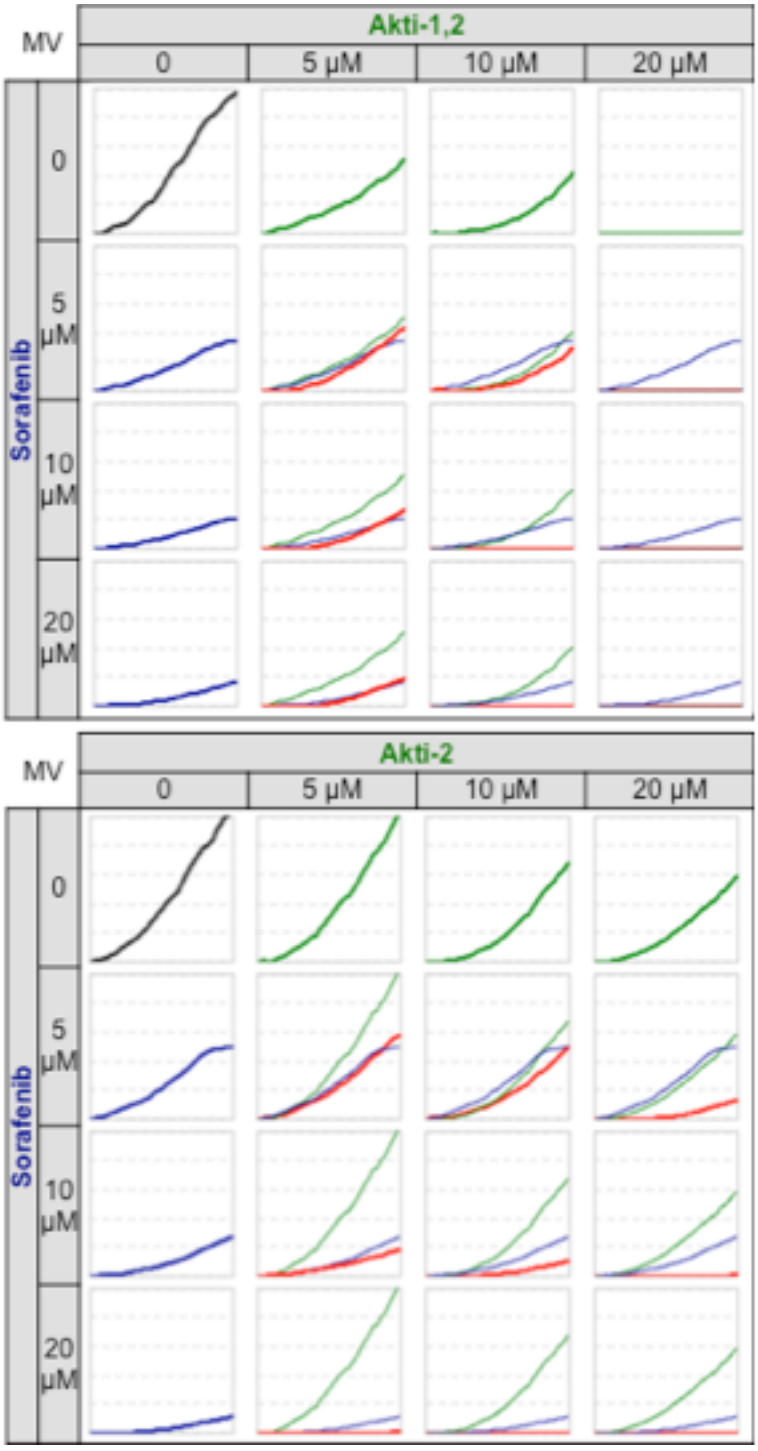

Figure 4.16: Real-time cell growth analysis of Mahlavu cells targeted with isoform-specific Akt inhibitors in combination with Sorafenib. Mahlavu cells were treated with the indicated kinase inhibitors for 72 hours. RTCES-based cell growth values (y-axis) were plotted against time (x-axis). Black line represents

control cells treated with DMSO. Growth of Sorafenib treated cells are represented in blue and Akt inhibitor treated cells are in green. Red plot represents the growth of cells treated with both Sorafenib and Akt inhibitor in combination.

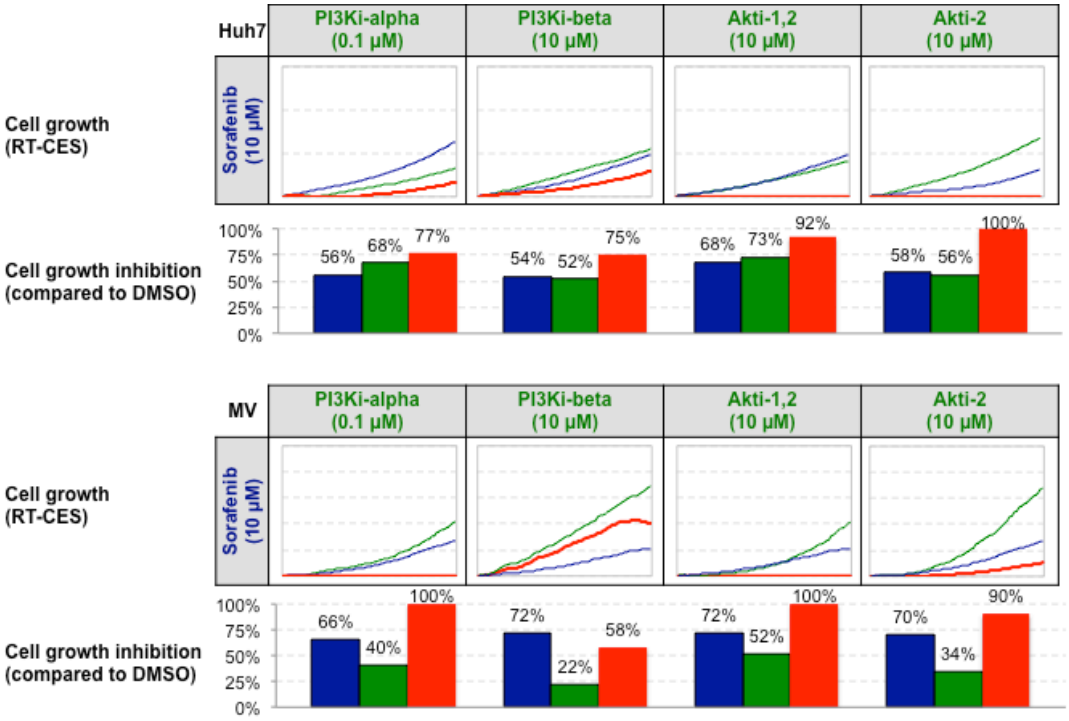

Figure 4.17: Synergistic growth-inhibitory effects of Sorafenib and PI3K/Akt inhibitors. RTCES-based cell growth values (y-axis) were plotted against time (x-axis). Cell growth inhibition was calculated as described in the methods section. Growth of cells treated with Sorafenib is represented in blue and growth of cells treated with other inhibitors is in green. Red plot represents the growth of cells treated with combination of two inhibitors.

4.8.2 Effect of combined therapy on downstream signaling

We showed that enhanced cytotoxicity in combination of Sorafenib with either PI3Ki-α or Akti-2 involves complete inhibition of p-Akt, p-Erk, cyclin D1 and Rb and activation of p21 (Figure 4.18).

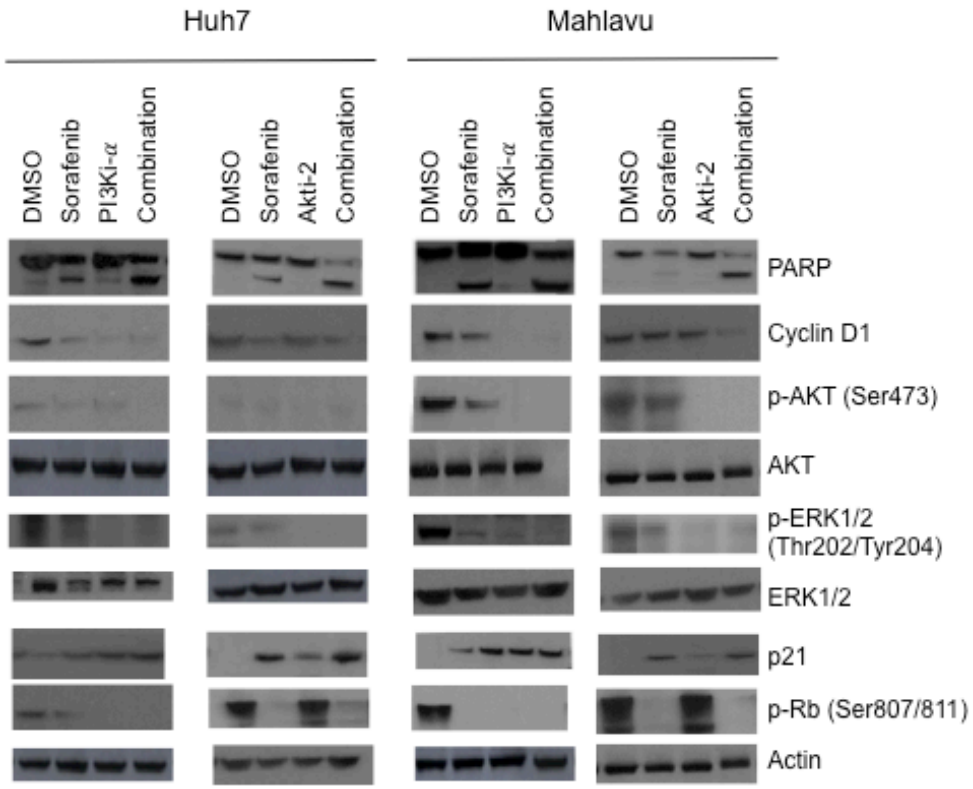

Figure 4.18: Inhibition of cell cycle progression in combined therapies.

4.8.3 Enhanced apoptotic cell death in combinational treatments

Synergistic growth-inhibitory effects of Sorafenib and PI3K/Akt inhibitors were in correlation with apoptotic morphology of cells. Co-treatment of Sorafenib with PI3Ki-α, Akti-1,2 and Akti-2 reduced the number of cells compared to single treatment of Sorafenib and induced apoptosis, as seen by rounded cells detaching from the surface (Figure 4.19).

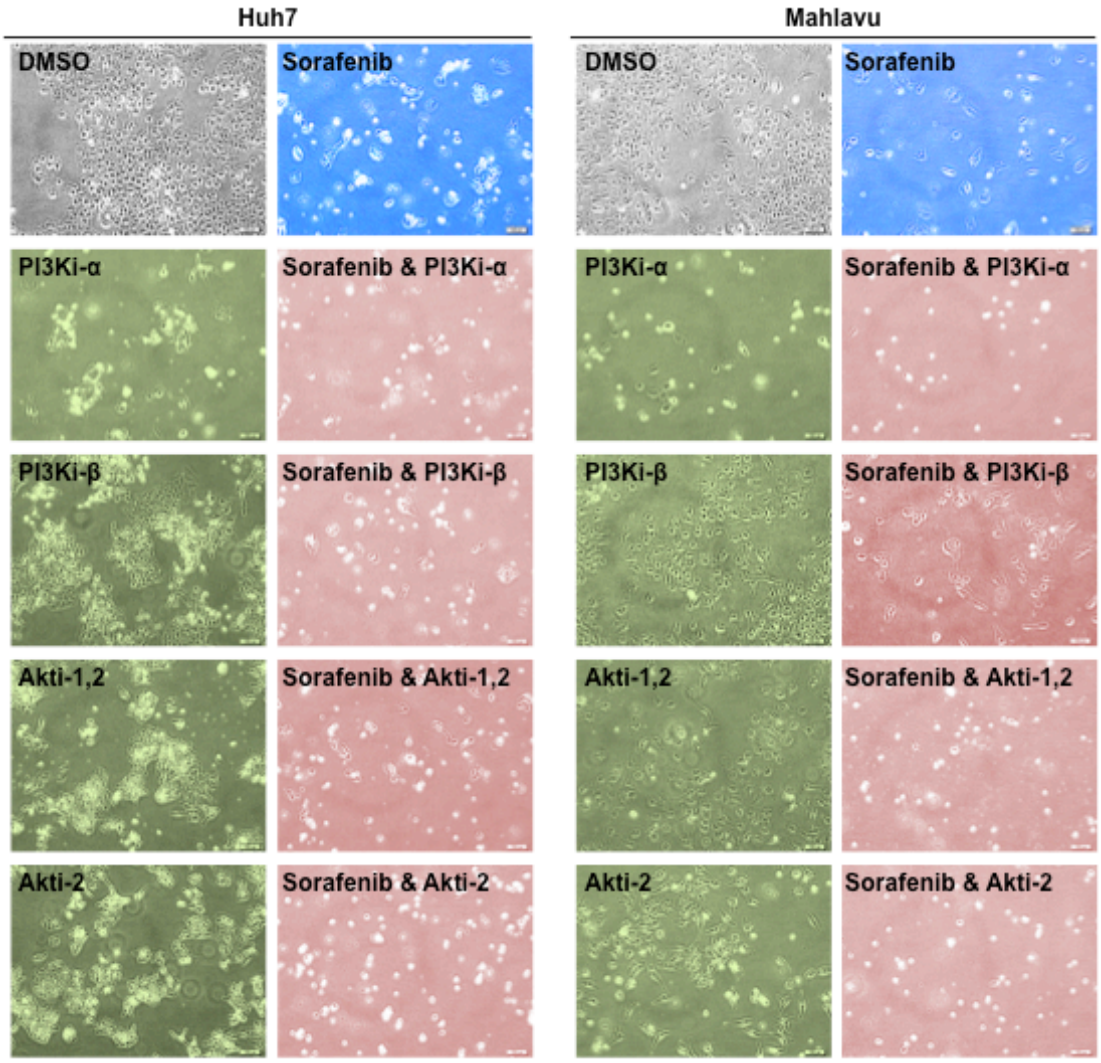

Figure 4.19: Light microscope images of HCC cells co-treated with Sorafenib and PI3K/Akt inhibitors. Images were color-coded for easier interpretation. DMSO controls are in gray. Blue pictures represent Sorafenib treated cells. Green pictures represent cells treated only with PI3K/Akt inhibitors. Images of cells co-treated with Sorafenib and PI3K/Akt inhibitors are in red.

We assessed cell viability with flow cytometric analysis using DNA-intercalating stain propidium iodide. Cells treated with Sorafenib were compared to co-targeted cells. Combination treatments with PI3Ki-α, Akti-1,2 and Akti-2 enhanced apoptotic sub-G1 population compared to single treatment with Sorafenib. Sorafenib/PI3Ki-β combination in Mahlavu showed antagonistic effect as anticipated from the previous RTCES results (Figure 4.20). Isoform-specific Akt inhibitor, Akti-

2, did not induce apoptosis by itself but enhanced pro-apoptotic effect of Sorafenib significantly (from 31% to 100% in Huh7 and from 22% to 87% in Mahlavu).

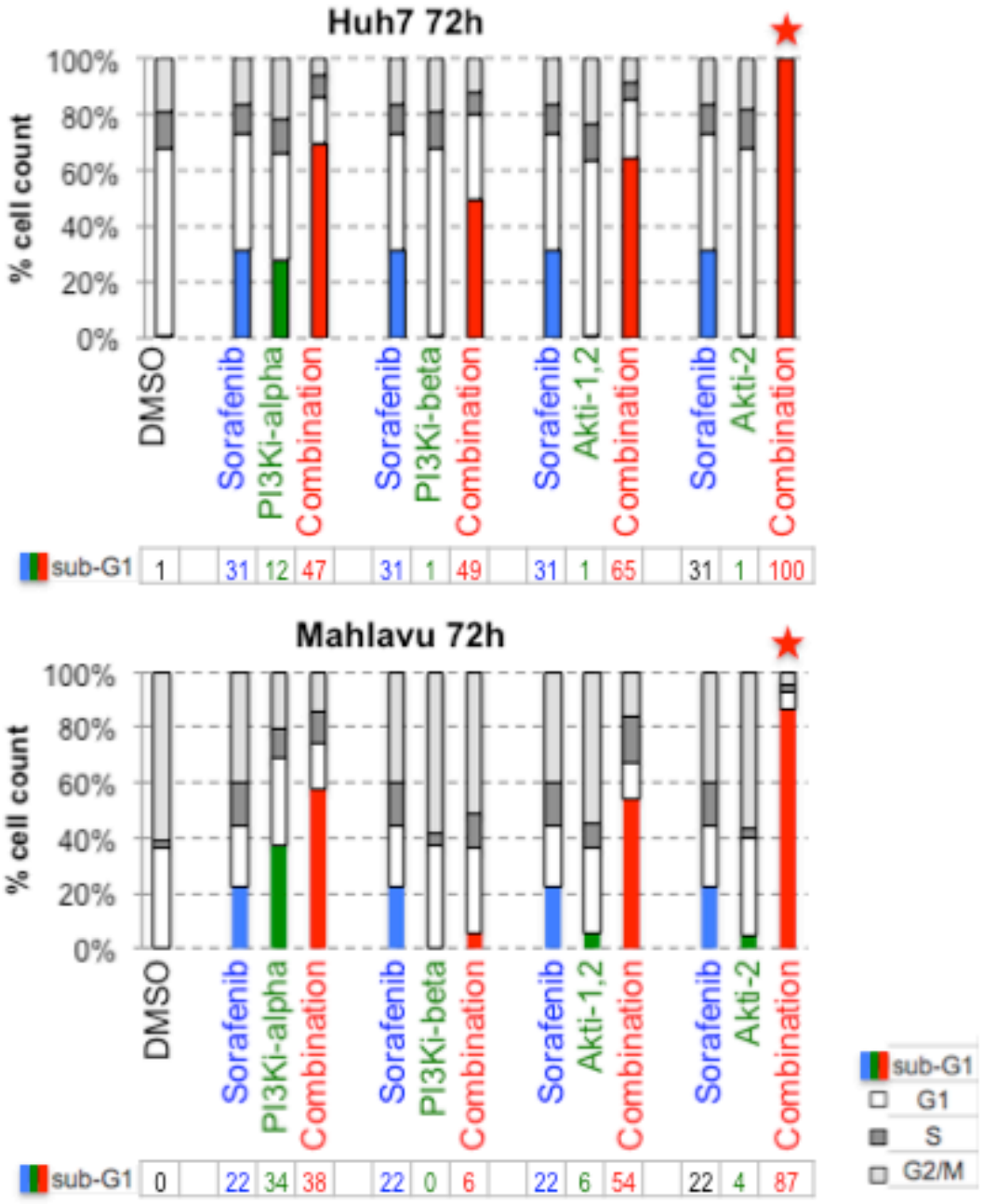

Figure 4.20: Flow Cytometric Analysis of Cellular Viability in cells co-treated with Sorafenib and PI3K/Akt inhibitors. Sub-G1 population represents apoptotic cells.

4.8.4 Synergistic anti-tumor activity of combinational treatments *in vivo*

Our *in vitro* experiments showed that combining Sorafenib with PI3Ki-*α* or Akti-2 synergistically inhibits growth and induces apoptosis in HCC cells as compared to single-agent treatment. While PI3Ki-*α* has cytotoxic activity as single agent at 0.1μM in both cell lines, Akti-2 has no effect as single agent even at 10μM. However, synergistic cytotoxicity induced by combination of Sorafenib with Akti-2 is much more striking. Therefore, we performed *in vivo* xenograft experiments to assess the anti-tumor effects of Sorafenib/Akti-2 combination.

Nude mice inoculated subcutaneously with Mahlavu cells were treated with 30 mg/kg Sorafenib or 7.5 mg/kg Akti-2 or combination of both 5 days a week for 3 weeks. At the end of the 3-week treatment, MRI images were taken and tumors were excised. MRI images showed reduction of tumor size in mice treated with combination compared to Sorafenib alone (Figure 4.21).

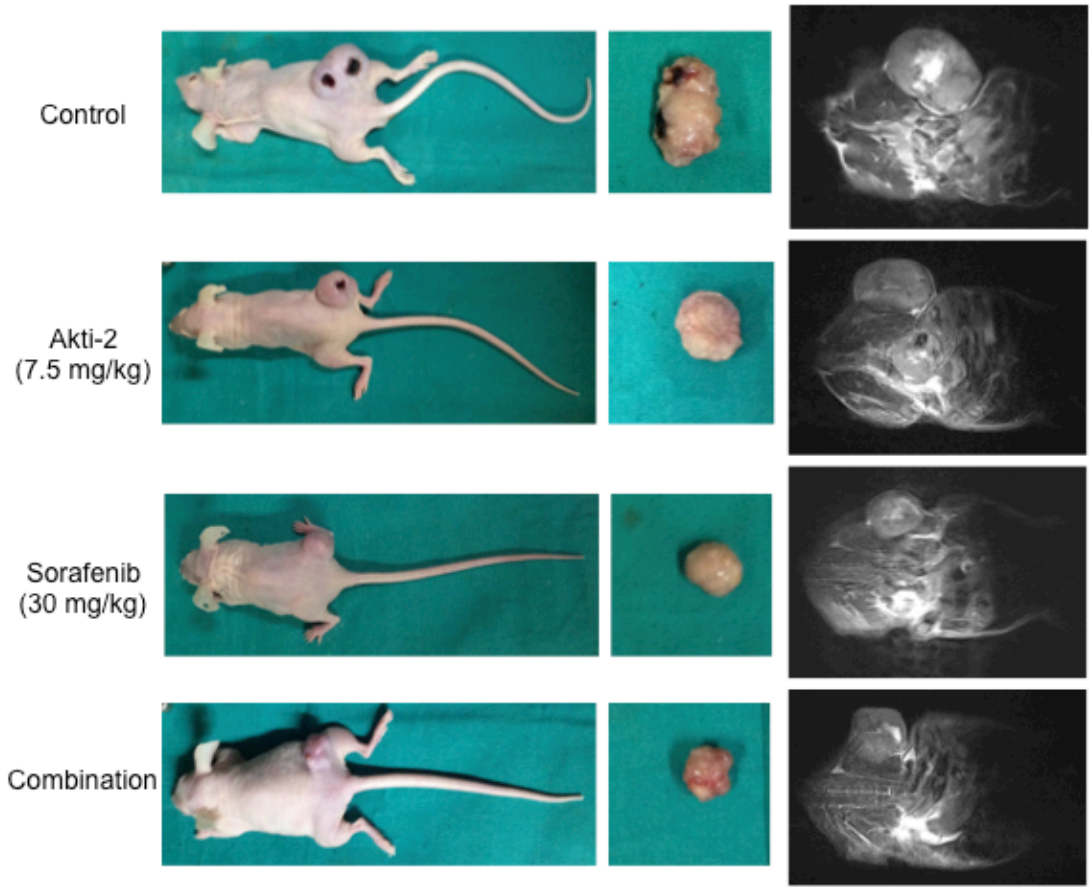

Figure 4.21: Synergistic anti-tumor activity of Sorafenib and Akti-2 *in vivo*. Mahlavu xenograft nude mice were treated with 30 mg/kg Sorafenib or 7.5 mg/kg Akti-2 or combination of both 5 days a week for 3 weeks by oral gavage. At the end of 3-week treatment, MRI images were taken.

Reduction of the tumor size was significant in all treatments compared to control group ($p<0.005$). However, combination of Sorafenib and Akti-2 did not result in significant reduction in tumor volume compared to Sorafenib as single agent (Figure 4.22). Large tumors in combination-treated mice became softer than tumors of Sorafenib-treated mice after 1 weeks of treatment, suggesting presence of necrosis-induced inflammation and swelling. After 2 weeks of treatment, 2 out of 5 mice developed large visible intra-tumoral necrotic areas (Figure 4.23).

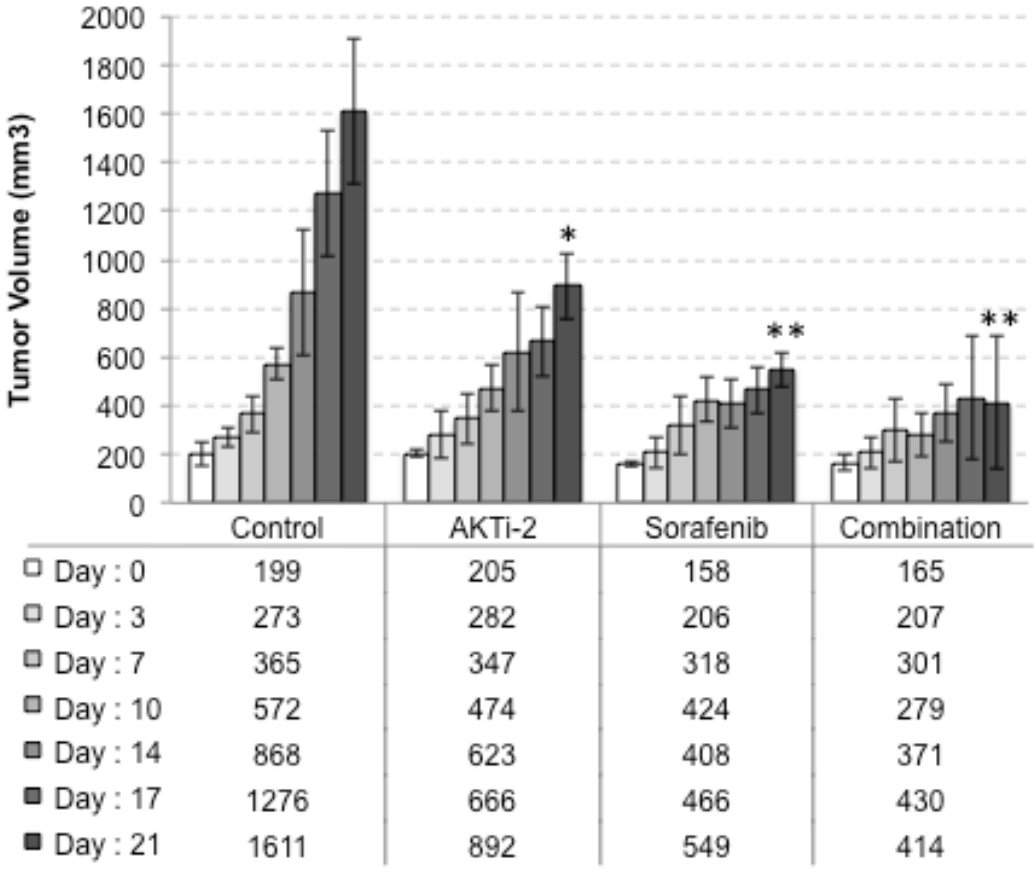

	Control	AKTi-2	Sorafenib	Combination
Day : 0	199	205	158	165
Day : 3	273	282	206	207
Day : 7	365	347	318	301
Day : 10	572	474	424	279
Day : 14	868	623	408	371
Day : 17	1276	666	466	430
Day : 21	1611	892	549	414

Figure 4.22: Reduced tumor size in mice treated with Sorafenib and Akti-2. Mahlavu xenograft nude mice were treated with 30 mg/kg Sorafenib or 7.5 mg/kg Akti-2 or combination of both 5 days a week for 3 weeks by oral gavage. Reduction of tumor size was significant in all treatments compared to control group (*: $p<0.005$, **: $p<0.001$).

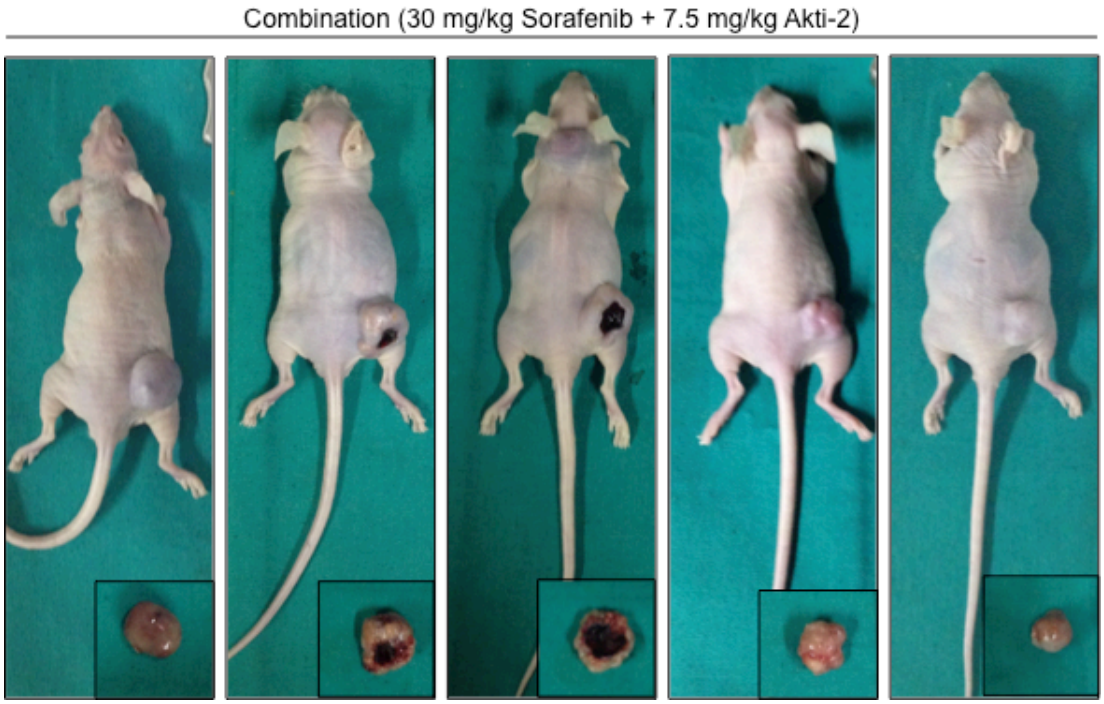

Figure 4.23: Temporary increase in tumor size associated with intra-tumoral necrosis in combination-treated mice. Mahlavu xenograft nude mice were treated with 30 mg/kg Sorafenib and 7.5 mg/kg Akti-2 for 3 weeks.

In HCC patients, anti-angiogenic effect of Sorafenib is characterized by intra-tumoral necrosis and a temporary, but substantial, increase in tumor size (Horger et al., 2009). Studies in HCC xenograft models showed that Sorafenib causes growth inhibition at 30 mg/kg and partial tumor regressions at 100 mg/kg (Liu, Ho, Chen, & Lai, 2012; Liu et al., 2006). Since Sorafenib is a multi-kinase inhibitor with systemic side effects, we addressed whether low dose (30 mg/kg) Sorafenib can establish higher anti-tumor efficacy when combined with a specific inhibitor, Akti-2. Single treatment with Sorafenib initiated intra-tumoral necrosis in 1 out of 5 mice 3 weeks post-treatment, while combination treatment resulted in substantial tumor necrosis and reduced tumor density (Figure 4.24). Enhanced anti-angiogenic effects of combination therapy promoted tumor necrosis and reduced tumor mass significantly (Sorafenib: 85% reduction, Combination: 93% reduction, $p<0.001$) (Figure 4.25).

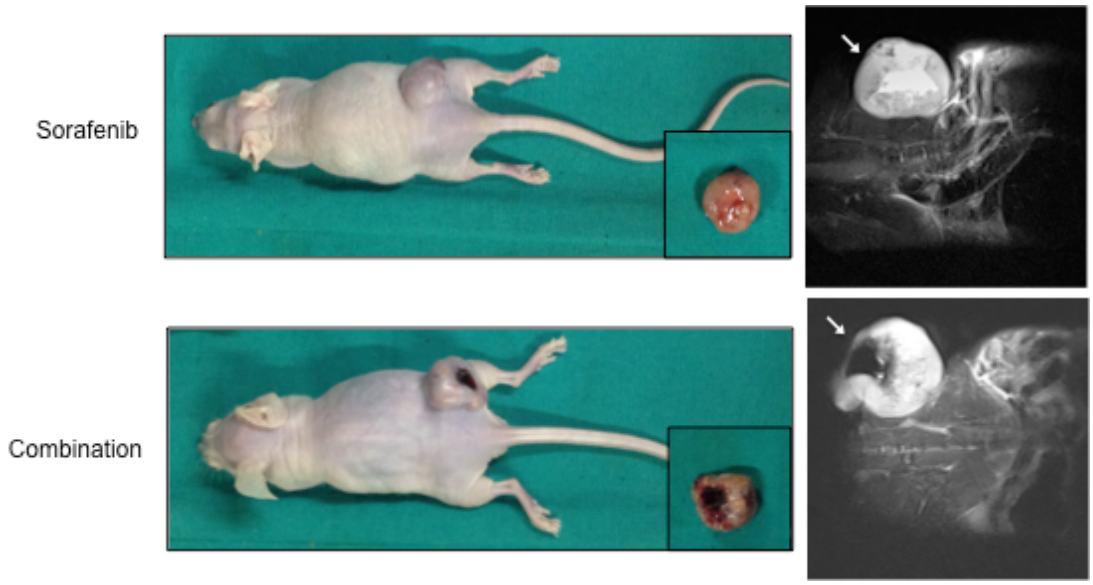

Figure 4.24: Enhanced anti-angiogenic effects of combination therapy supporting tumor necrosis. Mahlavu xenograft nude mice were treated with 30 mg/kg Sorafenib and 7.5 mg/kg Akti-2 for 3 weeks.

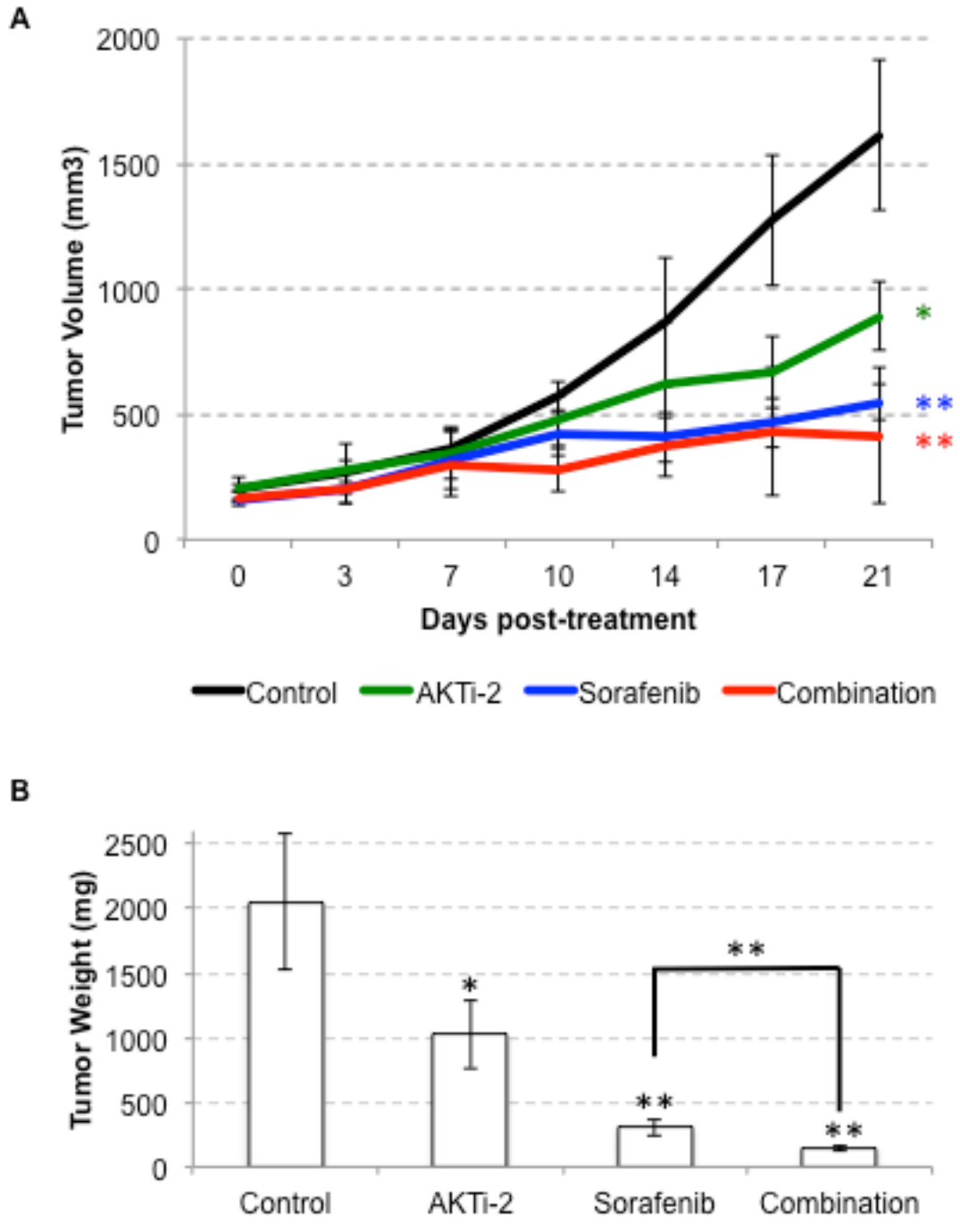

Figure 4.25: Reduced tumor mass in mice treated with Sorafenib and Akti-2. Mahlavu xenograft nude mice were treated with 30 mg/kg Sorafenib or 7.5 mg/kg Akti-2 or combination of both 5 days a week for 3 weeks by oral gavage. A) Line-graph representation of tumor growth. B) Bar-graph representation of tumor weight. (*: $p<0.005$, **: $p\leq0.001$)

4.9. Identification of optimal reference genes for microarray normalization

We performed microarray experiments to reveal transcriptome level alterations in HCC cells in response to drug treatment. The basic, yet the most critical requirement of microarray analysis and all other platforms that process omics data is selection of reference genes in order to ensure reliable and statistically accurate comparison of samples. Housekeeping genes are constitutively expressed in all cells in all conditions and are involved in the maintenance of basal cellular functions such as metabolism, gene expression, protein synthesis and cell signaling (Hsiao et al., 2001; Warrington, Nair, Mahadevappa, & Tsyganskaya, 2000). Hence, they are presumed to have steady expression levels unaffected by tissue type or experimental condition and therefore have been used as reference genes for normalization of transcriptome data. However, even the most commonly used reference genes (ACTB, GAPDH, TBP) are differentially expressed in different pathological stages of HCC (Gao et al., 2008; Waxman & Wurmbach, 2007). Moreover, GAPDH and ACTB are direct targets of miR-644a and have several pseudogenes, making them less reliable to be used as reference genes (Sikand, Singh, Ebron, & Shukla, 2012; Stark, Brennecke, Bushati, Russell, & Cohen, 2005; Sun, Li, Luo, & Liao, 2012). Therefore, first step in the analysis of transcriptome data should be selection of the most suitable reference genes. In order to confirm the reliability of available housekeeping gene sets and to determine a global list of constitutively and invariably expressed genes that can be used as reference genes in HCC, we analyzed expression patterns of 9090 microarray samples grouped into 381 NCBI-GEO datasets. We identified novel reference genes based on their coefficient of variation and percentage of occurrence in all GEO datasets using Receiver Operating Characteristic (ROC) curves and classified them based on Medical Subject Headings (MeSH) associated with the transcriptome study that was published and indexed by the National Library of Medicine.

Expressions of 17 genes (AARS, ACTB, CFL1, EEF2, GAPDH, GSTO1, H2AFZ, HBXIP, RPL30, RPL41, RPL7, RPN2, RPS10, RPS17, RPS3A, SOD1, TPT1), which were most commonly observed in gene sets associated with various MeSH categories, were compared in 8 HCC cell lines (HepG2, FOCUS, Mahlavu, Hep3B, Hep3B-TR, Huh7, SkHep1, and PLC) by RT-qPCR. Coefficient of Variation (CV) of each gene was calculated as the ratio of standard deviation to the

mean relative expression. geNorm and NormFinder software were used for stability analysis (Table 4.5). GeNorm calculates an expression stability value for each gene based on the average pairwise variation between all tested genes. The genes are ranked according to their expression stability through stepwise exclusion of the least stable gene (Vandesompele et al., 2002). NormFinder ranks the candidate reference genes with minimal estimated intra- and inter-group variation and calculates an expression stability value for each gene (Andersen, Jensen, & Ørntoft, 2004). The selected reference genes were ranked according to their CV determined by qPCR and stability measures determined by geNorm and NormFinder (Table 4.6, Figure 4.26). Ribosomal genes are the optimal reference genes for normalization of HCC cell lines.

Table 4.5: Stability values of reference genes calculated by NormFinder and geNorm. Genes with the lowest values are the most stable genes.

	NormFinder	**geNorm**
RPS10	0.19	0.00
RPL41	0.29	0.00
RPL7	0.19	0.22
RPS17	0.19	0.27
RPS3A	0.23	0.30
RPL30	0.11	0.31
GAPDH	0.25	0.38
CFL1	0.29	0.42
HBXIP	0.29	0.45
H2AFZ	0.33	0.48
ACTB	0.43	0.50
EEF2	0.38	0.53
AARS	0.60	0.58
SOD1	0.75	0.65
TPT1	0.72	0.72
RPN2	0.78	0.79
GSTO1	1.17	0.91

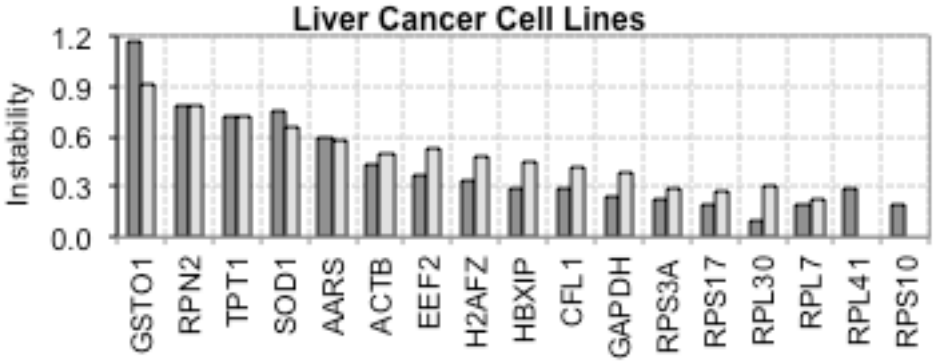

Figure 4.26: Stability of reference genes in HCC cell lines. NormFinder and geNorm results were represented in dark gray and light gray respectively.

Table 4.6: Stability order of reference genes based on CV, NormFinder and geNorm analysis. Genes are sorted from the most stable to the least stable.

CV	NormFinder	geNorm
RPL7	RPL30	RPL41
RPS17	RPL7	RPS10
RPL30	RPS17	RPL7
CFL1	RPS10	RPS17
EEF2	RPS3A	RPS3A
GAPDH	GAPDH	RPL30
RPS10	CFL1	GAPDH
RPS3A	HBXIP	CFL1
H2AFZ	RPL41	HBXIP
RPL41	H2AFZ	H2AFZ
ACTB	EEF2	ACTB
HBXIP	ACTB	EEF2
AARS	AARS	AARS
TPT1	TPT1	SOD1
RPN2	SOD1	TPT1
SOD1	RPN2	RPN2
GSTO1	GSTO1	GSTO1

4.10 Large-scale gene expression analysis of classic PI3K/AKT pathway inhibitors

In order to identify the effect of kinase inhibitors at the gene expression level, we performed microarray experiments. Initially we analyzed the effect of classic PI3K/AKT/mTOR inhibitors, LY294002, Wortmannin, Akti-1,2 and Rapamycin on gene expression in Huh7 and Mahlavu cells. Most differentially expressed top 100 genes ($p < 0.05$, fold-change ≥ 2) in response to treatment with LY294002, Wortmannin and Rapamycin for 48 hours were similar in cells, while Akti-1,2 treatment led to a different gene expression profile (Figure 4.27). All treatments lead to alterations in genes associated with metabolic processed in Huh7. LY294002 regulates chromatin assembly and nucleosome organization in both cell lines. LY294002, Wortmannin and Rapamycin promote expression of pro-apoptotic genes in Mahlavu cell line. Wortmannin and Rapamycin also regulate genes involved in cell cycle in Mahlavu. Additionally, Wortmannin regulates development, angiogenesis, migration and immune response in Mahlavu cells. Akti-1,2, on the other hand, regulates migration in Huh7 and is associated mostly with anti-apoptotic processes in Mahlavu (Tables 4.7 and 4.8).

Although *in vitro* experiments showed that inhibiting the PI3K/AKT/mTOR pathway with LY294002, Wortmannin, Akti-1,2 and Rapamycin is cytotoxic in HCC cells, transcriptome-level gene expression changes in inhibitor treated cells compared to untreated cells were not more than 1.5 fold ($\log2(\text{fold change}) \leq 1.5$). Therefore, we implemented a signal transduction score-flow algorithm that uses transcriptome data to imitate protein-level signal flow inside cells and assigns a quantitative score for each gene in the interactome networks gathered from KEGG database as described in the methods section (Isik et al., 2012). Network-level signaling analysis showed that kinase inhibitors targeting PI3K/AKT/mTOR pathway regulate cell cycle, apoptosis, migration, angiogenesis and DNA repair processes, through differential regulation of downstream effectors (Figures 4.28 – 4.31).

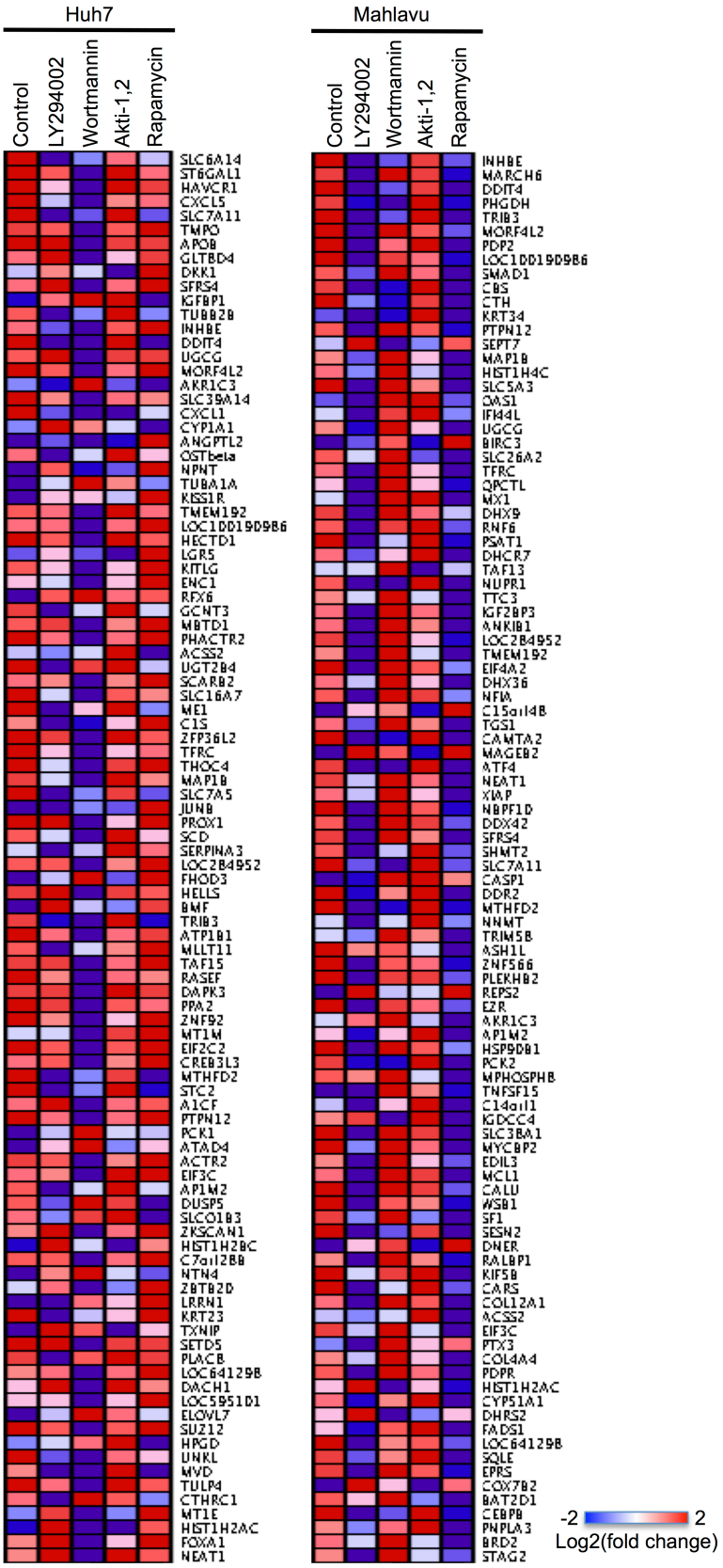

Figure 4.27: Heatmap representation of top 100 differentially expressed genes.

Table 4.7: Biological processes associated with top 100 differentially expressed genes in Huh7 cells (enriched with p<0.05)

Treatment	GO ID	GO Term
LY294002	GO:0006334	nucleosome assembly
	GO:0031497	chromatin assembly
	GO:0065004	protein-DNA complex assembly
	GO:0034728	nucleosome organization
	GO:0006323	DNA packaging
	GO:0006333	chromatin assembly or disassembly
	GO:0034622	cellular macromolecular complex assembly
	GO:0045661	regulation of myoblast differentiation
	GO:0034621	cellular macromolecular complex subunit organization
	GO:0008203	cholesterol metabolic process
Wortmannin	GO:0043434	response to peptide hormone stimulus
	GO:0007398	ectoderm development
	GO:0042493	response to drug
	GO:0015838	betaine transport
	GO:0015879	carnitine transport
	GO:0000050	urea cycle
	GO:0019627	urea metabolic process
Akti-1,2	GO:0016125	sterol metabolic process
	GO:0019318	hexose metabolic process
	GO:0008202	steroid metabolic process
	GO:0033555	multicellular organismal response to stress
	GO:0005996	monosaccharide metabolic process

	GO:0006952	defense response
	GO:0006006	glucose metabolic process
	GO:0009611	response to wounding
Rapamycin	GO:0042493	response to drug
	GO:0016125	sterol metabolic process
	GO:0015838	betaine transport
	GO:0015879	carnitine transport
	GO:0008203	cholesterol metabolic process
	GO:0015697	quaternary ammonium group transport
	GO:0008202	steroid metabolic process
	GO:0051181	cofactor transport
	GO:0015695	organic cation transport
	GO:0051180	vitamin transport
	GO:0006694	steroid biosynthetic process
	GO:0016126	sterol biosynthetic process

Table 4.8: Biological processes associated with top 100 differentially expressed genes in Mahlavu cells (enriched with p<0.05)

Treatment	GO ID	GO Term
LY294002	GO:0034621	cellular macromolecular complex subunit organization
	GO:0034728	nucleosome organization
	GO:0034622	cellular macromolecular complex assembly
	GO:0030203	glycosaminoglycan metabolic process
	GO:0042981	regulation of apoptosis

	GO:0043067	regulation of programmed cell death
	GO:0010941	regulation of cell death
	GO:0006022	aminoglycan metabolic process
	GO:0043933	macromolecular complex subunit organization
	GO:0030212	hyaluronan metabolic process
Wortmannin	GO:0001525	angiogenesis
	GO:0001944	vasculature development
	GO:0042981	regulation of apoptosis
	GO:0051094	positive regulation of developmental process
	GO:0043067	regulation of programmed cell death
	GO:0010941	regulation of cell death
	GO:0032570	response to progesterone stimulus
	GO:0048514	blood vessel morphogenesis
	GO:0043525	positive regulation of neuron apoptosis
	GO:0001568	blood vessel development
	GO:0048641	regulation of skeletal muscle tissue development
	GO:0022402	cell cycle process
	GO:0006955	immune response
	GO:0008219	cell death
	GO:0010033	response to organic substance
	GO:0016265	death
	GO:0040017	positive regulation of locomotion
	GO:0002520	immune system development
	GO:0051329	interphase of mitotic cell cycle
	GO:0007050	cell cycle arrest

	GO:0051325	interphase
	GO:0007049	cell cycle
	GO:0016202	regulation of striated muscle tissue development
	GO:0048634	regulation of muscle development
	GO:0051726	regulation of cell cycle
	GO:0045597	positive regulation of cell differentiation
	GO:0000082	G1/S transition of mitotic cell cycle
	GO:0045785	positive regulation of cell adhesion
	GO:0007179	transforming growth factor beta receptor signaling pathway
	GO:0043066	negative regulation of apoptosis
	GO:0007184	SMAD protein nuclear translocation
	GO:0032026	response to magnesium ion
	GO:0051240	positive regulation of multicellular organismal process
	GO:0006915	apoptosis
	GO:0043069	negative regulation of programmed cell death
	GO:0060548	negative regulation of cell death
	GO:0008285	negative regulation of cell proliferation
	GO:0045765	regulation of angiogenesis
	GO:0012501	programmed cell death
	GO:0043536	positive regulation of blood vessel endothelial cell migration
	GO:0009725	response to hormone stimulus
	GO:0000278	mitotic cell cycle
Akti-1,2	GO:0042981	regulation of apoptosis
	GO:0043067	regulation of programmed cell death
	GO:0010941	regulation of cell death

	GO:0006916	anti-apoptosis
	GO:0043066	negative regulation of apoptosis
	GO:0043069	negative regulation of programmed cell death
	GO:0060548	negative regulation of cell death
	GO:0032355	response to estradiol stimulus
	GO:0010639	negative regulation of organelle organization
Rapamycin	GO:0007049	cell cycle
	GO:0042981	regulation of apoptosis
	GO:0043067	regulation of programmed cell death
	GO:0010941	regulation of cell death
	GO:0043632	modification-dependent macromolecule catabolic process
	GO:0019941	modification-dependent protein catabolic process
	GO:0051603	proteolysis involved in cellular protein catabolic process
	GO:0044257	cellular protein catabolic process
	GO:0030163	protein catabolic process
	GO:0006508	proteolysis
	GO:0070271	protein complex biogenesis
	GO:0006461	protein complex assembly

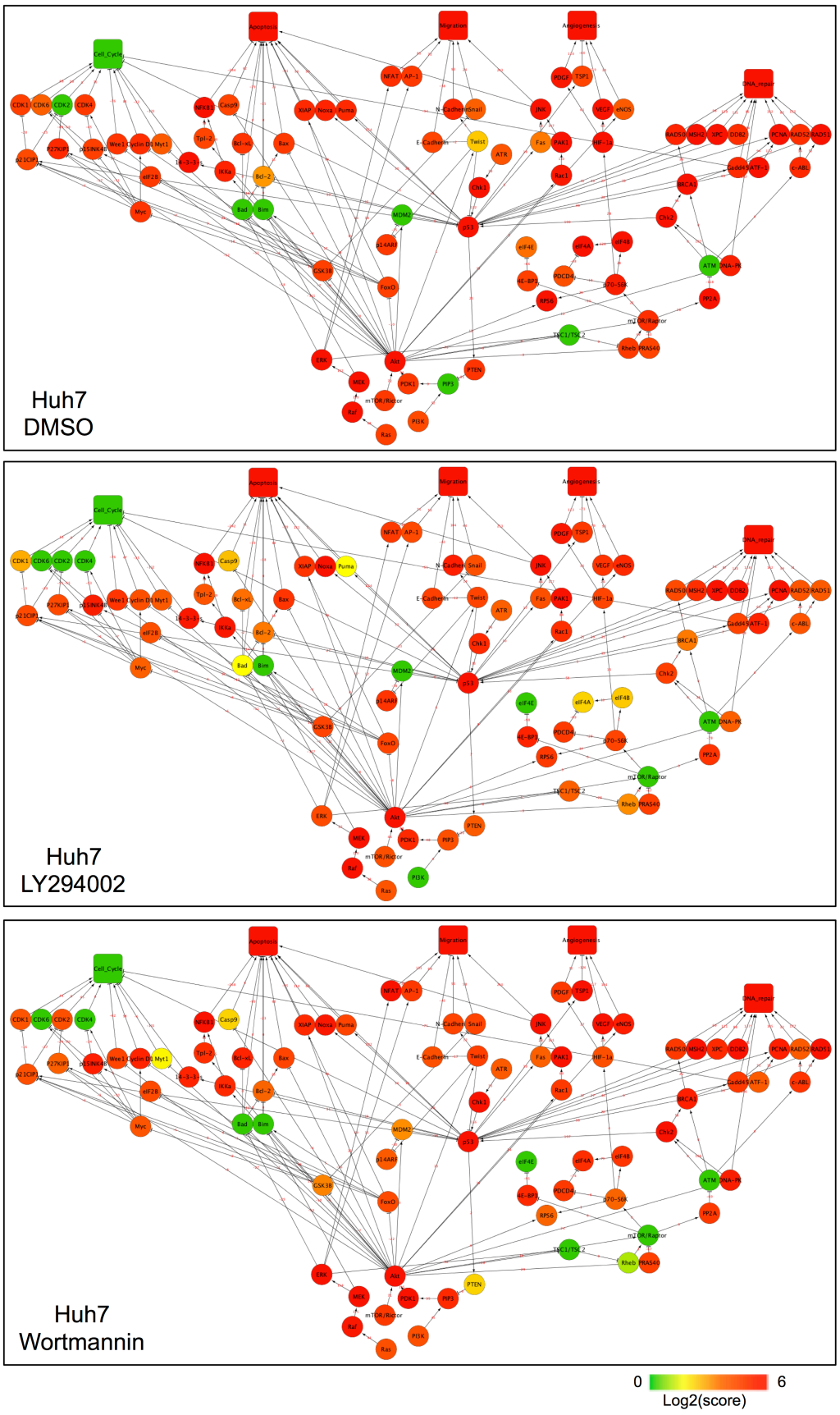

Figure 4.28: Cytoscape representation of differential regulation of PI3K/Akt pathway in Huh7 cells treated with LY294002 and Wortmannin.

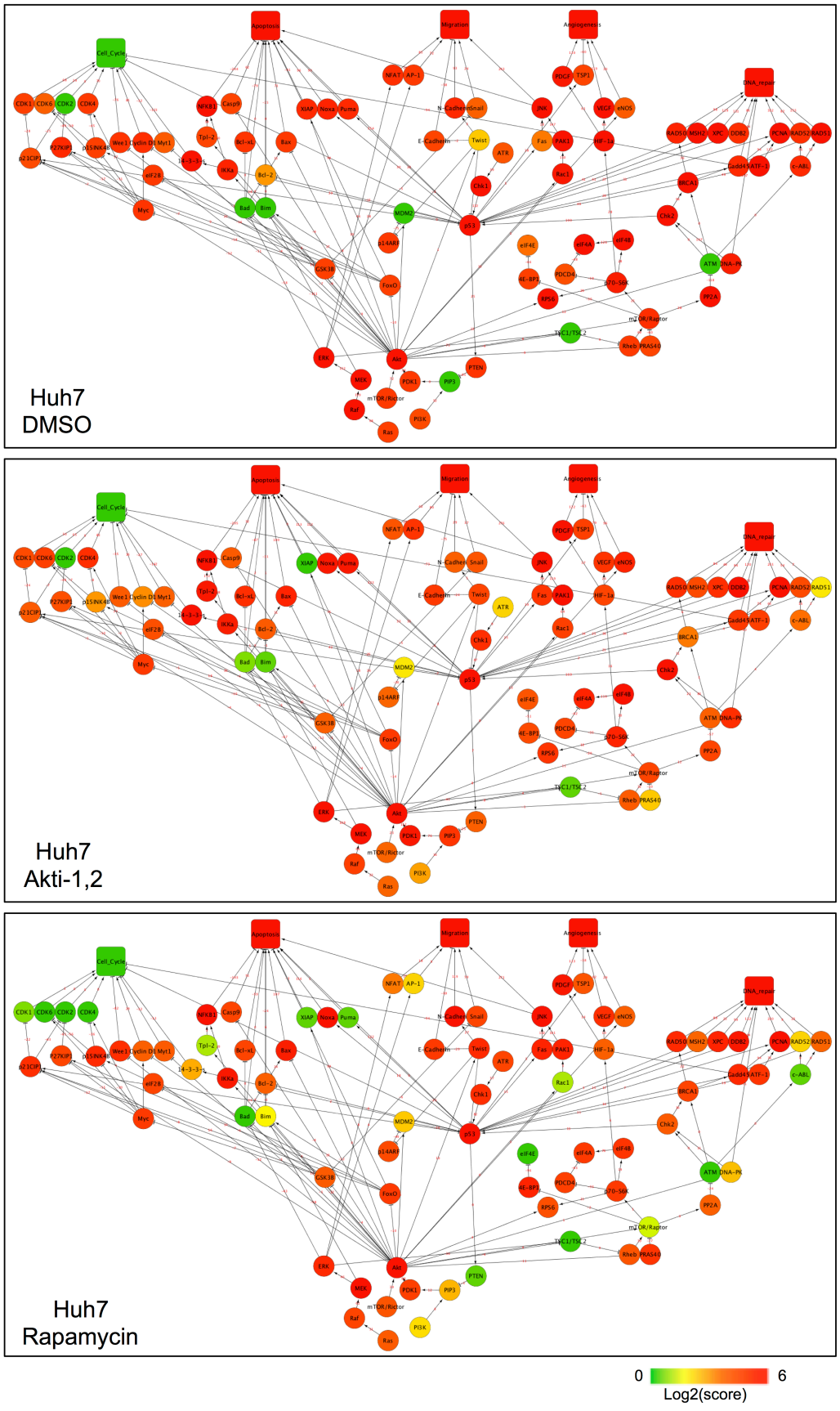

Figure 4.29: Cytoscape representation of differential regulation of PI3K/Akt pathway in Huh7 cells treated with Akti-1,2 and Rapamycin.

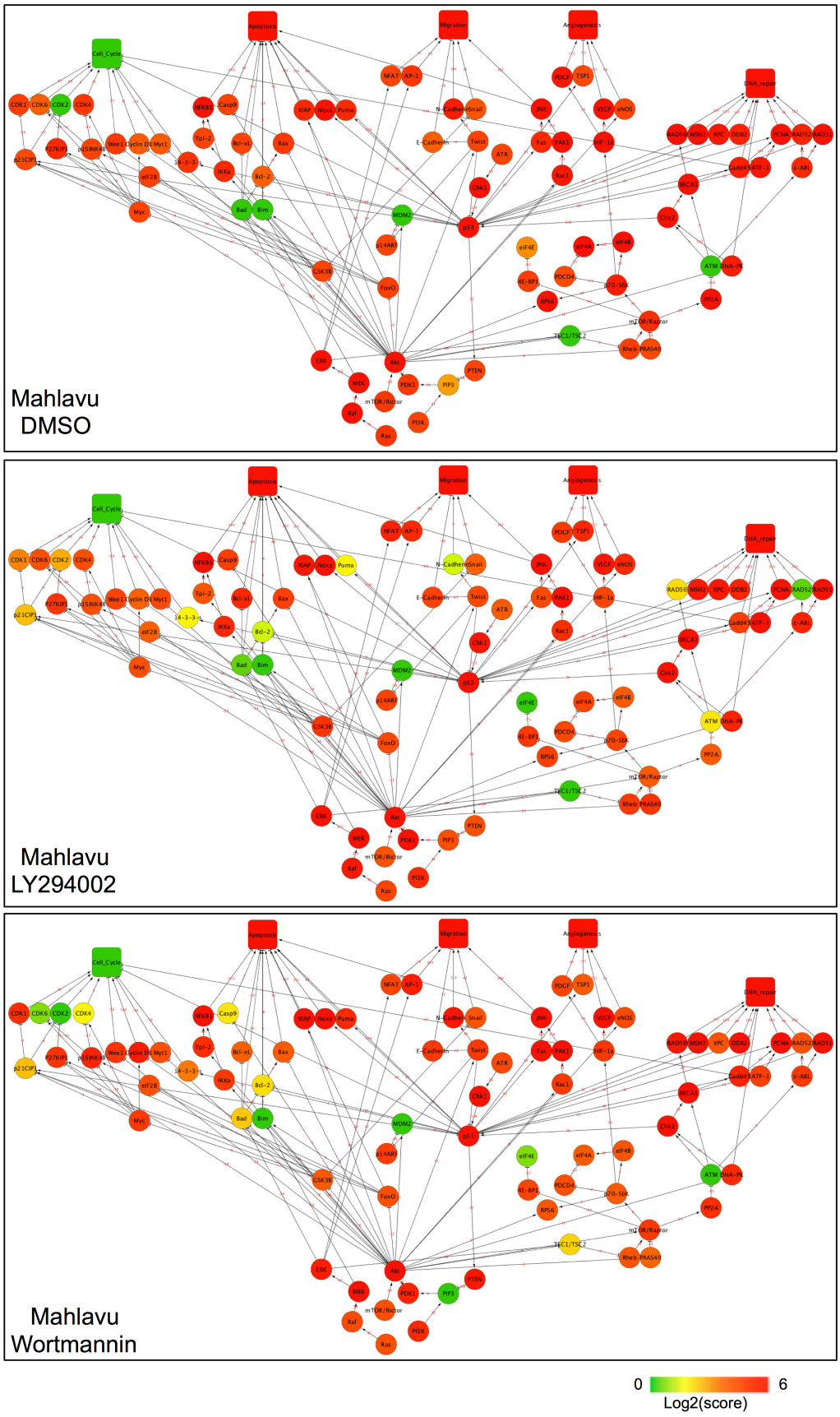

Figure 4.30: Cytoscape representation of differential regulation of PI3K/Akt pathway in Mahlavu cells treated with LY294002 and Wortmannin.

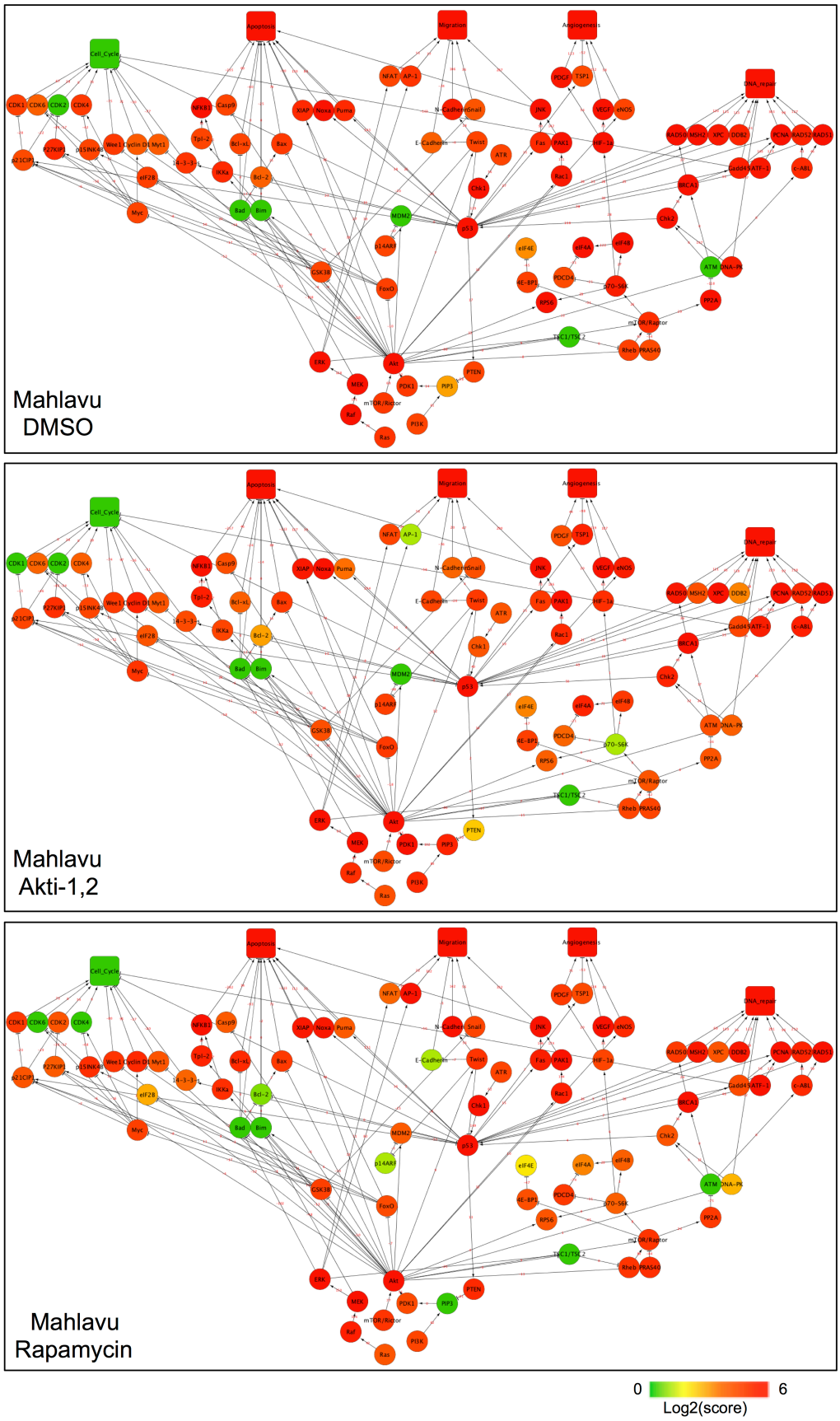

Figure 4.31: Cytoscape representation of differential regulation of PI3K/Akt pathway in Mahlavu cells treated with Akti-1,2 and Rapamycin.

4.11 Large-scale gene expression analysis of cells co-treated with Sorafenib and PI3K/AKT pathway inhibitors

We addressed transcriptome level alterations in HCC cells upon treatment with Sorafenib and PI3Ki-α as single agents or co-treatment with both inhibitors. Differentially expressed genes ($p < 0.01$, fold-change > 2) in response to treatment with Sorafenib, PI3Ki-α and combination for 48 hours revealed common and inhibitor-specific targets (Figure 4.32). Microarray experiments further identified genes that are uniquely targeted in cells receiving combination treatment. Biological processes enriched in treated cells (Tables 4.9, 4.10), molecular functions of differentially expressed genes involved in these processes (Tables 4.11, 4.12), and their contribution to pathways in KEGG database (Tables 4.13, 4.14) were analyzed with DAVID and GSEA (gene set enrichment analysis).

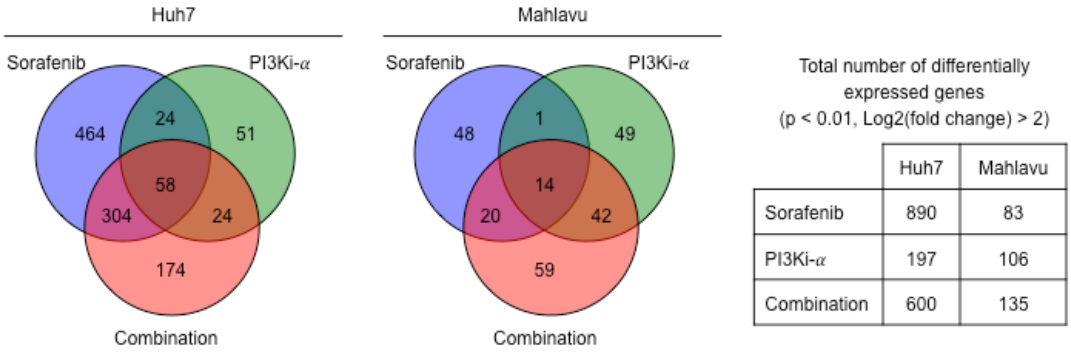

Total number of differentially expressed genes ($p < 0.01$, Log2(fold change) > 2)

	Huh7	Mahlavu
Sorafenib	890	83
PI3Ki-α	197	106
Combination	600	135

Figure 4.32: Venn diagram showing differentially expressed genes in HCC cells upon treatment with Sorafenib and PI3Ki-α as single agents or co-treatment with both inhibitors.

Table 4.9: Biological processes affected in treated Huh7 cells (p<0.01)

	GO ID	GO Term
Sorafenib	GO:0007584	response to nutrient
	GO:0010033	response to organic substance
	GO:0033273	response to vitamin
	GO:0016125	sterol metabolic process
	GO:0008203	cholesterol metabolic process
	GO:0032526	response to retinoic acid
	GO:0033189	response to vitamin A
	GO:0010038	response to metal ion
	GO:0008202	steroid metabolic process
	GO:0010035	response to inorganic substance
	GO:0031667	response to nutrient levels
	GO:0009891	positive regulation of biosynthetic process
	GO:0010560	positive regulation of glycoprotein biosynthetic process
	GO:0031328	positive regulation of cellular biosynthetic process
	GO:0009991	response to extracellular stimulus
	GO:0016126	sterol biosynthetic process
	GO:0009611	response to wounding
	GO:0009719	response to endogenous stimulus
	GO:0010876	lipid localization
	GO:0006869	lipid transport
	GO:0010557	positive regulation of macromolecule biosynthetic process
	GO:0001568	blood vessel development
	GO:0045935	positive regulation of nucleobase, nucleoside, nucleotide and nucleic acid metabolic process

	GO:0051173	positive regulation of nitrogen compound metabolic process
	GO:0015718	monocarboxylic acid transport
	GO:0033554	cellular response to stress
	GO:0001944	vasculature development
	GO:0042127	regulation of cell proliferation
	GO:0030522	intracellular receptor-mediated signaling pathway
	GO:0042921	glucocorticoid receptor signaling pathway
	GO:0051291	protein heterooligomerization
	GO:0009725	response to hormone stimulus
	GO:0007242	intracellular signaling cascade
	GO:0051592	response to calcium ion
	GO:0008283	cell proliferation
	GO:0031958	corticosteroid receptor signaling pathway
	GO:0042692	muscle cell differentiation
	GO:0043062	extracellular structure organization
	GO:0031175	neuron projection development
	GO:0006695	cholesterol biosynthetic process
	GO:0008610	lipid biosynthetic process
	GO:0009636	response to toxin
	GO:0070271	protein complex biogenesis
	GO:0006461	protein complex assembly
	GO:0043933	macromolecular complex subunit organization
PI3Ki-*α*	GO:0015031	protein transport
	GO:0045184	establishment of protein localization
	GO:0008104	protein localization
	GO:0044271	nitrogen compound biosynthetic process

Combination	GO:0001568	blood vessel development
	GO:0001944	vasculature development
	GO:0048514	blood vessel morphogenesis
	GO:0046907	intracellular transport
	GO:0001525	angiogenesis
	GO:0051270	regulation of cell motion
	GO:0009101	glycoprotein biosynthetic process
	GO:0016192	vesicle-mediated transport
	GO:0009611	response to wounding
	GO:0042551	neuron maturation
	GO:0009100	glycoprotein metabolic process
	GO:0042127	regulation of cell proliferation
	GO:0030334	regulation of cell migration
	GO:0042312	regulation of vasodilation
	GO:0040012	regulation of locomotion
	GO:0016125	sterol metabolic process
	GO:0034383	low-density lipoprotein particle clearance
	GO:0043062	extracellular structure organization
	GO:0010557	positive regulation of macromolecule biosynthetic process
	GO:0010604	positive regulation of macromolecule metabolic process
	GO:0008284	positive regulation of cell proliferation
	GO:0070085	glycosylation
	GO:0043413	biopolymer glycosylation
	GO:0006486	protein amino acid glycosylation
	GO:0031328	positive regulation of cellular biosynthetic process
	GO:0048878	chemical homeostasis

	GO:0016322	neuron remodeling
	GO:0008203	cholesterol metabolic process

Table 4.10: Biological processes affected in treated Mahlavu cells (p<0.01)

	GO ID	GO Term
Sorafenib	GO:0006952	defense response
	GO:0009611	response to wounding
	GO:0006954	inflammatory response
	GO:0009620	response to fungus
PI3Ki-α	GO:0051789	response to protein stimulus
	GO:0010604	positive regulation of macromolecule metabolic process
	GO:0045893	positive regulation of transcription, DNA-dependent
	GO:0051254	positive regulation of RNA metabolic process
	GO:0006357	regulation of transcription from RNA polymerase II promoter
	GO:0045935	positive regulation of nucleobase, nucleoside, nucleotide and nucleic acid metabolic process
	GO:0051173	positive regulation of nitrogen compound metabolic process
	GO:0031328	positive regulation of cellular biosynthetic process
	GO:0045941	positive regulation of transcription
	GO:0009891	positive regulation of biosynthetic process
	GO:0010628	positive regulation of gene expression
Combination	GO:0006888	ER to Golgi vesicle-mediated transport

Table 4.11: Molecular functions of differentially expressed genes in treated Huh7 cells (p<0.01)

	GO ID	GO Term
Sorafenib	GO:0046870	cadmium ion binding
	GO:0046914	transition metal ion binding
	GO:0046872	metal ion binding
	GO:0043169	cation binding
	GO:0043167	ion binding
	GO:0008270	zinc ion binding
	GO:0005507	copper ion binding
	GO:0016717	oxidoreductase activity
	GO:0004620	phospholipase activity
	GO:0005543	phospholipid binding
	GO:0019899	enzyme binding
	GO:0003712	transcription cofactor activity
	GO:0008289	lipid binding
	GO:0005545	phosphatidylinositol binding
	GO:0004768	stearoyl-CoA 9-desaturase activity
	GO:0001786	phosphatidylserine binding
PI3Ki-α	GO:0019904	protein domain specific binding
	GO:0032559	adenyl ribonucleotide binding
	GO:0030554	adenyl nucleotide binding
	GO:0019207	kinase regulator activity
	GO:0001883	purine nucleoside binding
	GO:0000166	nucleotide binding
	GO:0001882	nucleoside binding

	GO:0005524	ATP binding
	GO:0032553	ribonucleotide binding
	GO:0032555	purine ribonucleotide binding
	GO:0017076	purine nucleotide binding
	GO:0042623	ATPase activity, coupled
	GO:0016887	ATPase activity
	GO:0019887	protein kinase regulator activity
Combination	GO:0046870	cadmium ion binding
	GO:0005507	copper ion binding
	GO:0008375	acetylglucosaminyltransferase activity

Table 4.12: Molecular functions of differentially expressed genes in treated Mahlavu cells (p<0.01)

	GO ID	**GO Term**
Sorafenib	-	-
PI3Ki-α	-	-
Combination	GO:0003723	RNA binding

Table 4.13: KEGG pathways enriched in treated Huh7 cells (p<0.05)

	KEGG pathway	# of Genes
Sorafenib	hsa00100:Steroid biosynthesis	5
	hsa04110:Cell cycle	14
	hsa04520:Adherens junction	10
	hsa05215:Prostate cancer	10
	hsa04010:MAPK signaling pathway	21
	hsa01040:Biosynthesis of unsaturated fatty acids	4

PI3Ki-α	hsa04114:Oocyte meiosis	7
	hsa04110:Cell cycle	7
	hsa04914:Progesterone-mediated oocyte maturation	5
Combination	-	-

Table 4.14: KEGG pathways enriched in treated Mahlavu cells (p<0.05)

	KEGG pathway	# of Genes
Sorafenib	hsa04621:NOD-like receptor signaling pathway	3
	hsa04060:Cytokine-cytokine receptor interaction	5
PI3Ki-α	hsa04010:MAPK signaling pathway	5
Combination	-	-

Microarray analysis emphasized the wide-ranging effect of the multi-kinase inhibitor, Sorafenib. Cellular processes that are regulated specifically in response to treatment with combination of Sorafenib and PI3Ki-α but not with single treatment of Sorafenib were identified (Tables 4.15, 4.16). Additionally, identification of cellular processes affected specifically in response to treatment with Sorafenib but not with combination therapy revealed unanticipated side effects of Sorafenib therapy that could explain therapeutic resistance to Sorafenib (Tables 4.17, 4.18).

Table 4.15: Cellular processes affected specifically by up-regulated genes in response to treatment with combination of Sorafenib and PI3Ki-α but not with single treatment of Sorafenib in Huh7 cells ($p<0.05$)

GO ID	GO Term
GO:0006886	intracellular protein transport
GO:0016192	vesicle-mediated transport
GO:0033365	protein localization in organelle
GO:0031331	positive regulation of cellular catabolic process
GO:0048193	Golgi vesicle transport
GO:0006892	post-Golgi vesicle-mediated transport
GO:0034613	cellular protein localization
GO:0030162	regulation of proteolysis
GO:0043065	positive regulation of apoptosis
GO:0006917	induction of apoptosis
GO:0070727	cellular macromolecule localization
GO:0051247	positive regulation of protein metabolic process
GO:0010608	posttranscriptional regulation of gene expression
GO:0015031	protein transport
GO:0008104	protein localization
GO:0045184	establishment of protein localization

Table 4.16: Cellular processes affected specifically by up-regulated genes in response to treatment with combination of Sorafenib and PI3Ki-α but not with single treatment of Sorafenib in Mahlavu cells ($p<0.05$)

GO ID	GO Term
GO:0007218	neuropeptide signaling pathway
GO:0006888	ER to Golgi vesicle-mediated transport
GO:0010608	posttranscriptional regulation of gene expression
GO:0006334	nucleosome assembly
GO:0031497	chromatin assembly
GO:0006323	DNA packaging
GO:0051276	chromosome organization

Table 4.17: Cellular processes affected specifically by up-regulated genes in response to treatment with Sorafenib but not with combination therapy in Huh7 cells ($p<0.05$)

GO ID	GO Term
GO:0030522	intracellular receptor-mediated signaling pathway
GO:0007242	intracellular signaling cascade
GO:0030518	steroid hormone receptor signaling pathway
GO:0010628	positive regulation of gene expression
GO:0045893	positive regulation of transcription, DNA-dependent
GO:0043065	positive regulation of apoptosis
GO:0043068	positive regulation of programmed cell death
GO:0031667	response to nutrient levels
GO:0032526	response to retinoic acid
GO:0007584	response to nutrient

GO:0009719	response to endogenous stimulus
GO:0032869	cellular response to insulin stimulus
GO:0032870	cellular response to hormone stimulus
GO:0033554	cellular response to stress
GO:0006974	response to DNA damage stimulus
GO:0032321	positive regulation of Rho GTPase activity
GO:0043087	regulation of GTPase activity
GO:0007257	activation of JUN kinase activity
GO:0043507	positive regulation of JUN kinase activity
GO:0010557	positive regulation of macromolecule biosynthetic process
GO:0031328	positive regulation of cellular biosynthetic process
GO:0010560	positive regulation of glycoprotein biosynthetic process
GO:0051254	positive regulation of RNA metabolic process
GO:0045935	positive regulation of nucleobase, nucleoside, nucleotide and nucleic acid metabolic process
GO:0006796	phosphate metabolic process
GO:0010906	regulation of glucose metabolic process
GO:0046068	cGMP metabolic process
GO:0048812	neuron projection morphogenesis
GO:0000904	cell morphogenesis involved in differentiation
GO:0032330	regulation of chondrocyte differentiation
GO:0045453	bone resorption
GO:0048771	tissue remodeling
GO:0030182	neuron differentiation
GO:0030521	androgen receptor signaling pathway

Table 4.18: Cellular processes affected specifically by up-regulated genes in response to treatment with Sorafenib but not with combination therapy in Mahlavu cells ($p<0.05$)

GO Term	GO ID
GO:0006952	defense response
GO:0006955	immune response
GO:0009611	response to wounding
GO:0006954	inflammatory response
GO:0006968	cellular defense response
GO:0002252	immune effector process
GO:0045087	innate immune response

Collectively, our transcriptome level expression data delineate redundant functions and compensatory relationship between Raf/MEK/ERK and PI3K/AKT/mTOR pathways and explain mechanisms of resistance to Sorafenib. Therapeutic efficiency of Sorafenib is based on its ability to down-regulate MAPK signaling, reduce cell proliferation, growth, and angiogenesis and induce apoptosis. However, Sorafenib induces multiple other intracellular signaling cascades, activates Ras and Rho GTPase activities and consequent enhanced signaling through Ral/Rac/Rho cascades result in the activation of the PI3K/Akt pathway. Another unforeseen side effect of Sorafenib was the induction of pro-inflammatory and immune responses, which promote tumor growth. Combination of Sorafenib and PI3K inhibitor effectively down-regulated MAPK and PI3K pathways, overcame the compensatory activation of Ral/Rac/Rho cascades, and prevented production of pro-inflammatory and immune responses. These extremely encouraging results highlight the potential of combined targeted therapies with Sorafenib and PI3K inhibitors for the treatment of advanced HCC.

Although we included only significantly differentially expressed genes in our analysis, we realized that the fold changes between drug treated and control samples were low. Therefore, we decided to perform RNA sequencing with these inhibitors. RNA-seq analysis of Huh7 and Mahlavu cells treated with PI3Ki-α showed that

RNA-seq can capture more data on transcriptome level regulation. We analyzed modulation of gene expression regulated by the major transcription factors FOXO1 and p53 (Figures 4.33 and 4.34). RNA-seq analysis will be performed with Sorafenib and combination of Sorafenib and PI3Ki-α soon, in order to interpret differences between mono- and dual-treatments.

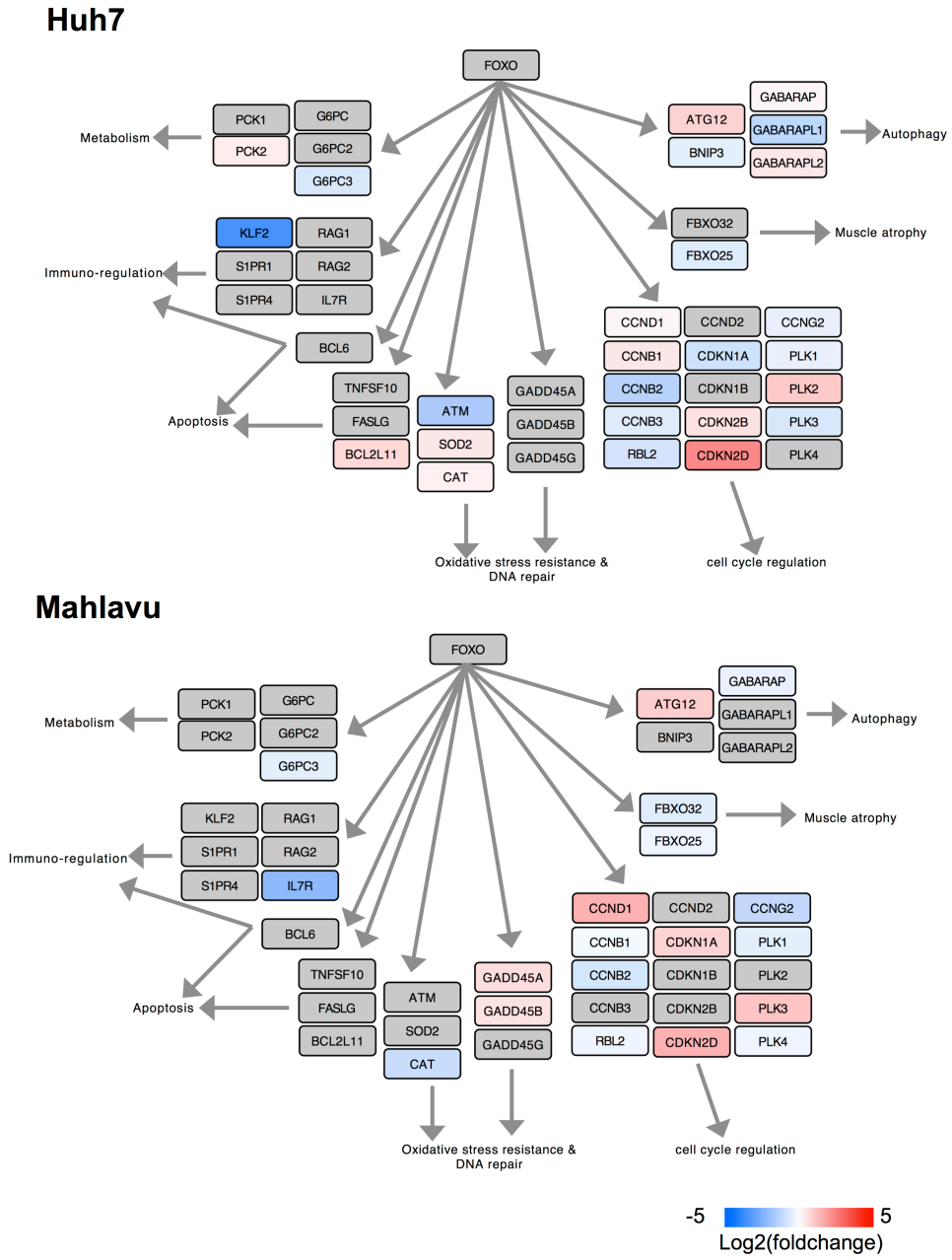

Figure 4.33: Effect of PI3Ki-α on FOXO-mediated gene expression. Genes regulated by FOXO transcription factor were obtained from KEGG database and visualized using Cytoscape based on the fold changes in gene expression between drug treated cells and control cells. Genes that were down-regulated and up-regulated

in response to PI3Ki-α treatment are shown in blue and red, respectively. Genes with gray color did not have significant alterations in their expression levels upon drug treatment.

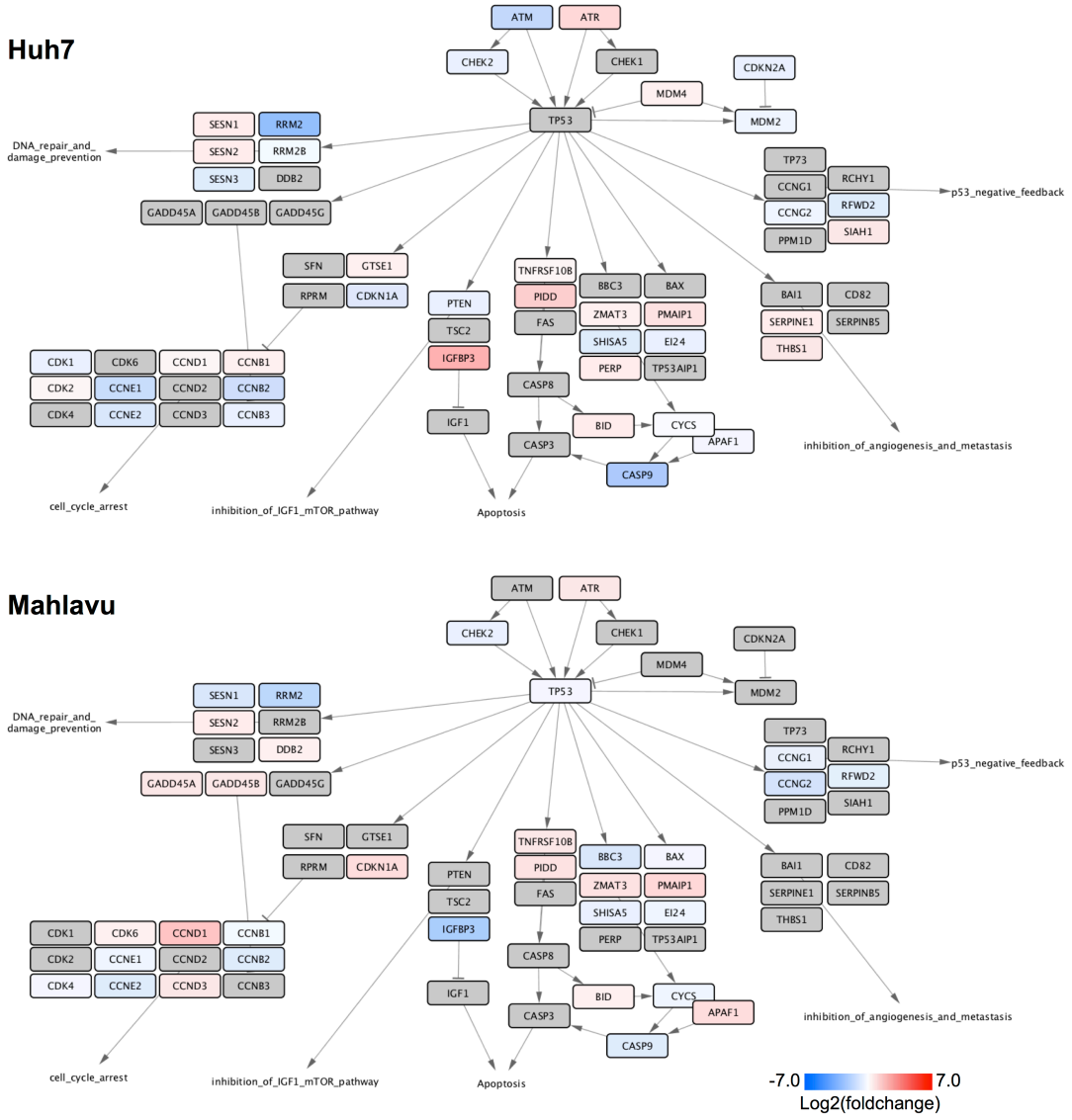

Figure 4.34: Effect of PI3Ki-α on p53-mediated gene expression. Genes regulated by FOXO transcription factor were obtained from KEGG database and visualized using Cytoscape based on the fold changes in gene expression between drug treated cells and control cells. Genes that were down-regulated and up-regulated in response to PI3Ki-α treatment are shown in blue and red, respectively. Genes with gray color did not have significant alterations in their expression levels upon drug treatment.

CHAPTER 5. DISCUSSION AND CONCLUSION

Extensive studies on resistance to Sorafenib and tumor recurrence in HCC patients suggest that Sorafenib-mediated anti-growth and anti-angiogenic signals mainly through the Raf/MEK/ERK cascade can facilitate signaling from the compensatory PI3K/AKT/mTOR pathway. Proliferation, growth, angiogenesis and metastasis are multifaceted cellular processes regulated by redundant and compensatory signaling. Besides, they are in close interaction with other processes whose deregulation confers hallmark capabilities of cancer, i.e. metabolism, inflammation, immune response. Growth factors and angiogenic signals are not exclusive inducers of compensatory pathways. Cytokines and chemokines, which are associated with tumor promoting pro-inflammatory and immune responses, also activate the Raf/MEK/ERK and PI3K/AKT/mTOR pathways. Yet, another obstacle in resolving therapeutic resistance is the variable predominance of isoform-specific signaling within a single pathway based on cellular context. Therefore, targeted therapy studies in HCC should focus not only on signaling redundancy and compensatory relationship between the Raf/MEK/ERK and PI3K/AKT/mTOR pathways, but also on how intra-pathway redundancies affect inter-pathway compensability. Here, we provide *in vitro* experimental evidence for therapeutic potential of combining Sorafenib with p110α-isoform specific inhibitor of PI3K kinase (PI3Ki-α, PIK-75) and *in vivo* evidence for the enhanced therapeutic efficiency of combining Sorafenib with the Akt2-isoform specific inhibitor of Akt kinase (Akti-2).

We showed that p110α isoform specific inhibition of PI3K results in synergistic inhibition of cell growth in both Huh7 and Mahlavu cells. The synergistic cytotoxicity was more pronounced in Mahlavu, since PTEN-loss mediated constitutive activation of PI3K/Akt pathway renders these cells more susceptible to PI3K inhibition. On the other hand, p110β isoform specific inhibition of PI3K results in synergistic inhibition of cell growth in Huh7, but produces an antagonistic effect in Mahlavu probably by enhancing signaling through p110α (Figure 5.1). These results indicate the predominant role of p110α in PTEN-deficient HCC cells.

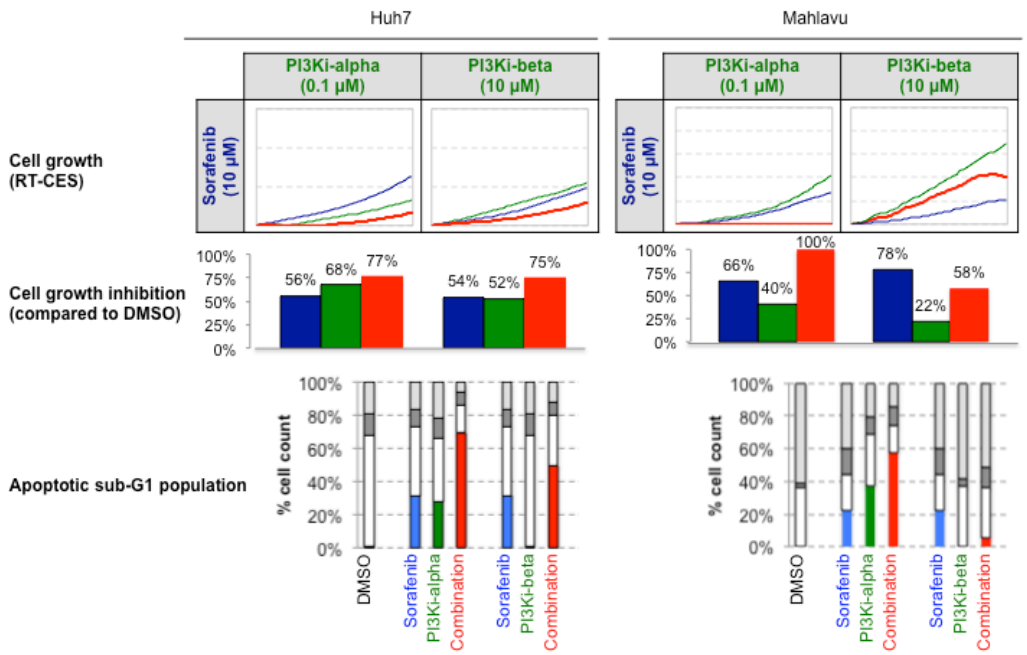

Figure 5.1: Differential cytotoxic effects of combining Sorafenib and isoform-specific PI3K inhibitors in HCC cells based on PTEN status.

Based on microarray results, cell cycle progression and cell proliferation (GO:0008283, GO:0022402, KEGG:hsa04110), wound healing (GO:0042060, GO:0009611), regulation of protein catabolic process (GO:0042176) and kinase regulator activity (GO:0019207) were down-regulated in both cell lines upon single treatment with Sorafenib, single treatment with PI3Ki-α and combined treatment of both. Moreover, up-regulation of MAPK kinase activity in cells treated with PI3Ki-α as single agent, was overcame upon co-treatment with Sorafenib, as a result of significant increase in MAP kinase phosphatase activity (GO:0017017, GO:0033549, hsa04010).

In Sorafenib treated HCC cells, there was a significant increase in inflammatory and immune responses (GO:0006954, GO:0006955). It is well established that release of pro-inflammatory cytokines and chemokines from cancer cells promote modulation of immune response in favor of tumor proliferation, angiogenesis and metastasis (Balkwill, 2004; Gerber, Hippe, Buhren, Müller, & Homey, 2009; Sethi & Kang, 2011; Zlotnik, Burkhardt, & Homey, 2011). Besides, activation of the chemokine pathway is suggested as a mechanism of therapeutic

resistance. Indeed, Sorafenib increases tumor hypoxia and subsequently intensifies chemokine network. Recent studies targeting pro-inflammatory chemokine network and related tumor-associated macrophages (TAMs) have shown increase in the efficacy of Sorafenib treatment (Chen et al., 2014; Duda et al., 2011; Tang, Mo, Wang, Wei, & Xiao, 2013). PI3K/Akt signaling also increases production of various pro-inflammatory cytokines and the immunosuppressive cytokine IL-10 (Antoniv & Ivashkiv, 2011; Martin et al., 2005; Thomson et al., 2009). Hence, targeting PI3K/Akt pathway can increase the efficacy of Sorafenib by modulating chemokine network.

HCC proceeds from chronic liver inflammation and is prominently regulated by inflammatory microenvironment and immune response (Aravalli, 2013; Brownell & Polyak, 2013; Capece et al., 2013). Under hypoxic conditions of tumor microenvironment, endothelial cells up-regulate CXCR7, and CXCL11/CXCR7 pathway supports HCC progression (Monnier et al., 2012). HCC patients exhibit significantly higher CXCR7 and CXCL11 in tumors compared to normal liver. Microarray analysis identified significant up-regulation of pro-inflammatory cytokines CXCL11, CCL5, and TSLP and pro-inflammatory receptor TNFRSF9 in Sorafenib treated Mahlavu cells. CCL5 secreted from stromal cells is known to induce migration and invasion of HCC cells through PI3K/Akt pathway, suggesting a compensatory activation of PI3K/Akt in response to Sorafenib treatment (Bai et al., 2014). As anticipated, up-regulation of tumor-promoting inflammation in response to Sorafenib treatment was effectively counteracted by co-treatment with PI3Ki-α.

Single treatment of PI3Ki-α did not provoke any inflammatory or immune responses in either Huh7 or Mahlavu cells. Combination of PI3Ki-α and Sorafenib resulted in reduced proliferation and enhanced apoptosis compared to single treatments in Mahlavu cells, without any tumor-promoting side effect. In Huh7, inflammatory response was enhanced in cells co-treated with Sorafenib and PI3Ki-α compared to cells treated only with PI3Ki-alpha, whereas there was no significant change in Mahlavu cells. Additionally, although apoptotic and anti-proliferative processes were up-regulated in combination treated Huh7 cells compared to Sorafenib treated cells, combined treatment of PI3Ki-α and Sorafenib resulted in increased angiogenesis and vasculature development (GO:0001525, GO:0048514, GO:0001944), migration (GO:0030334, GO:0051270), response to wounding

(GO:0009611) and inflammatory response (GO:0006954) compared to single treatment with PI3Ki-α. In Mahlavu cells there was no such compensatory up-regulation. These results suggest that although combination of Sorafenib and PI3Ki-α synergistically reduces proliferation and growth and increases apoptosis in both Huh7 and Mahlavu cells, it can also promote migration, angiogenesis and inflammatory response in Huh7, probably through p110β isoform of PI3K and therefore targeted therapies should be designed based on cellular context of HCC cells.

Microarray analysis revealed that in Sorafenib treated Huh7 cells, Ras GTPase binding (GO:0017016), Rac GTPase binding (GO:0048365), phosphatidylinositol binding (GO:0005545), steroid hormone receptor binding (GO:0035258) and transcription factor binding (GO:0008134) are elevated and protein serine/threonine kinase (GO:0004674) and transcription coactivator (GO:0003713) activities are increased. Ras effectors, include PI3K, MAPK and Ral/Rac/Rho cascades, which crosstalk with each other. PI3K is activated by Ras and Rho family small GTPases and RhoA, in turns, acts as an antagonist of PI3K via stimulating the phospholipid phosphatase activity of PTEN through RhoA-associated kinase (Rock) (Li et al., 2005; Yang et al., 2012). Recently, interactions of Ras and Rho GTPases with PI3K were identified to be isoform-specific. Ras cannot bind p110β, but instead RAC1 and CDC42 e Rho GTPases bind and activate p110β. Hence, in Huh7 cells, Sorafenib induced Rho GTPase activity can transmit signals predominantly through p110β rather than p110α. Therefore, combination of p110β isoform specific PI3K inhibitor with Sorafenib is highly synergistic and cytotoxic in Huh7 cells, but shows antagonistic actions in Mahlavu cells, which depend primarily on p110α isoform (Figure 4.18). The synergistic cytotoxic activity of Sorafenib and PI3Ki-β is partly mediated by reducing Sorafenib-induced Rho GTPase activity (Table 4.16). As expected, co-treatment of Sorafenib and PI3Ki-α was more effective on Mahlavu cells (Figure 4.18). Herein, we postulate that PTEN-loss mediated hyper-activation of PI3K signaling is dependent on p110α. In addition to blocking Akt-mediated survival signlas, ROCK is also known to affect membrane ion channels, which is in parallel with our microarray results in Sorafenib-treated Huh7 cells (Table 4.17).

Besides, it is known that the liver-specific tumor suppressor DLC1 (deleted in liver cancer), which is a Rho GTPase-activating protein, suppresses cell proliferation and invasion in HCC by negatively regulating the activity of Rho proteins (Wong et al., 2005). Hence compensatory positive regulation of Ral/Rac/Rho cascade in Sorafenib treated Huh7 cells can be a major mechanism of resistance. Combination of PI3Ki-α and Sorafenib prevented up-regulation of Ral/Rac/Rho cascade, suggesting a critical role of co-targeting PI3K pathway to overcome resistance. Yet, combining Sorafenib with PI3Ki-β instead of PI3Ki-α in Huh7 cells should be studied in transcriptomics level and *in vivo*.

Our microarray experiments revealed activation of JUN kinase activity (GO:0007257) specifically in Sorafenib treated Huh7 cells. However, our *in vitro* experiments and microarray analysis demonstrated that Sorafenib up-regulates cyclin-dependent kinase inhibitor, p21 to halt cell cycle progression (Figure 4.19). Yet, it is known that p21 inhibits apoptosis-signal-regulating kinase 1 (ASK1) and blocks activation of c-JUN N-terminal kinase (JNK) – mediated apoptosis. ASK1 is one of the common effectors of Raf/MEK/ERK and PI3K/AKT/mTOR pathways. Akt activates ASK1 through inhibiting p21 or activating mTORC1. Hence, inhibition of PI3K/AKT/mTOR signaling leads to activation of ASK1 and consequent induction of c-JUN N-terminal kinase (JNK) results in apoptosis (Bjornsti & Houghton, 2004). Therefore, combined use of PI3Ki-α and Sorafenib effectively intensifies apoptotic stimuli.

JNK and other mitogen-activated protein kinases (MAPK) family members p38 and ERK are activated in immune system to promote production of cytokines and inflammatory mediators. Dual-specificity MAP kinase phosphatases (DUSPs or MKPs) are negative regulators of MAPK. PI3K/Akt signaling increases production of the immunosuppressive cytokine Interleukin-10 (IL-10) and maintains anti-inflammatory processes through DUSP regulation and IL-10/Jak/Stat3 pathway (Antoniv & Ivashkiv, 2011; Martin et al., 2005). DUSP1 inhibits activity of p38 and JNK. We observed an increase in DUSP1 and the anti-inflammatory cytokine IL-10 in Sorafenib treated Huh7 cells. Co-treatment of Sorafenib with PI3Ki-α resulted in reduction of DUSP1 and IL-10 levels. Since IL-10 is also critical for immune evasion, combining Sorafenib and PI3Ki-α confers therapeutic advantage by targeting inflammatory- and immune-response based acquired capabilities of HCC.

Collectively, these results demonstrate isoform-specific functions of PI3K and selective dependence on different isoforms based on molecular alterations. Our transcriptome level expression data delineate redundant functions and compensatory relationship between Raf/MEK/ERK and PI3K/AKT/mTOR pathways and explain mechanisms of resistance to Sorafenib. Furthermore, *in vitro* microarray results of PI3K isoform alpha inhibitor emphasize therapeutic potential of using PI3K/AKT pathway inhibitors to overcome resistance to Sorafenib and increase its efficiency (Figure 5.2).

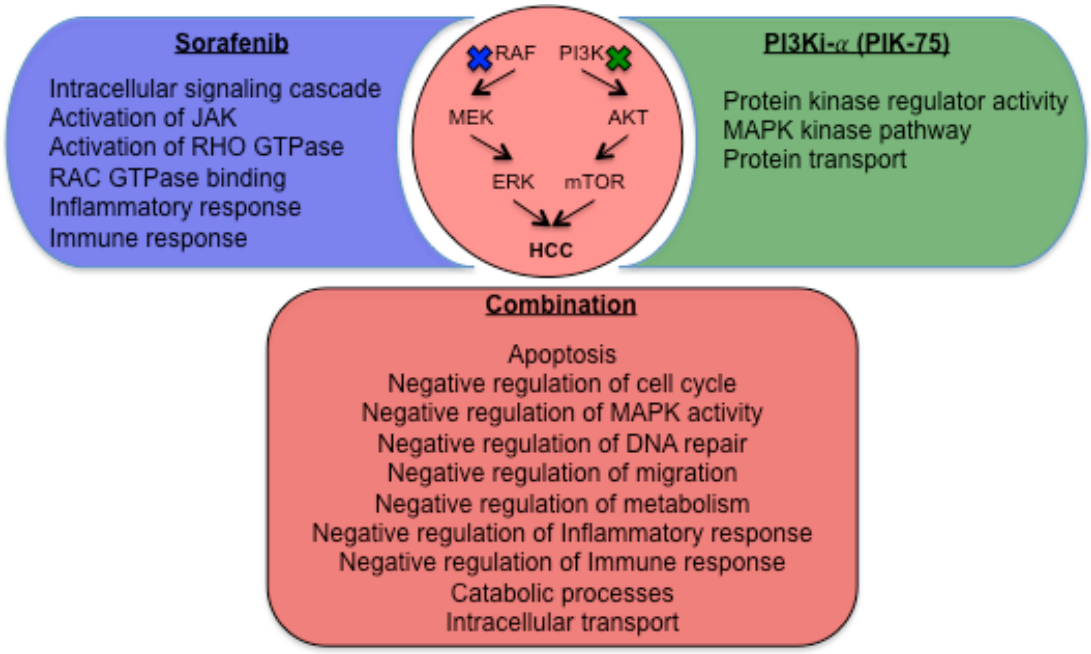

Figure 5.2: Therapeutic potential of using PI3K inhibitors to overcome resistance to Sorafenib

We showed that Akt2 isoform specific and non-specific inhibition of Akt cannot promote cell growth inhibition or apoptosis as single agents at 10 µM in both Huh7 and Mahlavu cells. Strikingly, combination of these inhibitors with Sorafenib results in synergistic inhibition of cell growth (Figure 5.3). These results indicate the therapeutic potential of combination therapies with Sorafenib and Akt inhibitors for the targeted therapy of HCC.

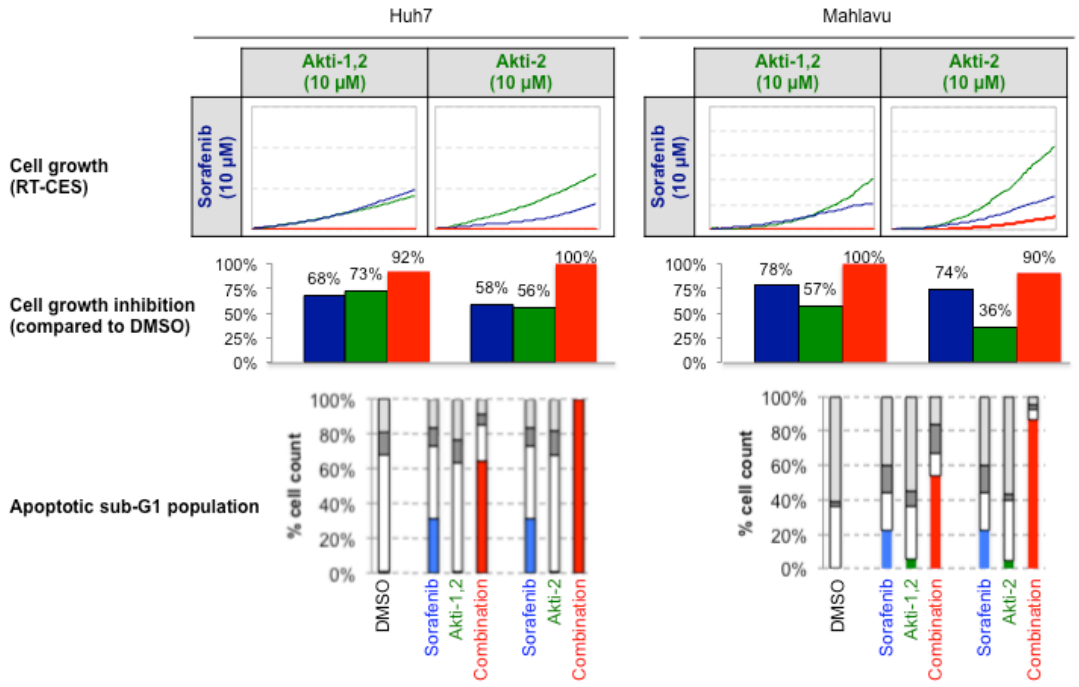

Figure 5.3: Cytotoxic effects of combining Sorafenib and isoform-specific and non-specific Akt inhibitors in HCC cells.

Although Akti-2 has not shown significant cytotoxicity *in vitro* when used as single agent, it produced significant reduction in tumor volume (45% compared to control) and tumor weight (50% compared to control). Sorafenib produced 66% reduction in tumor volume and 85% reduction in tumor weight compared to control. Combination of Sorafenib and Akti-2 showed significant superiority in reducing tumor volume (74% reduction compared to control) and tumor weight (93% compared to control). Tumor weight is a better measure of cytotoxic effects of drugs, since necrosis-induced inflammation and swelling in combination-treated mice produced a temporary increase in tumor size compared to Sorafenib-treated mice. 2 out of 5 mice developed visible intra-tumoral necrotic areas after 2 weeks of receiving combination treatment. In HCC patients, anti-angiogenic effect of Sorafenib is also characterized by intra-tumoral necrosis and a temporary, but substantial, increase in tumor size (Horger et al., 2009). Previous studies in HCC xenograft models showed that Sorafenib causes growth inhibition at 30 mg/kg and partial tumor regressions at 100 mg/kg (Liu et al., 2012; Liu et al., 2006). Here, we show that while 30 mg/kg Sorafenib causes tumor growth inhibition as single agent,

and co-treatment with 30 mg/kg Sorafenib and 7.5 mg/kg Akti-2 causes tumor regressions. Single treatment with Sorafenib initiated intra-tumoral necrosis in 1 out of 5 mice 3 weeks post-treatment, while combination treatment resulted in intra-tumoral necrosis in 4 out of 5 mice and reduced tumor density. Our results provide *in vivo* experimental evidence of the therapeutic potential of combination therapies with Sorafenib and Akt inhibitors for the treatment of advanced HCC (Figure 5.4).

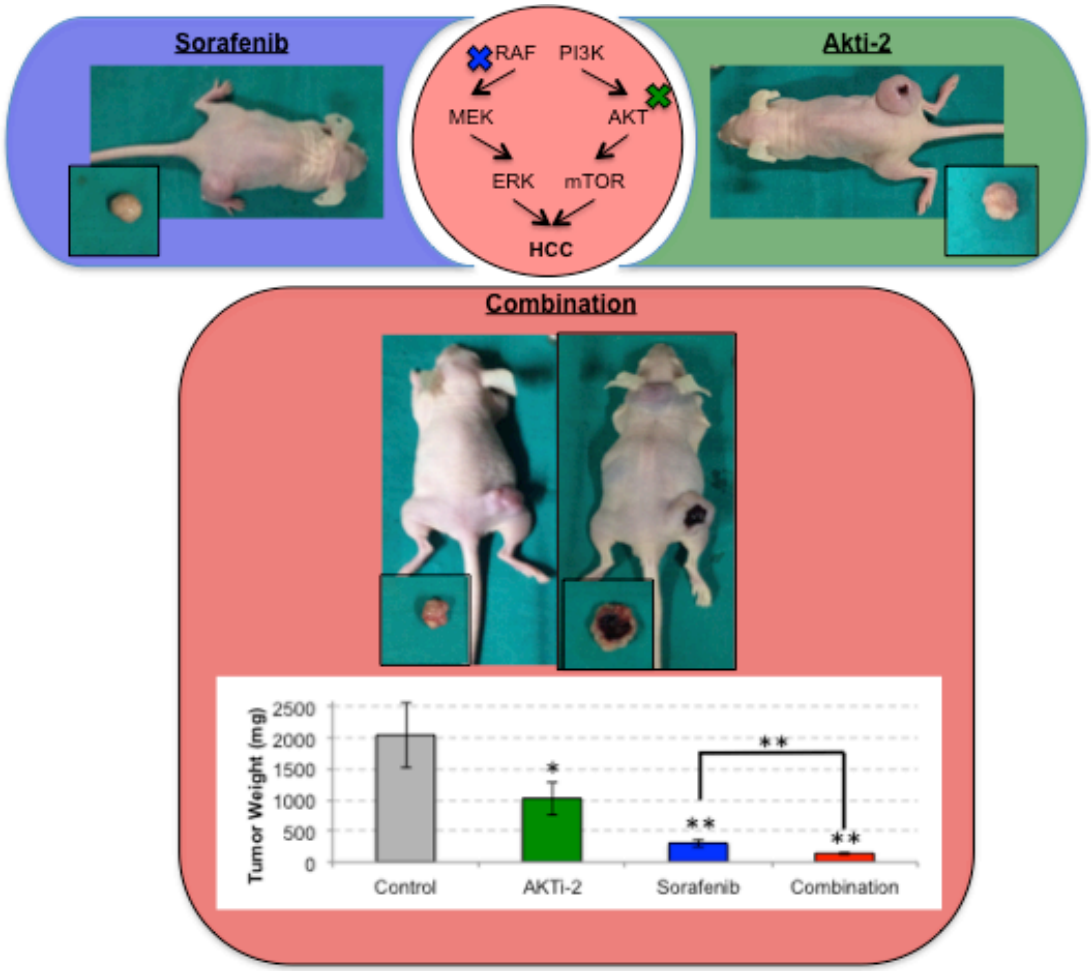

Figure 5.4: Therapeutic potential of using Akt inhibitors to enhance efficiency of Sorafenib. 1 out of 5 Sorafenib treated mice initiated intratumoral necrosis after 3 weeks of treatment. 4 out of 5 combination treated mice initiated intratumoral necrosis after 2 weeks of treatment. Substantial necrosis was clearly visible in 2 combination treated mice and others could be detected by MRI. 1 out of 5 combination treated mice directly reduced tumor volume without signs of necrosis.

CHAPTER 6. FUTURE PERSPECTIVES

Combining signal transduction inhibitors for simultaneous targeting of compensatory pathways with redundant functions is the most effective therapeutic strategy to overcome resistance to targeted agents. With the advance of high-throughput technologies and interpretation of various omics data, network-level understanding of molecular alterations enable identification of critical primary targets, anticipate possible side effects and facilitate design of optimal combinations to increase therapeutic efficiency. Our results showed the isoform-specific functions of PI3K and Akt kinases. Use of isoform-specific rather than general kinase inhibitors can minimize side effects and reduce the required dose thereby minimizing toxicity. We performed microarray experiments with Sorafenib, PI3Ki-α (PIK-75) and their combination in Huh7 and Mahlavu cell lines. Microarray experiments should also be performed for PI3Ki-β (TGX-221) and its combination with Sorafenib to better reveal isoform-specific functions of PI3K. We showed that PI3Ki-β and Sorafenib are antagonistic in Mahlavu cells. Microarray experiments will identify the molecular mechanism of compensatory growth-promoting signaling in Mahlavu cells treated with PI3Ki-β. PI3Ki-α (PIK-75), PI3Ki-β (TGX-221) and their combinations with Sorafenib should be tested in tumor xenografts *in vivo* to assess advantage of combination therapy over mono-therapy with Sorafenib.

Cytotoxic activities of PI3Ki-α (PIK-75), PI3Ki-β (TGX-221), Akti-1,2 and Akti-2 should be tested in normal cells, to ensure that they will specifically target cancer cells with minimum toxicity on normal healthy cells.

We demonstrated anti-tumor effect of Sorafenib and Akti-2 combination in Mahlavu xenografts *in vivo*. The significant reduction in tumor volume and weight should be supported with hematoxylin-eosin (H&E) staining and immunohistochemistry assays. Alterations in expression levels of critical effectors of PI3K/AKT/mTOR and RAF/MEK/ERK pathways upon combinational treatment *in vivo* should be determined with western blot. In order to identify molecular mechanism of synergy between Sorafenib and Akti-2, microarray or RNAseq experiments should be performed. Additionally, proteomics studies and

phosphorylation based kinase activity assays could be extremely informative on signaling pathway alterations since kinases regulate their downstream effectors through phosphorylation.

In order to validate the dependence of Mahlavu cells on the p110α isoform for cell survival, RNAi can be used to knock-down specific isoforms. Role of PTEN on the sensitivity of HCC cells to Sorafenib and PI3K/Akt inhibitor can be studied by knocking-down PTEN in Huh7 cells and comparing response of these cells to inhibitors with that of wild-type Huh7.

REFERENCES

Ackah, E., Yu, J., Zoellner, S., Iwakiri, Y., Skurk, C., Shibata, R., … Sessa, W. C. (2005). Akt1/protein kinase Balpha is critical for ischemic and VEGF-mediated angiogenesis. *The Journal of Clinical Investigation*, *115*(8), 2119–27. doi:10.1172/JCI24726

Andersen, C. L., Jensen, J. L., & Ørntoft, T. F. (2004). Normalization of Real-Time Quantitative Reverse Transcription-PCR Data: A Model-Based Variance Estimation Approach to Identify Genes Suited for Normalization, Applied to Bladder and Colon Cancer Data Sets. *Cancer Research* , *64* (15), 5245–5250. doi:10.1158/0008-5472.CAN-04-0496

Antoniv, T. T., & Ivashkiv, L. B. (2011). Interleukin-10-induced gene expression and suppressive function are selectively modulated by the PI3K-Akt-GSK3 pathway. *Immunology*, *132*(4), 567–77. doi:10.1111/j.1365-2567.2010.03402.x

Aravalli, R. N. (2013). Role of innate immunity in the development of hepatocellular carcinoma. *World Journal of Gastroenterology : WJG*, *19*(43), 7500–14. doi:10.3748/wjg.v19.i43.7500

Aston, N. S., Watt, N., Morton, I. E., Tanner, M. S., & Evans, G. S. (2000). Copper toxicity affects proliferation and viability of human hepatoma cells (HepG2 line). *Human & Experimental Toxicology*, *19*(6), 367–76. Retrieved from http://www.ncbi.nlm.nih.gov/pubmed/10962511

Audeh, M. W., Carmichael, J., Penson, R. T., Friedlander, M., Powell, B., Bell-McGuinn, K. M., … Tutt, A. (2010). Oral poly(ADP-ribose) polymerase inhibitor olaparib in patients with BRCA1 or BRCA2 mutations and recurrent ovarian cancer: a proof-of-concept trial. *Lancet*, *376*(9737), 245–51. doi:10.1016/S0140-6736(10)60893-8

Augustin, H. G., Koh, G. Y., Thurston, G., & Alitalo, K. (2009). Control of vascular

morphogenesis and homeostasis through the angiopoietin-Tie system. *Nature Reviews. Molecular Cell Biology*, *10*(3), 165–77. doi:10.1038/nrm2639

Bae, J.-J., Rho, J.-W., Lee, T.-J., Yun, S.-S., Kim, H.-J., Choi, J.-H., … Lee, T.-Y. (2007). Loss of heterozygosity on chromosome 10q23 and mutation of the phosphatase and tensin homolog deleted from chromosome 10 tumor suppressor gene in Korean hepatocellular carcinoma patients. *Oncology Reports*, *18*(4), 1007–13. Retrieved from http://www.ncbi.nlm.nih.gov/pubmed/17786367

Bai, H., Weng, Y., Bai, S., Jiang, Y., Li, B., He, F., … Shi, Q. (2014). CCL5 secreted from bone marrow stromal cells stimulates the migration and invasion of Huh7 hepatocellular carcinoma cells via the PI3K-Akt pathway. *International Journal of Oncology*, *45*(1), 333–43. doi:10.3892/ijo.2014.2421

Bai, P., & Virág, L. (2012). Role of poly(ADP-ribose) polymerases in the regulation of inflammatory processes. *FEBS Letters*, *586*(21), 3771–7. doi:10.1016/j.febslet.2012.09.026

Balkwill, F. (2004). Cancer and the chemokine network. *Nature Reviews. Cancer*, *4*(7), 540–50. doi:10.1038/nrc1388

Bensaad, K., Tsuruta, A., Selak, M. a, Vidal, M. N. C., Nakano, K., Bartrons, R., … Vousden, K. H. (2006). TIGAR, a p53-inducible regulator of glycolysis and apoptosis. *Cell*, *126*(1), 107–20. doi:10.1016/j.cell.2006.05.036

Berenjeno, I. M., Guillermet-Guibert, J., Pearce, W., Gray, A., Fleming, S., & Vanhaesebroeck, B. (2012). Both p110α and p110β isoforms of PI3K can modulate the impact of loss-of-function of the PTEN tumour suppressor. *The Biochemical Journal*, *442*(1), 151–9. doi:10.1042/BJ20111741

Bergers, G., & Hanahan, D. (2008). Modes of resistance to anti-angiogenic therapy. *Nature Reviews. Cancer*, *8*(8), 592–603. doi:10.1038/nrc2442

Beyoğlu, D., Imbeaud, S., Maurhofer, O., Bioulac-Sage, P., Zucman-Rossi, J., Dufour, J.-F., & Idle, J. R. (2013). Tissue metabolomics of hepatocellular carcinoma: tumor energy metabolism and the role of transcriptomic

classification. *Hepatology (Baltimore, Md.)*, *58*(1), 229–38. doi:10.1002/hep.26350

Bierie, B., & Moses, H. L. (2006). Tumour microenvironment: TGFbeta: the molecular Jekyll and Hyde of cancer. *Nature Reviews. Cancer*, *6*(7), 506–20. doi:10.1038/nrc1926

Bjornsti, M.-A., & Houghton, P. J. (2004). The TOR pathway: a target for cancer therapy. *Nature Reviews. Cancer*, *4*(5), 335–48. doi:10.1038/nrc1362

Boyault, S., Rickman, D. S., de Reyniès, A., Balabaud, C., Rebouissou, S., Jeannot, E., … Zucman-Rossi, J. (2007). Transcriptome classification of HCC is related to gene alterations and to new therapeutic targets. *Hepatology (Baltimore, Md.)*, *45*(1), 42–52. doi:10.1002/hep.21467

Brenndörfer, E. D., & Sällberg, M. (2012). Hepatitis C virus-mediated modulation of cellular immunity. *Archivum Immunologiae et Therapiae Experimentalis*, *60*(5), 315–29. doi:10.1007/s00005-012-0184-z

Brownell, J., & Polyak, S. J. (2013). Molecular pathways: hepatitis C virus, CXCL10, and the inflammatory road to liver cancer. *Clinical Cancer Research : An Official Journal of the American Association for Cancer Research*, *19*(6), 1347–52. doi:10.1158/1078-0432.CCR-12-0928

Bryant, H. E., Schultz, N., Thomas, H. D., Parker, K. M., Flower, D., Lopez, E., … Helleday, T. (2005). Specific killing of BRCA2-deficient tumours with inhibitors of poly(ADP-ribose) polymerase. *Nature*, *434*(7035), 913–7. doi:10.1038/nature03443

Budanov, A. V, & Karin, M. (2008). p53 target genes sestrin1 and sestrin2 connect genotoxic stress and mTOR signaling. *Cell*, *134*(3), 451–60. doi:10.1016/j.cell.2008.06.028

Budhu, A., Roessler, S., Zhao, X., Yu, Z., Forgues, M., Ji, J., … Wang, X. W. (2013). Integrated metabolite and gene expression profiles identify lipid biomarkers associated with progression of hepatocellular carcinoma and patient

outcomes. *Gastroenterology*, *144*(5), 1066–1075.e1. doi:10.1053/j.gastro.2013.01.054

Buontempo, F., Ersahin, T., Missiroli, S., Senturk, S., Etro, D., Ozturk, M., … Neri, M. L. (2011). Inhibition of Akt signaling in hepatoma cells induces apoptotic cell death independent of Akt activation status. *Investigational New Drugs*, *29*(6), 1303–13. doi:10.1007/s10637-010-9486-3

Caja, L., Sancho, P., Bertran, E., & Fabregat, I. (2011). Dissecting the effect of targeting the epidermal growth factor receptor on TGF-β-induced-apoptosis in human hepatocellular carcinoma cells. *Journal of Hepatology*, *55*(2), 351–8. doi:10.1016/j.jhep.2010.10.041

Caja, L., Sancho, P., Bertran, E., Iglesias-Serret, D., Gil, J., & Fabregat, I. (2009). Overactivation of the MEK/ERK pathway in liver tumor cells confers resistance to TGF-{beta}-induced cell death through impairing up-regulation of the NADPH oxidase NOX4. *Cancer Research*, *69*(19), 7595–602. doi:10.1158/0008-5472.CAN-09-1482

Calvisi, D. F., Ladu, S., Gorden, A., Farina, M., Conner, E. a, Lee, J.-S., … Thorgeirsson, S. S. (2006). Ubiquitous activation of Ras and Jak/Stat pathways in human HCC. *Gastroenterology*, *130*(4), 1117–28. doi:10.1053/j.gastro.2006.01.006

Campbell, J. S., Johnson, M. M., Bauer, R. L., Hudkins, K. L., Gilbertson, D. G., Riehle, K. J., … Fausto, N. (2007). Targeting stromal cells for the treatment of platelet-derived growth factor C-induced hepatocellular carcinogenesis. *Differentiation; Research in Biological Diversity*, *75*(9), 843–52. doi:10.1111/j.1432-0436.2007.00235.x

Cantor, J. R., & Sabatini, D. M. (2012). Cancer cell metabolism: one hallmark, many faces. *Cancer Discovery*, *2*(10), 881–98. doi:10.1158/2159-8290.CD-12-0345

Capece, D., Fischietti, M., Verzella, D., Gaggiano, A., Cicciarelli, G., Tessitore, A., … Alesse, E. (2013). The inflammatory microenvironment in hepatocellular carcinoma: a pivotal role for tumor-associated macrophages. *BioMed Research*

International, *2013*, 187204. doi:10.1155/2013/187204

Challen, C., Guo, K., Collier, J. D., Cavanagh, D., & Bassendine, M. F. (1992). Infrequent point mutations in codons 12 and 61 of ras oncogenes in human hepatocellular carcinomas. *Journal of Hepatology*, *14*(2-3), 342–6. Retrieved from http://www.ncbi.nlm.nih.gov/pubmed/1323601

Chan, I. S., Guy, C. D., Chen, Y., Lu, J., Swiderska-Syn, M., Michelotti, G. A., … Diehl, A. M. (2012). Paracrine Hedgehog signaling drives metabolic changes in hepatocellular carcinoma. *Cancer Research*, *72*(24), 6344–50. doi:10.1158/0008-5472.CAN-12-1068

Chen, W. S., Xu, P. Z., Gottlob, K., Chen, M. L., Sokol, K., Shiyanova, T., … Hay, N. (2001). Growth retardation and increased apoptosis in mice with homozygous disruption of the Akt1 gene. *Genes & Development*, *15*(17), 2203–8. doi:10.1101/gad.913901

Chen, Y., Huang, Y., Reiberger, T., Duyverman, A. M., Huang, P., Samuel, R., … Duda, D. G. (2014). Differential effects of sorafenib on liver versus tumor fibrosis mediated by stromal-derived factor 1 alpha/C-X-C receptor type 4 axis and myeloid differentiation antigen-positive myeloid cell infiltration in mice. *Hepatology (Baltimore, Md.)*, *59*(4), 1435–47. doi:10.1002/hep.26790

Cheng, A.-L., Guan, Z., Chen, Z., Tsao, C.-J., Qin, S., Kim, J. S., … Kang, Y.-K. (2012). Efficacy and safety of sorafenib in patients with advanced hepatocellular carcinoma according to baseline status: subset analyses of the phase III Sorafenib Asia-Pacific trial. *European Journal of Cancer (Oxford, England : 1990)*, *48*(10), 1452–65. doi:10.1016/j.ejca.2011.12.006

Cheng, A.-L., Kang, Y.-K., Chen, Z., Tsao, C.-J., Qin, S., Kim, J. S., … Guan, Z. (2009). Efficacy and safety of sorafenib in patients in the Asia-Pacific region with advanced hepatocellular carcinoma: a phase III randomised, double-blind, placebo-controlled trial. *The Lancet Oncology*, *10*(1), 25–34. doi:10.1016/S1470-2045(08)70285-7

Chiang, D. Y., Villanueva, A., Hoshida, Y., Peix, J., Newell, P., Minguez, B., …

Llovet, J. M. (2008). Focal gains of VEGFA and molecular classification of hepatocellular carcinoma. *Cancer Research*, *68*(16), 6779–88. doi:10.1158/0008-5472.CAN-08-0742

Chin, Y. R., & Toker, A. (2009). Function of Akt/PKB signaling to cell motility, invasion and the tumor stroma in cancer. *Cellular Signalling*, *21*(4), 470–6. doi:10.1016/j.cellsig.2008.11.015

Chin, Y. R., & Toker, A. (2011). Akt isoform-specific signaling in breast cancer: uncovering an anti-migratory role for palladin. *Cell Adhesion & Migration*, *5*(3), 211–4. Retrieved from http://www.pubmedcentral.nih.gov/articlerender.fcgi?artid=3210203&tool=pmcentrez&rendertype=abstract

Chin, Y. R., Yuan, X., Balk, S. P., & Toker, A. (2014). PTEN-Deficient Tumors Depend on AKT2 for Maintenance and Survival. *Cancer Discovery*. doi:10.1158/2159-8290.CD-13-0873

Cho, H., Mu, J., Kim, J. K., Thorvaldsen, J. L., Chu, Q., Crenshaw, E. B., … Birnbaum, M. J. (2001). Insulin resistance and a diabetes mellitus-like syndrome in mice lacking the protein kinase Akt2 (PKB beta). *Science (New York, N.Y.)*, *292*(5522), 1728–31. doi:10.1126/science.292.5522.1728

Cho, H., Thorvaldsen, J. L., Chu, Q., Feng, F., & Birnbaum, M. J. (2001). Akt1/PKBalpha is required for normal growth but dispensable for maintenance of glucose homeostasis in mice. *The Journal of Biological Chemistry*, *276*(42), 38349–52. doi:10.1074/jbc.C100462200

Copple, B. L. (2010). Hypoxia stimulates hepatocyte epithelial to mesenchymal transition by hypoxia-inducible factor and transforming growth factor-beta-dependent mechanisms. *Liver International : Official Journal of the International Association for the Study of the Liver*, *30*(5), 669–82. doi:10.1111/j.1478-3231.2010.02205.x

Dedes, K. J., Wetterskog, D., Mendes-Pereira, A. M., Natrajan, R., Lambros, M. B., Geyer, F. C., … Reis-Filho, J. S. (2010). PTEN deficiency in endometrioid

endometrial adenocarcinomas predicts sensitivity to PARP inhibitors. *Science Translational Medicine*, *2*(53), 53ra75. doi:10.1126/scitranslmed.3001538

Deng, Q., Wang, Q., Zong, W.-Y., Zheng, D.-L., Wen, Y.-X., Wang, K.-S., … Han, Z.-G. (2010). E2F8 contributes to human hepatocellular carcinoma via regulating cell proliferation. *Cancer Research*, *70*(2), 782–91. doi:10.1158/0008-5472.CAN-09-3082

Dong, L., Yang, G., Pan, Y., Chen, Y., Tan, Y., Dai, R., … Wang, H. (2011). The oncoprotein p28GANK establishes a positive feedback loop in β-catenin signaling. *Cell Research*, *21*(8), 1248–61. doi:10.1038/cr.2011.103

Drew, Y., Mulligan, E. A., Vong, W.-T., Thomas, H. D., Kahn, S., Kyle, S., … Curtin, N. J. (2011). Therapeutic potential of poly(ADP-ribose) polymerase inhibitor AG014699 in human cancers with mutated or methylated BRCA1 or BRCA2. *Journal of the National Cancer Institute*, *103*(4), 334–46. doi:10.1093/jnci/djq509

Duda, D. G., Kozin, S. V, Kirkpatrick, N. D., Xu, L., Fukumura, D., & Jain, R. K. (2011). CXCL12 (SDF1alpha)-CXCR4/CXCR7 pathway inhibition: an emerging sensitizer for anticancer therapies? *Clinical Cancer Research : An Official Journal of the American Association for Cancer Research*, *17*(8), 2074–80. doi:10.1158/1078-0432.CCR-10-2636

Dudgeon, C., Peng, R., Wang, P., Sebastiani, A., Yu, J., & Zhang, L. (2012). Inhibiting oncogenic signaling by sorafenib activates PUMA via GSK3β and NF-κB to suppress tumor cell growth. *Oncogene*, *31*(46), 4848–58. doi:10.1038/onc.2011.644

Dummler, B., Tschopp, O., Hynx, D., Yang, Z.-Z., Dirnhofer, S., & Hemmings, B. A. (2006). Life with a single isoform of Akt: mice lacking Akt2 and Akt3 are viable but display impaired glucose homeostasis and growth deficiencies. *Molecular and Cellular Biology*, *26*(21), 8042–51. doi:10.1128/MCB.00722-06

Eckers, A., Reimann, K., & Klotz, L.-O. (2009). Nickel and copper ion-induced stress signaling in human hepatoma cells: analysis of phosphoinositide 3'-

kinase/Akt signaling. *Biometals : An International Journal on the Role of Metal Ions in Biology, Biochemistry, and Medicine*, *22*(2), 307–16. doi:10.1007/s10534-008-9167-2

Eisenberg, E., & Levanon, E. Y. (2003). Human housekeeping genes are compact. *Trends in Genetics : TIG*, *19*(7), 356–62. doi:10.1016/S0168-9525(03)00137-9

El-Serag, H. B. (2011). Hepatocellular carcinoma. *The New England Journal of Medicine*, *365*(12), 1118–27. doi:10.1056/NEJMra1001683

Elstrom, R. L., Bauer, D. E., Buzzai, M., Karnauskas, R., Harris, M. H., Plas, D. R., … Thompson, C. B. (2004). Akt stimulates aerobic glycolysis in cancer cells. *Cancer Research*, *64*(11), 3892–9. doi:10.1158/0008-5472.CAN-03-2904

Engelman, J. a. (2009). Targeting PI3K signalling in cancer: opportunities, challenges and limitations. *Nature Reviews. Cancer*, *9*(8), 550–62. doi:10.1038/nrc2664

Fabregat, I., Roncero, C., & Fernández, M. (2007). Survival and apoptosis: a dysregulated balance in liver cancer. *Liver International : Official Journal of the International Association for the Study of the Liver*, *27*(2), 155–62. doi:10.1111/j.1478-3231.2006.01409.x

Fang, M., Shen, Z., Huang, S., Zhao, L., Chen, S., Mak, T. W., & Wang, X. (2010). The ER UDPase ENTPD5 promotes protein N-glycosylation, the Warburg effect, and proliferation in the PTEN pathway. *Cell*, *143*(5), 711–24. doi:10.1016/j.cell.2010.10.010

Farazi, P. A., & DePinho, R. A. (2006). Hepatocellular carcinoma pathogenesis: from genes to environment. *Nature Reviews. Cancer*, *6*(9), 674–87. doi:10.1038/nrc1934

Farmer, H., McCabe, N., Lord, C. J., Tutt, A. N. J., Johnson, D. A., Richardson, T. B., … Ashworth, A. (2005). Targeting the DNA repair defect in BRCA mutant cells as a therapeutic strategy. *Nature*, *434*(7035), 917–21. doi:10.1038/nature03445

Ferlay, J., Shin, H.-R., Bray, F., Forman, D., Mathers, C., & Parkin, D. M. (2010). Estimates of worldwide burden of cancer in 2008: GLOBOCAN 2008. *International Journal of Cancer. Journal International Du Cancer*, *127*(12), 2893–917. doi:10.1002/ijc.25516

Fong, P. C., Boss, D. S., Yap, T. A., Tutt, A., Wu, P., Mergui-Roelvink, M., … de Bono, J. S. (2009). Inhibition of poly(ADP-ribose) polymerase in tumors from BRCA mutation carriers. *The New England Journal of Medicine*, *361*(2), 123–34. doi:10.1056/NEJMoa0900212

Fruman, D. A., & Rommel, C. (2014). PI3K and cancer: lessons, challenges and opportunities. *Nature Reviews. Drug Discovery*, *13*(2), 140–56. doi:10.1038/nrd4204

Fujimoto, A., Totoki, Y., Abe, T., Boroevich, K. a, Hosoda, F., Nguyen, H. H., … Nakagawa, H. (2012). Whole-genome sequencing of liver cancers identifies etiological influences on mutation patterns and recurrent mutations in chromatin regulators. *Nature Genetics*, *44*(7), 760–4. doi:10.1038/ng.2291

Fujiwara, Y., Hoon, D. S., Yamada, T., Umeshita, K., Gotoh, M., Sakon, M., … Monden, M. (2000). PTEN / MMAC1 mutation and frequent loss of heterozygosity identified in chromosome 10q in a subset of hepatocellular carcinomas. *Japanese Journal of Cancer Research : Gann*, *91*(3), 287–92. Retrieved from http://www.ncbi.nlm.nih.gov/pubmed/10760687

Gao, Q., Wang, X.-Y., Fan, J., Qiu, S.-J., Zhou, J., Shi, Y.-H., … Sun, J. (2008). Selection of reference genes for real-time PCR in human hepatocellular carcinoma tissues. *Journal of Cancer Research and Clinical Oncology*, *134*(9), 979–86. doi:10.1007/s00432-008-0369-3

Garofalo, R. S., Orena, S. J., Rafidi, K., Torchia, A. J., Stock, J. L., Hildebrandt, A. L., … Coleman, K. G. (2003). Severe diabetes, age-dependent loss of adipose tissue, and mild growth deficiency in mice lacking Akt2/PKB beta. *The Journal of Clinical Investigation*, *112*(2), 197–208. doi:10.1172/JCI16885

Gerber, P. A., Hippe, A., Buhren, B. A., Müller, A., & Homey, B. (2009).

Chemokines in tumor-associated angiogenesis. *Biological Chemistry*, *390*(12), 1213–23. doi:10.1515/BC.2009.144

Goldstein, J. C., Waterhouse, N. J., Juin, P., Evan, G. I., & Green, D. R. (2000). The coordinate release of cytochrome c during apoptosis is rapid, complete and kinetically invariant. *Nature Cell Biology*, *2*(3), 156–62. doi:10.1038/35004029

Gonzalez, E., & McGraw, T. E. (2009). The Akt kinases: isoform specificity in metabolism and cancer. *Cell Cycle (Georgetown, Tex.)*, *8*(16), 2502–8. Retrieved from http://www.pubmedcentral.nih.gov/articlerender.fcgi?artid=2997486&tool=pmcentrez&rendertype=abstract

Graupera, M., Guillermet-Guibert, J., Foukas, L. C., Phng, L.-K., Cain, R. J., Salpekar, A., … Vanhaesebroeck, B. (2008). Angiogenesis selectively requires the p110alpha isoform of PI3K to control endothelial cell migration. *Nature*, *453*(7195), 662–6. doi:10.1038/nature06892

Graupera, M., & Potente, M. (2013). Regulation of angiogenesis by PI3K signaling networks. *Experimental Cell Research*, *319*(9), 1348–55. doi:10.1016/j.yexcr.2013.02.021

Guertin, D. a, & Sabatini, D. M. (2007). Defining the role of mTOR in cancer. *Cancer Cell*, *12*(1), 9–22. doi:10.1016/j.ccr.2007.05.008

Ha, H.-L., Shin, H.-J., Feitelson, M. A., & Yu, D.-Y. (2010). Oxidative stress and antioxidants in hepatic pathogenesis. *World Journal of Gastroenterology : WJG*, *16*(48), 6035–43. Retrieved from http://www.pubmedcentral.nih.gov/articlerender.fcgi?artid=3012582&tool=pmcentrez&rendertype=abstract

Haendeler, J., Hoffmann, J., Rahman, S., Zeiher, A. M., & Dimmeler, S. (2003). Regulation of telomerase activity and anti-apoptotic function by protein-protein interaction and phosphorylation. *FEBS Letters*, *536*(1-3), 180–6. Retrieved from http://www.ncbi.nlm.nih.gov/pubmed/12586360

Han, Z.-G. (2012). *Functional genomic studies: insights into the pathogenesis of liver cancer. Annual review of genomics and human genetics* (Vol. 13, pp. 171–205). doi:10.1146/annurev-genom-090711-163752

Hanahan, D., & Weinberg, R. a. (2011). Hallmarks of cancer: the next generation. *Cell*, *144*(5), 646–74. doi:10.1016/j.cell.2011.02.013

Harrold, J. M., Ramanathan, M., & Mager, D. E. (2013). Network-based approaches in drug discovery and early development. *Clinical Pharmacology and Therapeutics*, *94*(6), 651–8. doi:10.1038/clpt.2013.176

Hatano, E., & Brenner, D. A. (2001). Akt protects mouse hepatocytes from TNF-alpha- and Fas-mediated apoptosis through NK-kappa B activation. *American Journal of Physiology. Gastrointestinal and Liver Physiology*, *281*(6), G1357–68. Retrieved from http://www.ncbi.nlm.nih.gov/pubmed/11705740

He, A. R., & Goldenberg, A. S. (2013). Treating hepatocellular carcinoma progression following first-line sorafenib: therapeutic options and clinical observations. *Therapeutic Advances in Gastroenterology*, *6*(6), 447–58. doi:10.1177/1756283X13498540

Honda, K., Sbisà, E., Tullo, a, Papeo, P. a, Saccone, C., Poole, S., … Habib, N. a. (1998). P53 Mutation Is a Poor Prognostic Indicator for Survival in Patients With Hepatocellular Carcinoma Undergoing Surgical Tumour Ablation. *British Journal of Cancer*, *77*(5), 776–82. Retrieved from http://www.pubmedcentral.nih.gov/articlerender.fcgi?artid=2149958&tool=pmcentrez&rendertype=abstract

Horger, M., Lauer, U. M., Schraml, C., Berg, C. P., Koppenhöfer, U., Claussen, C. D., … Bitzer, M. (2009). Early MRI response monitoring of patients with advanced hepatocellular carcinoma under treatment with the multikinase inhibitor sorafenib. *BMC Cancer*, *9*, 208. doi:10.1186/1471-2407-9-208

Hsiao, L. L., Dangond, F., Yoshida, T., Hong, R., Jensen, R. V, Misra, J., … Gullans, S. R. (2001). A compendium of gene expression in normal human tissues. *Physiological Genomics*, *7*(2), 97–104.

doi:10.1152/physiolgenomics.00040.2001

Hu, T.-H., Huang, C.-C., Lin, P.-R., Chang, H.-W., Ger, L.-P., Lin, Y.-W., … Tai, M.-H. (2003). Expression and prognostic role of tumor suppressor gene PTEN/MMAC1/TEP1 in hepatocellular carcinoma. *Cancer*, *97*(8), 1929–40. doi:10.1002/cncr.11266

Hu, Y., Shen, Y., Ji, B., Yin, S., Ren, X., Chen, T., … Zhang, Y. (2011). Liver-specific gene therapy of hepatocellular carcinoma by targeting human telomerase reverse transcriptase with pegylated immuno-lipopolyplexes. *European Journal of Pharmaceutics and Biopharmaceutics : Official Journal of Arbeitsgemeinschaft Für Pharmazeutische Verfahrenstechnik e.V*, *78*(3), 320–5. doi:10.1016/j.ejpb.2010.12.036

Hussain, S. P., Schwank, J., Staib, F., Wang, X. W., & Harris, C. C. (2007). TP53 mutations and hepatocellular carcinoma: insights into the etiology and pathogenesis of liver cancer. *Oncogene*, *26*(15), 2166–76. doi:10.1038/sj.onc.1210279

Hwang, Y. H., Choi, J. Y., Kim, S., Chung, E. S., Kim, T., Koh, S. S., … Park, Y. M. (2004). Over-expression of c-raf-1 proto-oncogene in liver cirrhosis and hepatocellular carcinoma. *Hepatology Research : The Official Journal of the Japan Society of Hepatology*, *29*(2), 113–121. doi:10.1016/j.hepres.2004.02.009

Imose, M., Nagaki, M., Naiki, T., Osawa, Y., Brenner, D. A., Asano, T., … Moriwaki, H. (2003). Inhibition of nuclear factor kappaB and phosphatidylinositol 3-kinase/Akt is essential for massive hepatocyte apoptosis induced by tumor necrosis factor alpha in mice. *Liver International : Official Journal of the International Association for the Study of the Liver*, *23*(5), 386–96. Retrieved from http://www.ncbi.nlm.nih.gov/pubmed/14708901

Isik, Z., Ersahin, T., Atalay, V., Aykanat, C., & Cetin-Atalay, R. (2012). A signal transduction score flow algorithm for cyclic cellular pathway analysis, which combines transcriptome and ChIP-seq data. *Molecular bioSystems*, *8*(12), 3224–31. doi:10.1039/c2mb25215e

Jemal, A., Bray, F., & Ferlay, J. (2011). Global Cancer Statistics. *CA CANCER J CLIN*, *61*(2), 69–90. doi:10.3322/caac.20107.Available

Jia, S., Roberts, T. M., & Zhao, J. J. (2009). Should individual PI3 kinase isoforms be targeted in cancer? *Current Opinion in Cell Biology*, *21*(2), 199–208. doi:10.1016/j.ceb.2008.12.007

Jung, M., Drapier, J. C., Weidenbach, H., Renia, L., Oliveira, L., Wang, A., … Nussler, A. K. (2000). Effects of hepatocellular iron imbalance on nitric oxide and reactive oxygen intermediates production in a model of sepsis. *Journal of Hepatology*, *33*(3), 387–94. Retrieved from http://www.ncbi.nlm.nih.gov/pubmed/11019994

Juvekar, A., Burga, L. N., Hu, H., Lunsford, E. P., Ibrahim, Y. H., Balmañà, J., … Wulf, G. M. (2012). Combining a PI3K inhibitor with a PARP inhibitor provides an effective therapy for BRCA1-related breast cancer. *Cancer Discovery*, *2*(11), 1048–63. doi:10.1158/2159-8290.CD-11-0336

Kang, S. S., Kwon, T., Kwon, D. Y., & Do, S. I. (1999). Akt protein kinase enhances human telomerase activity through phosphorylation of telomerase reverse transcriptase subunit. *The Journal of Biological Chemistry*, *274*(19), 13085–90. Retrieved from http://www.ncbi.nlm.nih.gov/pubmed/10224060

Kawamura, N., Nagai, H., Bando, K., Koyama, M., Matsumoto, S., Tajiri, T., … Emi, M. (1999). PTEN/MMAC1 mutations in hepatocellular carcinomas: somatic inactivation of both alleles in tumors. *Japanese Journal of Cancer Research : Gann*, *90*(4), 413–8. Retrieved from http://www.ncbi.nlm.nih.gov/pubmed/10363579

Kedderis, G. L. (1996). Biochemical basis of hepatocellular injury. *Toxicologic Pathology*, *24*(1), 77–83. Retrieved from http://www.ncbi.nlm.nih.gov/pubmed/8839284

Kimbung, S., Biskup, E., Johansson, I., Aaltonen, K., Ottosson-Wadlund, A., Gruvberger-Saal, S., … Hedenfalk, I. (2012). Co-targeting of the PI3K pathway improves the response of BRCA1 deficient breast cancer cells to PARP1

inhibition. *Cancer Letters*, *319*(2), 232–41. doi:10.1016/j.canlet.2012.01.015

Ladu, S., Calvisi, D. F., Conner, E. A., Farina, M., Factor, V. M., & Thorgeirsson, S. S. (2008). E2F1 inhibits c-Myc-driven apoptosis via PIK3CA/Akt/mTOR and COX-2 in a mouse model of human liver cancer. *Gastroenterology*, *135*(4), 1322–32. doi:10.1053/j.gastro.2008.07.012

Lamouille, S., Xu, J., & Derynck, R. (2014). Molecular mechanisms of epithelial–mesenchymal transition. *Nature Reviews Molecular Cell Biology*, *15*(3), 178–196. doi:10.1038/nrm3758

Lee, J.-S., Kim, J. H., Park, Y.-Y., & Mills, G. B. (2011). Systems biology approaches to decoding the genome of liver cancer. *Cancer Research and Treatment : Official Journal of Korean Cancer Association*, *43*(4), 205–11. doi:10.4143/crt.2011.43.4.205

Lee, T. K., Poon, R. T. P., Yuen, A. P., Ling, M. T., Kwok, W. K., Wang, X. H., … Fan, S. T. (2006). Twist overexpression correlates with hepatocellular carcinoma metastasis through induction of epithelial-mesenchymal transition. *Clinical Cancer Research : An Official Journal of the American Association for Cancer Research*, *12*(18), 5369–76. doi:10.1158/1078-0432.CCR-05-2722

Levine, A. J., & Puzio-Kuter, A. M. (2010). The Control of the Metabolic Switch in Cancers by Oncogenes and Tumor Suppressor Genes. *Science (New York, N.Y.)*, *330*(December 2010), 1340–1345.

Li, W.-C., Ye, S.-L., Sun, R.-X., Liu, Y.-K., Tang, Z.-Y., Kim, Y., … Zhang, H. (2006). Inhibition of growth and metastasis of human hepatocellular carcinoma by antisense oligonucleotide targeting signal transducer and activator of transcription 3. *Clinical Cancer Research : An Official Journal of the American Association for Cancer Research*, *12*(23), 7140–8. doi:10.1158/1078-0432.CCR-06-0484

Li, X. M., Tang, Z. Y., Zhou, G., Lui, Y. K., & Ye, S. L. (1998). Significance of vascular endothelial growth factor mRNA expression in invasion and metastasis of hepatocellular carcinoma. *Journal of Experimental & Clinical Cancer*

Research : CR, *17*(1), 13–7. Retrieved from http://www.ncbi.nlm.nih.gov/pubmed/9646228

Li, Y. Y., & Jones, S. J. (2012). Drug repositioning for personalized medicine. *Genome Medicine*, *4*(3), 27. doi:10.1186/gm326

Li, Z., Dong, X., Dong, X., Wang, Z., Liu, W., Deng, N., … Wu, D. (2005). Regulation of PTEN by Rho small GTPases. *Nature Cell Biology*, *7*(4), 399–404. doi:10.1038/ncb1236

Liang, Y., Zheng, T., Song, R., Wang, J., Yin, D., Wang, L., … Liu, L. (2013). Hypoxia-mediated sorafenib resistance can be overcome by EF24 through Von Hippel-Lindau tumor suppressor-dependent HIF-1α inhibition in hepatocellular carcinoma. *Hepatology (Baltimore, Md.)*, *57*(5), 1847–57. doi:10.1002/hep.26224

Liu, J., Zhu, Q., Li, J., Zhao, S., & Li, L. (2008). The retrovirus-mediated antisense human telomerase RNA (hTR) gene limits the growth of hepatocellular carcinoma growth in cell culture and animals. *Digestive Diseases and Sciences*, *53*(4), 1122–30. doi:10.1007/s10620-007-9980-4

Liu, L., Cao, Y., Chen, C., Zhang, X., McNabola, A., Wilkie, D., … Carter, C. (2006). Sorafenib blocks the RAF/MEK/ERK pathway, inhibits tumor angiogenesis, and induces tumor cell apoptosis in hepatocellular carcinoma model PLC/PRF/5. *Cancer Research*, *66*(24), 11851–8. doi:10.1158/0008-5472.CAN-06-1377

Liu, L., Ho, R. L. K., Chen, G. G., & Lai, P. B. S. (2012). Sorafenib inhibits hypoxia-inducible factor-1α synthesis: implications for antiangiogenic activity in hepatocellular carcinoma. *Clinical Cancer Research : An Official Journal of the American Association for Cancer Research*, *18*(20), 5662–71. doi:10.1158/1078-0432.CCR-12-0552

Liu, L., Zhu, X.-D., Wang, W.-Q., Shen, Y., Qin, Y., Ren, Z.-G., … Tang, Z.-Y. (2010). Activation of beta-catenin by hypoxia in hepatocellular carcinoma contributes to enhanced metastatic potential and poor prognosis. *Clinical*

Cancer Research : An Official Journal of the American Association for Cancer Research, *16*(10), 2740–50. doi:10.1158/1078-0432.CCR-09-2610

Liu, P., Cheng, H., Roberts, T. M., & Zhao, J. J. (2009). Targeting the phosphoinositide 3-kinase pathway in cancer. *Nature Reviews. Drug Discovery*, *8*(8), 627–44. doi:10.1038/nrd2926

Liu, Y., Fuchs, J., Li, C., & Lin, J. (2010). IL-6, a risk factor for hepatocellular carcinoma: FLLL32 inhibits IL-6-induced STAT3 phosphorylation in human hepatocellular cancer cells. *Cell Cycle (Georgetown, Tex.)*, *9*(17), 3423–7. Retrieved from http://www.ncbi.nlm.nih.gov/pubmed/20818158

Llovet, J. M., Di Bisceglie, A. M., Bruix, J., Kramer, B. S., Lencioni, R., Zhu, A. X., … Gores, G. J. (2008). Design and endpoints of clinical trials in hepatocellular carcinoma. *Journal of the National Cancer Institute*, *100*(10), 698–711. doi:10.1093/jnci/djn134

Llovet, J. M., Ricci, S., Mazzaferro, V., Hilgard, P., Gane, E., Blanc, J.-F., … Bruix, J. (2008). Sorafenib in advanced hepatocellular carcinoma. *The New England Journal of Medicine*, *359*(4), 378–90. doi:10.1056/NEJMoa0708857

Manning, B. D., & Cantley, L. C. (2007). AKT/PKB signaling: navigating downstream. *Cell*, *129*(7), 1261–74. doi:10.1016/j.cell.2007.06.009

Martin, M., Rehani, K., Jope, R. S., & Michalek, S. M. (2005). Toll-like receptor-mediated cytokine production is differentially regulated by glycogen synthase kinase 3. *Nature Immunology*, *6*(8), 777–84. doi:10.1038/ni1221

Matsuo, N., Shiraha, H., Fujikawa, T., Takaoka, N., Ueda, N., Tanaka, S., … Yamamoto, K. (2009). Twist expression promotes migration and invasion in hepatocellular carcinoma. *BMC Cancer*, *9*, 240. doi:10.1186/1471-2407-9-240

Mazzocca, A., Fransvea, E., Dituri, F., Lupo, L., Antonaci, S., & Giannelli, G. (2010). Down-regulation of connective tissue growth factor by inhibition of transforming growth factor beta blocks the tumor-stroma cross-talk and tumor progression in hepatocellular carcinoma. *Hepatology (Baltimore, Md.)*, *51*(2),

523–34. doi:10.1002/hep.23285

McCabe, N., Turner, N. C., Lord, C. J., Kluzek, K., Bialkowska, A., Swift, S., … Ashworth, A. (2006). Deficiency in the repair of DNA damage by homologous recombination and sensitivity to poly(ADP-ribose) polymerase inhibition. *Cancer Research*, *66*(16), 8109–15. doi:10.1158/0008-5472.CAN-06-0140

McEllin, B., Camacho, C. V, Mukherjee, B., Hahm, B., Tomimatsu, N., Bachoo, R. M., & Burma, S. (2010). PTEN loss compromises homologous recombination repair in astrocytes: implications for glioblastoma therapy with temozolomide or poly(ADP-ribose) polymerase inhibitors. *Cancer Research*, *70*(13), 5457–64. doi:10.1158/0008-5472.CAN-09-4295

Mendes-Pereira, A. M., Martin, S. A., Brough, R., McCarthy, A., Taylor, J. R., Kim, J.-S., … Ashworth, A. (2009). Synthetic lethal targeting of PTEN mutant cells with PARP inhibitors. *EMBO Molecular Medicine*, *1*(6-7), 315–22. doi:10.1002/emmm.200900041

Mitsuhashi, N., Shimizu, H., Ohtsuka, M., Wakabayashi, Y., Ito, H., Kimura, F., … Miyazaki, M. (2003). Angiopoietins and Tie-2 expression in angiogenesis and proliferation of human hepatocellular carcinoma. *Hepatology (Baltimore, Md.)*, *37*(5), 1105–13. doi:10.1053/jhep.2003.50204

Monnier, J., Boissan, M., L'Helgoualc'h, A., Lacombe, M.-L., Turlin, B., Zucman-Rossi, J., … Samson, M. (2012). CXCR7 is up-regulated in human and murine hepatocellular carcinoma and is specifically expressed by endothelial cells. *European Journal of Cancer (Oxford, England : 1990)*, *48*(1), 138–48. doi:10.1016/j.ejca.2011.06.044

Nakagawa, H., & Shibata, T. (2013). Comprehensive genome sequencing of the liver cancer genome. *Cancer Letters*, *340*(2), 234–240. doi:10.1016/j.canlet.2012.10.035

Ng, I. O., Poon, R. T., Lee, J. M., Fan, S. T., Ng, M., & Tso, W. K. (2001). Microvessel density, vascular endothelial growth factor and its receptors Flt-1 and Flk-1/KDR in hepatocellular carcinoma. *American Journal of Clinical*

Pathology, *116*(6), 838–45. doi:10.1309/FXNL-QTN1-94FH-AB3A

Niu, R. F., Zhang, L., Xi, G. M., Wei, X. Y., Yang, Y., Shi, Y. R., & Hao, X. S. (2007). Up-regulation of Twist induces angiogenesis and correlates with metastasis in hepatocellular carcinoma. *Journal of Experimental & Clinical Cancer Research : CR*, *26*(3), 385–94. Retrieved from http://www.ncbi.nlm.nih.gov/pubmed/17987801

Niwa, Y., Kanda, H., Shikauchi, Y., Saiura, A., Matsubara, K., Kitagawa, T., … Yoshikawa, H. (2005). Methylation silencing of SOCS-3 promotes cell growth and migration by enhancing JAK/STAT and FAK signalings in human hepatocellular carcinoma. *Oncogene*, *24*(42), 6406–17. doi:10.1038/sj.onc.1208788

Noh, K. H., Kang, T. H., Kim, J. H., Pai, S. I., Lin, K. Y., Hung, C.-F., … Kim, T. W. (2009). Activation of Akt as a mechanism for tumor immune evasion. *Molecular Therapy : The Journal of the American Society of Gene Therapy*, *17*(3), 439–47. doi:10.1038/mt.2008.255

Nomura, F., Yaguchi, M., Togawa, A., Miyazaki, M., Isobe, K., Miyake, M., … Nakai, T. (2000). Enhancement of poly-adenosine diphosphate-ribosylation in human hepatocellular carcinoma. *Journal of Gastroenterology and Hepatology*, *15*(5), 529–35. Retrieved from http://www.ncbi.nlm.nih.gov/pubmed/10847440

Oh, B.-K., Jo Chae, K., Park, C., Kim, K., Jung Lee, W., Han, K., & Nyun Park, Y. (2003). Telomere shortening and telomerase reactivation in dysplastic nodules of human hepatocarcinogenesis. *Journal of Hepatology*, *39*(5), 786–792. doi:10.1016/S0168-8278(03)00395-7

Oh, B.-K., Kim, H., Park, Y. N., Yoo, J. E., Choi, J., Kim, K.-S., … Park, C. (2008). High telomerase activity and long telomeres in advanced hepatocellular carcinomas with poor prognosis. *Laboratory Investigation; a Journal of Technical Methods and Pathology*, *88*(2), 144–52. doi:10.1038/labinvest.3700710

Ozcelik, D., Ozaras, R., Gurel, Z., Uzun, H., & Aydin, S. (2003). Copper-mediated

oxidative stress in rat liver. *Biological Trace Element Research*, *96*(1-3), 209–15. doi:10.1385/BTER:96:1-3:209

Pan, Y., Tan, Y., Wang, M., Zhang, J., Zhang, B., Yang, C., … Wang, H. (2013). Signal regulatory protein α is associated with tumor-polarized macrophages phenotype switch and plays a pivotal role in tumor progression. *Hepatology (Baltimore, Md.)*, *58*(2), 680–91. doi:10.1002/hep.26391

Pang, R., & Poon, R. T. P. (2006). Angiogenesis and antiangiogenic therapy in hepatocellular carcinoma. *Cancer Letters*, *242*(2), 151–67. doi:10.1016/j.canlet.2006.01.008

Pedroza-Gonzalez, A., Verhoef, C., Ijzermans, J. N. M., Peppelenbosch, M. P., Kwekkeboom, J., Verheij, J., … Sprengers, D. (2013). Activated tumor-infiltrating CD4+ regulatory T cells restrain antitumor immunity in patients with primary or metastatic liver cancer. *Hepatology (Baltimore, Md.)*, *57*(1), 183–94. doi:10.1002/hep.26013

Perz, J. F., Armstrong, G. L., Farrington, L. a, Hutin, Y. J. F., & Bell, B. P. (2006). The contributions of hepatitis B virus and hepatitis C virus infections to cirrhosis and primary liver cancer worldwide. *Journal of Hepatology*, *45*(4), 529–38. doi:10.1016/j.jhep.2006.05.013

Plentz, R. R., Caselitz, M., Bleck, J. S., Gebel, M., Flemming, P., Kubicka, S., … Rudolph, K. L. (2004). Hepatocellular telomere shortening correlates with chromosomal instability and the development of human hepatoma. *Hepatology (Baltimore, Md.)*, *40*(1), 80–6. doi:10.1002/hep.20271

Poon, R. T. P., Ho, J. W. Y., Tong, C. S. W., Lau, C., Ng, I. O. L., & Fan, S.-T. (2004). Prognostic significance of serum vascular endothelial growth factor and endostatin in patients with hepatocellular carcinoma. *The British Journal of Surgery*, *91*(10), 1354–60. doi:10.1002/bjs.4594

Porta, C., De Amici, M., Quaglini, S., Paglino, C., Tagliani, F., Boncimino, A., … Corazza, G. R. (2008). Circulating interleukin-6 as a tumor marker for hepatocellular carcinoma. *Annals of Oncology : Official Journal of the*

European Society for Medical Oncology / ESMO, *19*(2), 353–8. doi:10.1093/annonc/mdm448

Porta, C., Paglino, C., & Mosca, A. (2014). Targeting PI3K/Akt/mTOR Signaling in Cancer. *Frontiers in Oncology*, *4*, 64. doi:10.3389/fonc.2014.00064

Potente, M., Urbich, C., Sasaki, K., Hofmann, W. K., Heeschen, C., Aicher, A., … Dimmeler, S. (2005). Involvement of Foxo transcription factors in angiogenesis and postnatal neovascularization. *The Journal of Clinical Investigation*, *115*(9), 2382–92. doi:10.1172/JCI23126

Raoul, J.-L., Bruix, J., Greten, T. F., Sherman, M., Mazzaferro, V., Hilgard, P., … Llovet, J. M. (2012). Relationship between baseline hepatic status and outcome, and effect of sorafenib on liver function: SHARP trial subanalyses. *Journal of Hepatology*, *56*(5), 1080–8. doi:10.1016/j.jhep.2011.12.009

Rebouissou, S., Amessou, M., Couchy, G., Poussin, K., Imbeaud, S., Pilati, C., … Zucman-Rossi, J. (2009). Frequent in-frame somatic deletions activate gp130 in inflammatory hepatocellular tumours. *Nature*, *457*(7226), 200–4. doi:10.1038/nature07475

Rodon, J., Dienstmann, R., Serra, V., & Tabernero, J. (2013). Development of PI3K inhibitors: lessons learned from early clinical trials. *Nature Reviews. Clinical Oncology*, *10*(3), 143–53. doi:10.1038/nrclinonc.2013.10

Sakurai, T., He, G., Matsuzawa, A., Yu, G.-Y., Maeda, S., Hardiman, G., & Karin, M. (2008). Hepatocyte necrosis induced by oxidative stress and IL-1 alpha release mediate carcinogen-induced compensatory proliferation and liver tumorigenesis. *Cancer Cell*, *14*(2), 156–65. doi:10.1016/j.ccr.2008.06.016

Sethi, N., & Kang, Y. (2011). Unravelling the complexity of metastasis - molecular understanding and targeted therapies. *Nature Reviews. Cancer*, *11*(10), 735–48. doi:10.1038/nrc3125

Shen, W. H., Balajee, A. S., Wang, J., Wu, H., Eng, C., Pandolfi, P. P., & Yin, Y. (2007). Essential role for nuclear PTEN in maintaining chromosomal integrity.

Cell, *128*(1), 157–70. doi:10.1016/j.cell.2006.11.042

Shen, Y.-C., Lin, Z.-Z., Hsu, C.-H., Hsu, C., Shao, Y.-Y., & Cheng, A.-L. (2013). Clinical Trials in Hepatocellular Carcinoma: An Update. *Liver Cancer*, *2*(3-4), 345–364. doi:10.1159/000343850

Shen, Z., Huang, S., Fang, M., & Wang, X. (2011). ENTPD5, an endoplasmic reticulum UDPase, alleviates ER stress induced by protein overloading in AKT-activated cancer cells. *Cold Spring Harbor Symposia on Quantitative Biology*, *76*, 217–23. doi:10.1101/sqb.2011.76.010876

Shim, J. S., & Liu, J. O. (2014). Recent Advances in Drug Repositioning for the Discovery of New Anticancer Drugs. *International Journal of Biological Sciences*, *10*(7), 654–663. doi:10.7150/ijbs.9224

Shimamura, T., Saito, S., Morita, K., Kitamura, T., Morimoto, M., Kiba, T., … Sekihara, H. (2000). Detection of vascular endothelial growth factor and its receptor expression in human hepatocellular carcinoma biopsy specimens. *Journal of Gastroenterology and Hepatology*, *15*(6), 640–6. Retrieved from http://www.ncbi.nlm.nih.gov/pubmed/10921418

Shimizu, S., Nomura, F., Tomonaga, T., Sunaga, M., Noda, M., Ebara, M., & Saisho, H. (2004). Expression of poly(ADP-ribose) polymerase in human hepatocellular carcinoma and analysis of biopsy specimens obtained under sonographic guidance. *Oncology Reports*, *12*(4), 821–5. Retrieved from http://www.ncbi.nlm.nih.gov/pubmed/15375506

Sikand, K., Singh, J., Ebron, J. S., & Shukla, G. C. (2012). Housekeeping Gene Selection Advisory: Glyceraldehyde-3-Phosphate Dehydrogenase (GAPDH) and β-Actin Are Targets of miR-644a. *PLoS ONE*, *7*(10), e47510. Retrieved from http://dx.doi.org/10.1371/journal.pone.0047510

Soldani, C., & Scovassi, A. I. (2002). Poly(ADP-ribose) polymerase-1 cleavage during apoptosis: an update. *Apoptosis : An International Journal on Programmed Cell Death*, *7*(4), 321–8. Retrieved from http://www.ncbi.nlm.nih.gov/pubmed/12101391

Song, M. S., Salmena, L., & Pandolfi, P. P. (2012). The functions and regulation of the PTEN tumour suppressor. *Nature Reviews. Molecular Cell Biology*, *13*(5), 283–96. doi:10.1038/nrm3330

Sonntag, R., Gassler, N., Bangen, J.-M., Trautwein, C., & Liedtke, C. (2014). Pro-apoptotic Sorafenib signaling in murine hepatocytes depends on malignancy and is associated with PUMA expression in vitro and in vivo. *Cell Death & Disease*, *5*, e1030. doi:10.1038/cddis.2013.557

Stark, A., Brennecke, J., Bushati, N., Russell, R. B., & Cohen, S. M. (2005, December 16). Animal MicroRNAs Confer Robustness to Gene Expression and Have a Significant Impact on 32UTR Evolution. *Cell*. Cell Press. Retrieved from http://linkinghub.elsevier.com/retrieve/pii/S0092867405012729

Sugano, Y., Matsuzaki, K., Tahashi, Y., Furukawa, F., Mori, S., Yamagata, H., … Inoue, K. (2003). Distortion of autocrine transforming growth factor beta signal accelerates malignant potential by enhancing cell growth as well as PAI-1 and VEGF production in human hepatocellular carcinoma cells. *Oncogene*, *22*(15), 2309–21. doi:10.1038/sj.onc.1206305

Sun, R. C., & Denko, N. C. (2014). Hypoxic Regulation of Glutamine Metabolism through HIF1 and SIAH2 Supports Lipid Synthesis that Is Necessary for Tumor Growth. *Cell Metabolism*, *19*(2), 285–92. doi:10.1016/j.cmet.2013.11.022

Sun, X., Sui, Q., Zhang, C., Tian, Z., & Zhang, J. (2013). Targeting blockage of STAT3 in hepatocellular carcinoma cells augments NK cell functions via reverse hepatocellular carcinoma-induced immune suppression. *Molecular Cancer Therapeutics*, *12*(12), 2885–96. doi:10.1158/1535-7163.MCT-12-1087

Sun, Y., Li, Y., Luo, D., & Liao, D. J. (2012). Pseudogenes as Weaknesses of ACTB (Actb) and GAPDH (Gapdh) Used as Reference Genes in Reverse Transcription and Polymerase Chain Reactions. *PLoS ONE*, *7*(8), e41659. Retrieved from http://dx.doi.org/10.1371/journal.pone.0041659

Tacke, R. S., Tosello-Trampont, A., Nguyen, V., Mullins, D. W., & Hahn, Y. S. (2011). Extracellular hepatitis C virus core protein activates STAT3 in human

monocytes/macrophages/dendritic cells via an IL-6 autocrine pathway. *The Journal of Biological Chemistry*, *286*(12), 10847–55. doi:10.1074/jbc.M110.217653

Takada, S., & Koike, K. (1989). Activated N-ras gene was found in human hepatoma tissue but only in a small fraction of the tumor cells. *Oncogene*, *4*(2), 189–93. Retrieved from http://www.ncbi.nlm.nih.gov/pubmed/2538792

Tang, X., Mo, C., Wang, Y., Wei, D., & Xiao, H. (2013). Anti-tumour strategies aiming to target tumour-associated macrophages. *Immunology*, *138*(2), 93–104. doi:10.1111/imm.12023

Teicher, B. A., Linehan, W. M., & Helman, L. J. (2012). Targeting cancer metabolism. *Clinical Cancer Research : An Official Journal of the American Association for Cancer Research*, *18*(20), 5537–45. doi:10.1158/1078-0432.CCR-12-2587

Thomson, A. W., Turnquist, H. R., & Raimondi, G. (2009). Immunoregulatory functions of mTOR inhibition. *Nature Reviews. Immunology*, *9*(5), 324–37. doi:10.1038/nri2546

Toh, S. T., Jin, Y., Liu, L., Wang, J., Babrzadeh, F., Gharizadeh, B., … Lee, C. G.-L. (2013). Deep sequencing of the hepatitis B virus in hepatocellular carcinoma patients reveals enriched integration events, structural alterations and sequence variations. *Carcinogenesis*, *34*(4), 787–98. doi:10.1093/carcin/bgs406

Totoki, Y., Tatsuno, K., Yamamoto, S., Arai, Y., Hosoda, F., Ishikawa, S., … Shibata, T. (2011). High-resolution characterization of a hepatocellular carcinoma genome. *Nature Genetics*, *43*(5), 464–9. doi:10.1038/ng.804

Trikha, M., Corringham, R., Klein, B., & Rossi, J.-F. (2003). Targeted anti-interleukin-6 monoclonal antibody therapy for cancer: a review of the rationale and clinical evidence. *Clinical Cancer Research : An Official Journal of the American Association for Cancer Research*, *9*(13), 4653–65. Retrieved from http://www.pubmedcentral.nih.gov/articlerender.fcgi?artid=2929399&tool=pmcentrez&rendertype=abstract

Tschopp, O., Yang, Z.-Z., Brodbeck, D., Dummler, B. A., Hemmings-Mieszczak, M., Watanabe, T., … Hemmings, B. A. (2005). Essential role of protein kinase B gamma (PKB gamma/Akt3) in postnatal brain development but not in glucose homeostasis. *Development (Cambridge, England)*, *132*(13), 2943–54. doi:10.1242/dev.01864

Tsuda, H., Hirohashi, S., Shimosato, Y., Ino, Y., Yoshida, T., & Terada, M. (1989). Low incidence of point mutation of c-Ki-ras and N-ras oncogenes in human hepatocellular carcinoma. *Japanese Journal of Cancer Research : Gann*, *80*(3), 196–9. Retrieved from http://www.ncbi.nlm.nih.gov/pubmed/2542205

Van Zijl, F., Mair, M., Csiszar, A., Schneller, D., Zulehner, G., Huber, H., … Mikulits, W. (2009). Hepatic tumor-stroma crosstalk guides epithelial to mesenchymal transition at the tumor edge. *Oncogene*, *28*(45), 4022–33. doi:10.1038/onc.2009.253

Van Zijl, F., Zulehner, G., Petz, M., Schneller, D., Kornauth, C., Hau, M., … Mikulits, W. (2009). Epithelial-mesenchymal transition in hepatocellular carcinoma. *Future Oncology (London, England)*, *5*(8), 1169–79. doi:10.2217/fon.09.91

Vandesompele, J., De Preter, K., Pattyn, F., Poppe, B., Van Roy, N., De Paepe, A., & Speleman, F. (2002). Accurate normalization of real-time quantitative RT-PCR data by geometric averaging of multiple internal control genes. *Genome Biology*, *3*(7), RESEARCH0034. Retrieved from http://www.pubmedcentral.nih.gov/articlerender.fcgi?artid=126239&tool=pmcentrez&rendertype=abstract

Vanhaesebroeck, B., Guillermet-Guibert, J., Graupera, M., & Bilanges, B. (2010). The emerging mechanisms of isoform-specific PI3K signalling. *Nature Reviews. Molecular Cell Biology*, *11*(5), 329–41. doi:10.1038/nrm2882

Villanueva, A., Chiang, D. Y., Newell, P., Peix, J., Thung, S., Alsinet, C., … Llovet, J. M. (2008). Pivotal role of mTOR signaling in hepatocellular carcinoma. *Gastroenterology*, *135*(6), 1972–83, 1983.e1–11.

doi:10.1053/j.gastro.2008.08.008

Villunger, A., Michalak, E. M., Coultas, L., Müllauer, F., Böck, G., Ausserlechner, M. J., … Strasser, A. (2003). p53- and drug-induced apoptotic responses mediated by BH3-only proteins puma and noxa. *Science (New York, N.Y.)*, *302*(5647), 1036–8. doi:10.1126/science.1090072

Vogt, P. K., & Hart, J. R. (2011). PI3K and STAT3: a new alliance. *Cancer Discovery*, *1*(6), 481–6. doi:10.1158/2159-8290.CD-11-0218

WARBURG, O. (1956). On the origin of cancer cells. *Science (New York, N.Y.)*, *123*(3191), 309–14. Retrieved from http://www.ncbi.nlm.nih.gov/pubmed/13298683

WARRINGTON, J. A., NAIR, A., MAHADEVAPPA, M., & TSYGANSKAYA, M. (2000). Comparison of human adult and fetal expression and identification of 535 housekeeping/maintenance genes. *Physiological Genomics* , *2* (3), 143–147. Retrieved from http://physiolgenomics.physiology.org/content/2/3/143.abstract

Waxman, S., & Wurmbach, E. (2007). De-regulation of common housekeeping genes in hepatocellular carcinoma. *BMC Genomics*, *8*, 243. doi:10.1186/1471-2164-8-243

Wilhelm, S., Carter, C., Lynch, M., Lowinger, T., Dumas, J., Smith, R. a, … Kelley, S. (2006). Discovery and development of sorafenib: a multikinase inhibitor for treating cancer. *Nature Reviews. Drug Discovery*, *5*(10), 835–44. doi:10.1038/nrd2130

Williamson, C. T., Muzik, H., Turhan, A. G., Zamò, A., O'Connor, M. J., Bebb, D. G., & Lees-Miller, S. P. (2010). ATM deficiency sensitizes mantle cell lymphoma cells to poly(ADP-ribose) polymerase-1 inhibitors. *Molecular Cancer Therapeutics*, *9*(2), 347–57. doi:10.1158/1535-7163.MCT-09-0872

Wong, C.-M., Yam, J. W.-P., Ching, Y.-P., Yau, T.-O., Leung, T. H.-Y., Jin, D.-Y., & Ng, I. O.-L. (2005). Rho GTPase-activating protein deleted in liver cancer

suppresses cell proliferation and invasion in hepatocellular carcinoma. *Cancer Research*, *65*(19), 8861–8. doi:10.1158/0008-5472.CAN-05-1318

Woo, H. G., Park, E. S., Lee, J.-S., Lee, Y.-H., Ishikawa, T., Kim, Y. J., & Thorgeirsson, S. S. (2009). Identification of potential driver genes in human liver carcinoma by genomewide screening. *Cancer Research*, *69*(9), 4059–66. doi:10.1158/0008-5472.CAN-09-0164

Wörns, M.-A., & Galle, P. R. (2014). HCC therapies-lessons learned. *Nature Reviews. Gastroenterology & Hepatology*, *11*(7), 447–52. doi:10.1038/nrgastro.2014.10

Wu, S.-D., Ma, Y.-S., Fang, Y., Liu, L.-L., Fu, D., & Shen, X.-Z. (2012). Role of the microenvironment in hepatocellular carcinoma development and progression. *Cancer Treatment Reviews*, *38*(3), 218–25. doi:10.1016/j.ctrv.2011.06.010

Wu, Z., Wang, Y., & Chen, L. (2013). Network-based drug repositioning. *Molecular bioSystems*, *9*(6), 1268–81. doi:10.1039/c3mb25382a

Xu, B., Di, J., Wang, Z., Han, X., Li, Z., Luo, X., & Zheng, Q. (2013). Quantitative analysis of RASSF1A promoter methylation in hepatocellular carcinoma and its prognostic implications. *Biochemical and Biophysical Research Communications*, *438*(2), 324–8. doi:10.1016/j.bbrc.2013.07.070

Xu, X., Sakon, M., Nagano, H., Hiraoka, N., Yamamoto, H., Hayashi, N., … Monden, M. (2004). Akt2 expression correlates with prognosis of human hepatocellular carcinoma. *Oncology Reports*, *11*(1), 25–32. Retrieved from http://www.ncbi.nlm.nih.gov/pubmed/14654898

Xu, X., Ye, L., Araki, K., & Ahmed, R. (2012). mTOR, linking metabolism and immunity. *Seminars in Immunology*, *24*(6), 429–35. doi:10.1016/j.smim.2012.12.005

Yamazaki, K., Masugi, Y., & Sakamoto, M. (2011). Molecular pathogenesis of hepatocellular carcinoma: altering transforming growth factor-β signaling in hepatocarcinogenesis. *Digestive Diseases (Basel, Switzerland)*, *29*(3), 284–8.

doi:10.1159/000327560

Yan, W., Fu, Y., Tian, D., Liao, J., Liu, M., Wang, B., … Luo, M. (2009). PI3 kinase/Akt signaling mediates epithelial-mesenchymal transition in hypoxic hepatocellular carcinoma cells. *Biochemical and Biophysical Research Communications*, *382*(3), 631–6. doi:10.1016/j.bbrc.2009.03.088

Yang, H. W., Shin, M.-G., Lee, S., Kim, J.-R., Park, W. S., Cho, K.-H., … Heo, W. Do. (2012). Cooperative activation of PI3K by Ras and Rho family small GTPases. *Molecular Cell*, *47*(2), 281–90. doi:10.1016/j.molcel.2012.05.007

Yang, L., Wang, K.-J., Wang, L.-S., Jegga, A. G., Qin, S.-Y., He, G., … He, L. (2011). Chemical-protein interactome and its application in off-target identification. *Interdisciplinary Sciences, Computational Life Sciences*, *3*(1), 22–30. doi:10.1007/s12539-011-0051-8

Yang, M.-H., Chen, C.-L., Chau, G.-Y., Chiou, S.-H., Su, C.-W., Chou, T.-Y., … Wu, J.-C. (2009). Comprehensive analysis of the independent effect of twist and snail in promoting metastasis of hepatocellular carcinoma. *Hepatology (Baltimore, Md.)*, *50*(5), 1464–74. doi:10.1002/hep.23221

Yao, Y. J., Ping, X. L., Zhang, H., Chen, F. F., Lee, P. K., Ahsan, H., … Tsou, H. C. (1999). PTEN/MMAC1 mutations in hepatocellular carcinomas. *Oncogene*, *18*(20), 3181–5. doi:10.1038/sj.onc.1202659

Yildiz, G., Arslan-Ergul, A., Bagislar, S., Konu, O., Yuzugullu, H., Gursoy-Yuzugullu, O., … Ozturk, M. (2013). Genome-wide transcriptional reorganization associated with senescence-to-immortality switch during human hepatocellular carcinogenesis. *PloS One*, *8*(5), e64016. doi:10.1371/journal.pone.0064016

Yoshikawa, H., Matsubara, K., Qian, G. S., Jackson, P., Groopman, J. D., Manning, J. E., … Herman, J. G. (2001). SOCS-1, a negative regulator of the JAK/STAT pathway, is silenced by methylation in human hepatocellular carcinoma and shows growth-suppression activity. *Nature Genetics*, *28*(1), 29–35. doi:10.1038/88225

Yu, H., Pardoll, D., & Jove, R. (2009). STATs in cancer inflammation and immunity: a leading role for STAT3. *Nature Reviews. Cancer*, *9*(11), 798–809. doi:10.1038/nrc2734

Yu, J., & Zhang, L. (2008). PUMA, a potent killer with or without p53. *Oncogene*, *27 Suppl 1*, S71–83. doi:10.1038/onc.2009.45

Zhang, L., Zhou, F., & ten Dijke, P. (2013). Signaling interplay between transforming growth factor-β receptor and PI3K/AKT pathways in cancer. *Trends in Biochemical Sciences*, *38*(12), 612–20. doi:10.1016/j.tibs.2013.10.001

Zhang, Q.-B., Sun, H.-C., Zhang, K.-Z., Jia, Q.-A., Bu, Y., Wang, M., … Tang, Z.-Y. (2013). Suppression of natural killer cells by sorafenib contributes to prometastatic effects in hepatocellular carcinoma. *PloS One*, *8*(2), e55945. doi:10.1371/journal.pone.0055945

Zheng, L., Yang, W., Wu, F., Wang, C., Yu, L., Tang, L., … Wang, H. (2013). Prognostic significance of AMPK activation and therapeutic effects of metformin in hepatocellular carcinoma. *Clinical Cancer Research : An Official Journal of the American Association for Cancer Research*, *19*(19), 5372–80. doi:10.1158/1078-0432.CCR-13-0203

Zlotnik, A., Burkhardt, A. M., & Homey, B. (2011). Homeostatic chemokine receptors and organ-specific metastasis. *Nature Reviews. Immunology*, *11*(9), 597–606. doi:10.1038/nri3049

APPENDIX

ELSEVIER LICENSE
TERMS AND CONDITIONS

Jul 21, 2014

This is a License Agreement between Tulin Ersahin ("You") and Elsevier ("Elsevier") provided by Copyright Clearance Center ("CCC"). The license consists of your order details, the terms and conditions provided by Elsevier, and the payment terms and conditions.

All payments must be made in full to CCC. For payment instructions, please see information listed at the bottom of this form.

Supplier	Elsevier Limited The Boulevard,Langford Lane Kidlington,Oxford,OX5 1GB,UK
Registered Company Number	1982084
Customer name	Tulin Ersahin
Customer address	Bilkent University Ankara, 06800
License number	3433770253849
License date	Jul 21, 2014
Licensed content publisher	Elsevier
Licensed content publication	Cell
Licensed content title	Hallmarks of Cancer: The Next Generation
Licensed content author	Douglas Hanahan,Robert A. Weinberg
Licensed content date	4 March 2011
Licensed content volume number	144
Licensed content issue number	5
Number of pages	29
Start Page	646
End Page	674
Type of Use	reuse in a thesis/dissertation
Intended publisher of new work	other
Portion	figures/tables/illustrations
Number of figures/tables/illustrations	1
Format	both print and electronic
Are you the author of this Elsevier article?	No
Will you be translating?	No

NATURE PUBLISHING GROUP LICENSE
TERMS AND CONDITIONS

Jul 21, 2014

This is a License Agreement between Tulin Ersahin ("You") and Nature Publishing Group ("Nature Publishing Group") provided by Copyright Clearance Center ("CCC"). The license consists of your order details, the terms and conditions provided by Nature Publishing Group, and the payment terms and conditions.

All payments must be made in full to CCC. For payment instructions, please see information listed at the bottom of this form.

License Number	3433821311713
License date	Jul 21, 2014
Licensed content publisher	Nature Publishing Group
Licensed content publication	Nature Reviews Clinical Oncology
Licensed content title	Development of PI3K inhibitors: lessons learned from early clinical trials
Licensed content author	Jordi Rodon, Rodrigo Dienstmann, Violeta Serra and Josep Tabernero
Licensed content date	Feb 12, 2013
Volume number	10
Issue number	3
Type of Use	reuse in a dissertation / thesis
Requestor type	academic/educational
Format	print and electronic
Portion	figures/tables/illustrations
Number of figures/tables/illustrations	1
High-res required	no
Figures	Figure 1: Signaling of PI3K and relevant drugs
Author of this NPG article	no
Your reference number	None
Title of your thesis / dissertation	Systems biology approach for targeted therapy of liver cancer
Expected completion date	Aug 2014
Estimated size (number of pages)	250
Total	0.00 USD
Terms and Conditions	

Terms and Conditions for Permissions

NATURE PUBLISHING GROUP LICENSE
TERMS AND CONDITIONS

Jul 21, 2014

This is a License Agreement between Tulin Ersahin ("You") and Nature Publishing Group ("Nature Publishing Group") provided by Copyright Clearance Center ("CCC"). The license consists of your order details, the terms and conditions provided by Nature Publishing Group, and the payment terms and conditions.

All payments must be made in full to CCC. For payment instructions, please see information listed at the bottom of this form.

License Number	3433770051467
License date	Jul 21, 2014
Licensed content publisher	Nature Publishing Group
Licensed content publication	Nature Reviews Drug Discovery
Licensed content title	Targeting the phosphoinositide 3-kinase pathway in cancer
Licensed content author	Pixu Liu, Hailing Cheng, Thomas M. Roberts and Jean J. Zhao
Licensed content date	Aug 1, 2009
Volume number	8
Issue number	8
Type of Use	reuse in a dissertation / thesis
Requestor type	academic/educational
Format	print and electronic
Portion	figures/tables/illustrations
Number of figures/tables/illustrations	3
High-res required	no
Figures	Figure 1: The class i Pi3K signalling pathway Figure 3: Targeting the Pi3K pathway in cancer Figure 5: Function and therapeutic targeting of p110 isoforms
Author of this NPG article	no
Your reference number	None
Title of your thesis / dissertation	Systems biology approach for targeted therapy of liver cancer
Expected completion date	Aug 2014
Estimated size (number of pages)	250
Total	0.00 USD
Terms and Conditions	

Terms and Conditions for Permissions

ELSEVIER LICENSE
TERMS AND CONDITIONS

Jul 21, 2014

This is a License Agreement between Tulin Ersahin ("You") and Elsevier ("Elsevier") provided by Copyright Clearance Center ("CCC"). The license consists of your order details, the terms and conditions provided by Elsevier, and the payment terms and conditions.

All payments must be made in full to CCC. For payment instructions, please see information listed at the bottom of this form.

Supplier	Elsevier Limited The Boulevard,Langford Lane Kidlington,Oxford,OX5 1GB,UK
Registered Company Number	1982084
Customer name	Tulin Ersahin
Customer address	Bilkent University Ankara, 06800
License number	3433810817720
License date	Jul 21, 2014
Licensed content publisher	Elsevier
Licensed content publication	Cellular Signalling
Licensed content title	Function of Akt/PKB signaling to cell motility, invasion and the tumor stroma in cancer
Licensed content author	Y. Rebecca Chin,Alex Toker
Licensed content date	April 2009
Licensed content volume number	21
Licensed content issue number	4
Number of pages	7
Start Page	470
End Page	476
Type of Use	reuse in a thesis/dissertation
Portion	figures/tables/illustrations
Number of figures/tables/illustrations	1
Format	both print and electronic
Are you the author of this Elsevier article?	No
Will you be translating?	No
Title of your	Systems biology approach for targeted therapy of liver cancer

Encyclopedia of Molecular Cell Biology and Molecular Medicine

Decision Letter (mcb.200400024/pub2)

From: emcbmm@wiley.com

To: rengul@bilkent.edu.tr, vatalay@metu.edu.tr

CC:

Subject: Encyclopedia of Molecular Cell Biology and Molecular Medicine - Manuscript ID mcb.200400024/pub2 has been accepted

Body: Dear Dr. Cetin-Atalay,

It is a pleasure to accept your manuscript entitled "Molecular Biology of Liver Cancer" in its current form for publication in Encyclopedia of Molecular Cell Biology and Molecular Medicine.

Thank you for your excellent contribution.

Sincerely,

Sarah Mellor
Managing Editor
Wiley-VCH
emcbmm@wiley.com
on behalf of
Dr Bob Meyers

Molecular Biology of Liver Cancer

Tulin Ersahin[1], Mehmet Ozturk[2], Rengul Cetin-Atalay[1,3]

[1]Department of Molecular Biology and Genetics, Bilkent University, Ankara, 06800, Turkey

[2]Dokuz Eylul University, Advanced Biomedical Research Center, 035340, Izmir, Turkey.

[3]Corresponding author

Keywords

HBV

A small DNA virus that infects hepatocytes in the liver, causing acute or chronic hepatitis.

HCV

A small RNA virus that infects hepatocytes in the liver, causing acute or chronic hepatitis.

Genome-wide expression

An experimental approach for the identification of disease-specific gene expression

profiles.

Gene signatures

Expression pattern of a set of genes associated with a clinical subtype of a disease.

PI3K/AKT pathway

A signaling pathway involved in cell survival that is hyper-activated in various cancers, including liver cancer.

MAPK/ERK pathway

Kinase protein cascade involved in cell survival that is up-regulated in various cancers, including liver cancer.

P53

A tumor suppressor protein that is inactivated by mutation in cancers, including liver cancer.

hTERT

Human telomerase reverse transcriptase that is inactivated by mutation in cancers, including liver cancer.

Hepatocellular carcinoma (HCC) is one of the leading causes of cancer-related mortality worldwide. Recent advances in the molecular profiling of HCC emphasize its intra-tumoral heterogeneity and reveal how cellular pathways are altered in favor of tumor progression. Malignant transformation of primary liver cancer is achieved through the acquisition of cancer hallmark capabilities that promote uncontrolled proliferation hepatocytes. Here, we review the characteristics and acquired capabilities of human primary liver cancer based on the HCC-specific genetic and epigenetic alterations.

1. Introduction

Primary liver cancer is the fifth most frequently diagnosed cancer in men, and the seventh in women. However, due to its aggressive behavior and resistance to conventional therapies, liver cancer is the second most frequent cause of cancer death in men, and the sixth in women [1]. 748,300 new liver cancer cases and 695,900 cancer deaths were reported worldwide in 2008 [2]. Hepatocellular carcinoma (HCC) is the major histological subtype of

primary liver cancers, accounting for about 80% of the total liver cancer cases worldwide [3].

The major risk factors for HCC are hepatitis B virus (HBV), hepatitis C virus (HCV) infections, alcohol, and aflatoxin B1 exposure. Development of HCC is a multistep process, where hepatic injury first leads to chronic liver disease and then continuous inflammation results in cycles of cell death and hepatocyte regeneration. The subsequent expansion of dysplastic nodules along with telomerase reactivation, and increased genomic instability is followed by malignant transformation [4]. Integration of HBV DNA into the host genome is frequent in HCC. On the other hand, RNA virus HCV leads to malignant transformation through oxidative stress and pro-inflammatory response induced by viral proteins [5–7]. In addition, exposure to exogenous (Aflatoxins) or endogenous (toxic metabolites such as steroids and cholesterol and metal ions such as copper, iron, nickel) hepatotoxic factors leads to liver injury and provokes an increase in the proliferating fraction of hepatocytes [8–12]. Therefore, chronic liver regeneration may itself be a source of spontaneous gene mutations leading to HCC [13].

The current classification system (Barcelona Clinic Liver Cancer - BCLC), considers HCC in five stages: very early, early, intermediate, advanced, and end-stage according to tumor size, nodule number, vascular invasion, metastasis and liver function [14]. Treatment strategy is determined based on the stage of the patient. Patients with very early and early HCC are treated with resection, liver transplantation or partial hepatectomy and patients with intermediate HCC are treated with chemoembolization [15]. However, patients are often diagnosed at advanced stage, where these treatments cannot be applied. Chemotherapy is the only treatment option for patients with advanced stage HCC. Yet, patients with the same BCLC stage can still have variable responses, due to high genomic heterogeneity of HCC [16, 17]. Therefore, a molecular level classification is necessary for effective diagnosis and personalized treatment options. Genome-wide expression analysis, exome sequencing and microRNA profiling techniques are being used for efficient molecular classification of HCCs.

Sorafenib (Nexavar, BAY43-9006), a multi-kinase inhibitor, is the only FDA-approved molecular-targeted agent for the treatment of patients with advanced HCC [18–20]. Sorafenib inhibits Raf, VEGFR, and PDGFR kinases, and thereby suppresses cell proliferation and angiogenesis. In the phase III randomized controlled trials, Sorafenib showed an overall survival benefit of three months [15, 21].

Primary liver cancer is a major public health problem, which requires in-depth

molecular analysis in order to discover optimal targeted therapeutics. Due to the presence of genomic variations, custom-designed therapies based on our understanding of the molecular biology of liver cancer will be indispensable for the treatment of HCC in the future.

2. Molecular Hallmarks of Hepatocellular Carcinoma

Malignant transformation requires the cancer cells to acquire several growth-promoting characteristics to become tumorigenic and eventually malignant. Hepatocellular cancers drive from initially quiescent hepatocytes, whose growth is tightly controlled. The appearance of tumor in this highly controlled microenvironment suggests that initial HCC cells acquire phenotypic hallmarks of cancer described by Hanahan and Weinberg. Six core and two emerging cancer hallmark capabilities have been suggested: sustaining proliferative signaling, evading growth suppressors, resisting cell death, enabling replicative immortality, inducing angiogenesis, and activating invasion and metastasis, along with deregulating cellular energetics, and avoiding immune destruction [22]. Acquisition of these capabilities is facilitated by two enabling characteristics: genome instability and tumor-promoting inflammation during stepwise progression of HCC.

2.1. Genome instability and Mutations

Tumorigenesis is a multistep process that initiates from dysplastic lesions which accumulates somatically acquired mutations and genomic instability [23]. Genomic instability, including chromosomal rearrangements and point mutations, is an enabling characteristic of multistep tumorigenesis and underlies the acquisition of hallmark capabilities [22].

HCC harbors chromosomal gains at 1q, 5, 6p, 7, 8q, 17q and 20 and losses at 1p, 4q, 6q, 8p, 13q, 16, 17p and 21 [24, 25]. The gain of 1q and the loss of 1p and 17p are associated with early stages of HCC, while the gain of 6p, 5q and 8q and loss of 4q and 8p are associated with advanced stage HCC [26, 27]. Moreover, integration of HBV DNA within or upstream of the TERT (telomerase reverse transcriptase) gene in the host genome was observed in patients with HBV-related HCCs [28, 29]. DNA-damaging reactive oxygen species can also contribute to genomic instability [30, 31].

The TERT gene is frequently mutated in HCC, allowing cells to gain replicative immortality. TERT promoter mutations in 44% of 61 HCC patients were shown to associate

with early stages of HCC independent of viral-infection, sex, age and ethnicity [32]. These mutations are associated with early stages of HCC and are independent of viral-infection, sex, age and ethnicity. TP53 is the second most frequently mutated tumor suppressor gene in HCC and is associated with poor prognosis [33]. Mutation rates are 50% and 20% in HCCs with or without aflatoxin exposure, respectively [34]. A hot spot mutation at codon 249 (R249S) is specific to AFB1 exposure in 36 % tumors from Africa and 32% of tumors from China [35, 36]. Aberrant activation of Wnt/β-catenin signaling pathway, which plays a key role in hepatocarcinogenesis, is achieved by activating mutations of β-catenin (CTNNB1) and inactivating mutations or LOH of AXIN1 [24, 37–39]. Although mutations of retinoblastoma gene (RB1) are rare, RB is frequently inactivated in HCC through the loss of heterozygosity (LOH) of 13q, proteosomal degradation or aberrant cyclin-dependent kinase activity [40–42]. The cyclin-dependent kinase inhibitor 2A gene (p16), which acts as a tumor suppressor downstream of p53 and Rb is inactivated frequently in HCC [43, 44].

Mutations in the downstream elements of receptor tyrosine kinase (RTK) signaling are also observed in HCC. The inactivating mutations of the tumor suppressor gene Phosphatase and tensin homolog (PTEN), which is a negative regulator of PI3K/Akt survival pathway, are observed in HCC, but not very frequently [45–49]. Ras proto-oncogenes (H-ras, K-Ras, N-ras) are also rarely mutated and activated in HCC [43, 50–52]. Runt-related transcription factor (RUNX) family genes induce a senescence-like growth arrest in response to oncogenic Ras. Expression of one of the members of this family, RUNX3, is decreased in more then 50% of HCC cases [53, 54]. Its down-regulation is associated with escape from apoptosis and sustained growth [55, 56]. Recently, its role in mediating angiogenesis and of epithelial-mesenchymal transition was also shown [57]. Thus, the loss of RUNX expression may explain the rarity of Ras mutations in these cancers.

Less frequent inactivating tumor suppressing mutations of P14, IGFR2, KLF6, HNF1α, SMAD2, SMAD4 and LKB1/STK11, and less frequent activating oncogenic mutations of EGFR, Erb2, and PIK3CA have also been reported in HCC [58, 59]. Molecular alterations of critical genes and their contribution to the acquisition of hallmark capabilities are presented in Table 1.

Table 1. Molecular Alterations of Critical Genes in HCC

Cellular Process	Molecule	Alteration in HCC	Acquired Capability
Growth factor signaling	EGF / EGFR	Up-regulation	Sustaining proliferative signaling
	HGF / MET	Up-regulation	
	IGF / IGFR	Overexpression	Resisting cell death
	VEGF / VEGFR	Up-regulation	Inducing angiogenesis
	PDGF / PDGFR	Up-regulation	
	FGF / FGFR	Up-regulation	
Cell Cycle Regulation	TP53	Inactivating mutation / LOH	Sustaining proliferative signaling Evading growth suppressors
	RB1	Inactivating mutation / LOH	
	c-myc	Overexpression	
	p16 (CDKN2A)	Inactivating mutation / Hypermethylation	
	Cyclin D1	Overexpression	
	IRF2	Inactivating mutation	
Ras/RAF pathway	RAS	Activating mutation	Sustaining proliferative signaling Evading growth suppressors Inducing angiogenesis Activating invasion and metastasis
	RPS6KA3	Inactivating mutation	
PI3K/AKT pathway	PI3K-alpha (PIK3CA)	Activating mutation	Sustaining proliferative signaling Evading growth suppressors Inducing angiogenesis Activating Invasion and Metastasis Reprogramming energy metabolism
	PTEN	Inactivating mutation / LOH	
	AKT	Constitutive activation	
	mTORC1	Up-regulation	

JAK/Stat pathway	Stat	Constitutive activation	Tumor-promoting inflammation
	SOCS1,SOCS3	Down-regulation	
NF-κB pathway	NF-κB	Constitutive activation	Sustaining proliferative signaling Resisting cell death Tumor-promoting inflammation
Wnt/β-catenin pathway	β-catenin (CTNNB1)	Activating mutation / Overexpression	Sustaining proliferative signaling Tumor-promoting inflammation
	AXIN1, AXIN2	Inactivating mutation / LOH	
	APC	Inactivating mutation	
Hedgehog pathway	SHH	Overexpression	Reprogramming energy metabolism
	SMO	Overexpression	
	HHIP	LOH, hypermethylation	
Histone modification	DNMT1, 3A, 3B	Up-regulation	Sustaining proliferative signaling Evading growth suppressors
	EZH2	Overexpression	
	ARID1, ARID2	Inactivating mutation	
Apoptosis	Fas	Down-regulation	Resisting cell death
	FasL	Up-regulation	
	DR5	Down-regulation	
Angiogenesis	Angiopoietin	Up-regulation	Inducing angiogenesis
	Tie-2	Up-regulation	
Immunity	Glypican-3	Up-regulation	Evading immune destruction

2.2. Sustaining Proliferative Signaling

Constitutive activation of survival pathways, inactivation of tumor suppressors TP53, Rb, and p16, overexpression of c-myc and Cyclin D1, epigenetic silencing of p16INK4 and overexpression of E2F family members promote cell cycle progression and sustained proliferation of HCC cells.

Growth factors and their corresponding activated tyrosine kinase receptors such as

EGF-EGFR, IGF-IGFR, and HGF-MET transmit the proliferation signal through Ras/Raf/MEK/ERK and PI3K/AKT/mTOR pathways. Constitutive activation of these pathways are maintained through the overexpression of MET and EGFR and the inactivation or down-regulation of the negative regulators PTEN and RASSF1A of PI3K/AKT/mTOR and Ras/Raf/MEK/ERK pathways respectively. Identification of potential driver genes in human liver carcinoma by genome-wide screening revealed genes with specific signaling pathways such as PI3K/Akt/mTOR, AMP-activated protein kinase (AMPK), and EGFR [60]. Cell proliferation in HCV-positive HCC is also associated with Myc and AKT activation [61]. Moreover, it is known that overexpression of E2F family members, which are responsible for the transcription of genes involved in cell cycle and proliferation, inhibits c-Myc-driven apoptosis through PI3K/AKT/mTOR pathway [62, 63].

Additionally, large-scale analysis with high number of HCC samples revealed proliferation gene signatures. Chen et al., in 2002, showed high expression of a “proliferation cluster” comprised of genes required for cell cycle progression in 102 primary HCC tumor samples and 10 HCC cell lines [64]. Ribosomal protein genes were highly expressed as expected in cells with unlimited cell growth. Up-regulated genes were related to DNA replication and G2/M progression. In another study from 91 human primary HCC, a proliferation gene signature (containing PCNA, Bub3, MCM2, MCM6, MCM7, cyclinA2, cyclinB1, CKS2 and CDK4) was able to distinguish two groups of HCC patients with distinct prognosis [65].

2.3. Evading Growth Suppressors

Inactivation of pRB, p53 and p16, and overexpression of c-myc and cyclin D1 confer growth advantages in HCC. Activation of the MYC transcription signature is strongly associated with the malignant conversion of pre-neoplastic liver nodules and inactivation of MYC in invasive HCCs lead to sustained tumor regression as well as proliferation arrest, differentiation, and apoptosis of malignant cells [66, 67].

HCV Core protein induces promoter hypermethylation and down-regulation of p16 expression and subsequently induces Rb phosphorylation, leading to the activation of E2F1, that in turn stimulates cell growth [68]. This mechanism is also exploited to overcome stress-induced premature senescence in the presence of HCV-induced oxidative stress [69].

Furthermore, HCV Core protein up-regulates DNA methyltransferases 1 and 3b and induces promoter hypermethylation of retinoic acid receptor-β2 (RAR-β2). This mechanism leads to escape from RB/E2F-related growth arrest induced by all-trans retinoic acid [70].

Up-regulation of the oncoprotein gankyrin enhances the transcriptional activity of β-catenin, which in turn transcriptionally activates gankyrin by a positive feedback loop [71]. Gankyrin is highly expressed in HCC and its overexpression mediates the degradation of the tumor suppressor proteins Rb and p53 and thereby accelerates cell cycle progression.

Growth arrest and DNA damage 45G (GADD45G) is commonly down-regulated in oncogene-transformed HCC [72]. Ectopic expression of GADD45G induces senescence in HCC through repression of Jak/Stat3 pathway, independently of p53, p16INK4a, and Rb. Expression of constitutively activated Stat3 or human telomerase reverse transcriptase (hTERT) reverts GADD45G-induced senescence.

Transforming growth factor-beta (TGF-β) signaling has a growth suppressive role in the early stages of HCC. Resistance to TGF-β signaling-mediated growth inhibition is a frequent event during malignant transformation of hepatocytes. In the advanced stages of HCC, TGF-β is secreted by the stromal cells in tumor microenvironment and therefore induces apoptosis in hepatocytes. However, the down-regulation of the receptors of TGF-β and up-regulation of the EGFR and MEK/ERK pathways confers resistance to TGF-β-induced cell death in liver tumor cells [73–79].

2.4. Resisting Cell Death

Presence of elevated levels of growth factors such as IGF, up-regulation of anti-apoptotic pathways such as NF-κB pathway, down-regulation of death receptors such as DR5 and Fas, mutations in the tumor suppressor genes such as p53, contribute to evasion of apoptosis in many cancers including liver cancer. The IGF/IGFR signaling pathway that is constitutively activated in 20% of HCC via IGF2 or IGFR1 overexpression, regulates proliferation, motility, invasion and inhibition of apoptosis. This is correlated with stage, metastasis and survival of HCC [80–84]. The IGF pathway activates cell survival pathways PI3K/AKT and RAF/MEK/ERK and provides a mechanism to evade apoptosis [80].

Mutations in the tumor suppressor gene p53 cause the loss of apoptotic response. Large scale gene expression analysis showed that cell cycle-related genes (CCNG2,

BZAP45) and cell proliferation-related genes (SSR1, ANXA2, S100A10, and PTMA) were overexpressed in mutant-p53 tumors compared to wild type-p53 tumors in HCV-related HCC [85].

Tumor Necrosis Factor (TNF) activates the anti-apoptotic NF-κB pathway, the pro-apoptotic caspase–cascade, and JNK kinases in HCC. Inhibition of NF-κB by NEMO results in the up-regulation of the death receptor DR5, whose ligand (TRAIL) is predominantly expressed by natural killer (NK) cells and is essentially involved in liver injury in NEMO-deficient hepatocytes [86]. Furthermore, Caspase-8 is frequently inactivated in HCC and therefore interferes with the pro-apoptotic caspase–cascade [87]. Down-regulation of Fas expression, up-regulation of its ligand (FasL) expression in hepatocytes, and elevation of serum soluble Fas levels were also identified as critical players of evasion from immune surveillance, and hepatic carcinogenesis [88].

2.5. Enabling Replicative Immortality

It is known that reactivation of telomerase maintains the telomere length and replicative immortality during cirrhosis and therefore leads to HCC progression [89, 90]. Not only telomere dysfunction, but also oncogene activation, persistent DNA damage and ROS-induced oxidative stress can cause permanent cell cycle arrest, known as senescence [31, 91]. Bypass of senescence is a characteristic of liver cancer cells to gain replicative immortality.

TGF-beta, Ras, Raf, Mos, Mek, Myc, E2F, Stat5, Cyclin E and PTEN are key players of oncogene-induced senescence [92]. Re-activation of telomerase and inactivation of p53, p15, p16, p21 may play critical roles in the bypass of senescence and maintaining immortality [91]. Indeed, expression of human hTERT was able to revert GADD455 - induced senescence in HCC [72]. Up-regulation of hTERT expression by low-dose cisplatin contributed to cell death resistance in a HCC cell line and this resistance was reverted by inhibition of hTERT [93]. Two independent mutations were identified within the core promoter of TERT. These mutations increased transcriptional activity from the TERT promoter by two- to four- fold and were shown to occur frequently in HCC [94]. Recurrent integration of HBV into the promoter of the TERT gene was correlated with increased TERT expression in HBV-related HCC patient samples [95]. Furthermore, a recent study showed that HCCs expressing

"stemness"-related proteins (K19, EpCAM, CD133) have increased telomere length, increased expression of hTERT and shelterin complex proteins (TRF1, TRF2, TIN2, POT1, TPP1, RAP1), and increased chromosomal instability compared to HCCs without these markers [96]. Hence, high telomerase activity and long telomeres in HCCs are associated with aggressive behaviour and poor prognosis [95, 97]. We reported recently that there is a major shift from senescence-associated gene expression to immortality-associated gene expression during transition from dysplasia to early HCC lesions. Moreover, a senescence bypass signature was able to differentiate HCC from cirrhosis [98]. Therefore, targeting senescence in liver cancer treatment can be considered as an alternative mechanism in addition to classical chemotherapeutic agents [99].

2.6. Inducing Angiogenesis

Angiogenesis and neo-vascularization involves interactions between tumor cells, vascular endothelial cells and their supporting pericytes in order to supply oxygen and nutrients to the growing tumor [30]. In HCC, the balance between pro-angiogenic and anti-angiogenic factors is disrupted due to excess secretion of angiogenic factors by endothelial cells and pericytes in the tumor microenvironment [100]. Angiogenic factors including vascular endothelial growth factor (VEGF), fibroblast growth factors (FGF), platelet-derived growth factor (PDGF) and angiopoietin-2, Tie-2 are up-regulated in HCC. This process induces angiogenic signaling through activation of the RAF/MEK/ERK, PI3K/AKT/mTOR, JAK/Stat and HGF/MET pathways [101–106].

VEGF and its receptors VEGFR-1 and VEGFR-2 are over-expressed in HCC, and are associated with aggressiveness and poor prognosis [107–111]. The HBV x antigen also up-regulates VEGFR-3 [112]. VEGF acts synergistically with FGF, whose overexpression is correlated with HCC angiogenesis [113, 114].

Hypoxia, which occurs during fibrosis, cirrhosis and malignant transformation, enhances proliferation, angiogenesis, metastasis, chemoresistance, and radioresistance of HCC [100]. Hypoxia induced factor 1 alpha (HIF-1α) promotes hepatocyte epithelial-mesenchymal transition (EMT) through PI3K/Akt, TGF-β and β-catenin signaling and this is associated with enhanced metastatic potential and poor prognosis in HCC [115–117]. Bone morphogenetic protein 4 (BMP-4) is also induced in hypoxic conditions and promotes

vasculogenesis and tumor progression in HCC [118].

2.7. Activating Invasion and Metastasis

Cell detachment is an early step of tumor invasion, requiring alterations of the adhesive properties of cancer cells in general. Therefore, epithelial-mesenchymal transition (EMT) is critical for activating invasion and metastasis of HCC. Up-regulation and activation of Twist, Snail, Slug, Zeb1/2, and Vimentin, and down-regulation of E-cadherin and hepatocyte nuclear factor (HNF)-4α frequently occur during EMT and correlate with poor prognosis in liver cancer [119–122]. Furthermore, p53 regulates EMT through miR-200 family members and miR-192, which targets Zeb1 and Zeb2 [123]. HBx expression was shown to induce EMT by activating the PI3K/Akt/GSK-3β pathway, which stabilizes Snail and mediates integrin α6β1 signaling, thus facilitating tumor invasion and metastasis during HCC progression [124, 125]. In HCV-positive HCC patients, expression of a four gene signature, including E-cadherin, inhibitor of DNA binding 2 (ID2), MMP9, and transcription factor 3 (TCF3), is correlated with poor prognosis [126].

Osteopontin is over-expressed in metastatic HBV-related HCC and invasion and metastasis are effectively blocked by an osteopontin-specific antibody both in vitro and in vivo [127]. This observation suggests that osteopontin can be considered as a diagnostic marker and a potential therapeutic target for HBV-related metastatic HCC [128, 129]. Tumor suppressor DLC1 and cytoskeletal protein RhoA are also involved in the prevention of dissemination and metastasis of human HCC cells in nude mice [130, 131]. Additionally, intra-tumoral hypoxia triggers invasion and metastasis of HCC through oncogenic HGF/MET signaling pathway [132]. A Met-regulated gene expression signature defines an aggressive subtype of HCC with increased vascular invasion rate, microvessel density and decreased mean survival time of HCC patients [103].

2.8. Reprogramming Energy Metabolism

Cancer cells reprogram their energy metabolism so that they can use glucose to supply energy through aerobic glycolysis and glutamine to provide intermediates of the tricarboxylic acid (TCA) cycle [133]. In addition, autophagy enables fast growing cells to break down cellular organelles, resulting in recycled catabolites that can be used for biosynthesis

and energy metabolism [22]. mTOR, an evolutionarily conserved serine/threonine kinase located downstream in the PI3K/AKT pathway, also works as a nutrition sensor to monitor cellular metabolism [134]. In the presence of sufficient energy and nutrients, active mTOR promotes translation and biosynthesis, hence suppresses autophagy. In the absence of sufficient energy and nutrients, mTOR with down-regulated activity leads to the reduction of biosynthesis and promotes autophagy [135]. PI3K/AKT pathway also stimulates glucose uptake and metabolism for continued growth and survival of cancer cells [136].

On the other hand, glutamine uptake and metabolism is under the control of c-myc [137]. Elevated energy consumption and addiction to mitochondrial glutaminolysis is dependent on the AMPK-related kinase 5 (ARK5) through oncogenic c-myc expression in HCC cells. ARK5 limits protein synthesis via inhibition of mTORC1 and maintains a high respiratory capacity required for efficient glutamine metabolism [138]. Therefore, targeting cellular energy homeostasis is a promising therapeutic strategy for HCC cells with higher c-myc expression. AMP-activated protein kinase (AMPK), which is activated in response to reduced energy levels, promotes ATP production by increasing catabolism and conserves ATP by switching off biosynthetic pathways. AMPK was found to be dysfunctional in patients with HCC, and low p-AMPK levels correlated with aggressiveness and poor prognosis [139]. Moreover, AMPK is also activated by the p53 targets, Sestrin1 and Sestrin2 [140]. p53 stimulates oxidative phosphorylation and reduces the rate of glycolysis through the upregulation of TP53-induced glycolysis and apoptosis regulator (TIGAR) [141]. Therefore, energy metabolism is shifted from mitochondrial respiration towards glycolysis by the loss of p53 in cancer cells.

During HCC development metabolic remodeling from mitochondrial oxidation to glycolysis was assessed by a combined transcriptomics and metabolomics study in 6 sub-groups of HCC tissues defined by Boyault et al. [142]. HCC has lower levels of glucose and other metabolites (glycerol 3-phosphate, glycerol 2-phosphate, malate, alanine, and myo-inositol) involved in energy production compared to healthy liver. Moreover, concentrations of certain saturated lipids are reduced in a sub-group of HCC cells associated with high serum alpha-fetoprotein (AFP) levels. This is consistent with the previous observations on the up-regulation of lipid catabolism accompanied by elevated AFP expression. Another study identified 28 metabolites and 169 genes involved in energy metabolism associated with aggressive HCC [143]. Metabolic activities in HCC microenvironment are also promoted by

Hedgehog signaling activation by malignant hepatocytes. Hedgehog ligands produced by these cells stimulate glycolysis in the neighboring myofibroblasts, resulting in the release of myofibroblast-derived lactate, which is used as an energy source by the malignant hepatocytes [144].

Mutations that activate oncogenes (such as c-myc, HIF-1α, and PI3K/AKT) or inactivate tumor suppressors (such as p53, PTEN, TSC2 and LKB1) have been shown to contribute to metabolic alterations in various types of cancer [145]. Oncogene-altered energy metabolism presents a new class of target molecules for tumor therapy. Indeed, activating oxidative phosphorylation by a pyruvate dehydrogenase kinase inhibitor (Dichloroacetate) overcame sorafenib resistance of HCC and combination of Sorafenib and Dichloroacetate resulted in elevated tumor regression compared to Sorafenib alone [146]. Therefore, tumor bioenergetics can be further exploited for HCC therapy.

2.9. Tumor-promoting inflammation

Tissue microenvironment plays a critical role in HCC formation and development [100]. HCC microenvironment is composed of cancer-associated fibroblasts (CAFs), invading inflammatory cells, endothelial cells (ECs), pericytes adjacent to the ECs, hepatic stellate cells (HSCs), macrophages (Kupffer cells), dendritic cells, and stem/progenitor cells. Extracellular matrix (ECM) components including collagen, fibronectin, laminin, glycosaminoglycans, and proteoglycans provide a support of microenvironment for these cells [100, 147]. All of these components of the microenvironment interact with each other and produce growth factors, cytokines, chemokines and free radicals that contribute to liver fibrosis, therefore tumor initiation and progression. Overexpression of highly negatively charged extracellular matrix protein osteopontin is associated with large tumor size, advanced tumor stage, capsular infiltration, vascular invasion, lymph node invasion, intrahepatic metastasis, early recurrence and poor prognosis of HCC [148–154]. Furthermore, plasma osteopontin levels were significantly higher in HCC patients and therefore, can be considered for early HCC marker together with AFP [151, 155, 156].

During HBV- or HCV- infection-associated chronic liver disease, hepatocyte injury leads to inflammatory cell infiltration, where host immune cells destroy virus-infected hepatocytes [157, 158]. Continuous inflammation results in a cycle of hepatocyte death and

proliferation leading to an increased genomic instability and mutations [4]. When stimulated with pro-inflammatory cytokines (IL-1β, TNF-α, and PDGF), Kupffer cells and HSCs produce osteopontin that plays an important role in inflammation, growth, invasion, metastasis, angiogenesis and inhibition of apoptosis [159–162]. TNF-α, produced by Kupffer cells and other immune cells promotes tumor progression mainly through NF-κB and Akt pathways [159].

Kupffer cells express and release pro-inflammatory cytokine interleukin-6 (IL-6). IL-6 is one of the major mediators of inflammation and activates STAT3 pathway to mediate its signal through the gp130 protein. IL-6 protects liver cells against apoptosis via STAT3 pathway following viral infection or chemical ingestion [163, 164]. This mechanism is also exploited during tumor promotion [165]. Constitutively activated Stat3 protein maintains NF-κB activity in tumors by preventing nuclear export of NF-κB complex through RelA acetylation [166]). RelA, in turn, maintains persistent activation of STAT3 and IL-6 in HCC microenvironment [167]. Therefore, conditional knock-out of STAT3 expression impairs liver regeneration, but tissue-specific knock-out of hepatic STAT3 effects glucose homeostasis and induction of insulin resistance [168, 169].

Oncogenic β-catenin also triggers an inflammatory response, including activation of the NF-κB pathway in hepatocytes, which promotes aggressiveness of HCC in mice [170]. Elevated IL-6 levels and constitutively activated STAT3 has been frequently detected in HCC patients and in cell lines [171–176]. In addition, the Jak-Stat inhibitors SOCS1 and SOCS3 are downregulated in HCC via promoter hypermethylation [177] . Moreover, somatic gain-of-function mutations in the IL6ST gene (gp130), have been identified in inflammatory hepatocellular adenomas [178]. IL-6/STAT3 further activates several interleukins and growth factors.

A low-grade inflammatory response is induced upon lipid accumulation in obesity, which in turn increases IL-6 and TNF expression by adipose tissue and Kupffer cells [179, 180]. IL-6 and TNF signaling promotes proliferation of damaged hepatocytes via activation of JAK/STAT and AKT/ERK, respectively [159, 181].

A unique 17 gene immune response signature of the liver microenvironment could predict venous metastases, recurrence, and prognosis in HCC [182]. A global Th1- to Th2-like cytokine shift is associated with HCC metastasis, which is promoted through a shift toward anti-inflammatory/immune-suppressive responses.

2.10. Evading Immune Destruction

Liver cancer develops usually on top of chronic inflammation during fibrosis and cirrhosis. Even though tumor cells exploit inflammation in favor of their growth as mentioned above, they still need to escape from immune destruction. HCC cells evade immune destruction by expressing immunosuppressive molecules such as PD-L1 and indolamine 2,3-dioxygenase (IDO), and secreting cytokines and chemokines such as IL6, IL10, TGF-β, and VEGF [183]. The resulting immunosuppressive microenvironment is supported by the induction of regulatory Dendritic cells (DCregs), regulatory T cells (Tregs) and tumor-associated macrophages (TAMs) and suppression of DCs, effector T cells and natural killer (NK) cells.

Macrophages are the major infiltrating leukocytes and are involved in both innate and adaptive immune responses [184]. During HBV- or HCV- infection, fibrotic and cirrhotic liver causes inflammatory cell infiltration due to necrosis of hepatocytes. Therefore, the status of TAMs and other immune cells in the tumor microenvironment is closely associated with suppression of anti-tumor immunity and progression of HCC. Polarizing inflammatory responses towards the preferential recruitment of Th2 type cells and Tregs rather than Th1 type cells promotes tumor immune evasion. While M2-type 'alternatively activated' macrophages promote tumor progression, M1-type 'classically activated' macrophages can exert anti-tumor activity by killing tumor cells. Therefore, shifting the macrophage balance from tumor promotion by innate immunity-driven inflammation towards tumor surveillance by adaptive immune responses can be an effective therapeutic strategy [185].

Dendritic cells (DCs), which are important for chronic liver inflammation, express and present antigens to infiltrating cytotoxic T lymphocytes (CTLs). Dendritic cells express Glypican 3 (GPC3), whose up-regulation is associated with poor prognosis in HCC [186]. Indeed, tumor-induced regulatory Dendritic cells with hyper-activate Stat3 can facilitate tumor immune evasion independent of Stat3 hyper-activation status in tumors [187]. Additionally, CTL-mediated immune response can be impaired by Kupffer cells through programmed death ligand 1(PD-L1), and regulatory DCs (CD14+ CTLA4+) through CTLA4-dependent IL-10 and IDO production, enabling immune evasion [188, 189].

Cytokine production by natural killer (NK) cells in chronic HCV infection is shifted toward secretion of Th2 type cytokines promoting an environment, which is more permissive for HCV [190]. In chronic HCV patients, NK cells have reduced cytotoxicity and IFN-γ

production, and secrete IL-10 and TGF-β resulting in the induction of Th2 cells and Tregs, maintaining immune evasion. Furthermore, many immune system-related genes, including SATB1, TNFRSF5, CTLA4, GITR, SIRPα, PD-L1 and ICOS have altered expression in HCC [85, 191, 192].

It has been shown that the only FDA-approved chemotherapeutic agent Sorafenib also suppresses proliferation and activation of natural killer (NK) cells in addition to malignant hepatocytes. Consequently, reduced cytotoxicity of NK cells handicaps HCC patients during treatment by rendering the host more susceptive to tumor growth and metastasis [193]. Therefore, immunotherapeutic approaches activating NK cells can enhance the efficacy of Sorafenib.

In light of above described cellular mechanisms, hallmarks of cancer are represented in parallel with the altered genes involved in the development of the multistep progression of liver cancer in Figure 1. This overall picture demonstrates that genome instability and mutations along with sustaining proliferative signaling having the highest number of altered genes, are the most studied hallmarks in HCC. Yet, the new emerging capabilities of tumor cells should be further studied in this disease in order to identify novel genes associated with HCC malignancy.

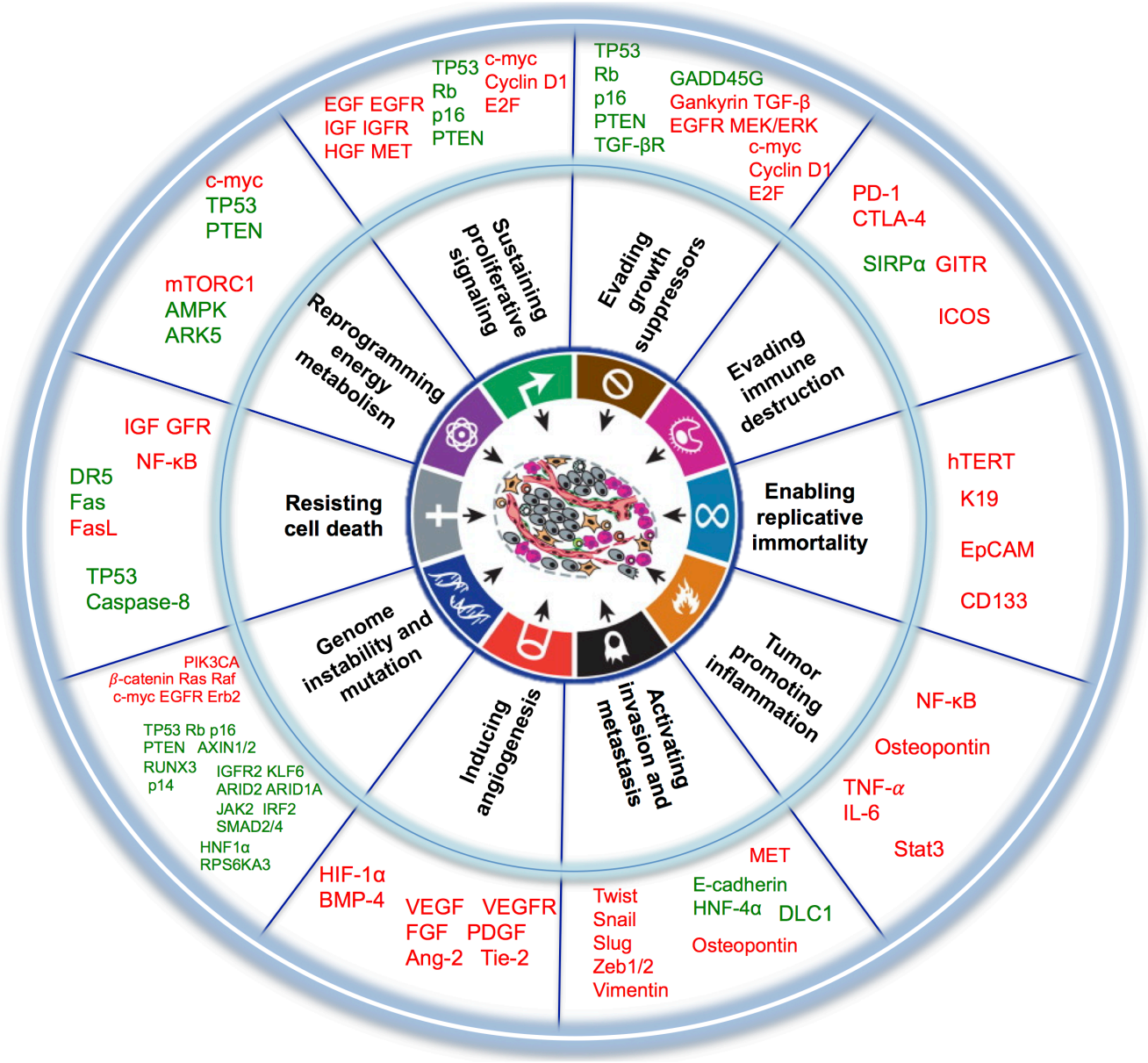

Figure 1. Molecular Hallmarks of Hepatocellular Carcinoma. Molecular alterations promote the hallmark capabilities through either activation/expression/up-regulation are in red or inactivation/loss/down-regulation are in green. (Modified from Hanahan and Weinberg with permission [22]).

3. Genome-wide changes in Hepatocellular Carcinoma

During the last decade, several high-throughput analyses on HCC samples have been published. Microarray, whole-genome sequencing and exome sequencing studies will enlighten the intra-tumoral heterogeneity of HCCs from various etiologies and histological pathologies. These large-scale studies revealed novel HCC-related pathways or gene signatures that can distinguish subgroups of HCC based on etiology, molecular background and histopathology. These signatures also predict survival, metastasis and recurrence. Major findings of recent high-throughput analyses on HCC are presented in Table 2. Some of the novel important genes associated with HCC are also included in the table along with their respective study.

Table 2: Major findings of recent high-throughput analyses on HCC

Classification of HCC based on altered gene expression	**Reference**
Highly expressed “proliferation cluster” genes in HCC	[64]
“proliferation cluster” genes predict survival by 406 gene signature	[65]
HCC classified into two groups based on IFN-regulated and apoptosis-relevant genes	[194]
Identify 240 gene signature for low- to high- grade dyplastic nodules and HCC	[195]
6 subgroups of HCC related to genetic alterations G1: IGFR1 activation, AKT activation, developmental imprinting G2: PIK3CA and TP53 mutations, AKT activation G3: TP53 mutation and overexpression of cell-cycle genes G4: a heterogeneous subgroup G5: β-catenin mutations, Wnt/β-catenin activation G6: G5 with satellite nodules, having higher activation of the Wnt pathway and low E-cadherin expression	[43]
4 neoplastic stages of HCV-positive HCC: control vs. cirrhosis: 8 gene signature	[196]

cirrhosis vs. dysplasia: 24 gene signature dysplasia vs. early HCC: 93 gene signature early vs. advanced HCC: 9 gene signature	
Subclasses of HCC with different genetic backgrounds c-Myc induced, 6p/1q-amplified, 17q-amplified	[197]
5 classes of HCV-positive HCC: CTNNB1 class: β-catenin mutations Proliferation class: IGF1R activation and RPS6 phosphorylation IFN-related class: a novel class defined by polysomy of chromosome 7	[111]
3 molecular subclasses of HCC: S1: Wnt/β-catenin activation S2: proliferation with Myc and AKT activation and IFN repression S3: tumor size, differentiation, and serum AFP levels	[61]
Cirrhosis vs. HCC Immortality and senescent signature: 15 immortality gene	[98]
Classification of HCC based on chromosomal imbalance	**Reference**
Early vs. advanced stages of HCC	[198]
3 HBV-positive HCC subgroups predict survival	[199]
Classification of HCC based on different etiologies	**Reference**
Invasiveness gene signatures of HBV- or HCV- associated HCC	[200]
HBV- or HCV- positivity: HBV-positive HCC: 31 genes relating to signal transduction, transcription, metastasis HCV-positive HCC: 52 genes related to detoxification and immune response	[201]
HBV-positive HCC vs. non-tumor liver tissues 44 gene signature	[202]
Early vs. late stages of HBV-positive HCC: 65 gene signature	[203]
Susceptibility to HBV-positive HCC 1p36.22 locus, and KIF1B-, UBE4B-, PGD-related pathways	[204]

Susceptibility to HCV-positive HCC common variants within the DEPDC5 locus on chromosome 22	[205]
HCV-positive HCC Strong association of a locus in the 5' flanking region of MICA, which leads to activation of natural killer cells and CD8+ T cells	[206]
Molecular profile of specific gene alterations	**Reference**
HCV-positive HCC with mutant-p53 vs. wild-type-p53 Overexpressed: cell cycle- and cell proliferation-related genes Underexpressed: immune system-related genes	[85]
Myc signature in cirrhosis vs. nodules vs. HCC	[66]
Met knock-out signature: HGF/Met activation associated with poor survival	[103]
RB knock-out signature: increased proliferation and RB/E2F activity	[207]
TGF-ß knock-out signature: invasive phenotype and increased tumor recurrence	[208]
Identification of genetic alterations	**Reference**
Somatic substitutions in HCV-positive HCC : T>C / A>G and C>T / G>A 11,731 mutations, including TP53, AXIN1, ADAM22, JAK2, KHDRBS2, NEK8 and TRRAP	[209]
Frequent mutations in HCV-associated HCC, including CTNNB1, TP53, ARID2, DMXL1 and NLP1 ARID2 as a tumor suppressor gene in HCV-associated HCC	[210]
Cirrhotic vs. non-cirrhotic HCC: G>T and C>A transversions are more frequent in tumors from non-cirrhotic liver new recurrent alterations in ARID1A, RPS6KA3, NFE2L2 and IRF2	[24]
Identification of epigenetic alterations	**Reference**
Predict survival: aberrant DNA methylation signature at promoter sites	[211]
High frequency chromatin regulating gene mutation Mutation in ARID2	[29]
Identification of potential tumor driver mutations	**Reference**
50 potential genes with specific signaling pathways (mTOR, AMPK, and EGFR)	[60]

3 tumor mutations (CCNG1, P62, and an indel/fusion gene) from sequencing of 3 HCC nodules from 1 HBV-positive HCC patient	[212]
13 potential tumor suppressor genes, including XPO4	[213]
Prediction of metastasis from gene signatures	**Reference**
153 gene signature in HBV-positive HCC Osteopontin overexpression	[127]
17 gene stromal tissue signature to predict metastasis	[182]
HBV-positive HCC patients with portal vein tumor thromboses Transversions: C:G > A:T and T:A > A:T mutation in ARID1A	[214]
Prediction of recurrence from gene signatures	**Reference**
12 gene signature	[215]
early intrahepatic recurrence	[216]
57 gene signature	[217]
early recurrence in HBV-positive HCC CD24	[218]
late recurrence from stromal tissues	[219]
Molecular profile of poorly-differentiated cells	**Reference**
Hepatoblast-like subclass with AP1 activation associated with poor prognosis	[220]
Progenitor-like class with EPCAM and AFP in HBV-positive HCC EPCAM-/AFP+ are associated with poor prognosis	[221]

4. microRNA Profiling of Hepatocellular Carcinoma

Recent findings highlight the importance of microRNAs in mediating the acquired capabilities of HCC. Comprehensive analysis of microRNA expression patterns revealed differential expression of miRNAs in metastatic HCC and non-metastatic HCC compared to healthy liver (Table 3). Hence, miRNAs can be utilized as prognostic markers in HCC patients

with various clinical phenotypes. miR-26a, whose expression is reduced in HCC, inhibits angiogenesis by down-regulating VEGFA through PIK3C2α/Akt/HIF-1α and suppresses growth and metastasis through IL-6/Stat3 signaling [222, 223]. miRNA replacement therapy, where miR-26a is administrated in a mouse model of HCC, inhibits cancer cell proliferation and induces apoptosis [224]. Delivery of downregulated miRNAs that are highly expressed and therefore tolerated in normal liver inhibits tumorigenicity without toxicity. Therefore, this approach can be a valuable strategy for miRNA-mediated HCC therapies.

Table 3: Alterations in microRNAs and their mechanisms of promoting HCC progression

microRNA	**Mechanism**	**Alteration in HCC**	**Reference**
miR-101	Targets EZH2 and inhibits HCC progression	Down-regulation	[225]
miR-122	Sensitize HCC cells to chemotherapeutic drugs by downregulating MDR related genes	Down-regulation	[226]
miR-124	- Targets PIK3CA, suppresses PI3K/AKT pathway - Suppresses the HCC growth through targeting STAT3. - Transient inhibition of HNF4α initiates HCC through a microRNA-inflammatory feedback loop of miR-124, IL6R, STAT3, miR-24, and miR-629.	Down-regulation	[227–229]
miR-139	Promotes cell proliferation and invasion through the WNT/TCF-4 pathway	Down-regulation	[230]
miR-140-5p	Suppresses cell proliferation and metastasis by targeting TGFBR1 and FGF9	Down-regulation	[231]
miR-148a	- Suppresses EMT and metastasis by targeting Met/Snail. - Reduces HPIP, represses AKT and ERK and inhibits mTOR through AKT/ERK/FOXO4/ATF5	Down-regulation	[232, 233]
miR-155	Targets APC, promotes hepatocyte proliferation and tumorigenesis by activating Wnt signaling	Overexpression	[234]
miR-17	Inhibits cell migration and invasion via suppression of MMP-3 and Akt	Down-regulation	[235]

miR-195	Blocks G1/S transition by repressing Rb/E2F signaling	Down-regulation	[236]
miR-199a/b-3p	Suppress HCC growth through targeting PAK4 and inhibiting PAK4/Raf/MEK/ERK pathway	Down-regulation	[237]
miR-21	Suppresses PTEN, hSulf-1, PDCD4 and RECK and activates EMT via AKT and ERK pathways	Overexpression	[238, 239]
miR-214	Contributes to angiogenesis through activation of HDGF paracrine pathway	Down-regulation	[240]
miR-216a/217	Activates the PI3K/Akt and TGF-β pathways by targeting PTEN and SMAD7	Overexpression	[241]
miR-221	Accelerates hepatocyte proliferation during liver regeneration	Overexpression	[242]
miR-222	Promotes metastasis through activating AKT signaling and targeting PPP2R2A	Overexpression	[243]
miR-224	Activates AKT signaling pathway by targeting PPP2R1B	Overexpression	[244]
miR-26a	Inhibits angiogenesis by down-Regulating VEGFA through PIK3C2α/Akt/HIF-1α Suppress HCC growth and metastasis through IL-6-Stat3 signaling	Down-regulation	[222, 223]
miR-27a	Reverses drug resistance (MDR) by inhibiting the FZD7/β-catenin pathway	Down-regulation	[245]
miR-375	Inhibits autophagy by reducingATG7 expression	Down-regulation	[246]
miR-503	Blocks G1/S transition by repressing Rb/E2F signaling	Down-regulation	[247]
miR-519d	Targets CDKN1A/p21, PTEN, AKT3 and TIMP2. Promotes cell proliferation, invasion and impairs apoptosis	Overexpression	[248]
miR-520b	Contributes to escape from growth suppression by targeting MEKK2 and cyclin D1 through JNK and Rb	Down-regulation	[249]
miR-612	Suppresses EMT through Akt2	Down-regulation	[250]
miR-675	Increases proliferation and inhibits invasiveness by	Overexpression	[251]

	downregulating RB and Twist1		
miR-7	Inhibits HCC cell growth and metastasis by targeting PI3K/AKT pathway	Down-regulation	[252]

5. Epigenetic Mechanisms

Epigenetic regulation of gene expression involves DNA methylation, post-translational histone modifications and changes in expression profiles of chromatin-modifying enzymes, which are highly deregulated in cancers, including HCC [253].

Epigenetic alterations in HCC include global DNA hypomethylation, gene-specific DNA hypermethylation of Rb, E-cadherin, RASSF1A and p16, gene-specific DNA hypomethylation of Vimentin, uPA and CD147, upregulation of DNA methyltransferases DNMT1, DNMT3A, and DNMT3B, and altered histone modification patterns of H3K9, and H3K27 through deregulation of histone modifying enzymes HDAC1/2/3, SIRT1, EZH2 and ARID2 [24, 29, 210, 254–260].

The histone methyltransferase EZH2 is overexpressed in HCC and contributes to the epigenetic silencing of target genes that regulate cancer cell growth and survival. Sorafenib was shown to down-regulate EZH2 protein level through accelerating its proteasome-mediated degradation in hepatoma cells, and thereby altering the HCC epigenome by reducing H3K27 trimethylation [261]. Overexpression of EZH2 reverses sorafenib-induced cell cycle arrest, and apoptosis. This epigenetics-based study revealed a novel combinational therapy approach, where inhibition of EZH2 can be used to increase sensitivity of HCC cells to chemotherapeutic agents.

All hallmarks of HCC are under the control of epigenetic mechanisms. In return, altered metabolism in HCC cells can determine the availability of metabolites that are necessary for the functioning of epigenetic modifiers and thereby regulate the cancer epigenome [262]. Aberrant activity of epigenetic regulators and gene-specific methylation alterations in HCC are given in Tables 4 and 5.

Table 4: Epigenetic deregulations in HCC

DNA methyltransferases	**Alteration in HCC**	**References**
DNMT1, DNMT3A, DNMT3B	up-regulated	[256, 263–266]
Histone deacetylases	**Alteration in HCC**	**References**
HDAC-1, HDAC-2, HDAC-3	up-regulated	[267, 268]
SIRT1	up-regulated	[269, 270]
SIRT2	up-regulated	[271]
SIRT3	down-regulated	[272]
SIRT6	down-regulated	[273, 274]
Histone methyltransferases	**Alteration in HCC**	**References**
EZH2	up-regulated	[275, 276]
SUV39H1	up-regulated	[277]
SMYD3	up-regulated	[278]
MMSET (NSD2)	up-regulated	[279]

Table 5: Hypermethylated and hypomethylated genes in HCC

Hypermethylated genes	**Description**	**Role in HCC**	**References**
RASSF1A	Ras Association Domain Family Member 1	Ras signaling pathway	[280–285]
RASSF5 (NORE1B)	Ras association domain family member 5	Ras signaling pathway	[281]
DAB2IP	DAB2 (mitogen-responsive phosphoprotein) interacting protein	Ras GTPase-activating protein	[283–285]
PTEN	phosphatase and tensin homolog	PI3K/Akt/mTOR pathway	[280, 286]
TP53	tumor protein p53	survival, cell death, proliferation, growth	[287]
RB1	retinoblastoma 1	cell cycle, proliferation,	[288]

		growth	
CDKN2A (p16)	cyclin-dependent kinase inhibitor 2A	cell cycle, proliferation, growth	[283–285, 289–293]
CDKN2B (p15)	cyclin-dependent kinase inhibitor 2B	cell cycle, proliferation, growth	[290, 294]
CDKL2	cyclin-dependent kinase-like 2	cell cycle, proliferation, growth	[283–285]
DACH1	dachshund family transcription factor 1	proliferation, growth	[295]
BMP4	Bone Morphogenetic Protein 4	growth, metabolism, angiogenesis	[283–285]
BMP6	bone morphogenetic protein 6	growth, metabolism, angiogenesis	[296]
SOCS1	suppressor of cytokine signaling 1	Jak/Stat pathway	[176, 297, 298]
SOCS3	suppressor of cytokine signaling 3	Jak/Stat pathway	[174]
SYK	spleen tyrosine kinase	Immune response	[299]
MAT1A	methionine adenosyltransferase I, alpha (liver-specific)	metabolism	[300–302]
GLS2	glutaminase 2 (liver, mitochondrial)	metabolism	[303]
GSTP1	glutathione S-transferase pi 1	metabolism	[282, 304, 305]
NQO1	NAD(P)H dehydrogenase, quinone 1	metabolism	[306]
COX-1, COX- 2	Cyclooxygenases	metabolism	[307]
NKX6-2	NK6 homeobox 2	metabolism	[283–285]
CDH1	cadherin 1, type 1, E-cadherin	invasion, metastasis	[308]
SFRPs	Secreted frizzled-related proteins	Wnt/β-catenin pathway	[309–312]
DACT2	dishevelled-binding antagonist of beta-catenin 2	Wnt/β-catenin pathway	[313, 314]
PRDM2 (RIZ1)	PR domain containing 2, with	epigenetic regulation	[315, 316]

	ZNF domain		
PRDM5	PR domain containing 5	epigenetic regulation	[317]
CHD5	chromodomain helicase DNA binding protein 5	chromatin remodeling	[318]
DNM3	dynamin 3	microtubule dynamics, vesicular transport	[283–285]
Hypomethylated genes	**Description**	**Role in HCC**	**References**
MET	met proto-oncogene	growth, invasion, metastasis	[319]
AKT3	v-akt murine thymoma viral oncogene homolog 3	PI3K/Akt/mTOR pathway	[283–285]
CD147	basigin (Ok blood group)	invasion, metastasis	[257]
VIM	Vimentin	invasion, metastasis	[260]
TFF3	Frequent trefoil factor 3	inflammation, immune response	[320]
CCL20	chemokine (C-C motif) ligand 20	inflammation, immune response	[283–285]
CD1B	T-Cell Surface Glycoprotein CD1b	inflammation, immune response	[283–285]
CD1E	T-Cell Surface Glycoprotein CD1e	inflammation, immune response	[283–285]
CD300E	immune Receptor Expressed On Myeloid Cells 2	inflammation, immune response	[283–285]
MNDA	myeloid cell nuclear differentiation antigen	inflammation, immune response	[283–285]
MAT2A	methionine adenosyltransferase 2, alpha	metabolism	[302, 321]
CYP11B1	cytochrome P450, family 11, subfamily B, polypeptide 1	drug metabolism	[283–285]
LINE-1	long interspersed nuclear element 1	proliferation	[322]

6. Concluding Remarks

Hepatocellular carcinoma is one of the leading causes of cancer-related death. This cancer is mostly a viral infection-associated disease and its etiology is quite well known. Late diagnosis and the paucity of efficient therapeutic interventions are the major reasons why this cancer remains one of the most deadly cancers, worldwide. During the last decade, most of the research on liver cancer focused on molecular classification methods and the finding of novel therapeutic targets and targeted agents. High throughput analysis of genomic state and genome-wide expression analysis were the most frequently used approaches for molecular classification. The primary purpose of molecular classification studies is to reduce the heterogeneity of HCC in terms of therapeutic response and patient survival. These studies allowed the discovery of different molecular subtypes of liver cancer by using so called “gene signatures”. A gene signature is the expression pattern of a set of genes associated with a clinical subtype of a disease. With this regards, several gene signatures and associated molecular types of HCC have been described. Figure 2 represents heterogeneity of liver cancer in parallel to multi-step evolution of this cancer. During progression of HCC, various cellular mechanisms and their underlying genetic, epigenetic and proteomic alterations enable acquisition of malignant behavior. These findings demonstrated that indeed HCC is a heterogeneous disease that can be subdivided into more or less homogenous subclasses. Unfortunately, these findings did not help much to the clinical follow-up of HCC patients, mostly because gene signatures are composed of large sets of genes, not readily adaptable to routine use.

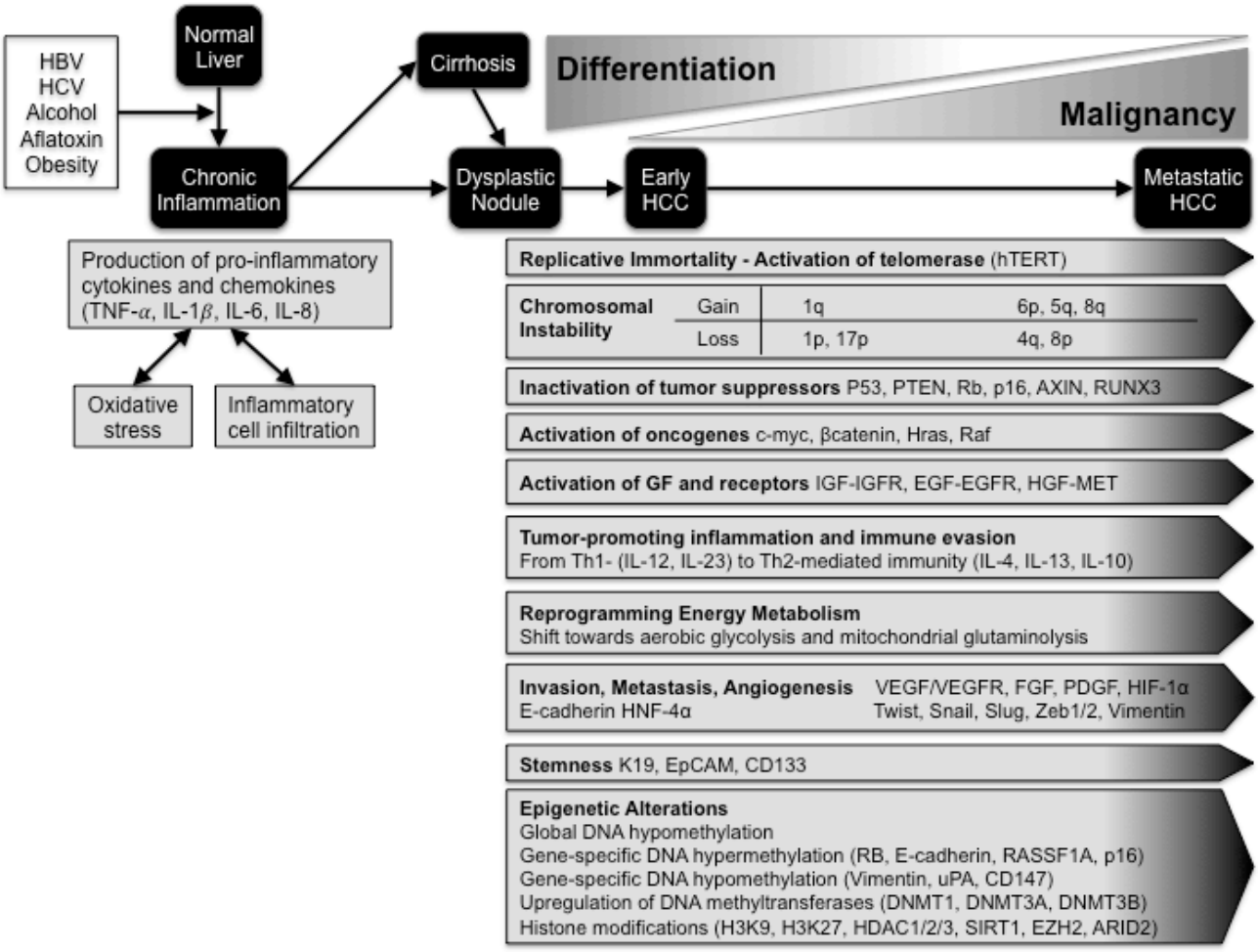

Figure 2. Multistep evolution of primary liver cancer. Development of HCC is a multistep process, where injured hepatocytes promote chronic inflammation leading to hepatocyte death and regeneration cycles during cirrhosis and enduring liver disease. The subsequent expansion of dysplastic nodules, telomerase reactivation, increased genomic instability, inactivation of tumor suppressors, activation of oncogenes and increase in growth factor signaling initiates HCC. Chromosomal instability and somatic mutations that favor the uncontrolled growth of HCC cells accumulate as the cancer advances. The acquisition of malignant phenotype is supported by tumor-promoting inflammation, capability to evade immune destruction and metabolic alterations that allow continued growth and survival of cancer cells. Onset of invasive, metastatic and angiogenetic capabilities promotes progression of carcinoma to the highly malignant metastatic state associated with stemness markers. Molecular alterations throughout the malignant transformation of HCC are regulated both in genetic and epigenetic levels.

The outputs of the efforts for finding novel targets for HCC treatment are so far less than satisfactory. There are several reasons for this. Firstly the number of mutant but targetable genes is limited. Secondly, the pathogenesis of HCC may be related to cellular signaling pathways rather than specific genes. Probably, some of the HCC-promoting signaling pathways are activated by mechanisms other than gene mutations. Changes in gene expression or protein networks (such as overall expression, stability, post-translational modifications) may be more critical for HCC pathology than gene mutations. The number of genes with dysregulated expression in HCC is extremely high. Consequently, a large set of signaling pathways appear to be deregulated in this cancer. The paucity of gene mutations together with such a high number of genes with expression changes strongly suggests that the epigenome of HCC is highly affected. DNA methylation changes appear to predominate HCC epigenome. In addition, a few published data on histone methylation patterns suggests that there are profound changes in the organization of HCC nucleosomes and chromatin. Future studies aiming to decipher the status of HCC epigenome and its effect on HCC proteome may lead to a better understanding of this unusual cancer and may then lead to the discovery of novel therapeutic targets.

References

1 Jemal, A., Bray, F., and Ferlay, J. (2011). Global Cancer Statistics. *CA CANCER J CLIN* ***61***, 69–90.

2 Ferlay, J., Shin, H.-R., Bray, F., Forman, D., Mathers, C., and Parkin, D. M. (2010). Estimates of worldwide burden of cancer in 2008: GLOBOCAN 2008. *Int. J. Cancer* ***127***, 2893–917. Available at: http://www.ncbi.nlm.nih.gov/pubmed/21351269 [Accessed November 6, 2013].

3 Perz, J. F., Armstrong, G. L., Farrington, L. a, Hutin, Y. J. F., and Bell, B. P. (2006). The contributions of hepatitis B virus and hepatitis C virus infections to cirrhosis and primary liver cancer worldwide. *J. Hepatol.* ***45***, 529–38. Available at: http://www.ncbi.nlm.nih.gov/pubmed/16879891 [Accessed November 7, 2013].

4 Farazi, P. A., and DePinho, R. A. (2006). Hepatocellular carcinoma pathogenesis: from genes to environment. *Nat. Rev. Cancer* ***6***, 674–87. Available at: http://www.ncbi.nlm.nih.gov/pubmed/16929323 [Accessed November 14, 2013].

5 Hino, O., Kajino, K., Umeda, T., and Arakawa, Y. (2002). Understanding the hypercarcinogenic state in chronic hepatitis: a clue to the prevention of human hepatocellular carcinoma. *J. Gastroenterol.* ***37***, 883–7. Available at: http://www.ncbi.nlm.nih.gov/pubmed/12483242 [Accessed November 26, 2013].

6 Bureau, C., Bernad, J., Chaouche, N., Orfila, C., Béraud, M., Gonindard, C., Alric, L., Vinel, J. P., and Pipy, B. (2001). Nonstructural 3 protein of hepatitis C virus triggers an oxidative burst in human monocytes via activation of NADPH oxidase. *J. Biol. Chem.* ***276***, 23077–83. Available at: http://www.ncbi.nlm.nih.gov/pubmed/11304537 [Accessed November 26, 2013].

7 Gong, G., Waris, G., Tanveer, R., and Siddiqui, A. (2001). Human hepatitis C virus NS5A protein alters intracellular calcium levels, induces oxidative stress, and activates STAT-3 and NF-kappa B. *Proc. Natl. Acad. Sci. U. S. A.* ***98***, 9599–604. Available at: http://www.pubmedcentral.nih.gov/articlerender.fcgi?artid=55498&tool=pmcentrez&rendertype=abstract [Accessed November 26, 2013].

8 Kedderis, G. L. Biochemical basis of hepatocellular injury. *Toxicol. Pathol.* ***24***, 77–83. Available at: http://www.ncbi.nlm.nih.gov/pubmed/8839284 [Accessed March 18, 2014].

9 Aston, N. S., Watt, N., Morton, I. E., Tanner, M. S., and Evans, G. S. (2000). Copper toxicity affects proliferation and viability of human hepatoma cells (HepG2 line). *Hum. Exp. Toxicol.* ***19***, 367–76. Available at: http://www.ncbi.nlm.nih.gov/pubmed/10962511 [Accessed March 18, 2014].

10 Ozcelik, D., Ozaras, R., Gurel, Z., Uzun, H., and Aydin, S. (2003). Copper-mediated oxidative stress in rat liver. *Biol. Trace Elem. Res.* ***96***, 209–15. Available at: http://www.ncbi.nlm.nih.gov/pubmed/14716100 [Accessed March 18, 2014].

11 Jung, M., Drapier, J. C., Weidenbach, H., Renia, L., Oliveira, L., Wang, A., Beger, H. G., and Nussler, A. K. (2000). Effects of hepatocellular iron imbalance on nitric oxide and reactive oxygen intermediates production in a model of sepsis. *J. Hepatol.* ***33***, 387–94. Available at: http://www.ncbi.nlm.nih.gov/pubmed/11019994 [Accessed March 18, 2014].

12 Eckers, A., Reimann, K., and Klotz, L.-O. (2009). Nickel and copper ion-induced stress signaling in human hepatoma cells: analysis of phosphoinositide 3'-kinase/Akt signaling. *Biometals* ***22***, 307–16. Available at: http://www.ncbi.nlm.nih.gov/pubmed/18925359 [Accessed March 18, 2014].

13 Fausto, N., Campbell, J. S., and Riehle, K. J. (2006). Liver regeneration. *Hepatology* ***43***, S45–53. Available at: http://www.ncbi.nlm.nih.gov/pubmed/16447274 [Accessed November 8, 2013].

14 Forner, A., Reig, M. E., de Lope, C. R., and Bruix, J. (2010). Current strategy for staging and treatment: the BCLC update and future prospects. *Semin. Liver Dis.* ***30***, 61–74. Available at: http://www.ncbi.nlm.nih.gov/pubmed/20175034.

15 Llovet, J. M., Di Bisceglie, A. M., Bruix, J., Kramer, B. S., Lencioni, R., Zhu, A. X., Sherman, M., Schwartz, M., Lotze, M., Talwalkar, J., et al. (2008). Design and endpoints of clinical trials in hepatocellular carcinoma. *J. Natl. Cancer Inst.* ***100***, 698–711. Available at: http://www.ncbi.nlm.nih.gov/pubmed/18477802 [Accessed November 11, 2013].

16 El-Serag, H. B. (2011). Hepatocellular carcinoma. *N. Engl. J. Med.* ***365***, 1118–27. Available at: http://www.ncbi.nlm.nih.gov/pubmed/21992124.

17 Lee, J.-S., Kim, J. H., Park, Y.-Y., and Mills, G. B. (2011). Systems biology approaches to decoding the genome of liver cancer. *Cancer Res. Treat.* ***43***, 205–11. Available at: http://www.pubmedcentral.nih.gov/articlerender.fcgi?artid=3253861&tool=pmcentrez&rendertype=abstract.

18 Wilhelm, S., Carter, C., Lynch, M., Lowinger, T., Dumas, J., Smith, R. a, Schwartz, B., Simantov, R., and Kelley, S. (2006). Discovery and development of sorafenib: a multikinase inhibitor for treating cancer. *Nat. Rev. Drug Discov.* ***5***, 835–44. Available at: http://www.ncbi.nlm.nih.gov/pubmed/17016424 [Accessed November 7, 2013].

19 Cheng, A.-L., Guan, Z., Chen, Z., Tsao, C.-J., Qin, S., Kim, J. S., Yang, T.-S., Tak, W. Y., Pan, H., Yu, S., et al. (2012). Efficacy and safety of sorafenib in patients with advanced hepatocellular carcinoma according to baseline status: subset analyses of the phase III Sorafenib Asia-Pacific trial. *Eur. J. Cancer* ***48***, 1452–65. Available at: http://www.ncbi.nlm.nih.gov/pubmed/22240282 [Accessed November 25, 2013].

20 Raoul, J.-L., Bruix, J., Greten, T. F., Sherman, M., Mazzaferro, V., Hilgard, P., Scherubl, H., Scheulen, M. E., Germanidis, G., Dominguez, S., et al. (2012). Relationship between baseline hepatic status and outcome, and effect of sorafenib on liver function: SHARP trial subanalyses. *J. Hepatol.* ***56***, 1080–8. Available at: http://www.ncbi.nlm.nih.gov/pubmed/22245896 [Accessed November 14, 2013].

21 Cheng, A.-L., Kang, Y.-K., Chen, Z., Tsao, C.-J., Qin, S., Kim, J. S., Luo, R., Feng, J., Ye, S., Yang, T.-S., et al. (2009). Efficacy and safety of sorafenib in patients in the Asia-Pacific region with advanced hepatocellular carcinoma: a phase III randomised, double-blind, placebo-controlled trial. *Lancet Oncol.* ***10***, 25–34. Available at: http://www.ncbi.nlm.nih.gov/pubmed/19095497 [Accessed November 14, 2013].

22 Hanahan, D., and Weinberg, R. a (2011). Hallmarks of cancer: the next generation. *Cell* ***144***, 646–74. Available at: http://www.ncbi.nlm.nih.gov/pubmed/21376230 [Accessed November 6, 2013].

23 Stratton, M. R., Campbell, P. J., and Futreal, P. A. (2009). The cancer genome. *Nature* ***458***, 719–24. Available at:

http://www.pubmedcentral.nih.gov/articlerender.fcgi?artid=2821689&tool=pmcentrez&rendertype=abstract [Accessed November 6, 2013].

24 Guichard, C., Amaddeo, G., Imbeaud, S., Ladeiro, Y., Pelletier, L., Maad, I. Ben, Calderaro, J., Bioulac-Sage, P., Letexier, M., Degos, F., et al. (2012). Integrated analysis of somatic mutations and focal copy-number changes identifies key genes and pathways in hepatocellular carcinoma. *Nat. Genet.* ***44***, 694–8. Available at: http://www.ncbi.nlm.nih.gov/pubmed/22561517 [Accessed November 6, 2013].

25 Nault, J.-C., and Zucman-Rossi, J. (2011). Genetics of hepatobiliary carcinogenesis. *Semin. Liver Dis.* ***31***, 173–87. Available at: http://www.ncbi.nlm.nih.gov/pubmed/21538283.

26 Midorikawa, Y., Yamamoto, S., Tsuji, S., Kamimura, N., Ishikawa, S., Igarashi, H., Makuuchi, M., Kokudo, N., Sugimura, H., and Aburatani, H. (2009). Allelic imbalances and homozygous deletion on 8p23.2 for stepwise progression of hepatocarcinogenesis. *Hepatology* ***49***, 513–22. Available at: http://www.ncbi.nlm.nih.gov/pubmed/19105209 [Accessed November 14, 2013].

27 Chochi, Y., Kawauchi, S., Nakao, M., Furuya, T., Hashimoto, K., and Oga, A. (2009). A copy number gain of the 6p arm is linked with advanced hepatocellular carcinoma : an array-based comparative genomic hybridization study. *J. Pathol.* ***217***, 677–684.

28 Bréchot, C., Gozuacik, D., Murakami, Y., and Paterlini-Bréchot, P. (2000). Molecular bases for the development of hepatitis B virus (HBV)-related hepatocellular carcinoma (HCC). *Semin. Cancer Biol.* ***10***, 211–31. Available at: http://www.ncbi.nlm.nih.gov/pubmed/10936070 [Accessed November 25, 2013].

29 Fujimoto, A., Totoki, Y., Abe, T., Boroevich, K. a, Hosoda, F., Nguyen, H. H., Aoki, M., Hosono, N., Kubo, M., Miya, F., et al. (2012). Whole-genome sequencing of liver cancers identifies etiological influences on mutation patterns and recurrent mutations in chromatin regulators. *Nat. Genet.* ***44***, 760–4. Available at: http://www.ncbi.nlm.nih.gov/pubmed/22634756 [Accessed November 15, 2013].

30 Hanahan, D., and Coussens, L. M. (2012). Accessories to the crime: functions of cells recruited to the tumor microenvironment. *Cancer Cell* ***21***, 309–22. Available at: http://www.ncbi.nlm.nih.gov/pubmed/22439926 [Accessed November 9, 2013].

31 Irmak, M. B., Ince, G., Ozturk, M., and Cetin-Atalay, R. (2003). Acquired tolerance of hepatocellular carcinoma cells to selenium deficiency: a selective survival mechanism? *Cancer Res.* ***63***, 6707–15. Available at: http://www.ncbi.nlm.nih.gov/pubmed/14583465.

32 Killela, P. J., Reitman, Z. J., Jiao, Y., Bettegowda, C., Agrawal, N., Diaz, L. a, Friedman, A. H., Friedman, H., Gallia, G. L., Giovanella, B. C., et al. (2013). TERT promoter mutations occur frequently in gliomas and a subset of tumors derived from cells with low rates of self-renewal. *Proc. Natl. Acad. Sci. U. S. A.* ***110***, 6021–6. Available at:

http://www.pubmedcentral.nih.gov/articlerender.fcgi?artid=3625331&tool=pmcentrez&rendertype=abstract [Accessed November 16, 2013].

33 Honda, K., Sbisà, E., Tullo, a, Papeo, P. a, Saccone, C., Poole, S., Pignatelli, M., Mitry, R. R., Ding, S., Isla, a, et al. (1998). P53 Mutation Is a Poor Prognostic Indicator for Survival in Patients With Hepatocellular Carcinoma Undergoing Surgical Tumour Ablation. *Br. J. Cancer* ***77***, 776–82. Available at: http://www.pubmedcentral.nih.gov/articlerender.fcgi?artid=2149958&tool=pmcentrez&rendertype=abstract.

34 Hussain, S. P., Schwank, J., Staib, F., Wang, X. W., and Harris, C. C. (2007). TP53 mutations and hepatocellular carcinoma: insights into the etiology and pathogenesis of liver cancer. *Oncogene* ***26***, 2166–76. Available at: http://www.ncbi.nlm.nih.gov/pubmed/17401425 [Accessed November 14, 2013].

35 Bressac, B., Kew, M., Wands, J., and Ozturk, M. (1991). Selective G to T mutations of p53 gene in hepatocellular carcinoma from southern Africa. *Nature* ***350***.

36 Hsu, I. C., Metcalf, R. A., Sun, T., Welsh, J. A., Wang, N. J., and Harris, C. C. (1991). Mutational hotspot in the p53 gene in human hepatocellular carcinomas. *Nature* ***350***, 427–8. Available at: http://www.ncbi.nlm.nih.gov/pubmed/1849234 [Accessed November 20, 2013].

37 Ishizaki, Y., Ikeda, S., Fujimori, M., Shimizu, Y., Kurihara, T., Itamoto, T., Kikuchi, A., Okajima, M., and Asahara, T. (2004). Immunohistochemical analysis and mutational analyses of beta-catenin, Axin family and APC genes in hepatocellular carcinomas. *Int. J. Oncol.* ***24***, 1077–83. Available at: http://www.ncbi.nlm.nih.gov/pubmed/15067328 [Accessed November 26, 2013].

38 Taniguchi, K., Roberts, L. R., Aderca, I. N., Dong, X., Qian, C., Murphy, L. M., Nagorney, D. M., Burgart, L. J., Roche, P. C., Smith, D. I., et al. (2002). Mutational spectrum of beta-catenin, AXIN1, and AXIN2 in hepatocellular carcinomas and hepatoblastomas. *Oncogene* ***21***, 4863–71. Available at: http://www.ncbi.nlm.nih.gov/pubmed/12101426 [Accessed November 14, 2013].

39 Laurent-Puig, P., and Zucman-Rossi, J. (2006). Genetics of hepatocellular tumors. *Oncogene* ***25***, 3778–86. Available at: http://www.ncbi.nlm.nih.gov/pubmed/16799619 [Accessed November 14, 2013].

40 Ozturk, M. (1999). Genetic aspects of hepatocellular carcinogenesis. *Semin. Liver Dis.* ***19***, 235–42. Available at: http://www.ncbi.nlm.nih.gov/pubmed/10518303 [Accessed November 26, 2013].

41 Higashitsuji, H., Itoh, K., Nagao, T., Dawson, S., Nonoguchi, K., Kido, T., Mayer, R. J., Arii, S., and Fujita, J. (2000). Reduced stability of retinoblastoma protein by gankyrin, an oncogenic ankyrin-repeat protein overexpressed in hepatomas. *Nat. Med.* ***6***, 96–9.

Available at: http://www.ncbi.nlm.nih.gov/pubmed/10613832 [Accessed November 26, 2013].

42 Zhang, X., Xu, H. J., Murakami, Y., Sachse, R., Yashima, K., Hirohashi, S., Hu, S. X., Benedict, W. F., and Sekiya, T. (1994). Deletions of chromosome 13q, mutations in Retinoblastoma 1, and retinoblastoma protein state in human hepatocellular carcinoma. *Cancer Res.* ***54***, 4177–82. Available at: http://www.ncbi.nlm.nih.gov/pubmed/8033150 [Accessed November 26, 2013].

43 Boyault, S., Rickman, D. S., de Reyniès, A., Balabaud, C., Rebouissou, S., Jeannot, E., Hérault, A., Saric, J., Belghiti, J., Franco, D., et al. (2007). Transcriptome classification of HCC is related to gene alterations and to new therapeutic targets. *Hepatology* ***45***, 42–52. Available at: http://www.ncbi.nlm.nih.gov/pubmed/17187432 [Accessed November 14, 2013].

44 Liew, C. T., Li, H. M., Lo, K. W., Leow, C. K., Chan, J. Y., Hin, L. Y., Lau, W. Y., Lai, P. B., Lim, B. K., Huang, J., et al. (1999). High frequency of p16INK4A gene alterations in hepatocellular carcinoma. *Oncogene* ***18***, 789–95. Available at: http://www.ncbi.nlm.nih.gov/pubmed/9989830 [Accessed November 26, 2013].

45 Bae, J.-J., Rho, J.-W., Lee, T.-J., Yun, S.-S., Kim, H.-J., Choi, J.-H., Jeong, D., Jang, B.-C., and Lee, T.-Y. (2007). Loss of heterozygosity on chromosome 10q23 and mutation of the phosphatase and tensin homolog deleted from chromosome 10 tumor suppressor gene in Korean hepatocellular carcinoma patients. *Oncol. Rep.* ***18***, 1007–13. Available at: http://www.ncbi.nlm.nih.gov/pubmed/17786367 [Accessed November 26, 2013].

46 Fujiwara, Y., Hoon, D. S., Yamada, T., Umeshita, K., Gotoh, M., Sakon, M., Nishisho, I., and Monden, M. (2000). PTEN / MMAC1 mutation and frequent loss of heterozygosity identified in chromosome 10q in a subset of hepatocellular carcinomas. *Jpn. J. Cancer Res.* ***91***, 287–92. Available at: http://www.ncbi.nlm.nih.gov/pubmed/10760687 [Accessed November 26, 2013].

47 Kawamura, N., Nagai, H., Bando, K., Koyama, M., Matsumoto, S., Tajiri, T., Onda, M., Fujimoto, J., Ueki, T., Konishi, N., et al. (1999). PTEN/MMAC1 mutations in hepatocellular carcinomas: somatic inactivation of both alleles in tumors. *Jpn. J. Cancer Res.* ***90***, 413–8. Available at: http://www.ncbi.nlm.nih.gov/pubmed/10363579 [Accessed November 26, 2013].

48 Yao, Y. J., Ping, X. L., Zhang, H., Chen, F. F., Lee, P. K., Ahsan, H., Chen, C. J., Lee, P. H., Peacocke, M., Santella, R. M., et al. (1999). PTEN/MMAC1 mutations in hepatocellular carcinomas. *Oncogene* ***18***, 3181–5. Available at: http://www.ncbi.nlm.nih.gov/pubmed/10340391 [Accessed November 26, 2013].

49 Buontempo, F., Ersahin, T., Missiroli, S., Senturk, S., Etro, D., Ozturk, M., Capitani, S., Cetin-Atalay, R., and Neri, M. L. (2011). Inhibition of Akt signaling in hepatoma cells induces apoptotic cell death independent of Akt activation status. *Invest. New Drugs* ***29***,

1303–13. Available at: http://www.ncbi.nlm.nih.gov/pubmed/20628892 [Accessed November 25, 2013].

50 Challen, C., Guo, K., Collier, J. D., Cavanagh, D., and Bassendine, M. F. (1992). Infrequent point mutations in codons 12 and 61 of ras oncogenes in human hepatocellular carcinomas. *J. Hepatol.* ***14***, 342–6. Available at: http://www.ncbi.nlm.nih.gov/pubmed/1323601 [Accessed November 26, 2013].

51 Takada, S., and Koike, K. (1989). Activated N-ras gene was found in human hepatoma tissue but only in a small fraction of the tumor cells. *Oncogene* ***4***, 189–93. Available at: http://www.ncbi.nlm.nih.gov/pubmed/2538792 [Accessed November 26, 2013].

52 Tsuda, H., Hirohashi, S., Shimosato, Y., Ino, Y., Yoshida, T., and Terada, M. (1989). Low incidence of point mutation of c-Ki-ras and N-ras oncogenes in human hepatocellular carcinoma. *Jpn. J. Cancer Res.* ***80***, 196–9. Available at: http://www.ncbi.nlm.nih.gov/pubmed/2542205 [Accessed November 26, 2013].

53 Mori, T., Nomoto, S., Koshikawa, K., Fujii, T., Sakai, M., Nishikawa, Y., Inoue, S., Takeda, S., Kaneko, T., and Nakao, A. (2005). Decreased expression and frequent allelic inactivation of the RUNX3 gene at 1p36 in human hepatocellular carcinoma. *Liver Int.* ***25***, 380–8. Available at: http://www.ncbi.nlm.nih.gov/pubmed/15780064 [Accessed November 26, 2013].

54 Miyagawa, K., Sakakura, C., Nakashima, S., Yoshikawa, T., Kin, S., Nakase, Y., Ito, K., Yamagishi, H., Ida, H., Yazumi, S., et al. Down-regulation of RUNX1, RUNX3 and CBFbeta in hepatocellular carcinomas in an early stage of hepatocarcinogenesis. *Anticancer Res.* ***26***, 3633–43. Available at: http://www.ncbi.nlm.nih.gov/pubmed/17094378 [Accessed November 26, 2013].

55 Nakanishi, Y., Shiraha, H., Nishina, S., Tanaka, S., Matsubara, M., Horiguchi, S., Iwamuro, M., Takaoka, N., Uemura, M., Kuwaki, K., et al. (2011). Loss of runt-related transcription factor 3 expression leads hepatocellular carcinoma cells to escape apoptosis. *BMC Cancer* ***11***, 3. Available at: http://www.pubmedcentral.nih.gov/articlerender.fcgi?artid=3022884&tool=pmcentrez&rendertype=abstract [Accessed November 26, 2013].

56 Li, X., Zhang, Y., Zhang, Y., Qiao, T., Wu, K., Ding, J., Liu, J., and Fan, D. (2008). RUNX3 inhibits growth of HCC cells and HCC xenografts in mice in combination with adriamycin. *Cancer Biol. Ther.* ***7***, 669–76. Available at: http://www.ncbi.nlm.nih.gov/pubmed/18259121 [Accessed November 26, 2013].

57 Tanaka, S., Shiraha, H., Nakanishi, Y., Nishina, S.-I., Matsubara, M., Horiguchi, S., Takaoka, N., Iwamuro, M., Kataoka, J., Kuwaki, K., et al. (2012). Runt-related transcription factor 3 reverses epithelial-mesenchymal transition in hepatocellular carcinoma. *Int. J. Cancer* ***131***, 2537–46. Available at: http://www.ncbi.nlm.nih.gov/pubmed/22488108 [Accessed November 26, 2013].

58 Imbeaud, S., Ladeiro, Y., and Zucman-Rossi, J. (2010). Identification of novel oncogenes and tumor suppressors in hepatocellular carcinoma. *Semin. Liver Dis.* ***30***, 75–86. Available at: http://www.ncbi.nlm.nih.gov/pubmed/20175035.

59 Villanueva, A., Newell, P., Chiang, D. Y., Ph, D., Friedman, S. L., and Llovet, J. M. (2007). Genomics and Signaling Pathways in Hepatocellular Carcinoma. *Semin. Liver Dis.* ***1***, 55–76.

60 Woo, H. G., Park, E. S., Lee, J.-S., Lee, Y.-H., Ishikawa, T., Kim, Y. J., and Thorgeirsson, S. S. (2009). Identification of potential driver genes in human liver carcinoma by genomewide screening. *Cancer Res.* ***69***, 4059–66. Available at: http://www.pubmedcentral.nih.gov/articlerender.fcgi?artid=2750086&tool=pmcentrez&rendertype=abstract [Accessed November 18, 2013].

61 Hoshida, Y., Nijman, S. M. B., Kobayashi, M., Chan, J. A., Brunet, J., Chiang, D. Y., Villanueva, A., Newell, P., Ikeda, K., Hashimoto, M., et al. (2009). Integrative Transcriptome Analysis Reveals Common Molecular Subclasses of Human Hepatocellular Carcinoma. 7385–7392.

62 Deng, Q., Wang, Q., Zong, W.-Y., Zheng, D.-L., Wen, Y.-X., Wang, K.-S., Teng, X.-M., Zhang, X., Huang, J., and Han, Z.-G. (2010). E2F8 contributes to human hepatocellular carcinoma via regulating cell proliferation. *Cancer Res.* ***70***, 782–91. Available at: http://www.ncbi.nlm.nih.gov/pubmed/20068156 [Accessed November 26, 2013].

63 Ladu, S., Calvisi, D. F., Conner, E. A., Farina, M., Factor, V. M., and Thorgeirsson, S. S. (2008). E2F1 inhibits c-Myc-driven apoptosis via PIK3CA/Akt/mTOR and COX-2 in a mouse model of human liver cancer. *Gastroenterology* ***135***, 1322–32. Available at: http://www.pubmedcentral.nih.gov/articlerender.fcgi?artid=2614075&tool=pmcentrez&rendertype=abstract [Accessed November 26, 2013].

64 Chen, X., Cheung, S. T., So, S., Fan, T., Barry, C., Higgins, J., Lai, K., Ji, J., Dudoit, S., Ng, I. O. L., et al. (2002). Gene Expression Patterns in Human Liver Cancers. *Mol. Biol. Cell* ***13***, 1929–1939.

65 Lee, J.-S., Chu, I.-S., Heo, J., Calvisi, D. F., Sun, Z., Roskams, T., Durnez, A., Demetris, A. J., and Thorgeirsson, S. S. (2004). Classification and prediction of survival in hepatocellular carcinoma by gene expression profiling. *Hepatology* ***40***, 667–76. Available at: http://www.ncbi.nlm.nih.gov/pubmed/15349906 [Accessed November 14, 2013].

66 Kaposi-Novak, P., Libbrecht, L., Woo, H. G., Lee, Y.-H., Sears, N. C., Coulouarn, C., Conner, E. a, Factor, V. M., Roskams, T., and Thorgeirsson, S. S. (2009). Central role of c-Myc during malignant conversion in human hepatocarcinogenesis. *Cancer Res.* ***69***, 2775–82. Available at: http://www.pubmedcentral.nih.gov/articlerender.fcgi?artid=2680077&tool=pmcentrez&rendertype=abstract [Accessed November 25, 2013].

67 Shachaf, C. M., Kopelman, A. M., and Arvanitis, C. (2004). MYC inactivation uncovers pluripotent differentiation and tumour dormancy in hepatocellular cancer. *Nature **431***.

68 Park, S.-H., Lim, J. S., Lim, S.-Y., Tiwari, I., and Jang, K. L. (2011). Hepatitis C virus Core protein stimulates cell growth by down-regulating p16 expression via DNA methylation. *Cancer Lett. **310***, 61–8. Available at: http://www.ncbi.nlm.nih.gov/pubmed/21757290 [Accessed November 25, 2013].

69 Lim, J. S., Park, S.-H., and Jang, K. L. (2012). Hepatitis C virus Core protein overcomes stress-induced premature senescence by down-regulating p16 expression via DNA methylation. *Cancer Lett. **321***, 154–61. Available at: http://www.ncbi.nlm.nih.gov/pubmed/22326283 [Accessed November 25, 2013].

70 Lee, H., Woo, Y.-J., Kim, S. S., Kim, S.-H., Park, B.-J., Choi, D., and Jang, K. L. (2013). Hepatitis C virus Core protein overcomes all-trans retinoic acid-induced cell growth arrest by inhibiting retinoic acid receptor-β2 expression via DNA methylation. *Cancer Lett. **335***, 372–9. Available at: http://www.ncbi.nlm.nih.gov/pubmed/23474497 [Accessed November 25, 2013].

71 Dong, L., Yang, G., Pan, Y., Chen, Y., Tan, Y., Dai, R., Ren, Y., Fu, J., and Wang, H. (2011). The oncoprotein p28GANK establishes a positive feedback loop in β-catenin signaling. *Cell Res. **21***, 1248–61. Available at: http://www.pubmedcentral.nih.gov/articlerender.fcgi?artid=3193485&tool=pmcentrez&rendertype=abstract [Accessed November 25, 2013].

72 Zhang, L., Yang, Z., Ma, A., Qu, Y., Xia, S., Xu, D., Ge, C., Qiu, B., Xia, Q., Li, J., et al. (2013). Growth arrest and DNA damage 45G down-regulation contributes to janus kinase/signal transducer and activator of transcription 3 activation and cellular senescence evasion in hepatocellular carcinoma. *Hepatology*. Available at: http://www.ncbi.nlm.nih.gov/pubmed/23897841 [Accessed November 26, 2013].

73 Sugano, Y., Matsuzaki, K., Tahashi, Y., Furukawa, F., Mori, S., Yamagata, H., Yoshida, K., Matsushita, M., Nishizawa, M., Fujisawa, J., et al. (2003). Distortion of autocrine transforming growth factor beta signal accelerates malignant potential by enhancing cell growth as well as PAI-1 and VEGF production in human hepatocellular carcinoma cells. *Oncogene **22***, 2309–21. Available at: http://www.ncbi.nlm.nih.gov/pubmed/12700666 [Accessed December 10, 2013].

74 Yamazaki, K., Masugi, Y., and Sakamoto, M. (2011). Molecular pathogenesis of hepatocellular carcinoma: altering transforming growth factor-β signaling in hepatocarcinogenesis. *Dig. Dis. **29***, 284–8. Available at: http://www.ncbi.nlm.nih.gov/pubmed/21829019 [Accessed November 26, 2013].

75 Caja, L., Sancho, P., Bertran, E., and Fabregat, I. (2011). Dissecting the effect of targeting the epidermal growth factor receptor on TGF-β-induced-apoptosis in human hepatocellular carcinoma cells. *J. Hepatol. **55***, 351–8. Available at: http://www.ncbi.nlm.nih.gov/pubmed/21147185 [Accessed December 3, 2013].

76 Mazzocca, A., Fransvea, E., Dituri, F., Lupo, L., Antonaci, S., and Giannelli, G. (2010). Down-regulation of connective tissue growth factor by inhibition of transforming growth factor beta blocks the tumor-stroma cross-talk and tumor progression in hepatocellular carcinoma. *Hepatology* ***51***, 523–34. Available at: http://www.ncbi.nlm.nih.gov/pubmed/19821534 [Accessed December 10, 2013].

77 Caja, L., Sancho, P., Bertran, E., Iglesias-Serret, D., Gil, J., and Fabregat, I. (2009). Overactivation of the MEK/ERK pathway in liver tumor cells confers resistance to TGF-{beta}-induced cell death through impairing up-regulation of the NADPH oxidase NOX4. *Cancer Res.* ***69***, 7595–602. Available at: http://www.ncbi.nlm.nih.gov/pubmed/19773433 [Accessed November 19, 2013].

78 Van Zijl, F., Mair, M., Csiszar, A., Schneller, D., Zulehner, G., Huber, H., Eferl, R., Beug, H., Dolznig, H., and Mikulits, W. (2009). Hepatic tumor-stroma crosstalk guides epithelial to mesenchymal transition at the tumor edge. *Oncogene* ***28***, 4022–33. Available at: http://www.pubmedcentral.nih.gov/articlerender.fcgi?artid=2900602&tool=pmcentrez&rendertype=abstract [Accessed November 8, 2013].

79 Bierie, B., and Moses, H. L. (2006). Tumour microenvironment: TGFbeta: the molecular Jekyll and Hyde of cancer. *Nat. Rev. Cancer* ***6***, 506–20. Available at: http://www.ncbi.nlm.nih.gov/pubmed/16794634 [Accessed November 7, 2013].

80 Tovar, V., Alsinet, C., Villanueva, A., Hoshida, Y., Chiang, D. Y., Solé, M., Thung, S., Moyano, S., Toffanin, S., Mínguez, B., et al. (2010). IGF activation in a molecular subclass of hepatocellular carcinoma and pre-clinical efficacy of IGF-1R blockage. *J. Hepatol.* ***52***, 550–9. Available at: http://www.pubmedcentral.nih.gov/articlerender.fcgi?artid=3662876&tool=pmcentrez&rendertype=abstract [Accessed November 25, 2013].

81 López-Calderero, I., Sánchez Chávez, E., and García-Carbonero, R. (2010). The insulin-like growth factor pathway as a target for cancer therapy. *Clin. Transl. Oncol.* ***12***, 326–38. Available at: http://www.ncbi.nlm.nih.gov/pubmed/20466617 [Accessed November 25, 2013].

82 Nussbaum, T., Samarin, J., Ehemann, V., Bissinger, M., Ryschich, E., Khamidjanov, A., Yu, X., Gretz, N., Schirmacher, P., and Breuhahn, K. (2008). Autocrine insulin-like growth factor-II stimulation of tumor cell migration is a progression step in human hepatocarcinogenesis. *Hepatology* ***48***, 146–56. Available at: http://www.ncbi.nlm.nih.gov/pubmed/18537183 [Accessed November 25, 2013].

83 Pollak, M. (2008). Insulin and insulin-like growth factor signalling in neoplasia. *Nat. Rev. Cancer* ***8***, 915–28. Available at: http://www.ncbi.nlm.nih.gov/pubmed/19029956 [Accessed November 19, 2013].

84 Cells, H. C., Chen, Y., Boyartchuk, V., and Lewis, B. C. (2009). Differential Roles of Insulin-like Growth Factor Receptor – and Insulin Receptor – mediated Signaling in the Phenotypes of. *Neoplasia **11***, 835–845.

85 Okada, T., Iizuka, N., Yamada-Okabe, H., Mori, N., Tamesa, T., Takemoto, N., Tangoku, A., Hamada, K., Nakayama, H., Miyamoto, T., et al. (2003). Gene expression profile linked to p53 status in hepatitis C virus-related hepatocellular carcinoma. *FEBS Lett. **555***, 583–590. Available at: http://linkinghub.elsevier.com/retrieve/pii/S0014579303013450 [Accessed November 14, 2013].

86 Liedtke, C., and Trautwein, C. (2012). The role of TNF and Fas dependent signaling in animal models of inflammatory liver injury and liver cancer. *Eur. J. Cell Biol. **91***, 582–9. Available at: http://www.ncbi.nlm.nih.gov/pubmed/22153863 [Accessed November 25, 2013].

87 Soung, Y. H., Lee, J. W., Kim, S. Y., Sung, Y. J., Park, W. S., Nam, S. W., Kim, S. H., Lee, J. Y., Yoo, N. J., and Lee, S. H. (2005). Caspase-8 gene is frequently inactivated by the frameshift somatic mutation 1225_1226delTG in hepatocellular carcinomas. *Oncogene **24***, 141–7. Available at: http://www.ncbi.nlm.nih.gov/pubmed/15531912 [Accessed November 14, 2013].

88 Hammam, O., Mahmoud, O., Zahran, M., Aly, S., Hosny, K., Helmy, A., and Anas, A. (2012). The role of fas/fas ligand system in the pathogenesis of liver cirrhosis and hepatocellular carcinoma. *Hepat. Mon. **12***, e6132. Available at: http://www.pubmedcentral.nih.gov/articlerender.fcgi?artid=3539063&tool=pmcentrez&rendertype=abstract [Accessed November 25, 2013].

89 Oh, B.-K., Jo Chae, K., Park, C., Kim, K., Jung Lee, W., Han, K., and Nyun Park, Y. (2003). Telomere shortening and telomerase reactivation in dysplastic nodules of human hepatocarcinogenesis. *J. Hepatol. **39***, 786–792. Available at: http://linkinghub.elsevier.com/retrieve/pii/S0168827803003957 [Accessed November 25, 2013].

90 Oh, B.-K., Kim, H., Park, Y. N., Yoo, J. E., Choi, J., Kim, K.-S., Lee, J. J., and Park, C. (2008). High telomerase activity and long telomeres in advanced hepatocellular carcinomas with poor prognosis. *Lab. Invest. **88***, 144–52. Available at: http://www.ncbi.nlm.nih.gov/pubmed/18158557 [Accessed November 25, 2013].

91 Ozturk, M., Arslan-Ergul, A., Bagislar, S., Senturk, S., and Yuzugullu, H. (2009). Senescence and immortality in hepatocellular carcinoma. *Cancer Lett. **286***, 103–13. Available at: http://www.ncbi.nlm.nih.gov/pubmed/19070423 [Accessed November 25, 2013].

92 Di Micco, R., Fumagalli, M., and d'Adda di Fagagna, F. (2007). Breaking news: high-speed race ends in arrest--how oncogenes induce senescence. *Trends Cell Biol. **17***,

529–36. Available at: http://www.ncbi.nlm.nih.gov/pubmed/17980599 [Accessed November 25, 2013].

93 Guo, X., Ma, N., Zhou, F., Zhang, L. I., and Bu, X. (2009). Up-regulation of hTERT expression by low-dose cisplatin contributes to chemotherapy resistance in human hepatocellular cancer cells. *Oncol. Rep.* ***22***, 549–556.

94 Huang, F. W., Hodis, E., Xu, M. J., Kryukov, G. V, Chin, L., and Garraway, L. A. (2013). Highly Recurrent TERT Promoter Mutations in Human Melanoma. *Science* ***339***, 957–959.

95 Toh, S. T., Jin, Y., Liu, L., Wang, J., Babrzadeh, F., Gharizadeh, B., Ronaghi, M., Toh, H. C., Chow, P. K.-H., Chung, A. Y.-F., et al. (2013). Deep sequencing of the hepatitis B virus in hepatocellular carcinoma patients reveals enriched integration events, structural alterations and sequence variations. *Carcinogenesis* ***34***, 787–98. Available at: http://www.ncbi.nlm.nih.gov/pubmed/23276797 [Accessed November 11, 2013].

96 Kim, H., Yoo, J. E., Cho, J. Y., Oh, B.-K., Yoon, Y.-S., Han, H.-S., Lee, H. S., Jang, J. J., Jeong, S. H., Kim, J. W., et al. (2013). Telomere length, TERT and shelterin complex proteins in hepatocellular carcinomas expressing “stemness”-related markers. *J. Hepatol.* ***59***, 746–52. Available at: http://www.ncbi.nlm.nih.gov/pubmed/23685049 [Accessed November 25, 2013].

97 Hu, Y., Shen, Y., Ji, B., Yin, S., Ren, X., Chen, T., Ma, Y., Zhang, Z., and Zhang, Y. (2011). Liver-specific gene therapy of hepatocellular carcinoma by targeting human telomerase reverse transcriptase with pegylated immuno-lipopolyplexes. *Eur. J. Pharm. Biopharm.* ***78***, 320–5. Available at: http://www.ncbi.nlm.nih.gov/pubmed/21220007 [Accessed November 25, 2013].

98 Yildiz, G., Arslan-Ergul, A., Bagislar, S., Konu, O., Yuzugullu, H., Gursoy-Yuzugullu, O., Ozturk, N., Ozen, C., Ozdag, H., Erdal, E., et al. (2013). Genome-wide transcriptional reorganization associated with senescence-to-immortality switch during human hepatocellular carcinogenesis. *PLoS One* ***8***, e64016. Available at: http://www.pubmedcentral.nih.gov/articlerender.fcgi?artid=3655073&tool=pmcentrez&rendertype=abstract [Accessed November 25, 2013].

99 Tuncbilek, M., Guven, E. B., Onder, T., and Cetin Atalay, R. (2012). Synthesis of novel 6-(4-substituted piperazine-1-yl)-9-(β-D-ribofuranosyl)purine derivatives, which lead to senescence-induced cell death in liver cancer cells. *J. Med. Chem.* ***55***, 3058–65. Available at: http://www.ncbi.nlm.nih.gov/pubmed/22409771 [Accessed December 10, 2013].

100 Wu, S.-D., Ma, Y.-S., Fang, Y., Liu, L.-L., Fu, D., and Shen, X.-Z. (2012). Role of the microenvironment in hepatocellular carcinoma development and progression. *Cancer Treat. Rev.* ***38***, 218–25. Available at: http://www.ncbi.nlm.nih.gov/pubmed/21763074 [Accessed November 25, 2013].

101 Roberts, L. R., and Gores, G. J. (2005). Hepatocellular carcinoma: molecular pathways and new therapeutic targets. *Semin. Liver Dis.* ***25***, 212–25. Available at: http://www.ncbi.nlm.nih.gov/pubmed/15918149.

102 Pang, R., and Poon, R. T. P. (2006). Angiogenesis and antiangiogenic therapy in hepatocellular carcinoma. *Cancer Lett.* ***242***, 151–67. Available at: http://www.ncbi.nlm.nih.gov/pubmed/16564617 [Accessed November 25, 2013].

103 Kaposi-novak, P., Lee, J.-S., Gòmez-quiroz, L., Coulouarn, C., Factor, V. M., and Thorgeirsson, S. S. (2006). Met-regulated expression signature defines a subset of human hepatocellular carcinomas with poor prognosis and aggressive phenotype. *J. Clin. Invest.* ***116***.

104 Mitsuhashi, N., Shimizu, H., Ohtsuka, M., Wakabayashi, Y., Ito, H., Kimura, F., Yoshidome, H., Kato, A., Nukui, Y., and Miyazaki, M. (2003). Angiopoietins and Tie-2 expression in angiogenesis and proliferation of human hepatocellular carcinoma. *Hepatology* ***37***, 1105–13. Available at: http://www.ncbi.nlm.nih.gov/pubmed/12717391 [Accessed November 26, 2013].

105 Ueki, T., Fujimoto, J., Suzuki, T., Yamamoto, H., and Okamoto, E. (1997). Expression of hepatocyte growth factor and its receptor c-met proto-oncogene in hepatocellular carcinoma. *Hepatology* ***25***, 862–6. Available at: http://www.ncbi.nlm.nih.gov/pubmed/9096589 [Accessed November 26, 2013].

106 Campbell, J. S., Johnson, M. M., Bauer, R. L., Hudkins, K. L., Gilbertson, D. G., Riehle, K. J., Yeh, M. M., Alpers, C. E., and Fausto, N. (2007). Targeting stromal cells for the treatment of platelet-derived growth factor C-induced hepatocellular carcinogenesis. *Differentiation.* ***75***, 843–52. Available at: http://www.ncbi.nlm.nih.gov/pubmed/17999742 [Accessed November 26, 2013].

107 Li, X. M., Tang, Z. Y., Zhou, G., Lui, Y. K., and Ye, S. L. (1998). Significance of vascular endothelial growth factor mRNA expression in invasion and metastasis of hepatocellular carcinoma. *J. Exp. Clin. Cancer Res.* ***17***, 13–7. Available at: http://www.ncbi.nlm.nih.gov/pubmed/9646228 [Accessed November 26, 2013].

108 Shimamura, T., Saito, S., Morita, K., Kitamura, T., Morimoto, M., Kiba, T., Numata, K., Tanaka, K., and Sekihara, H. (2000). Detection of vascular endothelial growth factor and its receptor expression in human hepatocellular carcinoma biopsy specimens. *J. Gastroenterol. Hepatol.* ***15***, 640–6. Available at: http://www.ncbi.nlm.nih.gov/pubmed/10921418 [Accessed November 26, 2013].

109 Poon, R. T. P., Ho, J. W. Y., Tong, C. S. W., Lau, C., Ng, I. O. L., and Fan, S.-T. (2004). Prognostic significance of serum vascular endothelial growth factor and endostatin in patients with hepatocellular carcinoma. *Br. J. Surg.* ***91***, 1354–60. Available at: http://www.ncbi.nlm.nih.gov/pubmed/15376182 [Accessed November 25, 2013].

110 Ng, I. O., Poon, R. T., Lee, J. M., Fan, S. T., Ng, M., and Tso, W. K. (2001). Microvessel density, vascular endothelial growth factor and its receptors Flt-1 and Flk-1/KDR in hepatocellular carcinoma. *Am. J. Clin. Pathol.* ***116***, 838–45. Available at: http://www.ncbi.nlm.nih.gov/pubmed/11764072.

111 Chiang, D. Y., Villanueva, A., Hoshida, Y., Peix, J., Newell, P., Minguez, B., LeBlanc, A. C., Donovan, D. J., Thung, S. N., Solé, M., et al. (2008). Focal gains of VEGFA and molecular classification of hepatocellular carcinoma. *Cancer Res.* ***68***, 6779–88. Available at: http://www.pubmedcentral.nih.gov/articlerender.fcgi?artid=2587454&tool=pmcentrez&rendertype=abstract [Accessed November 20, 2013].

112 Lian, Z., Liu, J., Wu, M., Wang, H.-Y., Arbuthnot, P., Kew, M., and Feitelson, M. a (2007). Hepatitis B x antigen up-regulates vascular endothelial growth factor receptor 3 in hepatocarcinogenesis. *Hepatology* ***45***, 1390–9. Available at: http://www.ncbi.nlm.nih.gov/pubmed/17539024 [Accessed November 25, 2013].

113 Imura, S., Miyake, H., Izumi, K., Tashiro, S., and Uehara, H. (2004). Correlation of vascular endothelial cell proliferation with microvessel density and expression of vascular endothelial growth factor and basic fibroblast growth factor in hepatocellular carcinoma. *J. Med. Invest.* ***51***, 202–9. Available at: http://www.ncbi.nlm.nih.gov/pubmed/15460907 [Accessed November 26, 2013].

114 Yoshiji, H., Kuriyama, S., Yoshii, J., Ikenaka, Y., Noguchi, R., Hicklin, D. J., Huber, J., Nakatani, T., Tsujinoue, H., Yanase, K., et al. (2002). Synergistic effect of basic fibroblast growth factor and vascular endothelial growth factor in murine hepatocellular carcinoma. *Hepatology* ***35***, 834–42. Available at: http://www.ncbi.nlm.nih.gov/pubmed/11915029 [Accessed November 26, 2013].

115 Yan, W., Fu, Y., Tian, D., Liao, J., Liu, M., Wang, B., Xia, L., Zhu, Q., and Luo, M. (2009). PI3 kinase/Akt signaling mediates epithelial-mesenchymal transition in hypoxic hepatocellular carcinoma cells. *Biochem. Biophys. Res. Commun.* ***382***, 631–6. Available at: http://www.ncbi.nlm.nih.gov/pubmed/19303863 [Accessed November 19, 2013].

116 Copple, B. L. (2010). Hypoxia stimulates hepatocyte epithelial to mesenchymal transition by hypoxia-inducible factor and transforming growth factor-beta-dependent mechanisms. *Liver Int.* ***30***, 669–82. Available at: http://www.pubmedcentral.nih.gov/articlerender.fcgi?artid=3111074&tool=pmcentrez&rendertype=abstract [Accessed November 11, 2013].

117 Liu, L., Zhu, X.-D., Wang, W.-Q., Shen, Y., Qin, Y., Ren, Z.-G., Sun, H.-C., and Tang, Z.-Y. (2010). Activation of beta-catenin by hypoxia in hepatocellular carcinoma contributes to enhanced metastatic potential and poor prognosis. *Clin. Cancer Res.* ***16***, 2740–50. Available at: http://www.ncbi.nlm.nih.gov/pubmed/20460486 [Accessed November 26, 2013].

118 Maegdefrau, U., Amann, T., Winklmeier, A., Braig, S., Schubert, T., Weiss, T. S., Schardt, K., Warnecke, C., Hellerbrand, C., and Bosserhoff, A.-K. (2009). Bone morphogenetic protein 4 is induced in hepatocellular carcinoma by hypoxia and promotes tumour progression. *J. Pathol.* ***218***, 520–9. Available at: http://www.ncbi.nlm.nih.gov/pubmed/19431154 [Accessed November 26, 2013].

119 Lee, T. K., Poon, R. T. P., Yuen, A. P., Ling, M. T., Kwok, W. K., Wang, X. H., Wong, Y. C., Guan, X. Y., Man, K., Chau, K. L., et al. (2006). Twist overexpression correlates with hepatocellular carcinoma metastasis through induction of epithelial-mesenchymal transition. *Clin. Cancer Res.* ***12***, 5369–76. Available at: http://www.ncbi.nlm.nih.gov/pubmed/17000670 [Accessed November 12, 2013].

120 Niu, R. F., Zhang, L., Xi, G. M., Wei, X. Y., Yang, Y., Shi, Y. R., and Hao, X. S. (2007). Up-regulation of Twist induces angiogenesis and correlates with metastasis in hepatocellular carcinoma. *J. Exp. Clin. Cancer Res.* ***26***, 385–94. Available at: http://www.ncbi.nlm.nih.gov/pubmed/17987801 [Accessed November 26, 2013].

121 Van Zijl, F., Zulehner, G., Petz, M., Schneller, D., Kornauth, C., Hau, M., Machat, G., Grubinger, M., Huber, H., and Mikulits, W. (2009). Epithelial-mesenchymal transition in hepatocellular carcinoma. *Future Oncol.* ***5***, 1169–79. Available at: http://www.pubmedcentral.nih.gov/articlerender.fcgi?artid=2963061&tool=pmcentrez&rendertype=abstract [Accessed November 12, 2013].

122 Yang, M.-H., Chen, C.-L., Chau, G.-Y., Chiou, S.-H., Su, C.-W., Chou, T.-Y., Peng, W.-L., and Wu, J.-C. (2009). Comprehensive analysis of the independent effect of twist and snail in promoting metastasis of hepatocellular carcinoma. *Hepatology* ***50***, 1464–74. Available at: http://www.ncbi.nlm.nih.gov/pubmed/19821482 [Accessed November 26, 2013].

123 Kim, T., Veronese, A., Pichiorri, F., Lee, T. J., Jeon, Y.-J., Volinia, S., Pineau, P., Marchio, A., Palatini, J., Suh, S.-S., et al. (2011). p53 regulates epithelial-mesenchymal transition through microRNAs targeting ZEB1 and ZEB2. *J. Exp. Med.* ***208***, 875–83. Available at: http://www.pubmedcentral.nih.gov/articlerender.fcgi?artid=3092351&tool=pmcentrez&rendertype=abstract [Accessed November 17, 2013].

124 Liu, H., Xu, L., He, H., Zhu, Y., Liu, J., Wang, S., Chen, L., Wu, Q., Xu, J., and Gu, J. (2012). Hepatitis B virus X protein promotes hepatoma cell invasion and metastasis by stabilizing Snail protein. *Cancer Sci.* ***103***, 2072–81. Available at: http://www.ncbi.nlm.nih.gov/pubmed/22957763 [Accessed November 25, 2013].

125 Ke, A.-W., Shi, G.-M., Zhou, J., Huang, X.-Y., Shi, Y.-H., Ding, Z.-B., Wang, X.-Y., Devbhandari, R. P., and Fan, J. (2011). CD151 amplifies signaling by integrin α6β1 to PI3K and induces the epithelial-mesenchymal transition in HCC cells. *Gastroenterology* ***140***, 1629–41.e15. Available at: http://www.ncbi.nlm.nih.gov/pubmed/21320503 [Accessed November 26, 2013].

126 Kim, J., Hong, S. J., Park, J. Y., Park, J. H., Yu, Y.-S., Park, S. Y., Lim, E. K., Choi, K. Y., Lee, E. K., Paik, S. S., et al. (2010). Epithelial-mesenchymal transition gene signature to predict clinical outcome of hepatocellular carcinoma. *Cancer Sci.* ***101***, 1521–8. Available at: http://www.ncbi.nlm.nih.gov/pubmed/20331628 [Accessed November 14, 2013].

127 Ye, Q.-H., Qin, L.-X., Forgues, M., He, P., Kim, J. W., Peng, A. C., Simon, R., Li, Y., Robles, A. I., Chen, Y., et al. (2003). Predicting hepatitis B virus-positive metastatic hepatocellular carcinomas using gene expression profiling and supervised machine learning. *Nat. Med.* ***9***, 416–23. Available at: http://www.ncbi.nlm.nih.gov/pubmed/12640447 [Accessed November 14, 2013].

128 Sun, B.-S., Dong, Q.-Z., Ye, Q.-H., Sun, H.-J., Jia, H.-L., Zhu, X.-Q., Liu, D.-Y., Chen, J., Xue, Q., Zhou, H.-J., et al. (2008). Lentiviral-mediated miRNA against osteopontin suppresses tumor growth and metastasis of human hepatocellular carcinoma. *Hepatology* ***48***, 1834–42. Available at: http://www.ncbi.nlm.nih.gov/pubmed/18972404 [Accessed November 20, 2013].

129 Zhao, J., Dong, L., Lu, B., Wu, G., Xu, D., Chen, J., Li, K., Tong, X., Dai, J., Yao, S., et al. (2008). Down-regulation of osteopontin suppresses growth and metastasis of hepatocellular carcinoma via induction of apoptosis. *Gastroenterology* ***135***, 956–68. Available at: http://www.ncbi.nlm.nih.gov/pubmed/18555021 [Accessed November 20, 2013].

130 Xue, W., Krasnitz, A., Lucito, R., Sordella, R., VanAelst, L., Cordon-Cardo, C., Singer, S., Kuehnel, F., Wigler, M., Powers, S., et al. (2008). DLC1 is a chromosome 8p tumor suppressor whose loss promotes hepatocellular carcinoma. *Genes Dev.* ***22***, 1439–1444. Available at: http://www.pubmedcentral.nih.gov/articlerender.fcgi?artid=2418580&tool=pmcentrez&rendertype=abstract [Accessed November 26, 2013].

131 Zhou, X., Zimonjic, D. B., Park, S.-W., Yang, X.-Y., Durkin, M. E., and Popescu, N. C. (2008). DLC1 suppresses distant dissemination of human hepatocellular carcinoma cells in nude mice through reduction of RhoA GTPase activity, actin cytoskeletal disruption and down-regulation of genes involved in metastasis. *Int. J. Oncol.* ***32***, 1285–91. Available at: http://www.ncbi.nlm.nih.gov/pubmed/18497990 [Accessed November 26, 2013].

132 Sullivan, R., and Graham, C. H. (2007). Hypoxia-driven selection of the metastatic phenotype. *Cancer Metastasis Rev.* ***26***, 319–31. Available at: http://www.ncbi.nlm.nih.gov/pubmed/17458507 [Accessed February 23, 2014].

133 Jang, M., Kim, S. S., and Lee, J. (2013). Cancer cell metabolism: implications for therapeutic targets. *Exp. Mol. Med.* ***45***, e45. Available at: http://www.pubmedcentral.nih.gov/articlerender.fcgi?artid=3809361&tool=pmcentrez&rendertype=abstract [Accessed November 12, 2013].

134 Guertin, D. a, and Sabatini, D. M. (2007). Defining the role of mTOR in cancer. *Cancer Cell* ***12***, 9–22. Available at: http://www.ncbi.nlm.nih.gov/pubmed/17613433 [Accessed November 11, 2013].

135 Xu, X., Ye, L., Araki, K., and Ahmed, R. (2012). mTOR, linking metabolism and immunity. *Semin. Immunol.* ***24***, 429–35. Available at: http://www.ncbi.nlm.nih.gov/pubmed/23352227 [Accessed November 25, 2013].

136 Elstrom, R. L., Bauer, D. E., Buzzai, M., Karnauskas, R., Harris, M. H., Plas, D. R., Zhuang, H., Cinalli, R. M., Alavi, A., Rudin, C. M., et al. (2004). Akt stimulates aerobic glycolysis in cancer cells. *Cancer Res.* ***64***, 3892–9. Available at: http://www.ncbi.nlm.nih.gov/pubmed/15172999.

137 Wise, D. R., DeBerardinis, R. J., Mancuso, A., Sayed, N., Zhang, X.-Y., Pfeiffer, H. K., Nissim, I., Daikhin, E., Yudkoff, M., McMahon, S. B., et al. (2008). Myc regulates a transcriptional program that stimulates mitochondrial glutaminolysis and leads to glutamine addiction. *Proc. Natl. Acad. Sci. U. S. A.* ***105***, 18782–7. Available at: http://www.pubmedcentral.nih.gov/articlerender.fcgi?artid=2596212&tool=pmcentrez&rendertype=abstract.

138 Liu, L., Ulbrich, J., Müller, J., Wüstefeld, T., Aeberhard, L., Kress, T. R., Muthalagu, N., Rycak, L., Rudalska, R., Moll, R., et al. (2012). Deregulated MYC expression induces dependence upon AMPK-related kinase 5. *Nature* ***483***, 608–12. Available at: http://www.ncbi.nlm.nih.gov/pubmed/22460906 [Accessed November 25, 2013].

139 Zheng, L., Yang, W., Wu, F., Wang, C., Yu, L., Tang, L., Qiu, B., Li, Y., Guo, L., Wu, M., et al. (2013). Prognostic significance of AMPK activation and therapeutic effects of metformin in hepatocellular carcinoma. *Clin. Cancer Res.* ***19***, 5372–80. Available at: http://www.ncbi.nlm.nih.gov/pubmed/23942093 [Accessed November 26, 2013].

140 Budanov, A. V, and Karin, M. (2008). p53 target genes sestrin1 and sestrin2 connect genotoxic stress and mTOR signaling. *Cell* ***134***, 451–60. Available at: http://www.pubmedcentral.nih.gov/articlerender.fcgi?artid=2758522&tool=pmcentrez&rendertype=abstract [Accessed November 14, 2013].

141 Bensaad, K., Tsuruta, A., Selak, M. a, Vidal, M. N. C., Nakano, K., Bartrons, R., Gottlieb, E., and Vousden, K. H. (2006). TIGAR, a p53-inducible regulator of glycolysis and apoptosis. *Cell* ***126***, 107–20. Available at: http://www.ncbi.nlm.nih.gov/pubmed/16839880 [Accessed November 17, 2013].

142 Beyoğlu, D., Imbeaud, S., Maurhofer, O., Bioulac-Sage, P., Zucman-Rossi, J., Dufour, J.-F., and Idle, J. R. (2013). Tissue metabolomics of hepatocellular carcinoma: tumor energy metabolism and the role of transcriptomic classification. *Hepatology* ***58***, 229–38. Available at: http://www.ncbi.nlm.nih.gov/pubmed/23463346 [Accessed November 8, 2013].

143 Budhu, A., Roessler, S., Zhao, X., Yu, Z., Forgues, M., Ji, J., Karoly, E., Qin, L.-X., Ye, Q.-H., Jia, H.-L., et al. (2013). Integrated metabolite and gene expression profiles identify lipid biomarkers associated with progression of hepatocellular carcinoma and patient outcomes. *Gastroenterology **144***, 1066–1075.e1. Available at: http://www.ncbi.nlm.nih.gov/pubmed/23376425 [Accessed November 20, 2013].

144 Chan, I. S., Guy, C. D., Chen, Y., Lu, J., Swiderska-Syn, M., Michelotti, G. A., Karaca, G., Xie, G., Krüger, L., Syn, W.-K., et al. (2012). Paracrine Hedgehog signaling drives metabolic changes in hepatocellular carcinoma. *Cancer Res. **72***, 6344–50. Available at: http://www.ncbi.nlm.nih.gov/pubmed/23066040 [Accessed November 26, 2013].

145 Levine, A. J., and Puzio-Kuter, A. M. (2010). The Control of the Metabolic Switch in Cancers by Oncogenes and Tumor Suppressor Genes. *Science **330***, 1340–1345.

146 Shen, Y.-C., Ou, D.-L., Hsu, C., Lin, K.-L., Chang, C.-Y., Lin, C.-Y., Liu, S.-H., and Cheng, a-L. (2013). Activating oxidative phosphorylation by a pyruvate dehydrogenase kinase inhibitor overcomes sorafenib resistance of hepatocellular carcinoma. *Br. J. Cancer **108***, 72–81. Available at: http://www.ncbi.nlm.nih.gov/pubmed/23257894 [Accessed November 25, 2013].

147 Schrader, J., and Iredale, J. P. (2011). The inflammatory microenvironment of HCC - the plot becomes complex. *J. Hepatol. **54***, 853–5. Available at: http://www.ncbi.nlm.nih.gov/pubmed/21185341 [Accessed November 26, 2013].

148 Nagoshi, S. (2013). Osteopontin: Versatile modulator of liver diseases. *Hepatol. Res.*, 1–9. Available at: http://www.ncbi.nlm.nih.gov/pubmed/23701387 [Accessed November 25, 2013].

149 Gotoh, M., Sakamoto, M., Kanetaka, K., Chuuma, M., and Hirohashi, S. (2002). Overexpression of osteopontin in hepatocellular carcinoma. *Pathol. Int. **52***, 19–24. Available at: http://www.ncbi.nlm.nih.gov/pubmed/11940202 [Accessed November 26, 2013].

150 Pan, H.-W., Ou, Y.-H., Peng, S.-Y., Liu, S.-H., Lai, P.-L., Lee, P.-H., Sheu, J.-C., Chen, C.-L., and Hsu, H.-C. (2003). Overexpression of osteopontin is associated with intrahepatic metastasis, early recurrence, and poorer prognosis of surgically resected hepatocellular carcinoma. *Cancer **98***, 119–27. Available at: http://www.ncbi.nlm.nih.gov/pubmed/12833464 [Accessed November 26, 2013].

151 Wu, J.-C., Sun, B.-S., Ren, N., Ye, Q.-H., and Qin, L.-X. (2010). Genomic aberrations in hepatocellular carcinoma related to osteopontin expression detected by array-CGH. *J. Cancer Res. Clin. Oncol. **136***, 595–601. Available at: http://www.ncbi.nlm.nih.gov/pubmed/19834740 [Accessed November 26, 2013].

152 Zhang, H., Ye, Q.-H., Ren, N., Zhao, L., Wang, Y.-F., Wu, X., Sun, H.-C., Wang, L., Zhang, B.-H., Liu, Y.-K., et al. (2006). The prognostic significance of preoperative plasma levels of osteopontin in patients with hepatocellular carcinoma. *J. Cancer Res.*

Clin. Oncol. ***132***, 709–17. Available at: http://www.ncbi.nlm.nih.gov/pubmed/16786357 [Accessed November 26, 2013].

153 Xie, H., Song, J., Du, R., Liu, K., Wang, J., Tang, H., Bai, F., Liang, J., Lin, T., Liu, J., et al. (2007). Prognostic significance of osteopontin in hepatitis B virus-related hepatocellular carcinoma. *Dig. Liver Dis.* ***39***, 167–72. Available at: http://www.ncbi.nlm.nih.gov/pubmed/17161983 [Accessed November 14, 2013].

154 Kim, J., Ki, S. S., Lee, S. D., Han, C. J., Kim, Y. C., Park, S. H., Cho, S. Y., Hong, Y.-J., Park, H. Y., Lee, M., et al. (2006). Elevated plasma osteopontin levels in patients with hepatocellular carcinoma. *Am. J. Gastroenterol.* ***101***, 2051–9. Available at: http://www.ncbi.nlm.nih.gov/pubmed/16848813 [Accessed November 26, 2013].

155 Abu El Makarem, M. A., Abdel-Aleem, A., Ali, A., Saber, R., Shatat, M., Rahem, D. A., and Sayed, D. Diagnostic significance of plasma osteopontin in hepatitis C virus-related hepatocellular carcinoma. *Ann. Hepatol.* ***10***, 296–305. Available at: http://www.ncbi.nlm.nih.gov/pubmed/21677331 [Accessed November 26, 2013].

156 Shang, S., Plymoth, A., Ge, S., Feng, Z., Rosen, H. R., Sangrajrang, S., Hainaut, P., Marrero, J. A., and Beretta, L. (2012). Identification of osteopontin as a novel marker for early hepatocellular carcinoma. *Hepatology* ***55***, 483–90. Available at: http://www.ncbi.nlm.nih.gov/pubmed/21953299 [Accessed November 14, 2013].

157 Nakamoto, Y., and Kaneko, S. (2003). Mechanisms of viral hepatitis induced liver injury. *Curr. Mol. Med.* ***3***, 537–44. Available at: http://www.ncbi.nlm.nih.gov/pubmed/14527085 [Accessed November 26, 2013].

158 Herzer, K., Sprinzl, M. F., and Galle, P. R. (2007). Hepatitis viruses: live and let die. *Liver Int.* ***27***, 293–301. Available at: http://www.ncbi.nlm.nih.gov/pubmed/17355449 [Accessed November 14, 2013].

159 Leonardi, G. C., Candido, S., Cervello, M., Nicolosi, D., Raiti, F., Travali, S., Spandidos, D. A., and Libra, M. (2012). The tumor microenvironment in hepatocellular carcinoma (review). *Int. J. Oncol.* ***40***, 1733–47. Available at: http://www.ncbi.nlm.nih.gov/pubmed/22447316 [Accessed November 26, 2013].

160 Ramaiah, S. K., and Rittling, S. (2008). Pathophysiological role of osteopontin in hepatic inflammation, toxicity, and cancer. *Toxicol. Sci.* ***103***, 4–13. Available at: http://www.ncbi.nlm.nih.gov/pubmed/17890765 [Accessed November 26, 2013].

161 Wai, P. Y., and Kuo, P. C. (2008). Osteopontin: regulation in tumor metastasis. *Cancer Metastasis Rev.* ***27***, 103–18. Available at: http://www.ncbi.nlm.nih.gov/pubmed/18049863 [Accessed November 26, 2013].

162 El-Tanani, M. K., Campbell, F. C., Kurisetty, V., Jin, D., McCann, M., and Rudland, P. S. (2006). The regulation and role of osteopontin in malignant transformation and

cancer. *Cytokine Growth Factor Rev.* ***17***, 463–74. Available at: http://www.ncbi.nlm.nih.gov/pubmed/17113338 [Accessed November 26, 2013].

163 Kovalovich, K., DeAngelis, R. A., Li, W., Furth, E. E., Ciliberto, G., and Taub, R. (2000). Increased toxin-induced liver injury and fibrosis in interleukin-6-deficient mice. *Hepatology* ***31***, 149–59. Available at: http://www.ncbi.nlm.nih.gov/pubmed/10613740 [Accessed November 26, 2013].

164 Haga, S., Terui, K., Zhang, H. Q., Enosawa, S., Ogawa, W., Inoue, H., Okuyama, T., Takeda, K., Akira, S., Ogino, T., et al. (2003). Stat3 protects against Fas-induced liver injury by redox-dependent and -independent mechanisms. *J. Clin. Invest.* ***112***, 989–98. Available at: http://www.pubmedcentral.nih.gov/articlerender.fcgi?artid=198521&tool=pmcentrez&rendertype=abstract [Accessed November 26, 2013].

165 Yu, H., Pardoll, D., and Jove, R. (2009). STATs in cancer inflammation and immunity: a leading role for STAT3. *Nat. Rev. Cancer* ***9***, 798–809. Available at: http://www.ncbi.nlm.nih.gov/pubmed/19851315 [Accessed November 6, 2013].

166 Lee, H., Herrmann, A., Deng, J.-H., Kujawski, M., Niu, G., Li, Z., Forman, S., Jove, R., Pardoll, D. M., and Yu, H. (2009). Persistently activated Stat3 maintains constitutive NF-kappaB activity in tumors. *Cancer Cell* ***15***, 283–93. Available at: http://www.pubmedcentral.nih.gov/articlerender.fcgi?artid=2777654&tool=pmcentrez&rendertype=abstract [Accessed November 7, 2013].

167 He, G., and Karin, M. (2011). NF-κB and STAT3 - key players in liver inflammation and cancer. *Cell Res.* ***21***, 159–68. Available at: http://www.pubmedcentral.nih.gov/articlerender.fcgi?artid=3193410&tool=pmcentrez&rendertype=abstract [Accessed November 14, 2013].

168 Li, W., Liang, X., Kellendonk, C., Poli, V., and Taub, R. (2002). STAT3 contributes to the mitogenic response of hepatocytes during liver regeneration. *J. Biol. Chem.* ***277***, 28411–7. Available at: http://www.ncbi.nlm.nih.gov/pubmed/12032149 [Accessed November 26, 2013].

169 Inoue, H., Ogawa, W., Ozaki, M., Haga, S., Matsumoto, M., Furukawa, K., Hashimoto, N., Kido, Y., Mori, T., Sakaue, H., et al. (2004). Role of STAT-3 in regulation of hepatic gluconeogenic genes and carbohydrate metabolism in vivo. *Nat. Med.* ***10***, 168–74. Available at: http://www.ncbi.nlm.nih.gov/pubmed/14716305 [Accessed November 26, 2013].

170 Anson, M., Crain-Denoyelle Anne-Marie, Baud, V., Chereau, F., Gougelet, A., Terris, B., Yamagoe, S., and Colnot, S. (2012). Oncogenic β-catenin triggers an inflammatory response that determines the aggressiveness of hepatocellular carcinoma in mice. *J. Clin. Invest.* ***122***.

171 Liu, Y., Fuchs, J., Li, C., and Lin, J. (2010). IL-6, a risk factor for hepatocellular carcinoma: FLLL32 inhibits IL-6-induced STAT3 phosphorylation in human hepatocellular cancer cells. *Cell Cycle* ***9***, 3423–7. Available at: http://www.ncbi.nlm.nih.gov/pubmed/20818158 [Accessed November 26, 2013].

172 Porta, C., De Amici, M., Quaglini, S., Paglino, C., Tagliani, F., Boncimino, A., Moratti, R., and Corazza, G. R. (2008). Circulating interleukin-6 as a tumor marker for hepatocellular carcinoma. *Ann. Oncol.* ***19***, 353–8. Available at: http://www.ncbi.nlm.nih.gov/pubmed/17962206 [Accessed November 26, 2013].

173 Li, W.-C., Ye, S.-L., Sun, R.-X., Liu, Y.-K., Tang, Z.-Y., Kim, Y., Karras, J. G., and Zhang, H. (2006). Inhibition of growth and metastasis of human hepatocellular carcinoma by antisense oligonucleotide targeting signal transducer and activator of transcription 3. *Clin. Cancer Res.* ***12***, 7140–8. Available at: http://www.ncbi.nlm.nih.gov/pubmed/17145839 [Accessed November 26, 2013].

174 Niwa, Y., Kanda, H., Shikauchi, Y., Saiura, A., Matsubara, K., Kitagawa, T., Yamamoto, J., Kubo, T., and Yoshikawa, H. (2005). Methylation silencing of SOCS-3 promotes cell growth and migration by enhancing JAK/STAT and FAK signalings in human hepatocellular carcinoma. *Oncogene* ***24***, 6406–17. Available at: http://www.ncbi.nlm.nih.gov/pubmed/16007195 [Accessed November 26, 2013].

175 Trikha, M., Corringham, R., Klein, B., and Rossi, J.-F. (2003). Targeted anti-interleukin-6 monoclonal antibody therapy for cancer: a review of the rationale and clinical evidence. *Clin. Cancer Res.* ***9***, 4653–65. Available at: http://www.pubmedcentral.nih.gov/articlerender.fcgi?artid=2929399&tool=pmcentrez&rendertype=abstract [Accessed November 26, 2013].

176 Yoshikawa, H., Matsubara, K., Qian, G. S., Jackson, P., Groopman, J. D., Manning, J. E., Harris, C. C., and Herman, J. G. (2001). SOCS-1, a negative regulator of the JAK/STAT pathway, is silenced by methylation in human hepatocellular carcinoma and shows growth-suppression activity. *Nat. Genet.* ***28***, 29–35. Available at: http://www.ncbi.nlm.nih.gov/pubmed/11326271 [Accessed November 13, 2013].

177 Calvisi, D. F., Ladu, S., Gorden, A., Farina, M., Conner, E. a, Lee, J.-S., Factor, V. M., and Thorgeirsson, S. S. (2006). Ubiquitous activation of Ras and Jak/Stat pathways in human HCC. *Gastroenterology* ***130***, 1117–28. Available at: http://www.ncbi.nlm.nih.gov/pubmed/16618406 [Accessed November 14, 2013].

178 Rebouissou, S., Amessou, M., Couchy, G., Poussin, K., Imbeaud, S., Pilati, C., Izard, T., Balabaud, C., Bioulac-Sage, P., and Zucman-Rossi, J. (2009). Frequent in-frame somatic deletions activate gp130 in inflammatory hepatocellular tumours. *Nature* ***457***, 200–4. Available at: http://www.pubmedcentral.nih.gov/articlerender.fcgi?artid=2695248&tool=pmcentrez&rendertype=abstract [Accessed November 26, 2013].

179 Park, E. J., Lee, J. H., Yu, G.-Y., He, G., Ali, S. R., Holzer, R. G., Osterreicher, C. H., Takahashi, H., and Karin, M. (2010). Dietary and genetic obesity promote liver inflammation and tumorigenesis by enhancing IL-6 and TNF expression. *Cell **140***, 197–208. Available at: http://www.pubmedcentral.nih.gov/articlerender.fcgi?artid=2836922&tool=pmcentrez&rendertype=abstract [Accessed November 6, 2013].

180 Toffanin, S., Friedman, S. L., and Llovet, J. M. (2010). Obesity, inflammatory signaling, and hepatocellular carcinoma-an enlarging link. *Cancer Cell **17***, 115–7. Available at: http://www.ncbi.nlm.nih.gov/pubmed/20159605 [Accessed November 14, 2013].

181 Wheelhouse, N. M., Chan, Y.-S., Gillies, S. E., Caldwell, H., Ross, J. A., Harrison, D. J., and Prost, S. (2003). TNF-alpha induced DNA damage in primary murine hepatocytes. *Int. J. Mol. Med. **12***, 889–94. Available at: http://www.ncbi.nlm.nih.gov/pubmed/14612962 [Accessed November 26, 2013].

182 Budhu, A., Forgues, M., Ye, Q.-H., Jia, H.-L., He, P., Zanetti, K. A., Kammula, U. S., Chen, Y., Qin, L.-X., Tang, Z.-Y., et al. (2006). Prediction of venous metastases, recurrence, and prognosis in hepatocellular carcinoma based on a unique immune response signature of the liver microenvironment. *Cancer Cell **10***, 99–111. Available at: http://www.ncbi.nlm.nih.gov/pubmed/16904609 [Accessed November 14, 2013].

183 Yaguchi, T., Sumimoto, H., Kudo-Saito, C., Tsukamoto, N., Ueda, R., Iwata-Kajihara, T., Nishio, H., Kawamura, N., and Kawakami, Y. (2011). The mechanisms of cancer immunoescape and development of overcoming strategies. *Int. J. Hematol. **93***, 294–300. Available at: http://www.ncbi.nlm.nih.gov/pubmed/21374075 [Accessed January 20, 2014].

184 Lewis, C. E., and Pollard, J. W. (2006). Distinct role of macrophages in different tumor microenvironments. *Cancer Res. **66***, 605–12. Available at: http://www.ncbi.nlm.nih.gov/pubmed/16423985 [Accessed November 8, 2013].

185 Allavena, P., Sica, A., Garlanda, C., and Mantovani, A. (2008). The Yin-Yang of tumor-associated macrophages in neoplastic progression and immune surveillance. *Immunol. Rev. **222***, 155–61. Available at: http://www.ncbi.nlm.nih.gov/pubmed/18364000.

186 Shirakawa, H., Suzuki, H., Shimomura, M., Kojima, M., Gotohda, N., Takahashi, S., Nakagohri, T., Konishi, M., Kobayashi, N., Kinoshita, T., et al. (2009). Glypican-3 expression is correlated with poor prognosis in hepatocellular carcinoma. *Cancer Sci. **100***, 1403–7. Available at: http://www.ncbi.nlm.nih.gov/pubmed/19496787 [Accessed November 26, 2013].

187 Cheng, F., Wang, H.-W., Cuenca, A., Huang, M., Ghansah, T., Brayer, J., Kerr, W. G., Takeda, K., Akira, S., Schoenberger, S. P., et al. (2003). A critical role for Stat3 signaling in immune tolerance. *Immunity **19***, 425–36. Available at: http://www.ncbi.nlm.nih.gov/pubmed/14499117.

188 Wu, K., Kryczek, I., Chen, L., Zou, W., and Welling, T. H. (2009). Kupffer cell suppression of CD8+ T cells in human hepatocellular carcinoma is mediated by B7-H1/programmed death-1 interactions. *Cancer Res.* ***69***, 8067–75. Available at: http://www.ncbi.nlm.nih.gov/pubmed/19826049 [Accessed November 24, 2013].

189 Han, Y., Chen, Z., Yang, Y., Jiang, Z., Gu, Y., Liu, Y., Lin, C., Pan, Z., Yu, Y., Jiang, M., et al. (2014). Human CD14(+) CTLA-4(+) regulatory dendritic cells suppress T-cell response by cytotoxic T-lymphocyte antigen-4-dependent IL-10 and indoleamine-2,3-dioxygenase production in hepatocellular carcinoma. *Hepatology* ***59***, 567–79. Available at: http://www.ncbi.nlm.nih.gov/pubmed/23960017 [Accessed February 1, 2014].

190 Brenndörfer, E. D., and Sällberg, M. (2012). Hepatitis C virus-mediated modulation of cellular immunity. *Arch. Immunol. Ther. Exp. (Warsz).* ***60***, 315–29. Available at: http://www.ncbi.nlm.nih.gov/pubmed/22911132 [Accessed November 25, 2013].

191 Zhao, F., Hoechst, B., Gamrekelashvili, J., Ormandy, L. a, Voigtländer, T., Wedemeyer, H., Ylaya, K., Wang, X. W., Hewitt, S. M., Manns, M. P., et al. (2012). Human CCR4+ CCR6+ Th17 cells suppress autologous CD8+ T cell responses. *J. Immunol.* ***188***, 6055–62. Available at: http://www.pubmedcentral.nih.gov/articlerender.fcgi?artid=3370143&tool=pmcentrez&rendertype=abstract [Accessed November 20, 2013].

192 Pan, Y., Tan, Y., Wang, M., Zhang, J., Zhang, B., Yang, C., Ding, Z., Dong, L., and Wang, H. (2013). Signal regulatory protein α is associated with tumor-polarized macrophages phenotype switch and plays a pivotal role in tumor progression. *Hepatology* ***58***, 680–91. Available at: http://www.ncbi.nlm.nih.gov/pubmed/23504854 [Accessed November 18, 2013].

193 Zhang, Q.-B., Sun, H.-C., Zhang, K.-Z., Jia, Q.-A., Bu, Y., Wang, M., Chai, Z.-T., Zhang, Q.-B., Wang, W.-Q., Kong, L.-Q., et al. (2013). Suppression of natural killer cells by sorafenib contributes to prometastatic effects in hepatocellular carcinoma. *PLoS One* ***8***, e55945. Available at: http://www.pubmedcentral.nih.gov/articlerender.fcgi?artid=3568028&tool=pmcentrez&rendertype=abstract [Accessed November 25, 2013].

194 Breuhahn, K., Vreden, S., Haddad, R., Beckebaum, S., Stippel, D., Flemming, P., Nussbaum, T., Caselmann, W. H., Haab, B. B., and Schirmacher, P. (2004). Molecular profiling of human hepatocellular carcinoma defines mutually exclusive interferon regulation and insulin-like growth factor II overexpression. *Cancer Res.* ***64***, 6058–64. Available at: http://www.ncbi.nlm.nih.gov/pubmed/15342387.

195 Nam, S. W., Park, J. Y., Ramasamy, A., Shevade, S., Islam, A., Long, P. M., Park, C. K., Park, S. E., Kim, S. Y., Lee, S. H., et al. (2005). Molecular changes from dysplastic nodule to hepatocellular carcinoma through gene expression profiling. *Hepatology* ***42***, 809–18. Available at: http://www.ncbi.nlm.nih.gov/pubmed/16175600 [Accessed November 14, 2013].

196 Wurmbach, E., Chen, Y., Khitrov, G., Zhang, W., Roayaie, S., Schwartz, M., Fiel, I., Thung, S., Mazzaferro, V., Bruix, J., et al. (2007). Genome-wide molecular profiles of HCV-induced dysplasia and hepatocellular carcinoma. *Hepatology* ***45***, 938–47. Available at: http://www.ncbi.nlm.nih.gov/pubmed/17393520 [Accessed November 14, 2013].

197 Katoh, H., Ojima, H., Kokubu, A., Saito, S., Kondo, T., Kosuge, T., Hosoda, F., Imoto, I., Inazawa, J., Hirohashi, S., et al. (2007). Genetically distinct and clinically relevant classification of hepatocellular carcinoma: putative therapeutic targets. *Gastroenterology* ***133***, 1475–86. Available at: http://www.ncbi.nlm.nih.gov/pubmed/17983802 [Accessed November 26, 2013].

198 Midorikawa, Y., Tsutsumi, S., Nishimura, K., Kamimura, N., Kano, M., Sakamoto, H., Makuuchi, M., and Aburatani, H. (2004). Distinct chromosomal bias of gene expression signatures in the progression of hepatocellular carcinoma. *Cancer Res.* ***64***, 7263–70. Available at: http://www.ncbi.nlm.nih.gov/pubmed/15492245.

199 Poon, T. C. W., Wong, N., Lai, P. B. S., Rattray, M., Johnson, P. J., and Sung, J. J. Y. (2006). A tumor progression model for hepatocellular carcinoma: bioinformatic analysis of genomic data. *Gastroenterology* ***131***, 1262–70. Available at: http://www.ncbi.nlm.nih.gov/pubmed/17030195 [Accessed November 14, 2013].

200 Okabe, H., Satoh, S., Kato, T., Kitahara, O., Yanagawa, R., Yamaoka, Y., Tsunoda, T., Furukawa, Y., and Nakamura, Y. (2001). Genome-wide analysis of gene expression in human hepatocellular carcinomas using cDNA microarray: identification of genes involved in viral carcinogenesis and tumor progression. *Cancer Res.* ***61***, 2129–37. Available at: http://www.ncbi.nlm.nih.gov/pubmed/11280777.

201 Iizuka, N., Oka, M., Yamada-Okabe, H., Mori, N., Tamesa, T., Okada, T., Takemoto, N., Tangoku, A., Hamada, K., Nakayama, H., et al. (2002). Comparison of gene expression profiles between hepatitis B virus- and hepatitis C virus-infected hepatocellular carcinoma by oligonucleotide microarray data on the basis of a supervised learning method. *Cancer Res.* ***62***, 3939–44. Available at: http://www.ncbi.nlm.nih.gov/pubmed/12124323.

202 Kim, B.-Y., Lee, J.-G., Park, S., Ahn, J.-Y., Ju, Y.-J., Chung, J.-H., Han, C. J., Jeong, S.-H., Yeom, Y. Il, Kim, S., et al. (2004). Feature genes of hepatitis B virus-positive hepatocellular carcinoma, established by its molecular discrimination approach using prediction analysis of microarray. *Biochim. Biophys. Acta* ***1739***, 50–61. Available at: http://www.ncbi.nlm.nih.gov/pubmed/15607117 [Accessed November 14, 2013].

203 Kim, S. M., Leem, S.-H., Chu, I.-S., Park, Y.-Y., Kim, S. C., Kim, S.-B., Park, E. S., Lim, J. Y., Heo, J., Kim, Y. J., et al. (2012). Sixty-five gene-based risk score classifier predicts overall survival in hepatocellular carcinoma. *Hepatology* ***55***, 1443–52. Available at: http://www.ncbi.nlm.nih.gov/pubmed/22105560 [Accessed November 26, 2013].

204 Zhang, H., Zhai, Y., Hu, Z., Wu, C., Qian, J., Jia, W., Ma, F., Huang, W., Yu, L., Yue, W., et al. (2010). Genome-wide association study identifies 1p36.22 as a new susceptibility locus for hepatocellular carcinoma in chronic hepatitis B virus carriers. *Nat. Genet.* ***42***, 755–8. Available at: http://www.ncbi.nlm.nih.gov/pubmed/20676096 [Accessed November 14, 2013].

205 Miki, D., Ochi, H., Hayes, C. N., Abe, H., Yoshima, T., Aikata, H., Ikeda, K., Kumada, H., Toyota, J., Morizono, T., et al. (2011). Variation in the DEPDC5 locus is associated with progression to hepatocellular carcinoma in chronic hepatitis C virus carriers. *Nat. Genet.* ***43***, 797–800. Available at: http://www.ncbi.nlm.nih.gov/pubmed/21725309 [Accessed November 7, 2013].

206 Kumar, V., Kato, N., Urabe, Y., Takahashi, A., Muroyama, R., Hosono, N., Otsuka, M., Tateishi, R., Omata, M., Nakagawa, H., et al. (2011). Genome-wide association study identifies a susceptibility locus for HCV-induced hepatocellular carcinoma. *Nat. Genet.* ***43***, 455–8. Available at: http://www.ncbi.nlm.nih.gov/pubmed/21499248 [Accessed November 14, 2013].

207 Mayhew, C. N., Carter, S. L., Fox, S. R., Sexton, C. R., Reed, C. A., Srinivasan, S. V, Liu, X., Wikenheiser-Brokamp, K., Boivin, G. P., Lee, J.-S., et al. (2007). RB loss abrogates cell cycle control and genome integrity to promote liver tumorigenesis. *Gastroenterology* ***133***, 976–84. Available at: http://www.ncbi.nlm.nih.gov/pubmed/17854601 [Accessed November 14, 2013].

208 Coulouarn, C., Factor, V. M., and Thorgeirsson, S. S. (2008). Transforming growth factor-beta gene expression signature in mouse hepatocytes predicts clinical outcome in human cancer. *Hepatology* ***47***, 2059–67. Available at: http://www.pubmedcentral.nih.gov/articlerender.fcgi?artid=2762280&tool=pmcentrez&rendertype=abstract [Accessed November 14, 2013].

209 Totoki, Y., Tatsuno, K., Yamamoto, S., Arai, Y., Hosoda, F., Ishikawa, S., Tsutsumi, S., Sonoda, K., Totsuka, H., Shirakihara, T., et al. (2011). High-resolution characterization of a hepatocellular carcinoma genome. *Nat. Genet.* ***43***, 464–9. Available at: http://www.ncbi.nlm.nih.gov/pubmed/21499249 [Accessed November 7, 2013].

210 Li, M., Zhao, H., Zhang, X., Wood, L. D., Anders, R. a, Choti, M. a, Pawlik, T. M., Daniel, H. D., Kannangai, R., Offerhaus, G. J. a, et al. (2011). Inactivating mutations of the chromatin remodeling gene ARID2 in hepatocellular carcinoma. *Nat. Genet.* ***43***, 828–9. Available at: http://www.pubmedcentral.nih.gov/articlerender.fcgi?artid=3163746&tool=pmcentrez&rendertype=abstract [Accessed November 7, 2013].

211 Hernandez-Vargas, H., Lambert, M.-P., Le Calvez-Kelm, F., Gouysse, G., McKay-Chopin, S., Tavtigian, S. V, Scoazec, J.-Y., and Herceg, Z. (2010). Hepatocellular carcinoma displays distinct DNA methylation signatures with potential as clinical predictors. *PLoS One* ***5***, e9749. Available at:

http://www.pubmedcentral.nih.gov/articlerender.fcgi?artid=2840036&tool=pmcentrez&rendertype=abstract [Accessed November 7, 2013].

212 Tao, Y., Ruan, J., Yeh, S.-H., Lu, X., Wang, Y., Zhai, W., Cai, J., Ling, S., Gong, Q., Chong, Z., et al. (2011). Rapid growth of a hepatocellular carcinoma and the driving mutations revealed by cell-population genetic analysis of whole-genome data. *Proc. Natl. Acad. Sci. U. S. A.* ***108***, 12042–7. Available at: http://www.pubmedcentral.nih.gov/articlerender.fcgi?artid=3141952&tool=pmcentrez&rendertype=abstract [Accessed November 19, 2013].

213 Zender, L., Xue, W., Zuber, J., Semighini, C. P., Krasnitz, A., Ma, B., Zender, P., Kubicka, S., Luk, J. M., Schirmacher, P., et al. (2008). An oncogenomics-based in vivo RNAi screen identifies tumor suppressors in liver cancer. *Cell* ***135***, 852–64. Available at: http://www.pubmedcentral.nih.gov/articlerender.fcgi?artid=2990916&tool=pmcentrez&rendertype=abstract [Accessed November 8, 2013].

214 Huang, J., Deng, Q., Wang, Q., Li, K.-Y., Dai, J.-H., Li, N., Zhu, Z.-D., Zhou, B., Liu, X.-Y., Liu, R.-F., et al. (2012). Exome sequencing of hepatitis B virus-associated hepatocellular carcinoma. *Nat. Genet.* ***44***, 1117–21. Available at: http://www.ncbi.nlm.nih.gov/pubmed/22922871 [Accessed November 14, 2013].

215 Iizuka, N., Oka, M., Yamada-Okabe, H., Nishida, M., Maeda, Y., Mori, N., Takao, T., Tamesa, T., Tangoku, A., Tabuchi, H., et al. (2003). Oligonucleotide microarray for prediction of early intrahepatic recurrence of hepatocellular carcinoma after curative resection. *Lancet* ***361***, 923–9. Available at: http://www.ncbi.nlm.nih.gov/pubmed/12648972.

216 Kurokawa, Y., Matoba, R., Takemasa, I., Nagano, H., Dono, K., Nakamori, S., Umeshita, K., Sakon, M., Ueno, N., Oba, S., et al. (2004). Molecular-based prediction of early recurrence in hepatocellular carcinoma. *J. Hepatol.* ***41***, 284–91. Available at: http://www.ncbi.nlm.nih.gov/pubmed/15288478 [Accessed November 7, 2013].

217 Wang, S. M., Ooi, L. L. P. J., and Hui, K. M. (2007). Identification and validation of a novel gene signature associated with the recurrence of human hepatocellular carcinoma. *Clin. Cancer Res.* ***13***, 6275–83. Available at: http://www.ncbi.nlm.nih.gov/pubmed/17975138 [Accessed November 14, 2013].

218 Woo, H. G., Park, E. S., Cheon, J. H., Kim, J. H., Lee, J.-S., Park, B. J., Kim, W., Park, S. C., Chung, Y. J., Kim, B. G., et al. (2008). Gene expression-based recurrence prediction of hepatitis B virus-related human hepatocellular carcinoma. *Clin. Cancer Res.* ***14***, 2056–64. Available at: http://www.ncbi.nlm.nih.gov/pubmed/18381945 [Accessed November 14, 2013].

219 Hoshida, Y., Villanueva, A., Kobayashi, M., Peix, J., Chiang, D. Y., Camargo, A., Gupta, S., Moore, J., Wrobel, M. J., Lerner, J., et al. (2008). Gene expression in fixed tissues and outcome in hepatocellular carcinoma. *N. Engl. J. Med.* ***359***, 1995–2004. Available

at:
http://www.pubmedcentral.nih.gov/articlerender.fcgi?artid=2963075&tool=pmcentrez&rendertype=abstract.

220 Lee, J.-S., Heo, J., Libbrecht, L., Chu, I.-S., Kaposi-Novak, P., Calvisi, D. F., Mikaelyan, A., Roberts, L. R., Demetris, A. J., Sun, Z., et al. (2006). A novel prognostic subtype of human hepatocellular carcinoma derived from hepatic progenitor cells. *Nat. Med.* ***12***, 410–6. Available at: http://www.ncbi.nlm.nih.gov/pubmed/16532004 [Accessed November 14, 2013].

221 Yamashita, T., Forgues, M., Wang, W., Kim, J. W., Ye, Q., Jia, H., Budhu, A., Zanetti, K. a, Chen, Y., Qin, L.-X., et al. (2008). EpCAM and alpha-fetoprotein expression defines novel prognostic subtypes of hepatocellular carcinoma. *Cancer Res.* ***68***, 1451–61. Available at: http://www.ncbi.nlm.nih.gov/pubmed/18316609 [Accessed November 14, 2013].

222 Chai, Z., Kong, J., Zhu, X., Zhang, Y., Lu, L., Zhou, J., Wang, L., Zhang, K., Zhang, Q., Ao, J., et al. (2013). MicroRNA-26a Inhibits Angiogenesis by Down-Regulating VEGFA through the PIK3C2α/Akt/HIF-1α Pathway in Hepatocellular Carcinoma. *PLoS One* ***8***.

223 Yang, X., Liang, L., Zhang, X.-F., Jia, H.-L., Qin, Y., Zhu, X.-C., Gao, X.-M., Qiao, P., Zheng, Y., Sheng, Y.-Y., et al. (2013). MicroRNA-26a suppresses tumor growth and metastasis of human hepatocellular carcinoma by targeting interleukin-6-Stat3 pathway. *Hepatology* ***58***, 158–70. Available at: http://www.ncbi.nlm.nih.gov/pubmed/23389848 [Accessed November 25, 2013].

224 Kota, J., Chivukula, R. R., O'Donnell, K. a, Wentzel, E. a, Montgomery, C. L., Hwang, H.-W., Chang, T.-C., Vivekanandan, P., Torbenson, M., Clark, K. R., et al. (2009). Therapeutic microRNA delivery suppresses tumorigenesis in a murine liver cancer model. *Cell* ***137***, 1005–17. Available at: http://www.pubmedcentral.nih.gov/articlerender.fcgi?artid=2722880&tool=pmcentrez&rendertype=abstract [Accessed November 14, 2013].

225 Xu, L., Beckebaum, S., Iacob, S., Wu, G., Kaiser, G. M., Radtke, A., Liu, C., Kabar, I., Schmidt, H. H., Zhang, X., et al. (2013). MicroRNA-101 inhibits human hepatocellular carcinoma progression through EZH2 downregulation and increased cytostatic drug sensitivity. *J. Hepatol.* Available at: http://www.ncbi.nlm.nih.gov/pubmed/24211739 [Accessed November 26, 2013].

226 Xu, Y., Xia, F., Ma, L., Shan, J., Shen, J., Yang, Z., Liu, J., Cui, Y., Bian, X., Bie, P., et al. (2011). MicroRNA-122 sensitizes HCC cancer cells to adriamycin and vincristine through modulating expression of MDR and inducing cell cycle arrest. *Cancer Lett.* ***310***, 160–9. Available at: http://www.ncbi.nlm.nih.gov/pubmed/21802841 [Accessed November 25, 2013].

227 Lu, Y., Yue, X., Cui, Y., Zhang, J., and Wang, K. (2013). MicroRNA-124 suppresses growth of human hepatocellular carcinoma by targeting STAT3. *Biochem. Biophys.*

Res. Commun. Available at: http://www.ncbi.nlm.nih.gov/pubmed/24211205 [Accessed November 25, 2013].

228 Hatziapostolou, M., Polytarchou, C., Aggelidou, E., Drakaki, A., Poultsides, G. a, Jaeger, S. a, Ogata, H., Karin, M., Struhl, K., Hadzopoulou-Cladaras, M., et al. (2011). An HNF4α-miRNA inflammatory feedback circuit regulates hepatocellular oncogenesis. *Cell* ***147***, 1233–47. Available at: http://www.pubmedcentral.nih.gov/articlerender.fcgi?artid=3251960&tool=pmcentrez&rendertype=abstract [Accessed November 14, 2013].

229 Lang, Q., and Ling, C. (2012). MiR-124 suppresses cell proliferation in hepatocellular carcinoma by targeting PIK3CA. *Biochem. Biophys. Res. Commun.* ***426***, 247–52. Available at: http://www.ncbi.nlm.nih.gov/pubmed/22940133 [Accessed November 26, 2013].

230 Gu, W., Li, X., and Wang, J. (2013). miR-139 regulates the proliferation and invasion of hepatocellular carcinoma through the WNT/TCF-4 pathway. *Oncol. Rep.* Available at: http://www.ncbi.nlm.nih.gov/pubmed/24190507 [Accessed November 26, 2013].

231 Yang, H., Fang, F., Chang, R., and Yang, L. (2013). MicroRNA-140-5p suppresses tumor growth and metastasis by targeting transforming growth factor β receptor 1 and fibroblast growth factor 9 in hepatocellular carcinoma. *Hepatology* ***58***, 205–17. Available at: http://www.ncbi.nlm.nih.gov/pubmed/23401231 [Accessed November 26, 2013].

232 Zhang, J.-P., Zeng, C., Xu, L., Gong, J., Fang, J.-H., and Zhuang, S.-M. (2013). MicroRNA-148a suppresses the epithelial-mesenchymal transition and metastasis of hepatoma cells by targeting Met/Snail signaling. *Oncogene*, 1–8. Available at: http://www.ncbi.nlm.nih.gov/pubmed/24013226 [Accessed November 15, 2013].

233 Xu, X., Fan, Z., Kang, L., Han, J., Jiang, C., Zheng, X., Zhu, Z., Jiao, H., Lin, J., Jiang, K., et al. (2013). Hepatitis B virus X protein represses miRNA-148a to enhance tumorigenesis. *J. Clin. Invest.* ***123***, 630–45. Available at: http://www.pubmedcentral.nih.gov/articlerender.fcgi?artid=3561812&tool=pmcentrez&rendertype=abstract [Accessed November 26, 2013].

234 Zhang, Y., Wei, W., Cheng, N., Wang, K., Li, B., Jiang, X., and Sun, S. (2012). Hepatitis C virus-induced up-regulation of microRNA-155 promotes hepatocarcinogenesis by activating Wnt signaling. *Hepatology* ***56***, 1631–40. Available at: http://www.ncbi.nlm.nih.gov/pubmed/22610915 [Accessed November 13, 2013].

235 Lin, Y.-H., Liao, C.-J., Huang, Y.-H., Wu, M.-H., Chi, H.-C., Wu, S.-M., Chen, C.-Y., Tseng, Y.-H., Tsai, C.-Y., Chung, I.-H., et al. (2013). Thyroid hormone receptor represses miR-17 expression to enhance tumor metastasis in human hepatoma cells. *Oncogene* ***32***, 4509–18. Available at: http://www.ncbi.nlm.nih.gov/pubmed/23912452 [Accessed November 25, 2013].

236 Xu, T., Zhu, Y., Xiong, Y., Ge, Y.-Y., Yun, J.-P., and Zhuang, S.-M. (2009). MicroRNA-195 suppresses tumorigenicity and regulates G1/S transition of human hepatocellular carcinoma cells. *Hepatology **50***, 113–21. Available at: http://www.ncbi.nlm.nih.gov/pubmed/19441017 [Accessed November 25, 2013].

237 Hou, J., Lin, L., Zhou, W., Wang, Z., Ding, G., Dong, Q., Qin, L., Wu, X., Zheng, Y., Yang, Y., et al. (2011). Identification of miRNomes in human liver and hepatocellular carcinoma reveals miR-199a/b-3p as therapeutic target for hepatocellular carcinoma. *Cancer Cell **19***, 232–43. Available at: http://www.ncbi.nlm.nih.gov/pubmed/21316602 [Accessed November 22, 2013].

238 Bao, L., Yan, Y., Xu, C., Ji, W., Shen, S., Xu, G., Zeng, Y., Sun, B., Qian, H., Chen, L., et al. (2013). MicroRNA-21 suppresses PTEN and hSulf-1 expression and promotes hepatocellular carcinoma progression through AKT/ERK pathways. *Cancer Lett. **337***, 226–36. Available at: http://www.ncbi.nlm.nih.gov/pubmed/23684551 [Accessed November 19, 2013].

239 Liu, C., Yu, J., Yu, S., Lavker, R. M., Cai, L., Liu, W., Yang, K., He, X., and Chen, S. (2010). MicroRNA-21 acts as an oncomir through multiple targets in human hepatocellular carcinoma. *J. Hepatol. **53***, 98–107. Available at: http://www.ncbi.nlm.nih.gov/pubmed/20447717 [Accessed November 26, 2013].

240 Shih, T.-C., Tien, Y.-J., Wen, C.-J., Yeh, T.-S., Yu, M.-C., Huang, C.-H., Lee, Y.-S., Yen, T.-C., and Hsieh, S.-Y. (2012). MicroRNA-214 downregulation contributes to tumor angiogenesis by inducing secretion of the hepatoma-derived growth factor in human hepatoma. *J. Hepatol. **57***, 584–91. Available at: http://www.ncbi.nlm.nih.gov/pubmed/22613005 [Accessed November 25, 2013].

241 Xia, H., Ooi, L. L. P. J., and Hui, K. M. (2013). MicroRNA-216a/217-induced epithelial-mesenchymal transition targets PTEN and SMAD7 to promote drug resistance and recurrence of liver cancer. *Hepatology **58***, 629–41. Available at: http://www.ncbi.nlm.nih.gov/pubmed/23471579 [Accessed November 25, 2013].

242 Yuan, Q., Loya, K., Rani, B., Möbus, S., Balakrishnan, A., Lamle, J., Cathomen, T., Vogel, A., Manns, M. P., Ott, M., et al. (2013). MicroRNA-221 overexpression accelerates hepatocyte proliferation during liver regeneration. *Hepatology **57***, 299–310. Available at: http://www.ncbi.nlm.nih.gov/pubmed/22821679 [Accessed November 25, 2013].

243 Wong, Q. W.-L., Ching, A. K.-K., Chan, A. W.-H., Choy, K.-W., To, K.-F., Lai, P. B.-S., and Wong, N. (2010). MiR-222 overexpression confers cell migratory advantages in hepatocellular carcinoma through enhancing AKT signaling. *Clin. Cancer Res. **16***, 867–75. Available at: http://www.ncbi.nlm.nih.gov/pubmed/20103675 [Accessed November 26, 2013].

244 Ma, D., Tao, X., Gao, F., Fan, C., and Wu, D. (2012). miR-224 functions as an onco-miRNA in hepatocellular carcinoma cells by activating AKT signaling. *Oncol. Lett. **4***,

483–488. Available at: http://www.pubmedcentral.nih.gov/articlerender.fcgi?artid=3673647&tool=pmcentrez&rendertype=abstract [Accessed November 25, 2013].

245 Chen, Z., Ma, T., Huang, C., Zhang, L., Lv, X., Xu, T., Hu, T., and Li, J. (2013). MiR-27a modulates the MDR1/P-glycoprotein expression by inhibiting FZD7/β-catenin pathway in hepatocellular carcinoma cells. *Cell. Signal.* ***25***, 2693–701. Available at: http://www.ncbi.nlm.nih.gov/pubmed/24018051 [Accessed November 26, 2013].

246 Chang, Y., Yan, W., He, X., Zhang, L., Li, C., Huang, H., Nace, G., Geller, D. A., Lin, J., and Tsung, A. (2012). miR-375 inhibits autophagy and reduces viability of hepatocellular carcinoma cells under hypoxic conditions. *Gastroenterology* ***143***, 177–87.e8. Available at: http://www.ncbi.nlm.nih.gov/pubmed/22504094 [Accessed November 26, 2013].

247 Xiao, F., Zhang, W., Chen, L., Chen, F., Xie, H., Xing, C., Yu, X., Ding, S., Chen, K., Guo, H., et al. (2013). MicroRNA-503 inhibits the G1/S transition by downregulating cyclin D3 and E2F3 in hepatocellular carcinoma. *J. Transl. Med.* ***11***, 195. Available at: http://www.pubmedcentral.nih.gov/articlerender.fcgi?artid=3765277&tool=pmcentrez&rendertype=abstract [Accessed November 25, 2013].

248 Fornari, F., Milazzo, M., Chieco, P., Negrini, M., Marasco, E., Capranico, G., Mantovani, V., Marinello, J., Sabbioni, S., Callegari, E., et al. (2012). In hepatocellular carcinoma miR-519d is up-regulated by p53 and DNA hypomethylation and targets CDKN1A/p21, PTEN, AKT3 and TIMP2. *J. Pathol.* ***227***, 275–85. Available at: http://www.ncbi.nlm.nih.gov/pubmed/22262409.

249 Zhang, W., Kong, G., Zhang, J., Wang, T., Ye, L., and Zhang, X. (2012). MicroRNA-520b inhibits growth of hepatoma cells by targeting MEKK2 and cyclin D1. *PLoS One* ***7***, e31450. Available at: http://www.pubmedcentral.nih.gov/articlerender.fcgi?artid=3272016&tool=pmcentrez&rendertype=abstract [Accessed November 25, 2013].

250 Tao, Z.-H., Wan, J.-L., Zeng, L.-Y., Xie, L., Sun, H.-C., Qin, L.-X., Wang, L., Zhou, J., Ren, Z.-G., Li, Y.-X., et al. (2013). miR-612 suppresses the invasive-metastatic cascade in hepatocellular carcinoma. *J. Exp. Med.* ***210***, 789–803. Available at: http://www.pubmedcentral.nih.gov/articlerender.fcgi?artid=3620363&tool=pmcentrez&rendertype=abstract [Accessed November 25, 2013].

251 Hernandez, J. M., Elahi, a, Clark, C. W., Wang, J., Humphries, L. a, Centeno, B., Bloom, G., Fuchs, B. C., Yeatman, T., and Shibata, D. (2013). miR-675 Mediates Downregulation of Twist1 and Rb in AFP-Secreting Hepatocellular Carcinoma. *Ann. Surg. Oncol.* Available at: http://www.ncbi.nlm.nih.gov/pubmed/23864307 [Accessed November 25, 2013].

252 Fang, Y., Xue, J.-L., Shen, Q., Chen, J., and Tian, L. (2012). MicroRNA-7 inhibits tumor growth and metastasis by targeting the phosphoinositide 3-kinase/Akt pathway in

hepatocellular carcinoma. *Hepatology* ***55***, 1852–62. Available at: http://www.ncbi.nlm.nih.gov/pubmed/22234835 [Accessed November 19, 2013].

253 Rodríguez-Paredes, M., and Esteller, M. (2011). Cancer epigenetics reaches mainstream oncology. *Nat. Med.* ***17***, 330–9. Available at: http://www.ncbi.nlm.nih.gov/pubmed/21386836 [Accessed November 7, 2013].

254 Zhai, B. (2008). Reduced expression of E-cadherin/catenin complex in hepatocellular carcinomas. *World J. Gastroenterol.* ***14***, 5665. Available at: http://www.wjgnet.com/1007-9327/14/5665.asp [Accessed November 25, 2013].

255 Xu, B., Di, J., Wang, Z., Han, X., Li, Z., Luo, X., and Zheng, Q. (2013). Quantitative analysis of RASSF1A promoter methylation in hepatocellular carcinoma and its prognostic implications. *Biochem. Biophys. Res. Commun.* ***438***, 324–8. Available at: http://www.ncbi.nlm.nih.gov/pubmed/23891693 [Accessed November 25, 2013].

256 Saito, Y., Kanai, Y., Nakagawa, T., Sakamoto, M., Saito, H., Ishii, H., and Hirohashi, S. (2003). Increased protein expression of DNA methyltransferase (DNMT) 1 is significantly correlated with the malignant potential and poor prognosis of human hepatocellular carcinomas. *Int. J. Cancer* ***105***, 527–32. Available at: http://www.ncbi.nlm.nih.gov/pubmed/12712445 [Accessed November 25, 2013].

257 Kong, L.-M., Liao, C.-G., Chen, L., Yang, H.-S., Zhang, S.-H., Zhang, Z., Bian, H.-J., Xing, J.-L., and Chen, Z.-N. (2011). Promoter hypomethylation up-regulates CD147 expression through increasing Sp1 binding and associates with poor prognosis in human hepatocellular carcinoma. *J. Cell. Mol. Med.* ***15***, 1415–28. Available at: http://www.ncbi.nlm.nih.gov/pubmed/20629990 [Accessed November 25, 2013].

258 Chan, C.-F., Yau, T.-O., Jin, D.-Y., Wong, C.-M., Fan, S.-T., and Ng, I. O.-L. (2004). Evaluation of nuclear factor-kappaB, urokinase-type plasminogen activator, and HBx and their clinicopathological significance in hepatocellular carcinoma. *Clin. Cancer Res.* ***10***, 4140–9. Available at: http://www.ncbi.nlm.nih.gov/pubmed/15217951.

259 Pogribny, I. P., and Rusyn, I. (2012). Role of epigenetic aberrations in the development and progression of human hepatocellular carcinoma. *Cancer Lett.* Available at: http://www.ncbi.nlm.nih.gov/pubmed/22306342 [Accessed November 14, 2013].

260 Kitamura, Y., Shirahata, A., Sakuraba, K., Goto, T., Mizukami, H., Saito, M., Ishibashi, K., Kigawa, G., Nemoto, H., Sanada, Y., et al. (2011). Aberrant methylation of the Vimentin gene in hepatocellular carcinoma. *Anticancer Res.* ***31***, 1289–91. Available at: http://www.ncbi.nlm.nih.gov/pubmed/21508377 [Accessed November 26, 2013].

261 Wang, S., Zhu, Y., He, H., Liu, J., Xu, L., Zhang, H., Liu, H., Liu, W., Liu, Y., Pan, D., et al. (2013). Sorafenib suppresses growth and survival of hepatoma cells by accelerating degradation of enhancer of zeste homolog 2. *Cancer Sci.* ***104***, 750–9. Available at: http://www.ncbi.nlm.nih.gov/pubmed/23421437 [Accessed November 25, 2013].

262 Puszyk, W. M., Trinh, T. Le, Chapple, S. J., and Liu, C. (2013). Linking metabolism and epigenetic regulation in development of hepatocellular carcinoma. *Lab. Invest.* ***93***, 983–90. Available at: http://www.ncbi.nlm.nih.gov/pubmed/23917878 [Accessed November 21, 2013].

263 Choi, M. S., Shim, Y.-H., Hwa, J. Y., Lee, S. K., Ro, J. Y., Kim, J.-S., and Yu, E. (2003). Expression of DNA methyltransferases in multistep hepatocarcinogenesis. *Hum. Pathol.* ***34***, 11–7. Available at: http://www.ncbi.nlm.nih.gov/pubmed/12605361 [Accessed March 17, 2014].

264 Oh, B.-K., Kim, H., Park, H.-J., Shim, Y.-H., Choi, J., Park, C., and Park, Y. N. (2007). DNA methyltransferase expression and DNA methylation in human hepatocellular carcinoma and their clinicopathological correlation. *Int. J. Mol. Med.* ***20***, 65–73. Available at: http://www.ncbi.nlm.nih.gov/pubmed/17549390 [Accessed March 17, 2014].

265 Park, H.-J., Yu, E., and Shim, Y.-H. (2006). DNA methyltransferase expression and DNA hypermethylation in human hepatocellular carcinoma. *Cancer Lett.* ***233***, 271–8. Available at: http://www.ncbi.nlm.nih.gov/pubmed/15885882 [Accessed March 17, 2014].

266 Nagai, M., Nakamura, A., Makino, R., and Mitamura, K. (2003). Expression of DNA (5-cytosin)-methyltransferases (DNMTs) in hepatocellular carcinomas. *Hepatol. Res.* ***26***, 186–191. Available at: http://www.ncbi.nlm.nih.gov/pubmed/12850690 [Accessed March 17, 2014].

267 Wu, L.-M., Yang, Z., Zhou, L., Zhang, F., Xie, H.-Y., Feng, X.-W., Wu, J., and Zheng, S.-S. (2010). Identification of histone deacetylase 3 as a biomarker for tumor recurrence following liver transplantation in HBV-associated hepatocellular carcinoma. *PLoS One* ***5***, e14460. Available at: http://www.pubmedcentral.nih.gov/articlerender.fcgi?artid=3012077&tool=pmcentrez&rendertype=abstract [Accessed March 19, 2014].

268 Quint, K., Agaimy, A., Di Fazio, P., Montalbano, R., Steindorf, C., Jung, R., Hellerbrand, C., Hartmann, A., Sitter, H., Neureiter, D., et al. (2011). Clinical significance of histone deacetylases 1, 2, 3, and 7: HDAC2 is an independent predictor of survival in HCC. *Virchows Arch.* ***459***, 129–39. Available at: http://www.ncbi.nlm.nih.gov/pubmed/21713366 [Accessed March 5, 2014].

269 Zhang, B., Chen, J., Cheng, A. S. L., and Ko, B. C. B. (2014). Depletion of sirtuin 1 (SIRT1) leads to epigenetic modifications of telomerase (TERT) gene in hepatocellular carcinoma cells. *PLoS One* ***9***, e84931. Available at: http://www.pubmedcentral.nih.gov/articlerender.fcgi?artid=3885646&tool=pmcentrez&rendertype=abstract [Accessed March 16, 2014].

270 Chen, J., Zhang, B., Wong, N., Lo, A. W. I., To, K.-F., Chan, A. W. H., Ng, M. H. L., Ho, C. Y. S., Cheng, S.-H., Lai, P. B. S., et al. (2011). Sirtuin 1 is upregulated in a subset of

hepatocellular carcinomas where it is essential for telomere maintenance and tumor cell growth. *Cancer Res.* ***71***, 4138–49. Available at: http://www.ncbi.nlm.nih.gov/pubmed/21527554 [Accessed March 4, 2014].

271 Chen, J., Chan, A. W. H., To, K.-F., Chen, W., Zhang, Z., Ren, J., Song, C., Cheung, Y.-S., Lai, P. B. S., Cheng, S.-H., et al. (2013). SIRT2 overexpression in hepatocellular carcinoma mediates epithelial to mesenchymal transition by protein kinase B/glycogen synthase kinase-3β/β-catenin signaling. *Hepatology* ***57***, 2287–98. Available at: http://www.ncbi.nlm.nih.gov/pubmed/23348706 [Accessed March 17, 2014].

272 Zhang, C. Z., Liu, L., Cai, M., Pan, Y., Fu, J., Cao, Y., and Yun, J. (2012). Low SIRT3 expression correlates with poor differentiation and unfavorable prognosis in primary hepatocellular carcinoma. *PLoS One* ***7***, e51703. Available at: http://www.pubmedcentral.nih.gov/articlerender.fcgi?artid=3522714&tool=pmcentrez&rendertype=abstract [Accessed March 17, 2014].

273 Zhang, Z.-G., and Qin, C.-Y. (2014). Sirt6 suppresses hepatocellular carcinoma cell growth via inhibiting the extracellular signal-regulated kinase signaling pathway. *Mol. Med. Rep.* ***9***, 882–8. Available at: http://www.ncbi.nlm.nih.gov/pubmed/24366394 [Accessed March 17, 2014].

274 Marquardt, J. U., Fischer, K., Baus, K., Kashyap, A., Ma, S., Krupp, M., Linke, M., Teufel, A., Zechner, U., Strand, D., et al. (2013). Sirtuin-6-dependent genetic and epigenetic alterations are associated with poor clinical outcome in hepatocellular carcinoma patients. *Hepatology* ***58***, 1054–64. Available at: http://www.ncbi.nlm.nih.gov/pubmed/23526469 [Accessed March 16, 2014].

275 Au, S. L.-K., Wong, C. C.-L., Lee, J. M.-F., Fan, D. N.-Y., Tsang, F. H., Ng, I. O.-L., and Wong, C.-M. (2012). Enhancer of zeste homolog 2 epigenetically silences multiple tumor suppressor microRNAs to promote liver cancer metastasis. *Hepatology* ***56***, 622–31. Available at: http://www.ncbi.nlm.nih.gov/pubmed/22370893 [Accessed March 12, 2014].

276 Kondo, Y., Shen, L., Suzuki, S., Kurokawa, T., Masuko, K., Tanaka, Y., Kato, H., Mizuno, Y., Yokoe, M., Sugauchi, F., et al. (2007). Alterations of DNA methylation and histone modifications contribute to gene silencing in hepatocellular carcinomas. *Hepatol. Res.* ***37***, 974–83. Available at: http://www.ncbi.nlm.nih.gov/pubmed/17584191 [Accessed March 5, 2014].

277 Fan, D. N.-Y., Tsang, F. H.-C., Tam, A. H.-K., Au, S. L.-K., Wong, C. C.-L., Wei, L., Lee, J. M.-F., He, X., Ng, I. O.-L., and Wong, C.-M. (2013). Histone lysine methyltransferase, suppressor of variegation 3-9 homolog 1, promotes hepatocellular carcinoma progression and is negatively regulated by microRNA-125b. *Hepatology* ***57***, 637–47. Available at: http://www.ncbi.nlm.nih.gov/pubmed/22991213 [Accessed March 5, 2014].

278 Hamamoto, R., Furukawa, Y., Morita, M., Iimura, Y., Silva, F. P., Li, M., Yagyu, R., and Nakamura, Y. (2004). SMYD3 encodes a histone methyltransferase involved in the

proliferation of cancer cells. *Nat. Cell Biol.* ***6***, 731–40. Available at: http://www.ncbi.nlm.nih.gov/pubmed/15235609 [Accessed February 14, 2014].

279 Zhou, P., Wu, L.-L., Wu, K.-M., Jiang, W., Li, J.-D., Zhou, L., Li, X.-Y., Chang, S., Huang, Y., Tan, H., et al. (2013). Overexpression of MMSET is correlation with poor prognosis in hepatocellular carcinoma. *Pathol. Oncol. Res.* ***19***, 303–9. Available at: http://www.ncbi.nlm.nih.gov/pubmed/23225158 [Accessed March 17, 2014].

280 Schagdarsurengin, U., Wilkens, L., Steinemann, D., Flemming, P., Kreipe, H. H., Pfeifer, G. P., Schlegelberger, B., and Dammann, R. (2003). Frequent epigenetic inactivation of the RASSF1A gene in hepatocellular carcinoma. *Oncogene* ***22***, 1866–71. Available at: http://www.ncbi.nlm.nih.gov/pubmed/12660822 [Accessed March 17, 2014].

281 Macheiner, D., Heller, G., Kappel, S., Bichler, C., Stättner, S., Ziegler, B., Kandioler, D., Wrba, F., Schulte-Hermann, R., Zöchbauer-Müller, S., et al. (2006). NORE1B, a candidate tumor suppressor, is epigenetically silenced in human hepatocellular carcinoma. *J. Hepatol.* ***45***, 81–9. Available at: http://www.ncbi.nlm.nih.gov/pubmed/16516329 [Accessed March 17, 2014].

282 Lambert, M.-P., Paliwal, A., Vaissière, T., Chemin, I., Zoulim, F., Tommasino, M., Hainaut, P., Sylla, B., Scoazec, J.-Y., Tost, J., et al. (2011). Aberrant DNA methylation distinguishes hepatocellular carcinoma associated with HBV and HCV infection and alcohol intake. *J. Hepatol.* ***54***, 705–15. Available at: http://www.ncbi.nlm.nih.gov/pubmed/21146512 [Accessed February 28, 2014].

283 Song, M.-A., Tiirikainen, M., Kwee, S., Okimoto, G., Yu, H., and Wong, L. L. (2013). Elucidating the landscape of aberrant DNA methylation in hepatocellular carcinoma. *PLoS One* ***8***, e55761. Available at: http://www.pubmedcentral.nih.gov/articlerender.fcgi?artid=3577824&tool=pmcentrez&rendertype=abstract [Accessed January 27, 2014].

284 Nishida, N., Kudo, M., Nagasaka, T., Ikai, I., and Goel, A. (2012). Characteristic patterns of altered DNA methylation predict emergence of human hepatocellular carcinoma. *Hepatology* ***56***, 994–1003. Available at: http://www.ncbi.nlm.nih.gov/pubmed/22407776 [Accessed February 4, 2014].

285 Shen, J., Wang, S., Zhang, Y.-J., Kappil, M., Wu, H.-C., Kibriya, M. G., Wang, Q., Jasmine, F., Ahsan, H., Lee, P.-H., et al. (2012). Genome-wide DNA methylation profiles in hepatocellular carcinoma. *Hepatology* ***55***, 1799–808. Available at: http://www.pubmedcentral.nih.gov/articlerender.fcgi?artid=3330167&tool=pmcentrez&rendertype=abstract [Accessed March 19, 2014].

286 Wang, L., Wang, W.-L., Zhang, Y., Guo, S.-P., Zhang, J., and Li, Q.-L. (2007). Epigenetic and genetic alterations of PTEN in hepatocellular carcinoma. *Hepatol. Res.* ***37***, 389–96. Available at: http://www.ncbi.nlm.nih.gov/pubmed/17441812 [Accessed March 17, 2014].

287 Pogribny, I. P., and James, S. J. (2002). Reduction of p53 gene expression in human primary hepatocellular carcinoma is associated with promoter region methylation without coding region mutation. *Cancer Lett.* ***176***, 169–74. Available at: http://www.ncbi.nlm.nih.gov/pubmed/11804744 [Accessed March 17, 2014].

288 Edamoto, Y., Hara, A., Biernat, W., Terracciano, L., Cathomas, G., Riehle, H.-M., Matsuda, M., Fujii, H., Scoazec, J.-Y., and Ohgaki, H. (2003). Alterations of RB1, p53 and Wnt pathways in hepatocellular carcinomas associated with hepatitis C, hepatitis B and alcoholic liver cirrhosis. *Int. J. Cancer* ***106***, 334–41. Available at: http://www.ncbi.nlm.nih.gov/pubmed/12845670 [Accessed March 17, 2014].

289 Matsuda, Y., Ichida, T., Matsuzawa, J., Sugimura, K., and Asakura, H. (1999). p16(INK4) is inactivated by extensive CpG methylation in human hepatocellular carcinoma. *Gastroenterology* ***116***, 394–400. Available at: http://www.ncbi.nlm.nih.gov/pubmed/9922321 [Accessed March 17, 2014].

290 Roncalli, M., Bianchi, P., Bruni, B., Laghi, L., Destro, A., Di Gioia, S., Gennari, L., Tommasini, M., Malesci, A., and Coggi, G. (2002). Methylation framework of cell cycle gene inhibitors in cirrhosis and associated hepatocellular carcinoma. *Hepatology* ***36***, 427–32. Available at: http://www.ncbi.nlm.nih.gov/pubmed/12143052 [Accessed March 17, 2014].

291 Shim, Y.-H., Yoon, G.-S., Choi, H.-J., Chung, Y. H., and Yu, E. (2003). p16 Hypermethylation in the early stage of hepatitis B virus-associated hepatocarcinogenesis. *Cancer Lett.* ***190***, 213–9. Available at: http://www.ncbi.nlm.nih.gov/pubmed/12565176 [Accessed March 17, 2014].

292 Li, X., Hui, A.-M., Sun, L., Hasegawa, K., Torzilli, G., Minagawa, M., Takayama, T., and Makuuchi, M. (2004). p16INK4A hypermethylation is associated with hepatitis virus infection, age, and gender in hepatocellular carcinoma. *Clin. Cancer Res.* ***10***, 7484–9. Available at: http://www.ncbi.nlm.nih.gov/pubmed/15569978 [Accessed March 17, 2014].

293 Csepregi, A., Ebert, M. P., Röcken, C., Schneider-Stock, R., Hoffmann, J., Schulz, H.-U., Roessner, A., and Malfertheiner, P. (2010). Promoter methylation of CDKN2A and lack of p16 expression characterize patients with hepatocellular carcinoma. *BMC Cancer* ***10***, 317. Available at: http://www.pubmedcentral.nih.gov/articlerender.fcgi?artid=2927998&tool=pmcentrez&rendertype=abstract [Accessed March 17, 2014].

294 Wong, I. H., Lo, Y. M., Yeo, W., Lau, W. Y., and Johnson, P. J. (2000). Frequent p15 promoter methylation in tumor and peripheral blood from hepatocellular carcinoma patients. *Clin. Cancer Res.* ***6***, 3516–21. Available at: http://www.ncbi.nlm.nih.gov/pubmed/10999738 [Accessed March 17, 2014].

295 Zhu, H., Wu, K., Yan, W., Hu, L., Yuan, J., Dong, Y., Li, Y., Jing, K., Yang, Y., and Guo, M. (2013). Epigenetic silencing of DACH1 induces loss of transforming growth factor-β1

antiproliferative response in human hepatocellular carcinoma. *Hepatology* ***58***, 2012–22. Available at: http://www.ncbi.nlm.nih.gov/pubmed/23787902 [Accessed March 16, 2014].

296 He, Y., Cui, Y., Xu, B., Gu, J., Wang, W., and Luo, X. (2014). Hypermethylation leads to bone morphogenetic protein 6 downregulation in hepatocellular carcinoma. *PLoS One* ***9***, e87994. Available at: http://www.pubmedcentral.nih.gov/articlerender.fcgi?artid=3907571&tool=pmcentrez&rendertype=abstract [Accessed March 17, 2014].

297 Okochi, O., Hibi, K., Sakai, M., Inoue, S., Takeda, S., Kaneko, T., and Nakao, A. (2003). Methylation-mediated silencing of SOCS-1 gene in hepatocellular carcinoma derived from cirrhosis. *Clin. Cancer Res.* ***9***, 5295–8. Available at: http://www.ncbi.nlm.nih.gov/pubmed/14614012 [Accessed March 17, 2014].

298 Miyoshi, H., Fujie, H., Moriya, K., Shintani, Y., Tsutsumi, T., Makuuchi, M., Kimura, S., and Koike, K. (2004). Methylation status of suppressor of cytokine signaling-1 gene in hepatocellular carcinoma. *J. Gastroenterol.* ***39***, 563–9. Available at: http://www.ncbi.nlm.nih.gov/pubmed/15235874 [Accessed March 17, 2014].

299 Yuan, Y., Wang, J., Li, J., Wang, L., Li, M., Yang, Z., Zhang, C., and Dai, J. Le (2006). Frequent epigenetic inactivation of spleen tyrosine kinase gene in human hepatocellular carcinoma. *Clin. Cancer Res.* ***12***, 6687–95. Available at: http://www.pubmedcentral.nih.gov/articlerender.fcgi?artid=1832152&tool=pmcentrez&rendertype=abstract [Accessed March 17, 2014].

300 Zhang, J., Gong, C., Bing, Y., Li, T., Liu, Z., and Liu, Q. (2013). Hypermethylation-repressed methionine adenosyltransferase 1A as a potential biomarker for hepatocellular carcinoma. *Hepatol. Res.* ***43***, 374–83. Available at: http://www.ncbi.nlm.nih.gov/pubmed/23072598 [Accessed March 17, 2014].

301 Tomasi, M. L., Li, T. W. H., Li, M., Mato, J. M., and Lu, S. C. (2012). Inhibition of human methionine adenosyltransferase 1A transcription by coding region methylation. *J. Cell. Physiol.* ***227***, 1583–91. Available at: http://www.pubmedcentral.nih.gov/articlerender.fcgi?artid=3183271&tool=pmcentrez&rendertype=abstract [Accessed March 17, 2014].

302 Frau, M., Tomasi, M. L., Simile, M. M., Demartis, M. I., Salis, F., Latte, G., Calvisi, D. F., Seddaiu, M. A., Daino, L., Feo, C. F., et al. (2012). Role of transcriptional and posttranscriptional regulation of methionine adenosyltransferases in liver cancer progression. *Hepatology* ***56***, 165–75. Available at: http://www.ncbi.nlm.nih.gov/pubmed/22318685 [Accessed March 17, 2014].

303 Zhang, J., Wang, C., Chen, M., Cao, J., Zhong, Y., Chen, L., Shen, H.-M., and Xia, D. (2013). Epigenetic silencing of glutaminase 2 in human liver and colon cancers. *BMC Cancer* ***13***, 601. Available at:

http://www.pubmedcentral.nih.gov/articlerender.fcgi?artid=3878668&tool=pmcentrez&rendertype=abstract [Accessed March 1, 2014].

304 Zhang, Y., Chen, Y., Ahsan, H., Lunn, R. M., Chen, S.-Y., Lee, P., Chen, C.-J., and Santella, R. M. (2005). Silencing of glutathione S-transferase P1 by promoter hypermethylation and its relationship to environmental chemical carcinogens in hepatocellular carcinoma. *Cancer Lett.* ***221***, 135–43. Available at: http://www.ncbi.nlm.nih.gov/pubmed/15808399 [Accessed March 17, 2014].

305 Zhong, S., Tang, M. W., Yeo, W., Liu, C., Lo, Y. M. D., and Johnson, P. J. (2002). Silencing of GSTP1 gene by CpG island DNA hypermethylation in HBV-associated hepatocellular carcinomas. *Clin. Cancer Res.* ***8***, 1087–92. Available at: http://www.ncbi.nlm.nih.gov/pubmed/11948118 [Accessed March 17, 2014].

306 Tada, M., Yokosuka, O., Fukai, K., Chiba, T., Imazeki, F., Tokuhisa, T., and Saisho, H. (2005). Hypermethylation of NAD(P)H: quinone oxidoreductase 1 (NQO1) gene in human hepatocellular carcinoma. *J. Hepatol.* ***42***, 511–9. Available at: http://www.ncbi.nlm.nih.gov/pubmed/15763338 [Accessed March 17, 2014].

307 Fernández-Alvarez, A., Llorente-Izquierdo, C., Mayoral, R., Agra, N., Boscá, L., Casado, M., and Martín-Sanz, P. (2012). Evaluation of epigenetic modulation of cyclooxygenase-2 as a prognostic marker for hepatocellular carcinoma. *Oncogenesis* ***1***, e23. Available at: http://www.pubmedcentral.nih.gov/articlerender.fcgi?artid=3412654&tool=pmcentrez&rendertype=abstract [Accessed February 28, 2014].

308 Jiang, L., Chan, J. Y.-W., and Fung, K.-P. (2012). Epigenetic loss of CDH1 correlates with multidrug resistance in human hepatocellular carcinoma cells. *Biochem. Biophys. Res. Commun.* ***422***, 739–44. Available at: http://www.ncbi.nlm.nih.gov/pubmed/22634315 [Accessed March 16, 2014].

309 Takagi, H., Sasaki, S., Suzuki, H., Toyota, M., Maruyama, R., Nojima, M., Yamamoto, H., Omata, M., Tokino, T., Imai, K., et al. (2008). Frequent epigenetic inactivation of SFRP genes in hepatocellular carcinoma. *J. Gastroenterol.* ***43***, 378–89. Available at: http://www.ncbi.nlm.nih.gov/pubmed/18592156 [Accessed January 23, 2014].

310 Quan, H., Zhou, F., Nie, D., Chen, Q., Cai, X., Shan, X., Zhou, Z., Chen, K., Huang, A., Li, S., et al. (2013). Hepatitis C virus core protein epigenetically silences SFRP1 and enhances HCC aggressiveness by inducing epithelial-mesenchymal transition. *Oncogene*. Available at: http://www.ncbi.nlm.nih.gov/pubmed/23770846 [Accessed March 3, 2014].

311 Xie, Q., Chen, L., Shan, X., Shan, X., Tang, J., Zhou, F., Chen, Q., Quan, H., Nie, D., Zhang, W., et al. (2013). Epigenetic silencing of SFRP1 and SFRP5 by Hepatitis B Virus X protein enhances hepatoma cell tumorigenicity through wnt signaling pathway. *Int. J. Cancer*. Available at: http://www.ncbi.nlm.nih.gov/pubmed/24374650 [Accessed February 1, 2014].

312 Shih, Y.-L., Hsieh, C.-B., Yan, M.-D., Tsao, C.-M., Hsieh, T.-Y., Liu, C.-H., and Lin, Y.-W. (2013). Frequent concomitant epigenetic silencing of SOX1 and secreted frizzled-related proteins (SFRPs) in human hepatocellular carcinoma. *J. Gastroenterol. Hepatol.* ***28***, 551–9. Available at: http://www.ncbi.nlm.nih.gov/pubmed/23215838 [Accessed January 23, 2014].

313 Zhang, X., Yang, Y., Liu, X., Herman, J. G., Brock, M. V, Licchesi, J. D. F., Yue, W., Pei, X., and Guo, M. (2013). Epigenetic regulation of the Wnt signaling inhibitor DACT2 in human hepatocellular carcinoma. *Epigenetics* ***8***. Available at: http://www.ncbi.nlm.nih.gov/pubmed/23449122 [Accessed March 16, 2014].

314 Gao, S., Yang, Z., Zheng, Z.-Y., Yao, J., Zhang, F., Wu, L.-M., Xie, H.-Y., Zhou, L., and Zheng, S.-S. (2013). Reduced expression of DACT2 promotes hepatocellular carcinoma progression: involvement of methylation-mediated gene silencing. *World J. Surg. Oncol.* ***11***, 57. Available at: http://www.pubmedcentral.nih.gov/articlerender.fcgi?artid=3605395&tool=pmcentrez&rendertype=abstract [Accessed March 17, 2014].

315 Zhang, C., Li, H., Wang, Y., Liu, W., Zhang, Q., Zhang, T., Zhang, X., Han, B., and Zhou, G. (2010). Epigenetic inactivation of the tumor suppressor gene RIZ1 in hepatocellular carcinoma involves both DNA methylation and histone modifications. *J. Hepatol.* ***53***, 889–95. Available at: http://www.ncbi.nlm.nih.gov/pubmed/20675009 [Accessed March 17, 2014].

316 Piao, G. H., Piao, W. H., He, Y., Zhang, H. H., Wang, G. Q., and Piao, Z. (2008). Hyper-methylation of RIZ1 tumor suppressor gene is involved in the early tumorigenesis of hepatocellular carcinoma. *Histol. Histopathol.* ***23***, 1171–5. Available at: http://www.ncbi.nlm.nih.gov/pubmed/18712668 [Accessed March 17, 2014].

317 Shu, X., Geng, H., Li, L., Ying, J., Ma, C., Wang, Y., Poon, F. F., Wang, X., Ying, Y., Yeo, W., et al. (2011). The epigenetic modifier PRDM5 functions as a tumor suppressor through modulating WNT/β-catenin signaling and is frequently silenced in multiple tumors. *PLoS One* ***6***, e27346. Available at: http://www.pubmedcentral.nih.gov/articlerender.fcgi?artid=3210799&tool=pmcentrez&rendertype=abstract [Accessed February 27, 2014].

318 Zhao, R., Wang, N., Huang, H., Ma, W., and Yan, Q. (2014). CHD5,a tumor suppressor is epigenetically silenced in hepatocellular carcinoma. *Liver Int.* Available at: http://www.ncbi.nlm.nih.gov/pubmed/24529164 [Accessed March 16, 2014].

319 Ogunwobi, O. O., Puszyk, W., Dong, H.-J., and Liu, C. (2013). Epigenetic upregulation of HGF and c-Met drives metastasis in hepatocellular carcinoma. *PLoS One* ***8***, e63765. Available at: http://www.pubmedcentral.nih.gov/articlerender.fcgi?artid=3665785&tool=pmcentrez&rendertype=abstract [Accessed March 16, 2014].

320 Okada, H., Kimura, M. T., Tan, D., Fujiwara, K., Igarashi, J., Makuuchi, M., Hui, A.-M., Tsurumaru, M., and Nagase, H. (2005). Frequent trefoil factor 3 (TFF3) overexpression and promoter hypomethylation in mouse and human hepatocellular carcinomas. *Int. J. Oncol.* ***26***, 369–77. Available at: http://www.pubmedcentral.nih.gov/articlerender.fcgi?artid=2292801&tool=pmcentrez&rendertype=abstract [Accessed March 17, 2014].

321 Yang, H., Huang, Z. Z., Zeng, Z., Chen, C., Selby, R. R., and Lu, S. C. (2001). Role of promoter methylation in increased methionine adenosyltransferase 2A expression in human liver cancer. *Am. J. Physiol. Gastrointest. Liver Physiol.* ***280***, G184–90. Available at: http://www.ncbi.nlm.nih.gov/pubmed/11208539 [Accessed March 17, 2014].

322 Gao, X., Qu, J., Chang, X., Lu, Y., Bai, W., Wang, H., Xu, Z., An, L., Wang, C., Zeng, Z., et al. (2014). Hypomethylation of long interspersed nuclear element-1 promoter is associated with poor outcomes for curative resected hepatocellular carcinoma. *Liver Int.* ***34***, 136–46. Available at: http://www.ncbi.nlm.nih.gov/pubmed/23875825 [Accessed March 16, 2014].

Invest New Drugs
DOI 10.1007/s10637-010-9486-3

PRECLINICAL STUDIES

Inhibition of Akt signaling in hepatoma cells induces apoptotic cell death independent of Akt activation status

Francesca Buontempo · Tulin Ersahin · Silvia Missiroli · Serif Senturk · Daniela Etro · Mehmet Ozturk · Silvano Capitani · Rengul Cetin-Atalay · Maria Luca Neri

Received: 1 April 2010 / Accepted: 24 June 2010

Summary The serine/threonine kinase Akt, a downstream effector of phosphatidylinositol 3-kinase (PI3K), is involved in cell survival and anti-apoptotic signaling. Akt has been shown to be constitutively expressed in a variety of human tumors including hepatocellular carcinoma (HCC). In this report we analyzed the status of Akt pathway in three HCC cell lines, and tested cytotoxic effects of Akt pathway inhibitors LY294002, Wortmannin and Inhibitor VIII. In Mahlavu human hepatoma cells Akt was constitutively activated, as demonstrated by its Ser473 phosphorylation, downstream hyperphosphorylation of BAD on Ser136, and by a specific cell-free kinase assay. In contrast, Huh7 and HepG2 did not show hyperactivation when tested by the same criteria. Akt enzyme hyperactivation in Mahlavu was associated with a loss of PTEN protein expression. Akt signaling was inhibited by the upstream kinase inhibitors, LY294002, Wortmannin, as well as by the specific Akt Inhibitor VIII in all three hepatoma cell lines. Cytotoxicity assays with Akt inhibitors in the same cell lines indicated that they were all sensitive, but with different IC50 values as assayed by RT-CES. We also demonstrated that the cytotoxic effect was through apoptotic cell death. Our findings provide evidence for its constitutive activation in one HCC cell line, and that HCC cell lines, independent of their Akt activation status respond to Akt inhibitors by apoptotic cell death. Thus, Akt inhibition may be considered as an attractive therapeutic intervention in liver cancer.

Keywords Akt · PI3K · PTEN · HCC · LY294002 · Inhibitor VIII · Wortmannin · RTCES

Francesca Buontempo and Tulin Ersahin have contributed equally to this work.

Electronic supplementary material The online version of this article (doi:10.1007/s10637-010-9486-3) contains supplementary material, which is available to authorized users.

F. Buontempo · S. Missiroli · D. Etro · S. Capitani · M. L. Neri (✉)
Dipartimento di Morfologia ed Embriologia,
Sezione di Anatomia Umana, Signal Transduction Unit,
Universita' di Ferrara,
via Fossato di Mortara 66,
44100 Ferrara, Italy
e-mail: luca.neri@unife.it

T. Ersahin · S. Senturk · M. Ozturk · R. Cetin-Atalay (✉)
Department of Molecular Biology and Genetics,
Bilkent University,
TR-06800 Ankara, Turkey
e-mail: rengul@bilkent.edu.tr

Introduction

Hepatocellular carcinoma (HCC) is one of the most common cancers worldwide occurs in patients with chronic viral hepatitis and cirrhosis at a high rate (3–5% annually) and is a major cause of morbidity and mortality in patients with advanced liver disease [1]. In healthy individuals, liver is a quiescent organ and adult hepatocytes are nondividing cells under normal physiological conditions. However, chronic liver injury due to viral diseases, exposure to chemicals and other environmental or host factors results in extensive cell death and consequently hepatocyte proliferation [2]. Chronic cell death in liver leads to a state where continuous hepatocyte regeneration is observed as a result of the inflammatory response. Continuous cycles of liver cell death and proliferation induce many cell signaling pathways including cell survival pathways such as Akt [3, 4]. Knowledge on the signaling pathways and the alterations involved in HCC is extending, however their role in molecular targeted therapy still remains to be described.

Published online: 14 July 2010

The most promising molecular targets in the generation of new chemotherapy agents are the protein kinases, including those in the PI3K/Akt pathway. The Akt pathway is involved in many cancers, as well as HCC development, through its activation by EGF or IGF signaling or the constitutive activation of Akt proteins or the inactivation of PTEN tumor suppressor [5–8]. The serine/threonine kinase Akt is a well-characterized downstream target of PI3K and resides within the cytoplasm in an inactive state, but binding of PtdIns (3,4,5)P3 to its pleckstrin homology (PH) domain recruits Akt to the plasma membrane and enables its activation by phosphorylation on the C-terminal hydrophobic tail [9]. Once activated, signaling through Akt can be propagated to a diverse array of substrates. Activated Akt is known to inhibit apoptosis through its ability to phosphorylate several targets, including BAD, FoxO transcription factors, Raf-1 and caspase-9, which are critical for cell survival [9]. Moreover, the tumor suppressor protein PTEN prevents Akt activation by acting as a lipid phosphatase on the PI3K product PtdIns (3,4,5)P3. Akt pathway hyper-activation has been reported due to the loss of tumor suppressor protein PTEN function through mutations, deletions, or epigenetic silencing [10, 11]. The PTEN gene is the second most frequently modified tumor suppressor gene, and is related to many cancers including brain, bladder, breast, prostate, endometrial and liver cancer [10–12].

In primary liver carcinoma, one of the major pathogenic mechanisms resides in the activated intracellular signal transduction caused by oncogenes and the tumor suppressor gene dysfunction that stimulates cell-cycle progression and enhance cell survival [13]. Despite this much information, the behavior and relevance of the Akt pathway in HCC and its therapeutic potential remain to be further elucidated. Since liver cancer usually develops on the background of chronic liver disease, conventional anticancer therapies are not effective. Moreover, the chemotherapeutics currently in use are non-selective cytotoxic drugs that can lead to systemic side effects in HCC patients with compromised liver function. Recently, Sorafenib, a multikinase inhibitor acting through VEGFR and PDGFR of the Raf kinase pathway, was approved for hepatocellular carcinoma treatment [4]. The Sorafenib Hepatocellular Carcinoma Assessment Randomized Protocol (SHARP) three-year clinical trial included 602 advanced-stage HCC patients (ClinicalTrials.gov number, NCT00105443) [4]. The average survival rate for the group taking Sorafenib was 10.7 months, and that for the group taking the placebo was 7.9 months. For the Sorafenib group a one-year survival rate of 44% was observed, whereas it was 33% for the placebo group. FDA- and EU- approved chemotherapeutic Sorafenib thus prolongs median survival and the time to progression by nearly three months in patients with advanced hepatocellular carcinoma. Therefore FDA and EU approved chemotherapeutic Sorafenib prolongs median survival and the time to progression by nearly 3 months in patients with advanced hepatocellular carcinoma. Therefore, there is a need for new liver cancer specific drugs based on the molecular mechanisms involved in liver carcinogenesis.

In this study, we investigated the Akt activation status in HCC cell lines the differential effects of three Akt pathway inhibitors and the extent of the inhibition of Akt signaling as a major molecular mechanism in determining inhibitor-induced apoptosis in these cells. The Akt pathway can be blocked by cell line specific doses of pathway inhibitors. Therefore, our findings suggested that PI3K/Akt could represent an attractive target mitigating in liver cancer.

Materials and methods

Materials

DMEM (cat.12-614F), FCS (cat.DE 14-801F), antibiotics (cat.DE 17-602E), glutamine and non essential amino acids (cat.BE 13-114E) were from Lonza (Milan). Calnexin, β-actin antibody, and Sulforhodamine B (SRB) (cat.86183-5 g) were from Sigma (St. Louis, MO). Lumi-Light detection kit (cat.12 015 196001) was from Roche M.B. (Germany). Akt Inhibitor VIII (cat.124018), Wortmannin (cat. BML-ST415-0005) and LY294002 (cat.440202) were from Calbiochem (La Jolla, CA). The DMSO concentration for drug solubilization was always less than 1% in the cell culture medium.

The Akt Antibody (cat.610861) was from BD Transduction Laboratories (Franklin Lakes, NJ) and anti-p-473Ser Akt (cat.587F11), anti-BAD (cat.185D10), anti-p-BAD (cat.#9292), recGSK3α/β fusion protein (cat.#9237 L), anti-p-GSK3α/β (cat.#9331 L), anti-PTEN and anti-PARP (cat.46D11) antibodies were from Cell Signaling (Danvers, MA). The immunoprecipitation matrix (cat.sc-45042) was from Santa Cruz Biotechnology (Santa Cruz, CA).

Cell culture

Hepatoma cells (Huh7, HepG2, Mahlavu) were cultured at 37°C, 5% CO_2 in standard medium (2 mML-Glutamine, 0.1 mM NEA, 1xPS in DMEM) with 10% FCS.

Western blotting analysis

Proteins, from cells grown to 60–70% confluence, were separated on 10% SDS-PAGE, transferred onto nitrocellulose membranes and visualized as described previously [14].

Akt kinase activity assay

Total homogenates from cells were resuspended in 50 mM Tris-HCl pH 7.4, 1 mM EDTA, 1 mM EGTA, 150 mM NaCl, 1% Triton X-100, 0.1% SDS plus phosphatase and proteases inhibitors. IP was performed according to the manufacturer's instruction. Akt IP was resuspended in 20 mM HEPES pH 7.4, 10 mM $MgCl_2$ and 10 mM $MnCl_2$. The reaction was started by incubating 10 μl IP, 100 μM ATP and 1 μg recGSK3α/β for 40 min at RT, and then stopped by 1 M Tris-HCl pH 6.8, 8% SDS, 40% glycerol, 20% β-ME. GSK3α/β phosphorylation was detected by western blotting.

NCI-60 Sulforhodamine B (SRB) cytotoxicity assay

The cytotoxicities of LY294002, Akt Inhibitor VIII and Wortmannin were tested as previously described [15]. Hepatoma cells (5000) were inoculated into 96 well plates,100 μl/well. Next day, inhibitors with the indicated concentrations were applied in a total of 200 μl of medium. After 72 h of treatment, cells were fixed by cold 10% (w/v) TCA and then the wells were washed and dried. One hundred μl of 0.4% SRB dye was applied to each well and incubated at RT for 10 min then removed and wells were dried. SRB dye was solubilized in 200 μl 10 mM Tris-Base and the absorbance was measured at 515 nm.

Real-time cell growth surveillance by cell electronic sensing

Hepatoma cells (2000cell/well in 150 μl) were inoculated into 96 E-Plates (Roche) containing 50 μl medium/well. Proliferation was monitored in real-time cell electronic sensing RT-CES (xCELLigence-Roche Applied Science), and the cell index (CI) was measured every 30 min for 24 h [16]. Next day, 100 μl medium was discarded and 50 μl fresh medium was added to each well. Inhibitors with indicated concentrations were applied to150 μl of medium. CI values were taken every 10 min for 4 h to visualize the fast drug response and then every 30 min to visualize the long-term drug response. Impedance measurements are displayed as Cell Index (CI) values and the effect of the inhibitors on cell growth is calculated as CI_{DRUG}/CI_{DMSO}. When the cells adhered to electrodes on the bottom of the wells, CI values increased in parallel to the cell growth due to the insulating properties of the cell membrane. As the number of cells covering the electrodes increases the electrical impedance (Z) increased ($Z_0=0$ --->$Z=Z_{cell}$).

Fluorescence microscopy

Cells were seeded at 3×10^4 cells/cm^2 on coverslips, allowed to grow for 24 h, as indicated in the figure legends, then washed twice with PBS and fixed with 4% paraformaldehyde. Subsequently, cells were washed once more with PBS and stained with 0.5 mg/ml DAPI. Preparations were dehydrated with increasing concentrations of ethanol and embedded in glycerol containing the antifading agent to be analyzed with Zeiss Axiophot epifluorescence microscope coupled with a Photometric Cool Snap CCD camera for image acquisition. The percentage of apoptotic cells was determined by counting fragmented nuclei in a minimum of 4 fields containing at least 150 cells. These experiments were performed in triplicate. As a positive control for apoptosis, cells were treated with 100 ng/ml Doxorubicine.

RT-PCR

Total RNA was isolated with NucleoSpin RNA II Kit (MN, Germany). cDNAs synthesized from 4 μg RNA with RevertAid kit (MBI Fermentas, Lithuania) were amplified by PCR with the primers (PTEN: intron-3-F_5′-AAAGATTCAGGCAATGTTTGTT-3′, intron-4-R_5′-TCTCACTCGATAATCTGGATGAC-3′, exon-4-F_5′-GACATTATGACACCGCCAAA-3′, exon-5-R_5′-TTCGTCCCTTTCCAGCTTTA-3′, exon-7-F_5′-CGACGGGAAGACAAGTTCAT-3′, exon-8-R_5′AGGTTTCCTCTGGTCCTGGT-3′, and GAPDH: F-5′-GGCTGAGAACGGGAAGCTTGTCAT-3′ and R-5′CAGCCTTCTCCATGGTGGTGAAGA-3′).

Results

Akt hyperphosphorylation in Mahlavu HCC cells

Hyperactivation of Akt was previously reported in HCC [17]. Therefore, we sought first to analyze the Akt levels and its serine-473 phosphorylation in hepatoma cells. Akt total amount seems comparable albeit a slight higher expression could be observed in Mahlavu cells when compared to Huh7 and HepG2 cells (Fig. 1a). In addition, significant Akt phosphorylation was detectable in Mahlavu cells, whereas only a slight Akt phosphorylation was detectable in HepG2 and Huh7 cells under native conditions.

Therefore, our initial observation suggested that the poorly differentiated Mahlavu cell line might have hyperactivated Akt signaling in comparison to the well-differentiated HCC

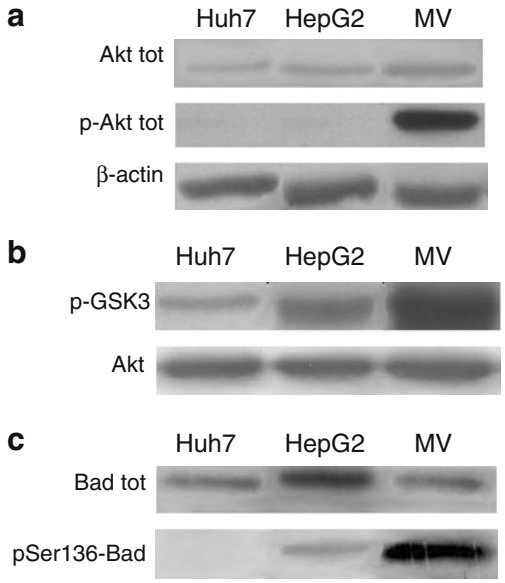

Fig. 1 Akt activity analysis in HCC cell lines. **a** Western blot analysis of untreated Huh7, HepG2, and Mahlavu cell lines, detected with anti Akt antibody or anti-p-Akt antibody. **b** Kinase assay on the fusion protein of GSK3α/β added to the reaction mixture as an exogenous substrate. As a control for equal loading, samples of immunoprecipitated Akt for the kinase assay were used. **c** Western blot analysis of untreated HCC cell lines was performed with anti-total BAD antibody or anti-p-BAD antibody. 20 μg of proteins were loaded for each lane. Data given here are representative of three independent experiments. SDS are less than 10%. The Mahlavu cell line displays high a Akt phosphorylation level and the highest enzymatic activity tested on both exogenous (GSK3α/β) and endogenous (BAD) substrate

cell lines; Huh7 and HepG2 [18]. To further assess whether Akt hyperphosphorylation in Mahlavu cells is related to the hyperactivation of its kinase enzymatic activity, we performed a kinase assay on the fusion protein GSK3 containing Akt target-phosphorylation residues. The results of this assay (Fig. 1b) showed the presence of a very low intrinsic activity in Huh7 cells, an intermediate activity in HepG2 cells but a very high kinase activity in Mahlavu cells. As a control for equal loading, samples of immunoprecipitated total Akt for the kinase assay were used. These data correlate very well with those obtained by western blot data on p-Akt (Fig. 1a).

We sought to further verify Akt pathway activation on a native target of Akt. To this end, we analyzed the phosphorylation status of BAD, a well-known protein downstream of Akt, whose phosphorylation prevents cells from undergoing apoptosis and confers them a proliferative advantage. The p-BAD antibody used in our study was specific to the Ser136 target of Akt kinase. In this way we excluded the possibility of BAD being phosphorylated by other kinases such as Erk-p90RSK kinase, which targets Ser122 [19]. pSer136-BAD was absent in Huh7 cells, and barely detectable in HepG2 cells, whereas a high level of pSer136-BAD was detected in Mahlavu cells (Fig. 1c).

Interestingly, total BAD protein levels were not equal in the cell lines analyzed although each lane contained 20 μg of total cell lysate, in particular Mahlavu showed lower BAD protein levels than HepG2 (Fig. 1c). However, we observed an intense phosphorylation by endogenous BAD in this cell line, which might explain the faint pSer136-BAD band in HepG2.

Determination of IC50 values for the HCC cells with SRB cytotoxicity assay

After the analysis of the hyperphosphorylation state of the Akt protein in well differentiated Huh7, HepG2 cells and poorly differentiated Mahlavu cells under native conditions, we decided to see the effect of PI3K inhibitors (LY294002, Wortmannin) and the specific Akt inhibitor (Inhibitor VIII) on this signaling pathway. Akt Inhibitor VIII selectively prevents Akt1 and Akt2 activity through pleckstrin homology (PH) domain [20, 21].

Initially we assessed their cytotoxicity by NCI-60 conventional Sulforhodamine B assay that was performed in quadruplicate and for 5 different concentrations following the NCI's drug screening protocol. The inhibitory effect of each drug of treatment was plotted (Fig. 2). IC50 values were calculated from these graphs for 24, 48, and 72 h (Fig. 2). IC50 values of LY294002 were 3.65 μM, 25.03 μM and 7.19 μM for 24 h and 3.75 μM, 5.82 μM and 8.71 μM for 72 h in Huh7, HepG2 and Mahlavu cell lines, respectively. For Wortmannin IC50 values in Huh7, HepG2 and Mahlavu cell lines were 26.07 μM, 29.23 μM and 20.19 μM for 24 h and 17.78 μM, 11.27 μM and 36.88 μM for 72 h, respectively. For 24 h, the IC50 values of Inhibitor VIII were 4.42 μM and 17.16 μM for Huh7 and HepG2, while there was not a significant inhibition observed in Mahlavu with NCI-60 assay. For 72 h, the IC50 values of Inhibitor VIII were 5.27 μM, 4.48 μM and 9.04 μM for Huh7, HepG2 and Mahlavu cells, respectively.

Real-time, dynamic monitoring of cell growth in HCC cells treated with the inhibitors

In order to further analyze if the growth inhibition of HCC cells is permanent or temporary, we used a novel cell surveillance system to monitor real-time, dynamic changes in cell growth based on the electrical impedance measurement technique. The RT-CES system allowed us to monitor the effects of LY294002, Wortmannin, and Inhibitor VIII on the hepatoma cells by a label-free and a real-time native approach. The proliferation and cytotoxicity of the inhibitors were followed by real-time through electronic cell sensors, integrated in the bottom of the 96 E-Plates in triplicates with 5 different concentrations (40 μM, 20 μM, 10 μM, 5 μM, 2.5 μM) (Fig. 3). When normalized to

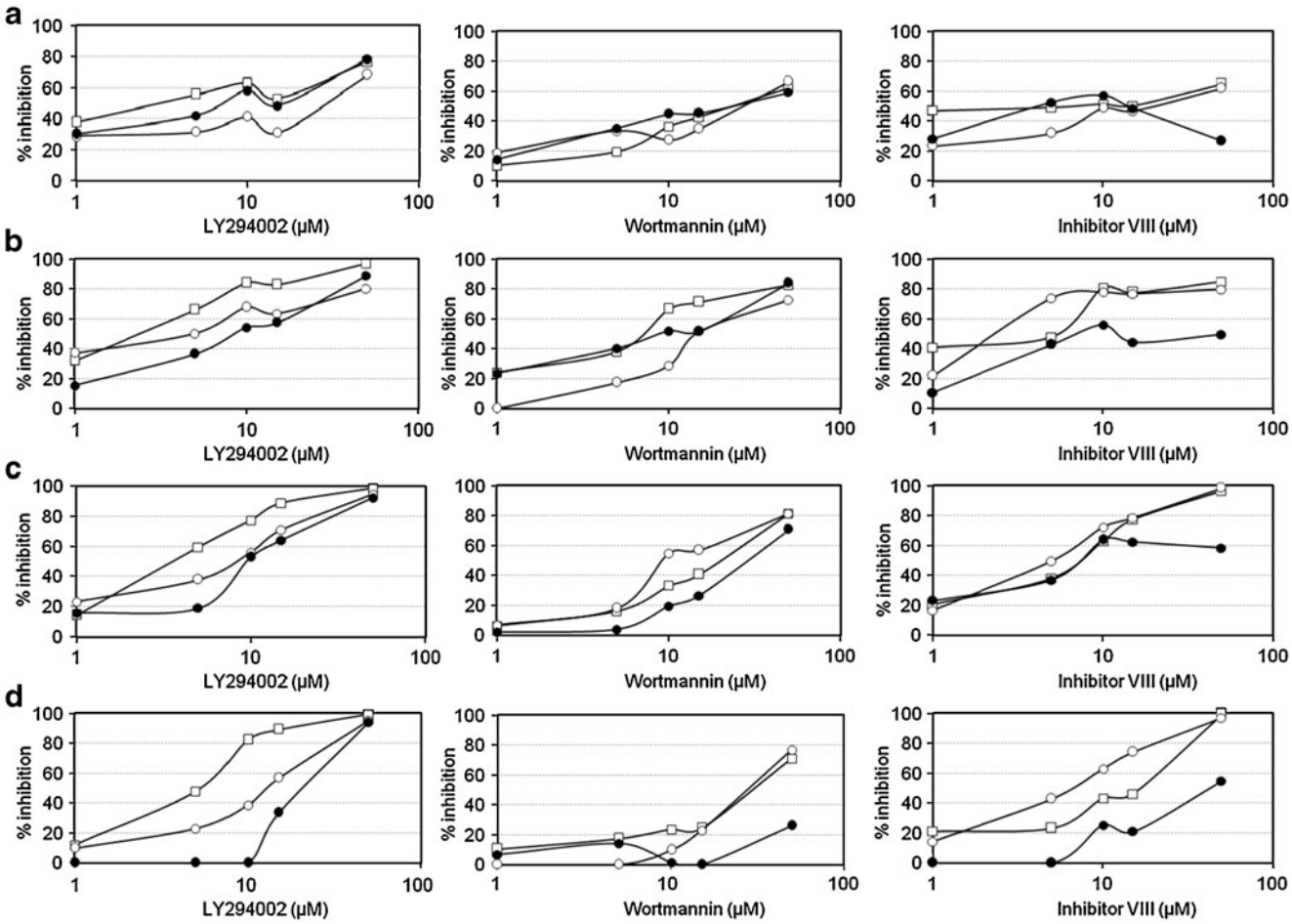

Fig. 2 Inhibitory effects of LY294002, Wortmannin and Akt Inhibitor VIII on HCC cell growth. % inhibition of cell growth after **a** 24, **b** 48, **c** 72 and **d** 96 hours of treatment with the inhibitors. Sulforhodamine B (SRB) colorimetric assay was performed in quadruplets with 5 different concentrations (50 μM, 15 μM, 10 μM, 5 μM, 1 μM) represented with error bars (Supplementary Figs. 1–3). The growth inhibitory effect for shorter exposure is relevant also for low concentrations. At longer exposure times growth inhibition requires higher drug concentrations. IC50 values were calculated based on the logarithmic regression line fitted on the % inhibition vs. log (concentration) graph, Huh7 (—□—), HepG2 (—○—), Mahlavu (—●—)

DMSO treated cell proliferation curves the cell growth plots demonstrated the concentration- and time-dependent cytotoxic effect of the inhibitors. In addition to provide also a visual demonstration of the effects of these drugs on these cells we treated cells with inhibitors and show their morphological changes by light microscope images at 24 and 48 hours in parallel with the RT-CES experiments with IC50 of 24 hours concentrations (Fig. 3b).

High dose treatment of LY294002 (40 μM) suppressed cell growth permanently after 8 h and continuing up to 84 h in Huh7 and Mahlavu cell lines. Lower doses (5 μM, 2.5 μM) of LY294002 had a minor effect on cell growth for up to 48 h but then the cells resumed growth, especially in the case of the Mahlavu cell line. With Inhibitor VIII treatment, cells responded similarly as to LY294002 exposure although Inhibitor VIII appeared more effective at short exposure times. Wortmannin treatment was effective in inhibiting cell growth only for about 24 h and then the cells gradually resumed normal growth. This real-time dynamic continuous analysis of cell growth and toxicity was essential to determine the optimal time points for performing biochemical endpoint assays. The continuous, dynamic analysis of cell growth of LY294002, Wortmannin and Akt Inhibitor VIII treated Huh7 and Mahlavu cells supported the time- and concentration-dependent effects of the three inhibitors on HCC cells as shown in Fig. 2.

We also analyzed Akt enzyme activity in the presence of inhibitors. The IC50 values of 72 h for LY294002, Wortmannin and Akt Inhibitor VIII were used to assess the effects of drug treatments on Akt kinase activity in HCC cell lines by a specific kinase assay using the fusion protein fusion protein of GSK3α/β as substrate similarly to that of Fig. 1b. Our results demonstrated the inhibitory effect of the three drugs on the kinase activity of the Akt protein, when compared to the kinase assay under native conditions. In all cases no Akt phosphorylation activity was

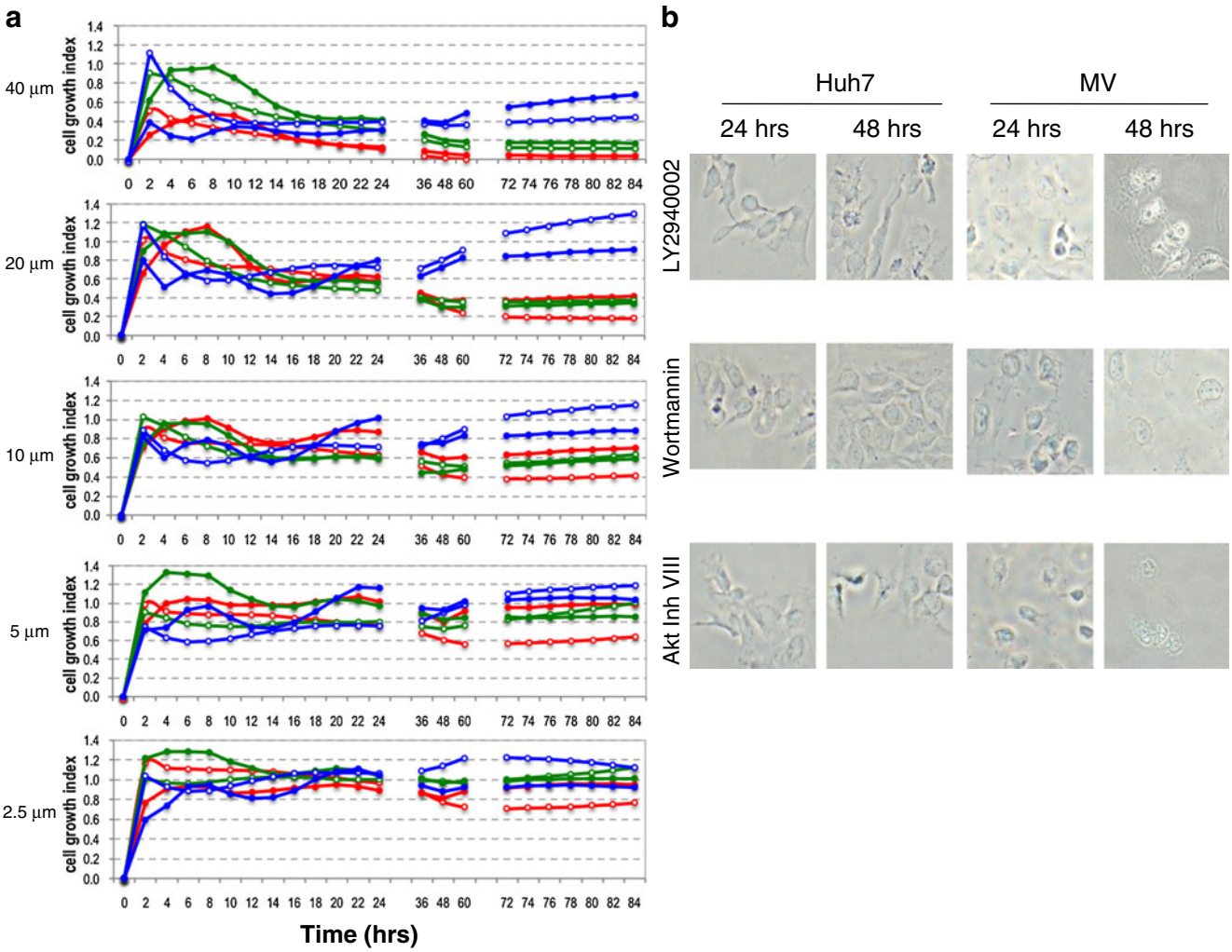

Fig. 3 Cell growth of LY294002, Wortmannin and Akt Inhibitor VIII treated Huh7 and Mahlavu cells. **a** Cell growth is assessed with the xCELLigence system that measures electrical impedance across micro-electrodes integrated on the bottom of tissue culture E-96 plates. Impedance measurements are displayed as Cell Index (CI) values, providing real-time quantitative information on cell growth. The effect of the inhibitors on cell growth is calculated as CI_{DRUG}/CI_{DMSO}. The cell growth assay was performed in triplicates with 5 different concentrations 40 µM, 20 µM, 10 µM, 5 µM, and 2.5 µM. Huh7-LY294002 (), Huh7-Akt Inhibitor VIII (), Huh7-Wortmannin (), Mahlavu-LY294002 (), Mahlavu-Akt Inhibitor VIII (), Mahlavu-Wortmannin (). **b** Analysis of apoptosis associated morphological changes with light microscopy. Huh7 and Mahlavu cells were treated with the indicated inhibitors at 24 and 48 hours. Huh7 cells : LY294002 (4 µM), Wortmannin (26 µM), Akt Inhibitor VIII (4.5 µM) ; Mahlavu cells : LY294002 (7 µM), Wortmannin (20 µM), Akt Inhibitor VIII (10 µM). 20X pictures were taken with OLYMPUS CKX41 microscope with DP72 camera

detected on the fusion protein of GSK3α/β (data not shown). These data indicate a very low Akt activity in each cell line, evidence of a significant inhibition of the pathway by these inhibitory molecules in HCC cells.

Cytotoxic effect of drugs on HCC cells through apoptosis

It is a well-documented fact that the Akt pathway has an important anti-apoptotic role in different cells [22, 23]. Morphological changes specific to apoptosis can be observed quite early after apoptotic stimuli [24, 25]. In order to see the morphological changes in Huh7, HepG2 and Mahlavu cells after treatment with each drug, cells were treated with inhibitors for 24 and 48 h. Each drug was used at its IC50 value obtained after 24 h of treatment. Apoptotic cells usually exhibit extensive DNA cleavage during the early stages of this controlled cell death mechanism. Cleavage may produce double-stranded, low molecular weight DNA fragments as well as single-stranded high molecular weight DNA fragments that manifests themselves as condensed aberrant nuclei, as shown by DAPI (Fig. 4) and the Hoechst 33258 stain (data not shown). This observation demonstrated that those cells displayed the type of cell death that is specific to apoptosis.

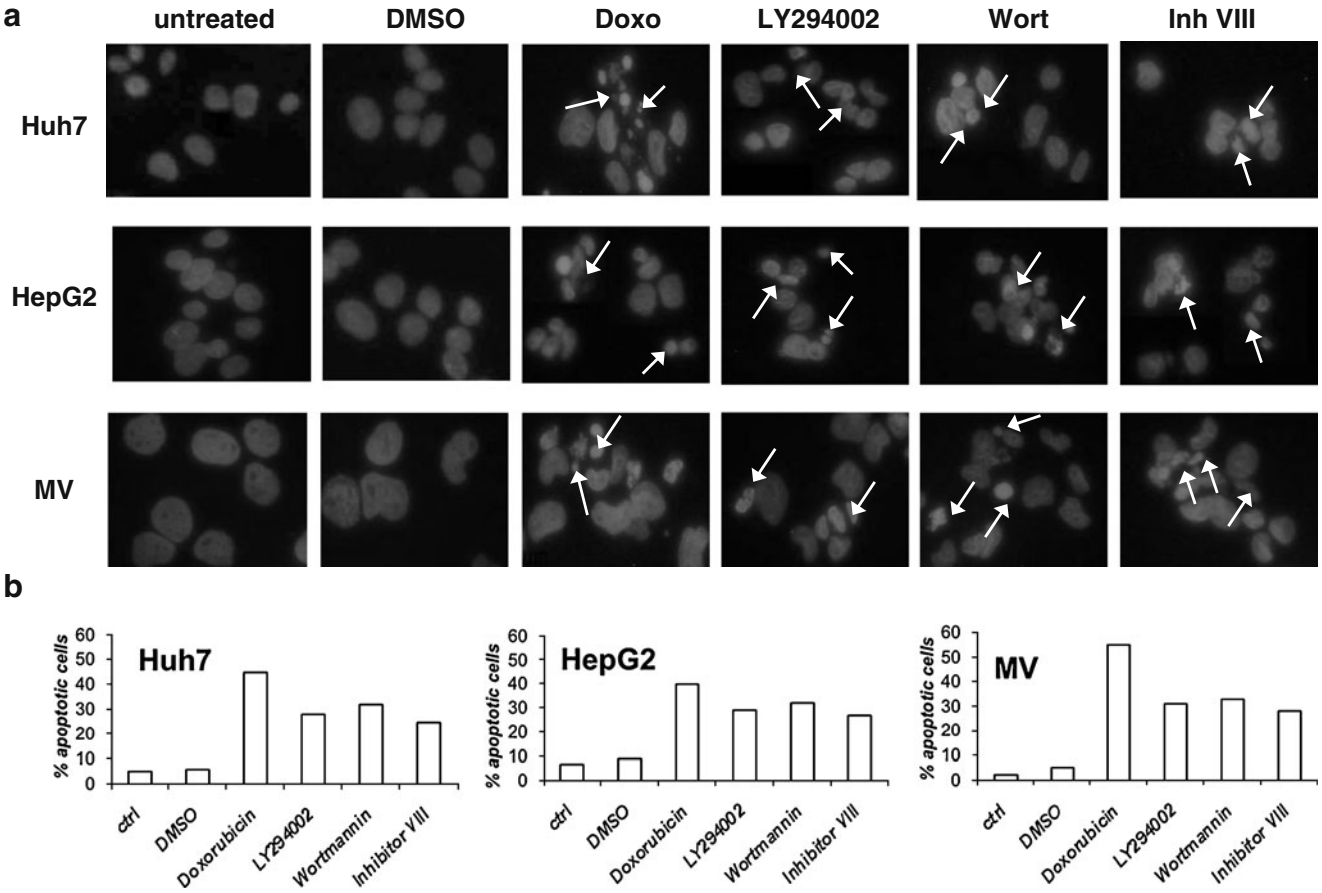

Fig. 4 DAPI staining showing the aberrant nuclear DNA due to the apoptotic cells with condensed nuclei (*white arrows*) in the presence of inhibitors with IC50 concentrations. **a** The pro-apoptotic effect of Akt pathway inhibitors on the morphology of the nuclear chromatin in HCC cells. Cells were treated for 24 h with the IC50 values **(**Huh7 : LY294002 (4 μM), Wortmannin (26 μM), Akt Inhibitor VIII (4.5 μM); HepG2 : LY294002 (25 μM), Wortmannin (29 μM), Akt Inhibitor VIII (18 μM); Mahlavu : LY294002 (7 μM), Wortmannin (20 μM), Akt Inhibitor VIII (10 μM)), then fixed and stained with DAPI. No changes were induced by DMSO. All samples treated with the positive control, Doxorubicine (100 ng/ml) showed evident apoptotic nuclei. Well markable, even if less present, are apoptotic nuclei after apoptosis induction with each drug. The results were from one experiment representative of three experiments. Bar=10 μm **b** Apoptotic cells were quantified by counting a minimum of 4 fields containing at least 150 cells. The results are presented as the mean of three independent experiments. Doxorubicine, an inhibitor of enzyme topoisomerase II progression by intercalation of DNA, induced a marked percentage of apoptosis. The three inhibitors used in this study within each cell line, gave similar results. SD was less then 10%

The pro-apoptotic effect of the drugs was assessed by counting aberrant nuclei in DAPI stained cells. The morphological features of apoptosis, i.e. condensation of chromatin and fragmentation of the nucleus, were examined. Control cells showed rounded and homogeneous nuclei, whereas drug treated-cells showed condensed and fragmented nuclei (Fig. 5a). The percentage of apoptosis ranged from 32% to 25% in Huh7, from 32% to 27% in HepG2 and from 35% to 28% in Mahlavu, (Fig. 4b).

In order to further clarify the type of cell death mechanism and the morphological changes that we observe in Figs. 3b, 4a, in the presence of the inhibitors as apoptosis, we performed Poly ADP-ribosyl polymerase (PARP) cleavage analysis by western blot. Huh7, HepG2 and Mahlavu cells were treated with each drug at the 24hours-IC50. PARP is typically cleaved from 113 kDa to 89 and 24 kDa fragments by caspase-3 during apoptosis. Although cleaved PARP is also detected during necrosis, the cleaved product's molecular size is different (50 kDa). As shown in Fig. 5, the cleaved band (89 kDa) is due to apoptosis, not necrosis [26]. Our observations clearly demonstrated that Akt pathway inhibitors had an apoptosis-dependent cytotoxic effect on HCC cell lines.

Comparative analysis of PTEN in HCC cells

With the aim of identifying differential responses of HCC cells to Akt pathway inhibitors, we further investigated PTEN, another pathway related molecule. PTEN protein expression in HCC cell lines exhibited differential expres-

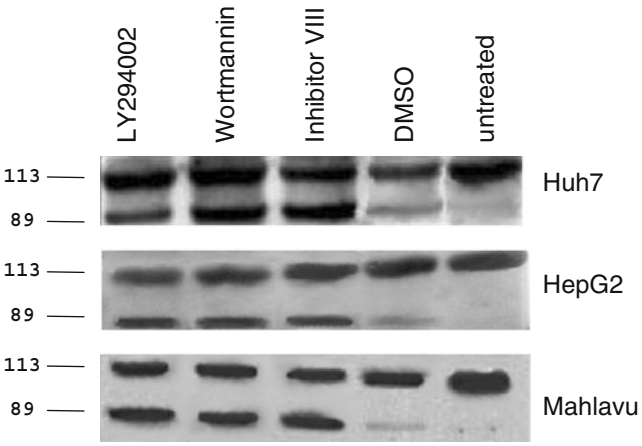

Fig. 5 Investigation of apoptotic cell death in the presence of Akt pathway inhibitors. Apoptosis activation was detected by means of PARP cleavage. The antibodies used recognize both the intact form (113 KDa) and the cleaved one (89 KDa). In each lane 20 μg proteins were loaded. . Almost no cleavage is observable in control and DMSO-treated samples. An evident PARP cleavage is induced by the three inhibitors used. Each cell line induced similar PARP cleavage. Data were representative of three independent experiments

sion patterns, ranging from marked expression in the Huh7 and HepG2 cell lines, to the absence of PTEN expression in Mahlavu cell line. The absence of PTEN protein expression was in correlation with the hyperphosphorylation of Akt, higher kinase activity on exogenous GSK3α/β fusion protein and on endogenous BAD protein in Mahlavu cell line. In correlation with the absence of PTEN protein expression, the Mahlavu cell line had mRNA expression with a partial deletion in the PTEN gene in exon 4 (Fig. 6), which may explain the lack of protein that results in the hyperactivation of the Akt protein in this cell line.

Discussion

In this study, we have shown hyperactivation of the Akt protein in hepatoma cell lines and apoptosis induction in time- and dose- dependent manners after treatment with three specific inhibitors of the PI3K/Akt pathway. The PI3K/Akt signaling pathway plays a significant role in carcinogenesis and drug resistance in different types of cancer including HCC, making Akt a potential target for cancer treatment [28, 29].

Tumors with activated PI3K/Akt signaling have been shown to become more aggressive, and Akt pathway activation has been identified as a significant risk factor for early disease recurrence and poor prognosis in HCC patients [30, 31]. Activated Akt correlates also with local metastasis of tumor cells from the primary liver cancer into the circulatory system and the survival of the circulating cells without cell-substratum interaction [32], showing the significance of this hyperactivated pathway not only in liver tumor aggressiveness but also in tumor diffusion and survival in different environments. Therefore we initially examined total Akt protein and native p-Akt levels in HCC cell lines. Mahlavu cells were previously reported to be poorly differentiated when compared to the well-differentiated "hepatocyte-like" Huh7 and HepG2 cells [18]. Although the cell lines included in this study showed similar total Akt protein expression (Fig. 1a), only Mahlavu cells displayed hyperphosphorylated Akt protein (Fig. 1a), which was determined by anti-p473Ser-Akt antibodies, because Ser473 Akt phosphorylation is a requirement for full Akt enzyme activity [33]. In Mahlavu cells, in parallel to the hyperphosphorylation of Akt, we also observed a lack of PTEN protein expression (Fig. 6) and increased phosphor-

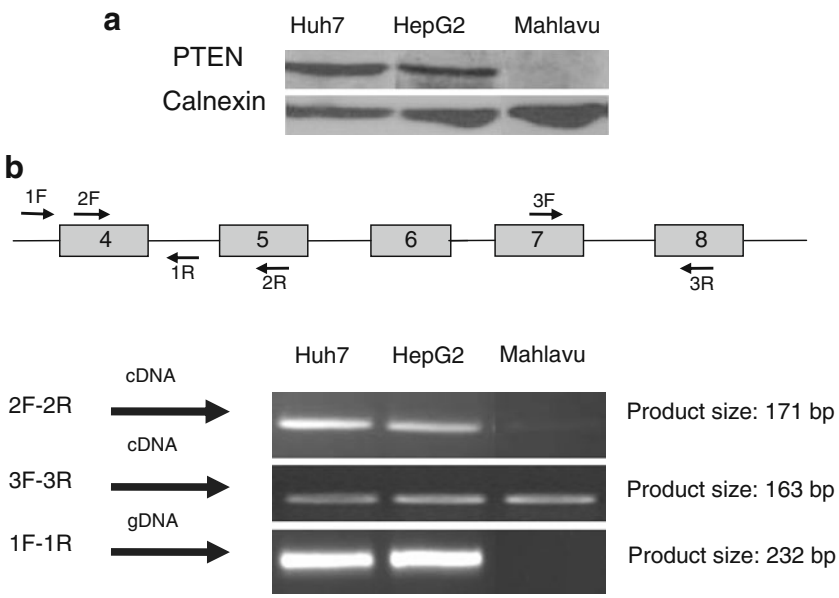

Fig. 6 Differential expression of the PTEN gene in human HCC cell lines. **a** Whole-cell lysates (40 μg) were analyzed by Western blotting using anti-PTEN antibody. Mahlavu cell line has no PTEN expression. **b** PCR analysis of PTEN gene in HCC cell lines. Figure describes the loss of PTEN gene fragment. The gene fragment that is lacking is located within exon 4 and 5

ylation of the downstream protein Bad on Ser136 and of the exogenous GSK3 substrate (Fig. 1b and c).

The activation of PI3K/Akt signaling frequently related to PTEN mutation has also been observed in nearly 50% of HCC [34], suggesting the importance of this pathway, since tumors with hyperactive Akt due to PTEN loss depend on hyperactivated Akt signaling for growth and survival [10]. Indeed, our results support the observations that a PTEN deficient cell line Mahlavu has hyperactivated Akt protein. Moreover Mahlavu has the higher IC50 values for Wortmannin than well differentiated Huh7 and HepG2 cell lines.

The great majority of protein kinase inhibitors that have been developed, bind at or near the ATP binding site [35]. These compounds were recommended for use in a concentration range of 0,1 to 100 μM to assess the roles of particular protein kinases. Depending on concentration, kinase inhibitors may act as multi-kinase inhibitors. Therefore in our study we analyzed the PI3K/Akt signaling inhibitors with concentrations between 40 μM–2.5 μM (Figs. 2 and 3) in order to identify their specific IC50 values on hepatoma cell lines. We think that with the concentration we used LY294002 and Wortmannin exhibit their cytotoxic activity through binding to the proximity of the active sites of their target kinases. Structural analysis of the p110γ isoform of PI3K in the presence of LY294002 demonstrated that this inhibitor binds to the active site. Cell death induced by LY294002 is through GSK3β activity, which is also demonstrated in the presence of lithium, a known inhibitor of GSK3β [36, 37]. Consistent with the structural similarity between the PI3K and mTOR kinase domains, LY294002 and Wortmannin act on both of these kinases with similar IC50 values [38]. Both PI3K and mTORC2 are the upstream proteins of the Akt pathway. Therefore, we focused also on the downstream analysis of Akt protein activation/inhibition regardless of the direct targets of LY294002 and Wortmannin in HCC cells. To stress the importance of Akt pathway signaling inhibition as a potential therapeutic target in liver cancer, we analyzed the effects of the selective Akt inhibitor, Akt Inhibitor VIII on HCC cells [20, 21].

We applied two different cytotoxicity assays, conventional NCI-60 method and novel RT-CES system. Both assays resulted in similar IC50 values for 24, 48, and 72 h for the specific PI3K/Akt signaling inhibitors LY294002, Wortmannin, and Akt inhibitor VIII, although it is possible to calculate IC50 for each time point with RT-CES. As expected, we were able to demonstrate that all three inhibitors had cytotoxic activity. At 24 h all three cells had comparable IC50s but with longer treatment times Mahlavu cells displayed higher IC50s when compared to Huh7 and HepG2 cells. RT-CES analysis demonstrated that normal cell growth has a cell index (CI) of around 1.2 (Fig. 3a). 20 μM inhibitor treatment did not influence the cell proliferation during the initial 10–16 h. The cytotoxic effect of the inhibitors became established toward the end of the 24 h (Fig. 3a, 40–10 μM) as it can be observed by the CI of 0.5. Between 36 h and to 60 h RT-CES data demonstrated whether they inhibit cell proliferation irreversibly or whether cells can survive afterwards. In the case of LY294002 and Akt inhibitor VIII, CI approached to 0.2 at the 60th hour meaning almost no cells attached to the bottom of the cell culture plates to form colonies. We confirmed this data in parallel experiments by direct light microscopy visualization of the cells at 24 and 48 h (Fig. 3b). Cells treated with Wortmannin displayed a similar growth curve with CI during first 24 h to that of LY294002 and Akt inhibitor VIII did. However starting from 36 h both Huh7 and Mahlavu cells continued to proliferate and expanded to cover the bottom of the E-plate parallel to the DMSO treated control cells even with very high (40 μM) concentrations. We confirmed again by microscopy that the cells presented a healthy morphology (Fig. 3b).

Continuous very low Cell Index data (0.2–0.3) with LY294002 and Akt inhibitor VIII treatments on the hepatoma cells were the indications of apoptotic cell death. In addition direct light microscopy visualization of the cell morphology showed that all the inhibitors induced apoptosis on hepatoma cells. From the above evidence the nature of the cell death exhibited in the presence of the PI3K/Akt signaling inhibitors LY294002, Wortmannin, and Akt inhibitor VIII was characterized as apoptosis (Figs. 4 and 5).

The three drugs, generated a PARP cleavage process on the HCC cell lines after being administered (Fig. 5). As shown above, the drugs appear to have similar apoptotic effects in all the cell lines tested. In addition, since PI3K-Class IIIs control autophagic proteolysis, we examined the possibility that the cytotoxic effect of these inhibitors might be through autophagy [27]. After 48 h of incubation with the three inhibitors we performed western blot analysis of autophagy related proteins BECN1 and p62 but did not observe any alterations that could be attributed to autophagy (data not shown).

This study suggests that targeting the PI3K/Akt signaling pathway provides a promising strategy for designing molecular targeted therapy in the case of solid tumors, especially HCC. Our data also suggest that PI3K/Akt activation status serve as a biomarker for identifying candidate patients for treatment with inhibitors of PI3K and/or of its downstream targets. However, it should be noted that drug transporters or IAPs (Inhibitors of Apoptosis Proteins) could contribute to the therapeutic resistance. Likewise, transcription factors, such as NF-κB, can up-regulate transporters like MRP2 to induce multidrug resistance in HCC [39]. Furthermore, we have previously

shown that during liver tumorigenesis HCC cells develop a "survivor phenotype" independent of the cause of oncogenic transformation under oxidative stress conditions [40].

It may also be important to raise questions about the stability of the drugs for longer treatments. We performed experiments, by monitoring cell growth real time, that demonstrated that when drug concentration increases, growth inhibition lasts longer. This observation could be due to a lower a decay rate of active drug molecule concentration. Our results obtained by the three PI3K/Akt pathway inhibitors used clearly demonstrated that the Akt pathway can still be a target when Akt and BAD are hyperphosphorylated and the PTEN protein is impaired, as we show in the Mahlavu cell line. In treatment, chemotherapeutic agents are usually given in a protocol with repeating dosages to target resistant cell populations.

Tumors with hyperactive Akt due to PTEN loss depend on Akt signaling for growth and survival [10]. Activated Akt pathway confers resistance to cancer therapy, making Akt a promising target for cancer treatment [34]. Increasing knowledge in the molecular mechanisms underlying hepatocarcinogenesis and the advent of molecular targeted therapies provide a promising treatment approach for HCC patients. Novel therapeutic targets, molecular oncogenic mechanisms and signaling cascades responsible for tumor growth should be investigated together with potential chemotherapeutic agents to improve clinical efficacy.

Acknowledgement We are indebted to Prof A. Esen (Virgina Tech) and Ms. R. Nelson for editing the English of the final version of our manuscript. This work was supported by The Scientific and Technical Research Council of Turkey, TUBITAK (project # 106 S359), the KANILTEK project Bilkent University local funds and MAE 2008, Fondazione CARIFE, Italian MIUR Cofin 2005, Fondazione CARICENTO, local funds of Ferrara University for Stamina Project (to SC), LMN and DE.

References

1. McGlynn KA, Tsao L, Hsing AW, Devesa SS, Fraumeni JF Jr (2001) International trends and patterns of primary liver cancer. Int J Cancer 94:290–296. doi:10.1002/ijc.1456
2. Ozturk N, Erdal E, Mumcuoglu M, Akcali KC, Yalcin O, Senturk S, Arslan-Ergul A, Gur B, Yulug I, Cetin-Atalay R, Yakicier C, Yagci T, Tez M, Ozturk M (2006) Reprogramming of replicative senescence in hepatocellular carcinoma-derived cells. Proc Natl Acad Sci USA 103:2178–2183. doi:10.1073/pnas.0510877103
3. Osaki M, Oshimura M, Ito H (2004) PI3K-Akt pathway: its functions and alterations in human cancer. Apoptosis 9:667–676. doi:10.1023/B:APPT.0000045801.15585.dd
4. Llovet JM, Ricci S, Mazzaferro V, Hilgard P, Gane E et al (2008) Sorafenib in advanced hepatocellular carcinoma. N Engl J Med 359:378–390. doi:10.1056/NEJMoa0708857
5. Engelman JA (2009) Targeting PI3K signalling in cancer: opportunities, challenges and limitations. Nat Rev Cancer 9:550–562. doi:10.1038/nrc2664
6. Liu P, Cheng H, Roberts TM, Zhao JJ (2009) Targeting the phosphoinositide 3-kinase pathway in cancer. Nat Rev Drug Discov 8:627–644. doi:10.1038/nrd2926
7. Tokunaga E, Oki E, Egashira A, Sadanaga N, Morita M, Kakeji Y, Maehara Y (2008) Deregulation of the Akt pathway in human cancer. Curr Cancer Drug Targets 8:27–36
8. Carnero A, Blanco-Aparicio C, Renner O, Link W, Leal JF (2008) The PTEN/PI3K/AKT signalling pathway in cancer, therapeutic implications. Curr Cancer Drug Targets 8:187–198
9. Hanada M, Feng J, Hemmings BA (2004) Structure, regulation and function of PKB/AKT–a major therapeutic target. Biochim Biophys Acta 1697:3–16. doi:10.1016/j.bbapap.2003.11.009
10. Salvesen HB, Stefansson I, Kretzschmar EI, Gruber P, MacDonald ND, Ryan A, Jacobs IJ, Akslen LA, Das S (2004) Significance of PTEN alterations in endometrial carcinoma: a population-based study of mutations, promoter methylation and PTEN protein expression. Int J Oncol 25:1615–1623
11. Xu G, Zhang W, Bertram P, Zheng XF, McLeod H (2004) Pharmacogenomic profiling of the PI3K/PTEN-AKT-mTOR pathway in common human tumors. Int J Oncol 24:893–900
12. Arcaro A, Guerreiro AS (2007) The phosphoinositide 3-kinase pathway in human cancer: genetic alterations and therapeutic implications. Curr Genomics 8:271–306. doi:10.2174/138920207782446160
13. Ozturk M EE, Ozturk N, Cetin-Atalay R and Irmak B (2005) Molecular Biology of Liver Cancer. In: RA M. Encyclopedia of Molecular Cell Biology and Molecular Medicine, Wiley-VCH, 2ed, vol. 7:323–335
14. Missiroli S, Etro D, Buontempo F, Ye K, Capitani S, Neri LM (2009) Nuclear translocation of active AKT is required for erythroid differentiation in erythropoietin treated K562 erythroleukemia cells. Int J Biochem Cell Biol 41(3):570–577
15. Monks A, Scudiero D, Skehan P, Shoemaker R, Paull K, Vistica D, Hose C, Langley J, Cronise P, Vaigro-Wolff A et al (1991) Feasibility of a high-flux anticancer drug screen using a diverse panel of cultured human tumor cell lines. J Natl Cancer Inst 83:757–766
16. Kirstein SL, Atienza JM, Xi B, Zhu J, Yu N, Wang X, Xu X, Abassi YA (2006) Live cell quality control and utility of real-time cell electronic sensing for assay development. Assay Drug Dev Technol 4(5):545–553
17. LoPiccolo J, Granville CA, Gills JJ, Dennis PA (2007) Targeting Akt in cancer therapy. Anticancer Drugs 18(8):861–874, Review
18. Sayan B, Tolga Emre NC, Irmak MB, Ozturk M, Cetin-Atalay R (2009) Nuclear exclusion of p33ING1b tumor suppressor protein: explored in HCC cells using a new highly specific antibody. Hybridoma 28:1–6. doi:10.1089/hyb.2008.0058
19. del Peso L, Gonzalez-Garcia M, Page C, Herrera R, Nunez G (1997) Interleukin-3-induced phosphorylation of BAD through the protein kinase Akt. Science 278:687–689
20. Barnett SF, Defeo-Jones D, Fu S, Hancock PJ, Haskell KM et al (2005) Identification and characterization of pleckstrin-homology-domain-dependent and isoenzyme-specific Akt inhibitors. Biochem J 385:399–408. doi:10.1042/BJ20041140
21. Zhao Z, Leister WH, Robinson RG, Barnett SF, Defeo-Jones D, Jones RE, Hartman GD, Huff JR, Huber HE, Duggan ME, Lindsley CW (2005) Discovery of 2, 3, 5-trisubstituted pyridine derivatives as potent Akt1 and Akt2 dual inhibitors. Bioorg Med Chem Lett 15:905–909. doi:10.1016/j.bmcl.2004.12.062
22. Manning BD, Cantley LC (2007) AKT/PKB signaling: navigating downstream. Cell 129:1261–1274. doi:10.1016/j.cell.2007.06.009
23. Fabregat I (2009) Dysregulation of apoptosis in hepatocellular carcinoma cells. World J Gastroenterol 15:513–520
24. Kim MJ, Oh SJ, Park SH, Kang HJ, Won MH, Kang TC, Hwang IK, Park JB, Kim JI, Kim J, Lee JY (2007) Hypoxia-induced cell

death of HepG2 cells involves a necrotic cell death mediated by calpain. Apoptosis 12:707–718. doi:10.1007/s10495-006-0002-3
25. Messam CA, Pittman RN (1998) Asynchrony and commitment to die during apoptosis. Exp Cell Res 238:389–398. doi:10.1006/excr.1997.3845
26. Gobeil S, Boucher CC, Nadeau D, Poirier GG (2001) Characterization of the necrotic cleavage of poly(ADP-ribose) polymerase (PARP-1): implication of lysosomal proteases. Cell Death Differ 8:588–594. doi:10.1038/sj.cdd.4400851
27. Blommaart EF, Krause U, Schellens JP, Vreeling-Sindelarova H, Meijer AJ (1997) The phosphatidylinositol 3-kinase inhibitors wortmannin and LY294002 inhibit autophagy in isolated rat hepatocytes. Eur J Biochem 243:240–246
28. Cully M, You H, Levine AJ, Mak TW (2006) Beyond PTEN mutations: the PI3K pathway as an integrator of multiple inputs during tumorigenesis. Nat Rev Cancer 6(3):184–192, Review
29. Schmitz KJ, Wohlschlaeger J, Lang H, Sotiropoulos GC, Malago M et al (2008) Activation of the ERK and AKT signalling pathway predicts poor prognosis in hepatocellular carcinoma and ERK activation in cancer tissue is associated with hepatitis C virus infection. J Hepatol 48:83–90. doi:10.1016/j.jhep.2007.08.018
30. Nakanishi K, Sakamoto M, Yamasaki S, Todo S, Hirohashi S (2005) Akt phosphorylation is a risk factor for early disease recurrence and poor prognosis in hepatocellular carcinoma. Cancer 103(2):307–312
31. Hu TH, Huang CC, Lin PR, Chang HW, Ger LP, Lin YW, Changchien CS, Lee CM, Tai MH (2003) Expression and prognostic role of tumor suppressor gene PTEN/MMAC1/TEP1 in hepatocellular carcinoma. Cancer 97(8):1929–1940
32. Boyault S, Rickman DS, de Reynies A, Balabaud C, Rebouissou S, Jeannot E, Herault A, Saric J, Belghiti J, Franco D (2007) (2008) Transcriptome classification of HCC is related to gene alterations and to new therapeutic targets. Hepatology 45:42–52
33. Recher C, Dos Santos C, Demur C, Payrastre B (2005) mTOR, a new therapeutic target in acute myeloid leukemia. Cell Cycle 4:1540–1549
34. Lindsley CW, Barnett SF, Layton ME, Bilodeau MT (2008) The PI3K/Akt pathway: recent progress in the development of ATP-competitive and allosteric Akt kinase inhibitors. Curr Cancer Drug Targets 8:7–18
35. Bain J, Plater L, Elliott M, Shpiro N, Hastie CJ, McLauchlan H, Klevernic I, Arthur JS, Alessi DR, Cohen P (2007) The selectivity of protein kinase inhibitors: a further update. Biochem J 408:297–315. doi:10.1042/BJ20070797
36. Beurel E, Kornprobst M, Blivet-Van Eggelpoel MJ, Cadoret A, Capeau J, Desbois-Mouthon C (2005) GSK-3beta reactivation with LY294002 sensitizes hepatoma cells to chemotherapy-induced apoptosis. Int J Oncol 27:215–222
37. Erdal E, Ozturk N, Cagatay T, Eksioglu-Demiralp E, Ozturk M (2005) Lithium-mediated downregulation of PKB/Akt and cyclin E with growth inhibition in hepatocellular carcinoma cells. Int J Cancer 115:903–910. doi:10.1002/ijc.20972
38. Ballou LM, Selinger ES, Choi JY, Drueckhammer DG, Lin RZ (2007) Inhibition of mammalian target of rapamycin signaling by 2-(morpholin-1-yl)pyrimido[2, 1-alpha]isoquinolin-4-one. J Biol Chem 282:24463–24470. doi:10.1074/jbc.M704741200
39. Okamoto T, Sanda T, Asamitsu K (2007) NF-kappa B signaling and carcinogenesis. Curr Pharm Des 13:447–462
40. Irmak MB, Ince G, Ozturk M, Cetin-Atalay R (2003) Acquired tolerance of hepatocellular carcinoma cells to selenium deficiency: a selective survival mechanism? Cancer Res 63:6707–6715

OPEN ACCESS Freely available online

PLOS ONE

Identification of Novel Reference Genes Based on MeSH Categories

Tulin Ersahin[1☯], Levent Carkacioglu[2☯], Tolga Can[2], Ozlen Konu[1], Volkan Atalay[2], Rengul Cetin-Atalay[1]*

1 Department of Molecular Biology and Genetics, Bilkent University, Ankara, Turkey, **2** Computer Engineering Department, Middle East Technical University, Ankara, Turkey

Abstract

Transcriptome experiments are performed to assess protein abundance through mRNA expression analysis. Expression levels of genes vary depending on the experimental conditions and the cell response. Transcriptome data must be diverse and yet comparable in reference to stably expressed genes, even if they are generated from different experiments on the same biological context from various laboratories. In this study, expression patterns of 9090 microarray samples grouped into 381 NCBI-GEO datasets were investigated to identify novel candidate reference genes using randomizations and Receiver Operating Characteristic (ROC) curves. The analysis demonstrated that cell type specific reference gene sets display less variability than a united set for all tissues. Therefore, constitutively and stably expressed, origin specific novel reference gene sets were identified based on their coefficient of variation and percentage of occurrence in all GEO datasets, which were classified using Medical Subject Headings (MeSH). A large number of MeSH grouped reference gene lists are presented as novel tissue specific reference gene lists. The most commonly observed 17 genes in these sets were compared for their expression in 8 hepatocellular, 5 breast and 3 colon carcinoma cells by RT-qPCR to verify tissue specificity. Indeed, commonly used housekeeping genes *GAPDH*, *Actin* and *EEF2* had tissue specific variations, whereas several ribosomal genes were among the most stably expressed genes *in vitro*. Our results confirm that two or more reference genes should be used in combination for differential expression analysis of large-scale data obtained from microarray or next generation sequencing studies. Therefore context dependent reference gene sets, as presented in this study, are required for normalization of expression data from diverse technological backgrounds.

Citation: Ersahin T, Carkacioglu L, Can T, Konu O, Atalay V, et al. (2014) Identification of Novel Reference Genes Based on MeSH Categories. PLoS ONE 9(3): e93341. doi:10.1371/journal.pone.0093341

Editor: Christian Schönbach, Nazarbayev University, Kazakhstan

Received October 10, 2013; **Accepted** March 3, 2014; **Published** March 28, 2014

Funding: This work was supported by grants from The Scientific and Technical Research Council of Turkey, (TUBITAK- project #110S338), Bilkent University and Middle East Technical University local funds. The funders had no role in study design, data collection and analysis, decision to publish, or preparation of the manuscript.

Competing Interests: The authors have declared that no competing interests exist.

* E-mail: rengul@bilkent.edu.tr

☯ These authors contributed equally to this work.

Introduction

During the last decade, there has been remarkable progress in the identification of human cells' transcriptome blueprint through small or large-scale quantitative gene expression studies. Since the gene expression is the major determinant of the protein abundance in the cell, transcriptome analysis experiments have been widely applied to reveal the molecular mechanisms of various cellular conditions. Depending on the cell fate, expression levels of genes vary. Although it seems straightforward to assess these variations through Real Time quantitative PCR or microarrays, there is a continuing and confusing debate on what basis these variations should be considered as deviations from normal physiology. Therefore, there is a need for compilation and comprehensive analysis of a gene of interest across several experiments from different sources. A gene's expression data must be scaled in a comparable platform. Various normalization methods are available to scale these data within the same experiment, yet it becomes problematic to compare arrays of different sources without using references.

Although most genes show variable expression depending on cellular context, tissue of origin or treatment conditions, some genes are constitutively expressed in all cells in all conditions. These constitutively expressed genes are required for the maintenance of the basal cellular functions such as metabolism, gene expression, protein synthesis and cell signaling [1,2]. These genes, called housekeeping genes, are generally assumed to have expression levels unaffected by tissue of origin or experimental condition. Therefore, they are widely used as reference genes for normalization of expression data. However, recent studies indicated that several widely used housekeeping genes have altered expressions under different experimental conditions [3–10]. Most of these studies focused on finding appropriate genes for normalization in individual cancer types. Yet, even the most commonly used reference genes (*ACTB*, *GAPDH*, *TBP*) were differentially expressed in different pathological stages of hepatocellular carcinoma [7,11]. These findings bring forward the need to process high-throughput data in order to determine a global list of constitutively and invariably expressed genes that can be used as reference genes [12–14]. For example, Hruz T. et al. measured the standard deviation of gene expression across large sets of Affymetrix arrays of human, mouse and *Arabidopsis* from the Genevestigator database and developed an online tool, Ref-Genes, that can be used to search for genes with minimal standard

Gene Symbol	Name	Ratio	Percentile Rank	
			Mean	Median
EEF2	(eukaryotic translation elongation factor 2)	0.979	95.2	98
RPS10	(ribosomal protein S10)	0.976	96.5	99
B2M	(beta-2-microglobulin)	0.975	96.4	99
CFL1	(cofilin 1 (non-muscle))	0.974	94.9	99
UBC	(ubiquitin C)	0.974	96.4	98.8
RPL27	(ribosomal protein L27)	0.973	94.5	99
RPL3	(ribosomal protein L3)	0.973	95.9	99
RPL7	(ribosomal protein L7)	0.972	96.1	99
ACTG1	(actin; gamma 1)	0.971	95.3	99
COPS6	(COP9 constitutive photomorphogenic homolog subunit 6 (Arabidopsis))	0.971	86.6	88
RPS17	(ribosomal protein S17)	0.971	96.3	99
RPL38	(ribosomal protein L38)	0.97	94	97.3
ATP5I	(ATP synthase; H+ transporting; mitochondrial F0 complex; subunit E)	0.969	92.4	94.5
RPS13	(ribosomal protein S13)	0.969	96.2	99
NACA	(nascent-polypeptide-associated complex alpha polypeptide)	0.968	95.6	98.5
PSMC1	(proteasome (prosome; macropain) 26S subunit; ATPase; 1)	0.968	92.3	95
RPL9	(ribosomal protein L9)	0.968	93.8	99
TPT1	(tumor protein; translationally-controlled 1)	0.968	96.1	99
OAZ1	(ornithine decarboxylase antizyme 1)	0.967	93.5	98.5
RPL22	(ribosomal protein L22)	0.967	94.8	97.2
RPS16	(ribosomal protein S16)	0.967	95.9	99
UBB	(ubiquitin B)	0.967	93.7	97
COX7C	(cytochrome c oxidase subunit VIIc)	0.965	92.6	95.7
H3F3A	(H3 histone; family 3A)	0.965	95.5	98
RPL13	(ribosomal protein L13)	0.965	92.8	98.8
RPL13A	(ribosomal protein L13a)	0.965	96	99
RPN2	(ribophorin II)	0.965	91.5	95
RPS27A	(ribosomal protein S27a)	0.964	94	98
TUBB	(tubulin; beta)	0.964	93	96
NDUFS5	(NADH dehydrogenase (ubiquinone) Fe-S protein 5; 15kDa (NADH-coenzyme Q reductase))	0.963	92.7	96
FAU	(Finkel-Biskis-Reilly murine sarcoma virus (FBR-MuSV) ubiquitously expressed (fox derived); ribosomal protein S30)	0.962	93.7	98
RPL30	(ribosomal protein L30)	0.962	94.4	99
RPS11	(ribosomal protein S11)	0.962	92.2	99
RPS3A	(ribosomal protein S3A)	0.962	96.1	99
SOD1	(superoxide dismutase 1; soluble (amyotrophic lateral sclerosis 1 (adult)))	0.962	93.6	97
COX7A2	(cytochrome c oxidase subunit VIIa polypeptide 2 (liver))	0.961	93.6	97
NCL	(nucleolin)	0.961	93.3	97
RPL21	(ribosomal protein L21)	0.961	94.2	99
SRP14	(signal recognition particle 14kDa (homologous Alu RNA binding protein))	0.961	92.7	97
RPS6	(ribosomal protein S6)	0.96	95.2	99
EEF1B2	(eukaryotic translation elongation factor 1 beta 2)	0.959	94.6	98

Figure 1. Screenshot of the first 40 lines from reference gene lists. Complete set of MeSH classified reference gene lists from 9090 array samples are given in hyperlinked Supporting Information S1 spreadsheet.
doi:10.1371/journal.pone.0093341.g001

deviation across a chosen set of arrays [15,16]. They concluded that no genes are universally stable, but a subset of stable genes with minimal variance exists for each biological context that can be used for the normalization of RT-qPCR data.

Although publicly available microarray or next generation sequencing (NGS) experiments were used to generate lists of candidate reference genes, novel statistical approaches for testing accuracy of a reference gene are still needed. Herein, we aimed to confirm the reliability of available housekeeping gene sets using randomization as well as to determine other invariably expressed gene sets based on Receiver Operating Characteristic (ROC) curves for classifiers under large number of experimental conditions and across a wide panel of tissue types.

Our method provides reference gene lists for global and cell-type specific normalization of transcriptome data. Gene lists are scored based on their expression stability, and classified according to the Medical Subject Headings (MeSH) associated with the transcriptome study that was published and indexed by National Library of Medicine. Gene lists are provided in the supporting dataset (Supporting Information S1). RT-qPCR assessment of selected reference genes is also provided for various tissue-specific cancer cell lines *in vitro*.

Results and Discussion

Development of a methodology to identify consistently stable genes

Housekeeping/reference genes should exhibit relatively constant expression levels when compared to non-housekeeping genes. To identify the consistency of the so-called housekeeping genes across large-scale experiment sets, the gene expression data were downloaded from the NCBI Gene Expression Omnibus (NCBI-GEO) database [17], and all spot data were extracted along with their associated metadata from the platform files. The data set approximately contained 142 million oligonucleotide microarray spots from 9090 microarray samples, which were grouped into 381 GEO datasets. Percentile-ranking method was applied independently on the global mean normalized data within each sample in each GEO dataset. This process provided a rank value for each gene within a sample. Therefore, the rank measure was

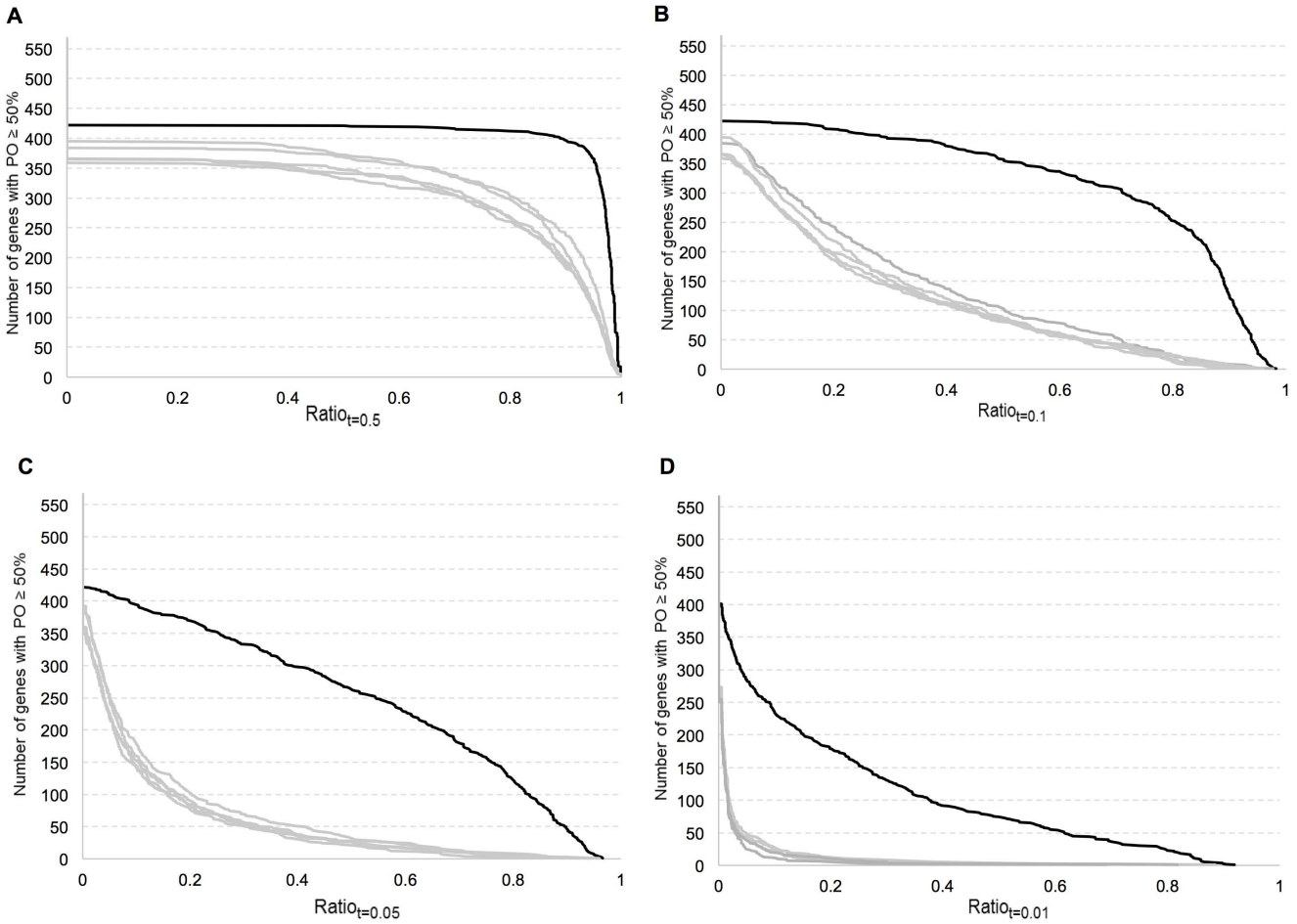

Figure 2. Graph of ratio of the number of sets in which a gene has a coefficient of variation (CV) less than a threshold (t), to the number of sets in which the gene is observed. Graphs were plotted for CV value thresholds t = 0.5 t = 0.1, t = 0.05 and t = 0.01. Percentage of occurrence (PO) is at least 50% of the total sets. The y-axis indicates the number of genes having a ratio greater than the ratio value at the corresponding x-axis. This function is described in the methods section, as x-axis being r and y-axis being $f_{PO}(r)$. The black curve represents housekeeping genes while curves with grey colors show 5 random sets of genes excluding the housekeeping genes. Random sets of genes have the same mean rank distribution as of those housekeeping genes.
doi:10.1371/journal.pone.0093341.g002

comparable across experiments and platforms, allowing the analysis of the behavior of a gene globally across GEO datasets. Using ranks of genes is a standard method as also employed in Quantile Normalization, which is a common microarray normalization technique [18].

The average changes in the rank of each gene in each GEO dataset (GDS) was computed based on the ratio of the standard deviation to the mean and termed as its coefficient of variation value (CV) (see Methods). CV, as a standardized measure of sample variability, help suggest candidate reference genes whose expression is stable and unaffected by the experimental condition since it has been successfully applied in identification of reference genes in multiple studies with varying thresholds [19–22]. Most genes had coefficient of variation values only for a subset of the available GDSs. Therefore, for each gene G_i and a predefined CV threshold t, the ratio of GEO datasets, where CV is less than t, $\text{Ratio}_t(G_i)$, is calculated as the measure of stable expression. $\text{Ratio}_t(G_i)$ is the ratio of GEO datasets, in which a gene exhibits a coefficient of variation less than t. The $\text{Ratio}_t(G_i)$ value, by itself, is not a sufficient measure to identify statistically significant reference genes. A gene that has a small enough CV value can get a perfect ratio even if it is observed in only a single GEO dataset. Therefore, a new parameter, $\text{PO}(G_i)$, calculated as the percentage of datasets that each gene has been observed in at least once, was used to adjust $\text{Ratio}_t(G_i)$ parameter (Methods). $\text{Ratio}_t(G_i)$ in the context of $\text{PO}(G_i)$ allowed for accurate normalization of a large set of microarray data, since it takes into account the information about the differences in probe/clone composition of the arrays. We assessed the utility of these measures by implementing a simple threshold based classifier and computing the sensitivity and specificity of this classifier using a published reference gene set as the ground truth (Methods). Two sets of reference genes were generated. First list contains reference gene lists with a CV threshold of 0.12 and with various sensitivity values while the second list is built with sensitivity of 0.5 for a range of CV threshold values. Figure 1 shows the first 40 genes from 342 reference genes with a CV of at most 0.12, sensitivity equal or over 0.5, specificity of 0.97 and minimum percentage of occurrence of 0.75 in all 9090 array samples from 381 GEO datasets (See Reference Gene Lists in Supporting Information S1 for the complete list). The high specificity shows that the CV measure coupled with percentage of occurrence is an accurate measure for identification of reference gene sets.

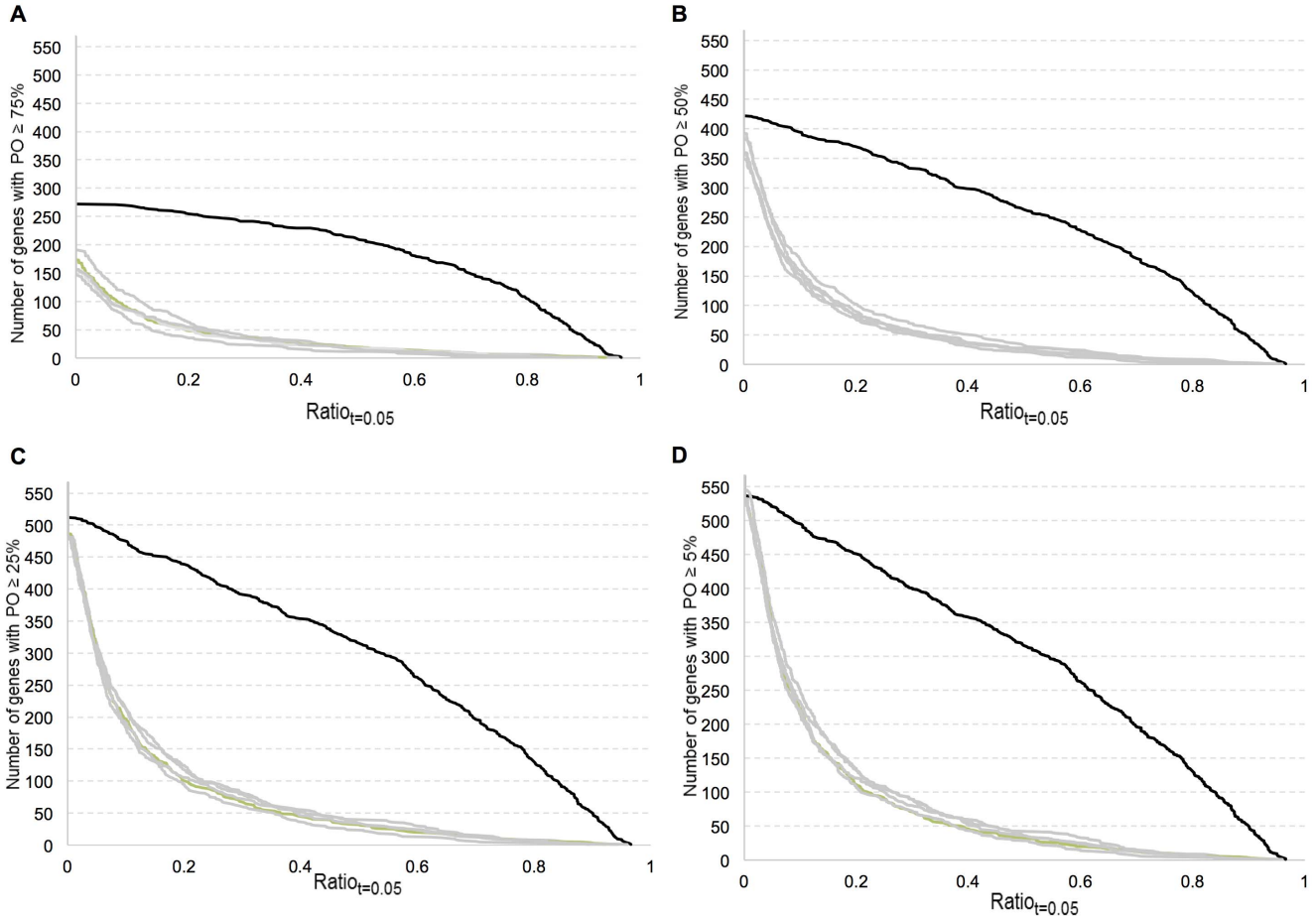

Figure 3. Graph of ratio of the number of sets in which gene has coefficient of variation less than 0.05 to the number of sets in which the gene is observed. Gene is observed at least a-) 75%, b-) 50%, c-) 25% and d-) 5% of the total sets. The y axis indicates the number of genes having a ratio greater than ratio value at the corresponding x axis. The curve with red color represents housekeeping genes while curves with other colors shows 5 random sets of genes excluding the housekeeping genes. Random sets of genes have the same mean rank distribution as of those housekeeping genes.
doi:10.1371/journal.pone.0093341.g003

Housekeeping/Reference genes should exhibit relatively constant expression levels and their average rank change should be lower than that of remaining genes. Hence, we assumed that the candidate reference genes should have lower CV and higher Ratio$_t(G_i)$ than that of randomly selected genes. In order to compare the expression behaviors of reference genes to that of random genes, we first analyzed the largest previously reported housekeeping datasets [1,23]. There was high variation between genes in the first dataset, in parallel with the authors' observations. Therefore, the dataset provided by Eisenberg *et al.* was used in our analysis. The 566 housekeeping genes in this dataset were compared to five different randomly selected sets of non-housekeeping genes having the same mean rank distribution as that of the housekeeping gene set.

Normalized gene expression values were analyzed for the CV thresholds $t=0.5$, $t=0.1$, $t=0.05$, and $t=0.01$ and minimum percentage of occurrences PO = 75%, 50%, 25% and 5%. When coefficient of variation, CV, was less than 0.5 ($t=0.5$), percentile-ranked GEO datasets showed high Ratio$_t$ values for nearly all of the analyzed genes (housekeeping or not), for all PO values. At lower CV thresholds, $t=0.1$, $t=0.05$ and $t=0.01$, housekeeping genes had significantly higher Ratio$_t$ values than those of random gene sets for all PO values. The randomization approach allowed us to test an optimum range of t and PO values that can discriminate between reference and non-reference genes. Graphs of Ratio$_t$ at PO = 50% with four different CV thresholds (Figure 2) and graphs of Ratio$_t$ at CV $t=0.05$ with four different PO thresholds were plotted (Figure 3). These graphs showed that measures could accurately distinguish previously identified reference genes from the randomly selected ones.

The difference in the ratio distribution of housekeeping genes compared to that of the randomly selected non-housekeeping gene sets was statistically significant, as shown by Kolmogorov-Simirnov tests (Table S1 in Supporting Information S2, $p<0.0001$). The random gene sets, excluding the housekeeping genes, did not show any significant ratio distribution difference, as shown by using Bonferroni adjusted Kolmogorov-Simirnov tests (Table S2 in Supporting Information S2). These observations proved that the expression of the tested housekeeping genes was less variable across different experiment sets compared to that of randomly selected gene sets.

In addition, we assessed the sensitivity and specificity of a simple threshold based classifier using the CV threshold using the published housekeeping gene set as the ground truth. The receiver operator characteristic (ROC) curve in Figure 4 shows that more than half of the published reference genes can be identified with a

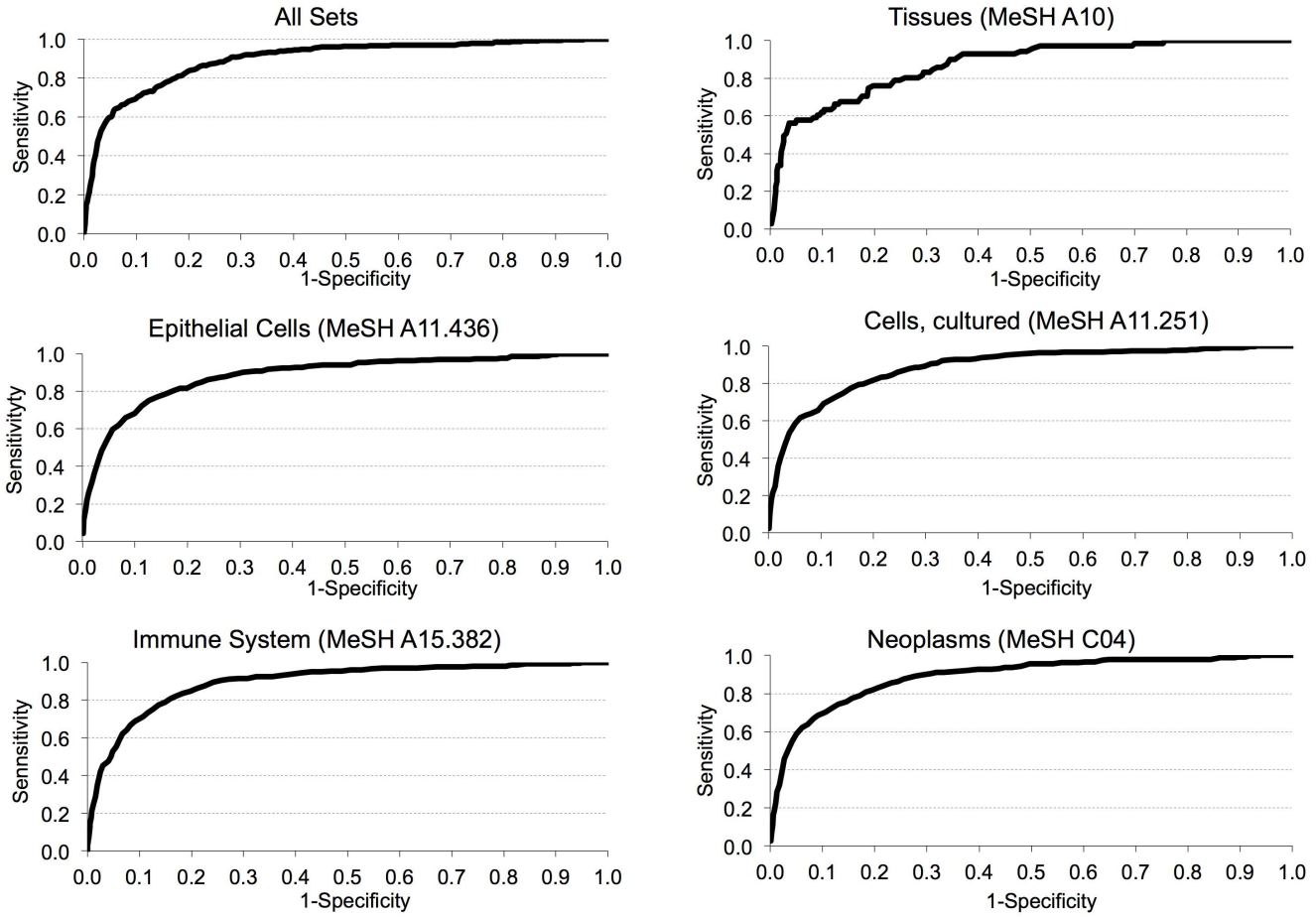

Figure 4. Receiver Operator Characteristic (ROC) curve of the simple threshold based classifier. The receiver operator characteristic (ROC) curve of a simple threshold classifier over all datasets and some MeSH categories. The housekeeping gene set by Eisenberg et al. [22] is used as the ground truth. The simple threshold classifier classifies all the genes with CV values below a threshold as housekeeping genes. By using different CV thresholds the stringency of the classifier can be varied and the ROC curve can be plotted accordingly. Sensitivity is the ratio of correctly classified ground truth genes over all ground truth genes and specificity is the ratio of correctly identified non-housekeeping genes over all non-housekeeping genes. Complete set of MeSH classified RO-curves are given in hyperlinked Supporting Information S3 spreadsheet.
doi:10.1371/journal.pone.0093341.g004

specificity of 0.97. Similar analyses performed on datasets grouped by MeSH are available in Supporting Information S3.

Identification of novel reference genes

Our primary goal in this study was to define a novel reference gene set that can be used for both global and cell type-specific normalization of expression experiments. For this purpose, a classifier that can be used to identify novel reference genes was built. Based on our analysis with the known 566-housekeeping gene set, coefficient of variation (CV) measure was set as the variable for building the classifier while minimum percentage of occurrence (PO) and Ratio_t values were fixed at 75% and 0.90 respectively. The accuracy of this classifier in predicting reference genes was assessed in comparison with the previously reported 566 housekeeping gene set [23]. Among the candidate reference genes that were identified by our classifier at each CV threshold, the known 566 housekeeping genes were regarded as true positives (TP) and the other genes were regarded as false positives (FP) to plot a receiver-operating characteristic (ROC) curve. In the supporting gene lists, the sensitivity was set to 0.5, implying that half of the identified reference genes are the known housekeeping genes. The ROC curve of our classifier for CV values ranging from 0.01 to 10 showed its effectiveness in finding true positives (sensitivity) (Figure 4). Curves for the overall (Figure 4A) and specific reference gene sets are available in the supporting hyperlinked dataset (Supporting Information S3).

According to a classic ROC curve, a good classifier should capture most of the known housekeeping genes while providing a relatively small number of false positives. However, in this particular case, the false positives could be the newly identified candidate reference genes. Therefore, their CV and $Ratio_t$ values should still be considered for their potential as a reference gene. CV, Ratio and Percentile Rank values are provided for each gene in the supporting hyperlinked dataset. The global reference genes were given in this list under the category of *All* with CV of 0.12, sensitivity equal or over 0.5, specificity of 0.97 and minimum percentage of occurrence of 0.75 (Figure 2A and Supporting Information S1).

In order to determine origin- and cell type-specific reference genes, the GEO sets were classified according to the Medical Subject Headings (MeSH) associated with their experimental data, published and indexed by National Library of Medicine. Of the 381 GEO datasets analyzed in this study, 341 were associated with 272 different medical publications and 264 of these publications

Table 1. MeSH groups and number of NCBI-GEO data sets in each group.

MeSH Tree Number	MeSH Heading	Number of Sets
ALL	ALL	381
A10	Tissues	77
A10.272	Epithelium	16
A10.690	Muscles	46
A11	Cells	223
A11.118	Blood Cells	47
A11.148	Bone Marrow Cells	14
A11.251	Cells. Cultured	157
A11.284	Cellular Structures	40
A11.329	Connective Tissue Cells	34
A11.436	Epithelial Cells	48
A11.627	Myeloid Cells	17
A11.733	Phagocytes	14
A11.872	Stem Cells	22
A15	Hemic and Immune Systems	74
A15.145	Blood	51
A15.378	Hematopoietic System	14
A15.382	Immune System	60
C04	Neoplasms	108
C04.557	Neoplasms by Histologic Type	68
C04.588	Neoplasms by Site	68
C04.697	Neoplastic Processes	16

doi:10.1371/journal.pone.0093341.t001

were associated with a total of 5754 MeSH terms [24]. These gene sets were grouped into three anatomy (tissues, cells, hemic and immune systems), and one disease (neoplasms) based MeSH categories (Table 1). GDS identification numbers associated with each MeSH are given in Supporting Information S1. Two lists of reference gene sets based on CV and sensitivity, were provided for each MeSH category. First list was constructed based on a fixed threshold for CV$<$0.12 and the second on a fixed threshold of sensitivity$>$0.50. Both gene sets had a fixed PO threshold of 75%. The reference gene lists, which include CV, PO, specificity and sensitivity values for each MeSH category, are provided as supporting hyperlinked dataset (Supporting Information S1).

Experimental validation of selected reference genes in different cancer cells

Among the large panel of identified reference genes, 17 genes were selected for experimental validation (Table 2). Expression levels of these reference genes (*AARS, ACTB, CFL1, EEF2, GAPDH, GSTO1, H2AFZ, HBXIP, RPL30, RPL41, RPL7, RPN2, RPS10, RPS17, RPS3A, SOD1, TPT1*) were assessed by RT-qPCR in 16 different cell lines consisting of 8 Hepatocellular Carcinoma (HCC) (HepG2, FOCUS, Mahlavu, Hep3B, Hep3B-TR, Huh7, SkHep1, and PLC), 5 Breast Cancer (MDA-MB453, HCC1937, BT20, T47D and CAMA-I), and 3 Colon Cancer (HCT116, HT29, and SW620) cell lines. Housekeeping/reference genes are expected to have high expression and low variability in expression levels between cells. Therefore, in RT-qPCR amplification, they should have low threshold cycle (Cq $<$30) and low standard deviation. All of the tested reference genes met this requirement for Cq values and standard deviations (Figure 5). The best candidate reference genes appeared at the center of the graphs for each group (Figure 5 A–C). In order to emphasize the stability of these genes, a well-expressed non-housekeeping gene, *RECK*, was included into the CV analysis. It was not included in the analysis with NormFinder and geNorm due to its high variability (CV around 1.0). Genes were ranked by their stability based on their CV. Comparison of the expression values by analysis of variance (ANOVA) identified *RPL30* as the most stable gene with lowest variance within and between the Liver, Breast and Colon Carcinoma cell line groups, followed by *RPL41*, *RPS10* and *CFL1*. The variance within each of these three groups was low for *RPS3A, RPS17, RPL7, ACTB, H2AFZ,* and *HBXIP* reference gene expression. However, the variance between the three groups was relatively high. This implied that these reference genes are more suitable for normalization of cell lines from single tissue-origin than cell lines with different tissue-origins. *GSTO1, TPT1, RPN2, SOD1* showed the highest variability.

Real-time quantitative PCR gene expression stability was further determined using geNorm and NormFinder software [3,25]. GeNorm is a pairwise comparison-based model. For each gene, it calculates an expression stability value based on the average pairwise variation between all tested genes. The genes are ranked according to their expression stability through stepwise exclusion of the least stable gene (highest stability value). NormFinder is a model-based approach that estimates the variation between sample subgroups, such as liver, breast and colon cancer cell lines, as well as the overall expression variation of the tested genes. Unlike geNorm, the resulting stability value and the stability rank order changes in NormFinder depending on the input genes. Therefore, geNorm and NormFinder stability analysis

Table 2. Stability measures of the reference genes that were used in RT-qPCR analysis.

	All 381 GEO sets			MeSH A11.251 (cells,cultured)			MeSH C04 (Neoplasms)		
		Percentile Rank			Percentile Rank			Percentile Rank	
Gene Symbol *	Ratio	Mean	Median	Ratio	Mean	Median	Ratio	Mean	Median
RPS3A	1	96.1	99	1	94.7	99	1	97.3	99
RPL30	1	94.4	99	1	95.6	99	1	98.7	99
RPS10	1	96.5	99	1	95.4	99	1	98.2	99
RPL7	1	96.1	99	1	95	99	1	98	99
RPL41	0.9	93.8	99	0.9	92.2	99	0.9	96.7	99
CFL1	1	94.9	99	1	93.7	99	1	97.8	99
RPS17	1	96.3	99	1	94.7	99	1	97.7	99
H2AFZ	0.9	90.7	94	1	92.4	86	0.9	93.5	95
ACTB	0.9	95	99	1	95.3	99	1	98.7	99
HBXIP	1	89	92	1	88.7	92.5	1	90.4	92
EEF2	1	95.2	98	1	93.5	98.5	1	97	98.5
AARS	0.9	85.7	91	0.9	87.2	92	0.9	87.2	92
SOD1	1	93.6	97	1	92.2	97	1	95	97
TPT1	1	96.1	99	1	95.3	99	1	97.7	99
RPN2	1	91.5	95	1	91.4	96	1	94	96.7
GSTO1	0.9	90	94	0.9	89.4	94	0.9	90	93

*Selected genes with CV $\leq$0.12 and PO $\geq$75%. The complete results for all MeSH categories and all reference genes obtained from 381 GEO sets are given in the Supporting Reference Gene Lists dataset (Supporting Information S1).

doi:10.1371/journal.pone.0093341.t002

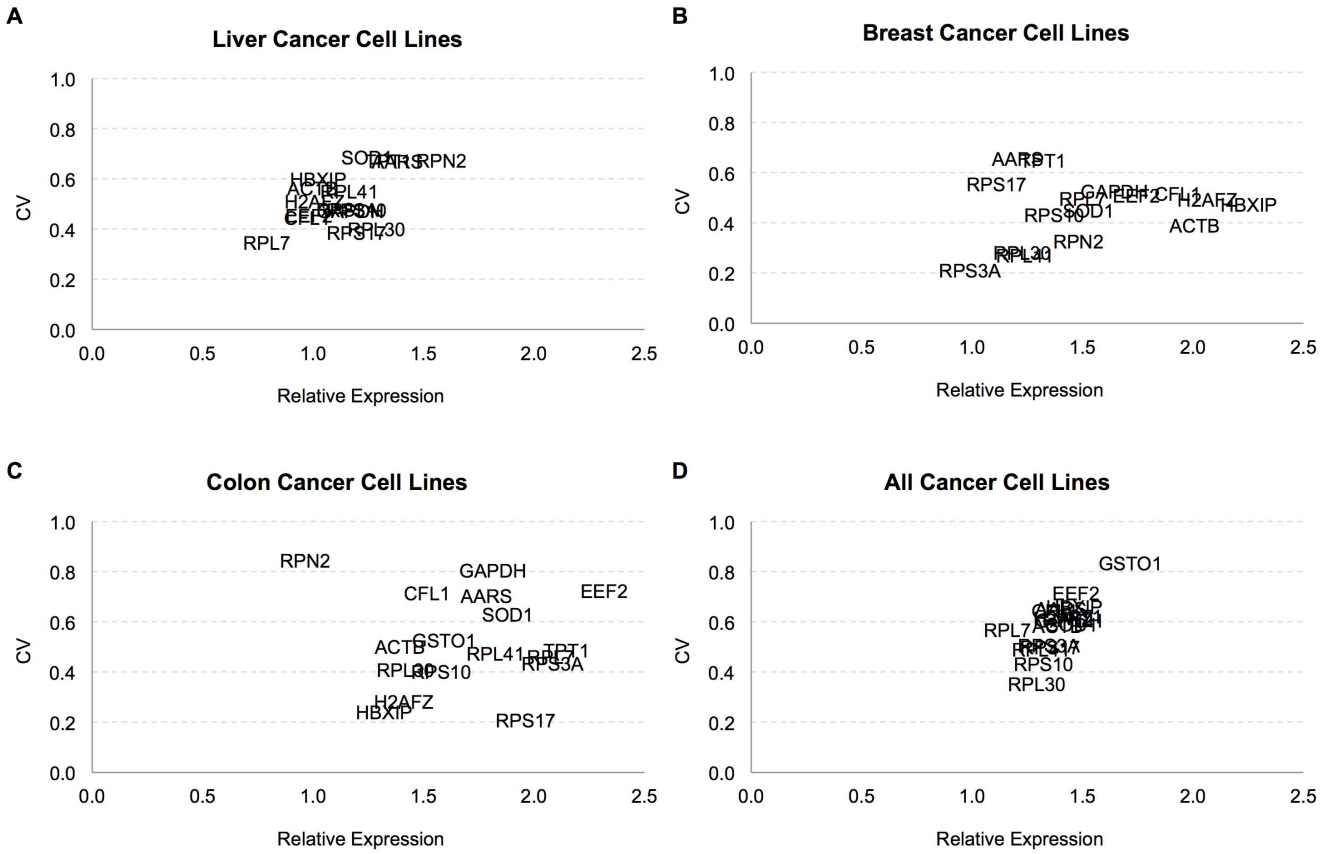

Figure 5. Graphs of coefficient of variations and relative expression levels of 17 reference genes in RT-qPCR. Coefficient of Variation (CV) was calculated based on the relative expression (efficiency$^{-\Delta Cq}$) of each housekeeping gene in (**A**) Liver, (**B**) Breast, (**C**) Colon and (**D**) All cancer cell lines.
doi:10.1371/journal.pone.0093341.g005

was performed with and without the least stable genes *EEF2*, *GSTO1*, *RPN2* and *TPT1*, which have a standard deviation value above the mean standard deviation (stdev = 1.42). The selected reference genes were ranked according to their overall stability values across 16 different cell lines, determined by geNorm and NormFinder (Table 3, Figure 6, Table S3 in Supporting Information S2). The ranking of these genes was similar for both methods. Ribosomal protein genes *RPS10*, *RPL41*, *RPL30*, and *RPS3A* were the most stable genes among all 16 cell lines according to geNorm and NormFinder respectively (Table 3, Tables S3–S4 in Supporting Information S2). Two traditional reference genes, *ACTB* and *GAPDH*, were less stable than the ribosomal genes and ranked lower in the stability rank list. *CFL1* and *HBXIP* were the most stable genes after the ribosomal protein genes in general (Figure 7A and Table 3). While the commonly used reference gene *GAPDH* was one of the stable genes within liver cancer cell lines, it was among the least stable genes within breast and colon cancer cell lines. It had a high variance in terms of stability value and expression value between the three types of carcinoma cell lines investigated. This implied that *GAPDH* could be used as a reference gene when comparing liver cancer cell lines, but not breast and colon cancer cell lines. *ACTB* was more stable than *GAPDH* in Breast and Colon Carcinoma cell lines and had a stability value similar to *GAPDH* in HCC cell lines. Moreover, even though reference genes were known to avoid regulation by miRNAs, recent findings showed that *GAPDH* and *ACTB* are direct targets of miR-644a [26,27]. Besides, several pseudogenes of *GAPDH* and *ACTB* were revealed, making them less reliable to be used as reference genes [28].

Stability within liver, breast and colon cancer cell lines was also analyzed separately. The ribosomal genes *RPL30*, *RPL41*, *RPL7*, *RPS10*, and *RPS3A* were stable within each cell line group (Figure 7B–D, Table 3, Tables S3, S4 in Supporting Information S2). *HBXIP*, *CFL1*, and *GAPDH* were among the most stable genes together with the ribosomal protein genes in 8 HCC cell lines analyzed. *HBXIP* was the third most stable gene in breast cancer cell lines according to geNorm, but ninth according to NormFinder ranking. *H2AFZ* and *HBXIP* were ranked among the most stable genes together with *RPS10*, *RPL41*, and *RPS3A* in colon cancer cell lines. The difference in the gene stability ranking order between the two softwares is due to the different methodologies. geNorm is based on the comparison of expression similarity of the tested genes. This may cause exclusion of a candidate reference gene with a relatively stable expression in early steps of the ranking procedure, if all other genes in the list have similar expression profiles. Another disadvantage of this approach may be a bias towards co-regulated genes, since these genes will have similar expression profiles and hence may be ranked top in the stability list, regardless of their expression stability. NormFinder does not have such a bias, since expression stability of each gene is determined independent of the rest of the genes. However, since NormFinder ranking is based on the variation between groups, when comparing groups like liver, breast, and colon carcinoma cell lines, if the variation within group

Table 3. Stability order of 17 housekeeping genes based on CV, NormFinder and geNorm analysis.

All			Liver			Breast			Colon		
CV	**NormFinder**	**geNorm**	**CV**	**NormFinder**	**geNorm**	**CV**	**NormFinder**	**geNorm**	**CV**	**NormFinder**	**geNorm**
RPL30	RPL30	RPL41	RPL7	RPL30	RPL41	RPS3A	RPS3A	RPL41	RPS17	RPS3A	RPL41
RPS10	RPS3A	RPS10	RPS17	RPL7	RPS10	RPL41	CFL1	RPS10	HBXIP	RPL41	RPS10
RPL41	RPS10	RPL7	RPL30	RPS17	RPL7	RPL30	ACTB	HBXIP	H2AFZ	RPS10	RPS3A
RPS17	RPL7	RPS3A	CFL1	RPS10	RPS17	RPN2	RPL30	RPL7	RPS10	RPL7	H2AFZ
RPS3A	RPL41	RPL30	EEF2	RPS3A	RPS3A	ACTB	RPL7	RPL30	RPL30	RPL30	HBXIP
RPL7	CFL1	HBXIP	GAPDH	GAPDH	RPL30	RPS10	RPL41	CFL1	RPS3A	H2AFZ	RPL30
ACTB	HBXIP	CFL1	RPS10	CFL1	GAPDH	SOD1	RPN2	RPS3A	RPL7	AARS	RPL7
SOD1	GAPDH	RPS17	RPS3A	HBXIP	CFL1	HBXIP	EEF2	EEF2	RPL41	HBXIP	RPS17
GAPDH	RPS17	EEF2	H2AFZ	RPL41	HBXIP	H2AFZ	HBXIP	ACTB	TPT1	ACTB	TPT1
RPN2	EEF2	ACTB	RPL41	H2AFZ	H2AFZ	RPL7	RPS10	RPS17	ACTB	CFL1	GSTO1
H2AFZ	ACTB	GAPDH	ACTB	EEF2	ACTB	EEF2	TPT1	TPT1	GSTO1	RPS17	ACTB
TPT1	H2AFZ	H2AFZ	HBXIP	ACTB	EEF2	CFL1	RPS17	RPN2	SOD1	TPT1	CFL1
CFL1	AARS	AARS	AARS	AARS	AARS	GAPDH	GAPDH	AARS	AARS	GAPDH	AARS
AARS	SOD1	TPT1	TPT1	TPT1	SOD1	RPS17	SOD1	SOD1	CFL1	GSTO1	GAPDH
HBXIP	TPT1	SOD1	RPN2	SOD1	TPT1	TPT1	H2AFZ	GAPDH	EEF2	SOD1	RPN2
EEF2	RPN2	RPN2	SOD1	RPN2	RPN2	AARS	AARS	H2AFZ	GAPDH	RPN2	SOD1
GSTO1	GSTO1	GSTO1	GSTO1	GSTO1	GSTO1	GSTO1	GSTO1	GSTO1	RPN2	EEF2	EEF2

doi:10.1371/journal.pone.0093341.t003

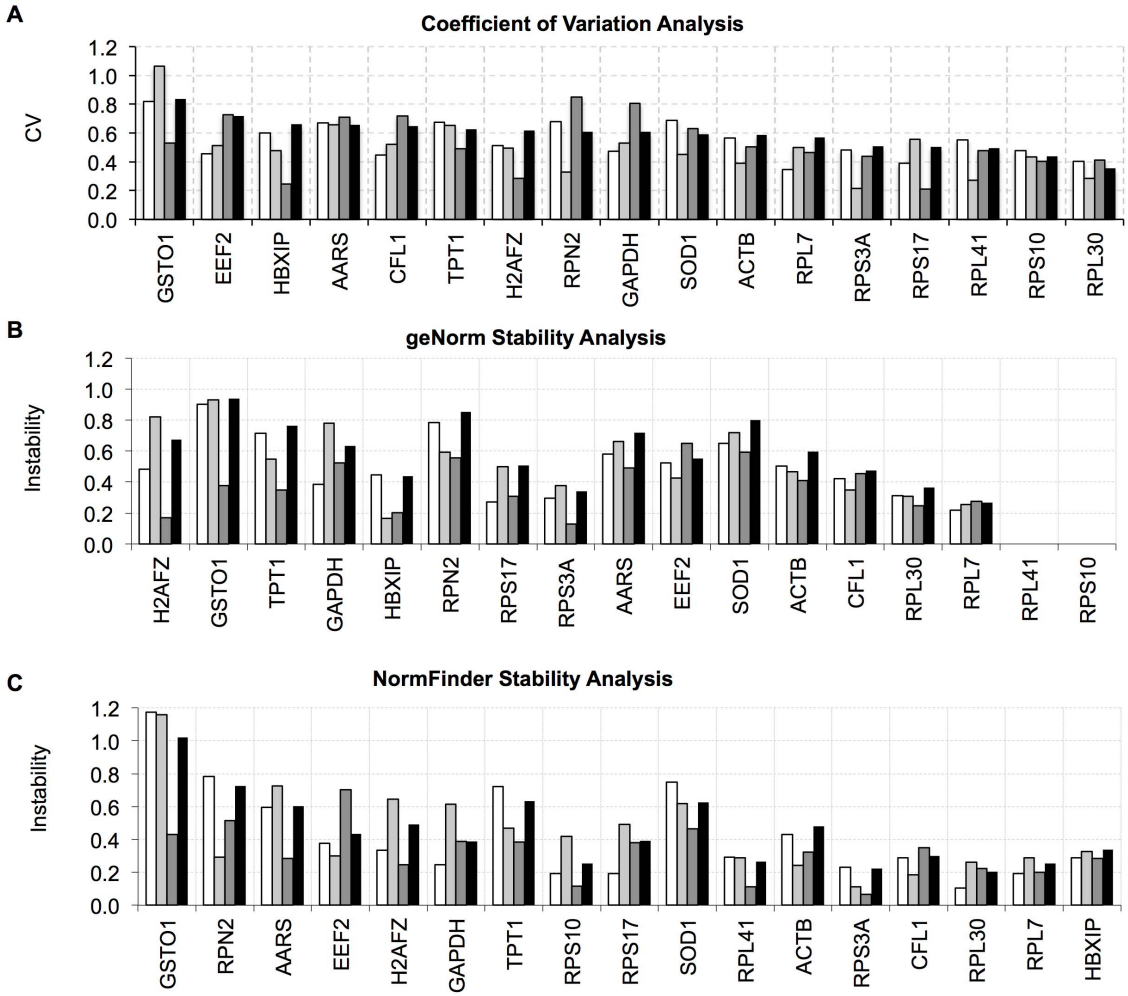

Figure 6. Stability analysis of reference genes in RT-qPCR based on CV, geNorm and NormFinder. Genes ranked by stability based on (**A**) CV, (**B**) geNorm and (**C**) NormFinder tools. White, light gray, dark gray and black bars represent Liver, Breast, Colon and All Cancer Cell lines respectively.
doi:10.1371/journal.pone.0093341.g006

is high, then the variation between groups may considered as lower, leading to false positive results.

In order to determine the optimal number of reference genes for accurate normalization, pairwise variation $V_{n/n+1}$ analysis was performed using the geNorm software. Taking 0.15 as a cut-off value as proposed, the use of *RPL41* and *RPS10* together as reference genes were enough for accurate normalization (V2/3 value = 0.134) when comparing Liver, Breast and Colon Carcinoma cell lines. An even more accurate normalization can be achieved if *RPL7* and *RPS3A* are also included as reference genes. (V3/4 value = 0.091 and V4/5 value = 0.067).

Conclusions

Even the most frequently used reference genes are subject to differential regulation under specific treatments or between different cell lines or tissues. Therefore, new reference gene sets should be determined instead of using traditional housekeeping/reference genes that are themselves prone to differential regulation. The use of two or more housekeeping genes for normalization can improve the reliability of normalization [5,9,29]. The largest meta-analysis for reference gene identification up-to-date compiled 1431 samples from 104 microarray data sets classified into 4 physiological states with 13 organ/tissue types and identified reference gene candidates mostly associated with transcription, RNA processing and translation [30]. Hruz et al. 2011 also performed a large scale meta-analysis across multiple species and sources using Genevestigator database [16]. They have used ranks of standard deviations using mouse Affymetrix datasets to support context specificity of reference gene sets. Our study also is comprehensive containing 142 million oligonucleotide microarray spots from 9090 microarray samples, grouped into 381 GEO datasets from multiple platforms. We also provide a novel methodology based on randomizations and ROC that allows testing the specificity and sensitivity of classifying a gene as reference or non-reference. Previously, a meta-analysis of 13,629 human gene array samples from GEO database identified candidate housekeeping genes, including *RPS13*, *RPL27*, *RPS20* and *OAZ1*. For each gene the coefficient of variation (CV) of its expression and the maximum fold change was calculated to identify genes with the minor variation in expression [19]. Recently, Eisenberg *et. al.* published an updated new housekeeping gene list based on analysis of RNA-seq data [31]. However, MeSH classification used in the present study has not been applied to reference gene set combinations previously. In this study, we

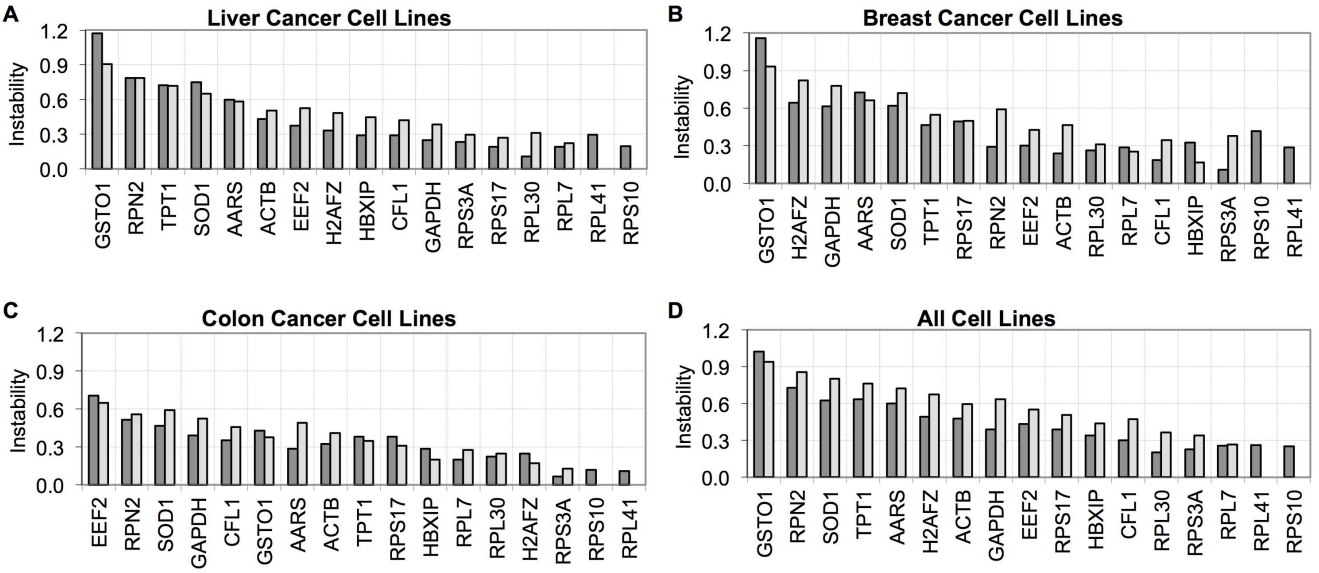

Figure 7. Stability analysis of reference genes in tissue-specific cell lines in RT-qPCR. Stability analysis in (A) Liver, (B) Breast, (C) Colon and (D) All cancer cell lines. NormFinder and geNorm results were represented in dark gray and light gray respectively.
doi:10.1371/journal.pone.0093341.g007

determined novel reference gene sets that can be used for both global and MeSH category-based normalization of gene expression data. Furthermore, we validated stability of known and novel reference genes obtained from meta-analysis with cancer cell line qPCR studies.

Our reference gene lists were dominated by the ribosomal protein genes and genes that are involved in maintenance of basal cellular activities such as translation and metabolism. Especially, *RPL30* and *RPL41* are good reference genes for comparing all cell lines regardless of their origin. Previously, 451 housekeeping genes that were expressed in all of the 19 distinct normal human tissue types studied, were shown to have variable expression levels among different tissues and ribosomal genes, which were among the most stable genes, were suggested as reference genes suitable for normalization purposes [1]. A more recent study however suggested that ribosomal protein genes, which display stable expression in meta-analysis, indeed exhibit variation in mRNA expression in a tissue-dependent manner [32]. These findings once more emphasize that finding a common reference gene, ribosomal or not, is not possible. The genes located at the top the reference gene set lists display the highest confidence based on CV and PO values therefore those genes are less likely to be wrong. However every computational analysis might have false positive results for this reason, users should select their reference gene of interest and experimentally validate the stability of the expression of that reference gene under their experimental conditions. Furthermore more than 2 reference genes per experiment would be a better measure for precision. Computational calculations present a road map to guide the experimentalists. The data sets we used to build MeSH dependent reference gene lists originated from various sources which aimed to identify differentially expressed gene sets under specific experimental conditions in order to minimize the homogeneity between and within data sets. Data set IDs are given together with reference gene lists in Supporting Information S1. Meta-analysis and consequent classification of tissue- or cell type-origin specificity of housekeeping genes appears to be the best approach to determine the most appropriate reference genes among the large number of known housekeeping genes. Furthermore identification of housekeeping genes enables normalization of transcriptome data not only for microarrays but also for RNA-seq experiments [33,34]. RNA-seq technology is advantageous for detecting genes that are expressed in low levels. Hence, similar studies with RNA-seq data may increase the reliability of housekeeping genes when large number of NGS data are available [14] and can be used to identify a universal reference gene set. The tissue specific reference gene lists presented in this study, provide housekeeping genes that can be exploited as references in differential expression analysis of data from variety of transcriptome and RT-qPCR experiments.

Methods

In order to normalize expression values, percentile ranking have been applied. For each gene G_i in a sample e_i, a single rank value, $r(G_i.e_j)$ was computed (Equation 1). For a gene that was covered by multiple probesets in a sample, the average gene probeset rank value was used [23].

$$\mathrm{r}(\mathrm{G_i},\mathrm{e_j}) = \frac{\left|\left\{G_k \middle| G_k \in G \wedge ex\left(G_k,e_j\right) \leq ex\left(G_i,e_j\right)\right\}\right|}{|G|} \times 100 \quad (1)$$

where $ex(g,e)$ is a function, which gives the mean normalized expression value of gene g in sample e and **G** is the set of all genes.

Computation of coefficient of variation value for each gene in each GEO dataset and identification of candidate reference genes

Let $G = \{G_1.....G_m\}$ be the set of genes and $\mathbf{S} = \{e_1.....e_n\}$ be a GEO dataset of n samples. For gene G_i in experiment e_j, a single rank value, $r(G_i.e_j)$, was computed. Given a set $\boldsymbol{S}$ with n experiments, we had at most n rank values for a gene. The average amount of change in the rank of gene G_i, in set $\boldsymbol{S}$ was then computed by the Coefficient of Variation $CV(S.G_i)$ as given below in Equation 2.

$$CV(S,G_i) = \frac{\sigma(S,G_i)}{\mu(S,G_i)} \quad (2)$$

where

$$\mu(S,G_i)=\frac{\sum_{j=1}^{n} r(G_i,e_j)}{n},\forall e_j\in S \quad (3)$$

and

$$\sigma(S,G_i)=\sqrt{\frac{1}{n}\sum_{j=1}^{n}\left(r(G_i,e_j)-\mu(S,G_i)\right)^2},\forall e_j\in S \quad (4)$$

In this analysis, we computed a coefficient of variation value for each gene G_i in each GEO dataset $\boldsymbol{S}$.

Next, we identified candidate reference genes with coefficient of variation values below a predefined threshold, t, observed in as many experiments as possible. In order to account for platform related differences, for each gene G_i and threshold t, we computed a ratio. $\text{Ratio}_t(G_i)$ as follows:

$$\text{Ratio}_t(G_i)=\frac{|\{CV(S,G_i)|CV(S,G_i)\le t\}|}{|\{CV(S,G_i)|CV(S,G_i)>0\}|} \quad (5)$$

Calculation of percentage of occurrence

Let $f_{\text{PO}}(r)$ be the function that gives the number of genes with $Ratio_t$ greater than a given r and occur in at least in PO% of the datasets (Equation 6).

$$f_{PO}(r)=|\{G_i|Ratio_t(G_i)<r\}| \quad (6)$$

We plotted and compared the graph of $f_{\text{PO}}(r)$, varying r from 0 to 1, for housekeeping genes and randomly selected non-housekeeping genes.

Calculation of specificity and sensitivity

We use the housekeeping gene set published by Eisenberg et al. [22] as the ground truth set of housekeeping genes. All the remaining genes are assumed to be non-housekeeping genes for the specificity and sensitivity analysis. The simple threshold classifier we use simply classifies all genes with a CV value below than a given threshold in at least Ratio_t of the datasets as housekeeping genes. All these analyses are performed at a fixed percentage of occurrence of 75% and with a fixed Ratio_t of 0.9. The ground truth genes that are identified as housekeeping genes by this classifier are true positives (TP) whereas, the ground truth genes that are identified as non-housekeeping genes are false negatives (FN). Similarly, genes not in the ground truth set but identified as housekeeping genes are false positive genes (FP) and genes not in the ground truth set identified as non-housekeeping genes by the classifier are true negatives (TN). Using these definitions, sensitivity is given by TP/(TP+FN) and specificity is computed as TN/(TN+FP).

Cell Lines

Cell lines were obtained from the following sources and validated by STR analysis: HepG2 (ATCC HB-8065), FOCUS [35], Mahlavu[36], Hep3B (ATCC HB-8064), Hep3B-TR [37], Huh7 (JCRB JCRB0403), SkHep1 (ATCC HTB- 52), PLC (ATCC CRL-8024), MDA-MB-453 (ATCC HTB-131), HCC1937 (ATCC CRL-2336), BT-20 (ATCC HTB-19), T47D (ATCC HTB-133), CAMA- 1 (ATCC HTB-21), HCT116 (ATCC CCL-247), HT29 (ATCC HTB-38), SW620 (ATCC CCL-227).

RNA extraction

RNA was extracted from 8 Hepatocellular Carcinoma cell lines (HepG2, FOCUS, Mahlavu, Hep3B, Hep3B-TR, Huh7, SkHep1, PLC), 5 Breast Carcinoma cell lines (MDA-MB453, HCC1937, BT20, T470, CAMA I) and 3 Colon Carcinoma cell lines (HCT116, HT29, SW620) with NucleoSpin Total RNA Isolation Kit and the concentration and purity of total RNA from each cell line was measured by using a NanoDrop Spectrophotometer (NanoDrop Technologies). Reverse transcription was performed using RevertAid First Strand cDNA Synthesis Kit (Fermentas) from 2 μg RNA with oligodT primer.

Real-time quantitative PCR and stability analysis

Primers for 17 selected housekeeping genes were designed using the Primer3 software (Table S5 in Supporting Information S2). A cDNA dilution series for each primer set in triplicate was analyzed to calculate efficiencies of the primers using the linear regression slope of the dilution series with the equation Efficiency = $10^{(-1/\text{slope})}$-1. Real-time quantitative PCR assays were performed in duplicate for each candidate gene using 1 μl of 1:100 diluted cDNA template with DyNAmo SYBR Green qPCR Kit (Finnzymes) on BioRad iCycler Real-Time qPCR System. The following program was used: Initial denaturation at 95°C 15 min amplification for 45 cycles (95°C 15 s followed by 57°C 30 s and 72°C 30 s), and final extension at 72°C 10 min. Melting curve analysis was done for each run, in addition to agarose gel electrophoresis, to confirm the amplicon size and presence of a single gene-specific peak free from any primer-dimer or genomic DNA amplification.

BioRad iCycler was programmed to set the Cq threshold on a fixed level. Cq values generated by BioRad iCycler system were transformed into quantities (relative expression values) according to Vandesompele *et al.* [25]. Relative expression values were calculated with the equation: Relative Expression = Efficiency$^{-\Delta Cq}$. Coefficient of Variation (CV) was calculated as the ratio of standard deviation to the mean relative expression. geNorm and NormFinder software were used for stability analysis.

Supporting Information

Supporting Information S1 Reference Gene Lists.
(ZIP)

Supporting Information S2 Tables S1–S5. Table S1. Kolmogorov–Simirnov Test results for the hypothesis comparing pair-wise equivalence of the ratio distribution of housekeeping gene set to the ratio distribution of random sets of genes excluding the housekeeping genes. Table S2. Kolmogorov–Simirnov Test results for the hypothesis comparing pair-wise equivalence of the ratio distribution of random sets of genes, excluding the housekeeping genes. Table S3. Stability values of 17 reference genes calculated by NormFinder and geNorm. Table S4. Stability values of 13 genes, with standard deviation lower than 1.42, calculated by NormFinder and geNorm. Table S5. Real-time quantitative PCR primers.
(PDF)

Supporting Information S3 ROC Curves.
(ZIP)

Author Contributions

Conceived and designed the experiments: RCA VA. Performed the experiments: TE LC. Analyzed the data: TE LC OK TC. Contributed reagents/materials/analysis tools: RCA TC OK. Wrote the paper: RCA VA TE LC TC.

References

1. Hsiao LL, Dangond F, Yoshida T, Hong R, Jensen RV, et al. (2001) A compendium of gene expression in normal human tissues. Physiol Genomics 7: 97–104. Available: http://www.ncbi.nlm.nih.gov/pubmed/11773596.
2. Warrington JA, Nair A, Mahadevappa M, Tsyganskaya M (2000) Comparison of human adult and fetal expression and identification of 535 housekeeping/maintenance genes. Physiol Genomics 2: 143–147. Available: http://physiolgenomics.physiology.org/content/2/3/143.abstract.
3. Andersen CL, Jensen JL, Ørntoft TF (2004) Normalization of Real-Time Quantitative Reverse Transcription-PCR Data: A Model-Based Variance Estimation Approach to Identify Genes Suited for Normalization, Applied to Bladder and Colon Cancer Data Sets. Cancer Res 64: 5245–5250. Available: http://cancerres.aacrjournals.org/content/64/15/5245.abstract.
4. Ohl F, Jung M, Xu C, Stephan C, Rabien A, et al. (2005) Gene expression studies in prostate cancer tissue: which reference gene should be selected for normalization? J Mol Med (Berl) 83: 1014–1024. Available: http://www.ncbi.nlm.nih.gov/pubmed/16211407. Accessed 20 March 2013.
5. Jung M, Ramankulov A, Roigas J, Johannsen M, Ringsdorf M, et al. (2007) In search of suitable reference genes for gene expression studies of human renal cell carcinoma by real-time PCR. BMC Mol Biol 8: 47. Available: http://www.pubmedcentral.nih.gov/articlerender.fcgi?artid = 1913536&tool = pmcentrez&rendertype = abstract. Accessed 20 March 2013.
6. Valenti MT, Bertoldo F, Dalle Carbonare L, Azzarello G, Zenari S, et al. (2006) The effect of bisphosphonates on gene expression: GAPDH as a housekeeping or a new target gene? BMC Cancer 6: 49. Available: http://www.pubmedcentral.nih.gov/articlerender.fcgi?artid = 1473200&tool = pmcentrez&rendertype = abstract. Accessed 12 March 2013.
7. Gao Q, Wang X-Y, Fan J, Qiu S-J, Zhou J, et al. (2008) Selection of reference genes for real-time PCR in human hepatocellular carcinoma tissues. J Cancer Res Clin Oncol 134: 979–986. Available: http://www.ncbi.nlm.nih.gov/pubmed/18317805. Accessed 20 March 2013.
8. Fu L-Y, Jia H-L, Dong Q-Z, Wu J-C, Zhao Y, et al. (2009) Suitable reference genes for real-time PCR in human HBV-related hepatocellular carcinoma with different clinical prognoses. BMC Cancer 9: 49. Available: http://www.pubmedcentral.nih.gov/articlerender.fcgi?artid = 2644316&tool = pmcentrez&rendertype = abstract. Accessed 20 March 2013.
9. De Kok JB, Roelofs RW, Giesendorf BA, Pennings JL, Waas ET, et al. (2005) Normalization of gene expression measurements in tumor tissues: comparison of 13 endogenous control genes. Lab Invest 85: 154–159. Available: http://www.ncbi.nlm.nih.gov/pubmed/15543203. Accessed 9 March 2013.
10. Dheda K, Huggett JF, Bustin SA, Johnson M a, Rook G, et al. (2004) Validation of housekeeping genes for normalizing RNA expression in real-time PCR. Biotechniques 37: 112–114, 116, 118–119. Available: http://www.ncbi.nlm.nih.gov/pubmed/15283208.
11. Waxman S, Wurmbach E (2007) De-regulation of common housekeeping genes in hepatocellular carcinoma. BMC Genomics 8: 243. Available: http://www.pubmedcentral.nih.gov/articlerender.fcgi?artid = 1937003&tool = pmcentrez&rendertype = abstract. Accessed 8 March 2013.
12. Popovici V, Goldstein DR, Antonov J, Jaggi R, Delorenzi M, et al. (2009) Selecting control genes for RT-QPCR using public microarray data. BMC Bioinformatics 10: 42. Available: http://www.pubmedcentral.nih.gov/articlerender.fcgi?artid = 2640357&tool = pmcentrez&rendertype = abstract. Accessed 20 March 2013.
13. Lee S, Jo M, Lee J, Koh SS, Kim S (2007) Identification of novel universal housekeeping genes by statistical analysis of microarray data. J Biochem Mol Biol 40: 226–231.
14. Srivastava S, Chen L (2010) A two-parameter generalized Poisson model to improve the analysis of RNA-seq data. Nucleic Acids Res 38: e170. Available: http://www.pubmedcentral.nih.gov/articlerender.fcgi?artid = 2943596&tool = pmcentrez&rendertype = abstract. Accessed 23 September 2013.
15. Hruz T, Laule O, Szabo G, Wessendorp F, Bleuler S, et al. (2008) Genevestigator v3: a reference expression database for the meta-analysis of transcriptomes. Adv Bioinformatics 2008: 420747. Available: http://www.pubmedcentral.nih.gov/articlerender.fcgi?artid = 2777001&tool = pmcentrez&rendertype = abstract. Accessed 18 November 2013.
16. Hruz T, Wyss M, Docquier M, Pfaffl MW, Masanetz S, et al. (2011) RefGenes: identification of reliable and condition specific reference genes for RT-qPCR data normalization. BMC Genomics 12: 156. Available: http://www.pubmedcentral.nih.gov/articlerender.fcgi?artid = 3072958&tool = pmcentrez&rendertype = abstract. Accessed 13 January 2014.
17. Edgar R, Domrachev M, Lash AE (2002) Gene Expression Omnibus: NCBI gene expression and hybridization array data repository. Nucleic Acids Res 30: 207–210. Available: http://nar.oxfordjournals.org/content/30/1/207.abstract.
18. Bolstad BM, Irizarry RA, Astrand M, Speed TP (2003) A comparison of normalization methods for high density oligonucleotide array data based on variance and bias. Bioinformatics 19: 185–193. Available: http://www.ncbi.nlm.nih.gov/pubmed/12538238.
19. De Jonge HJM, Fehrmann RSN, de Bont ESJM, Hofstra RMW, Gerbens F, et al. (2007) Evidence Based Selection of Housekeeping Genes. PLoS One 2: e898. Available: http://dx.plos.org/10.1371/journal.pone.0000898.
20. Czechowski T, Stitt M, Altmann T, Udvardi MK, Scheible W-R (2005) Genome-wide identification and testing of superior reference genes for transcript normalization in Arabidopsis. Plant Physiol 139: 5–17. Available: http://www.pubmedcentral.nih.gov/articlerender.fcgi?artid = 1203353&tool = pmcentrez&rendertype = abstract. Accessed 9 January 2014.
21. Hellemans J, Mortier G, De Paepe A, Speleman F, Vandesompele J (2007) qBase relative quantification framework and software for management and automated analysis of real-time quantitative PCR data. Genome Biol 8: R19. Available: http://www.pubmedcentral.nih.gov/articlerender.fcgi?artid = 1852402&tool = pmcentrez&rendertype = abstract. Accessed 10 January 2014.
22. Andersen CL, Jensen JL, Ørntoft TF (2004) Normalization of real-time quantitative reverse transcription-PCR data: a model-based variance estimation approach to identify genes suited for normalization, applied to bladder and colon cancer data sets. Cancer Res 64: 5245–5250. Available: http://www.ncbi.nlm.nih.gov/pubmed/15289330. Accessed 9 January 2014.
23. Eisenberg E, Levanon EY (2003) Human housekeeping genes are compact. Trends Genet 19: 356–362. Available: http://www.ncbi.nlm.nih.gov/pubmed/12850438. Accessed 8 March 2013.
24. Carkacioğlu L, Atalay RC, Konu O, Atalay V, Can T (2010) Bi-k-bi clustering: mining large scale gene expression data using two-level biclustering. Int J Data Min Bioinform 4: 701–721. Available: http://www.ncbi.nlm.nih.gov/pubmed/21355502. Accessed 13 January 2014.
25. Vandesompele J, De Preter K, Pattyn F, Poppe B, Van Roy N, et al. (2002) Accurate normalization of real-time quantitative RT-PCR data by geometric averaging of multiple internal control genes. Genome Biol 3: RESEARCH0034. Available: http://www.pubmedcentral.nih.gov/articlerender.fcgi?artid = 126239&tool = pmcentrez&rendertype = abstract.
26. Stark A, Brennecke J, Bushati N, Russell RB, Cohen SM (2005) Animal MicroRNAs Confer Robustness to Gene Expression and Have a Significant Impact on 32UTR Evolution. Cell 123: 1133–1146. Available: http://linkinghub.elsevier.com/retrieve/pii/S0092867405012729.
27. Sikand K, Singh J, Ebron JS, Shukla GC (2012) Housekeeping Gene Selection Advisory: Glyceraldehyde-3-Phosphate Dehydrogenase (GAPDH) and β-Actin Are Targets of miR-644a. PLoS One 7: e47510. Available: http://dx.doi.org/10.1371/journal.pone.0047510.
28. Sun Y, Li Y, Luo D, Liao DJ (2012) Pseudogenes as Weaknesses of ACTB (Actb) and GAPDH (Gapdh) Used as Reference Genes in Reverse Transcription and Polymerase Chain Reactions. PLoS One 7: e41659. Available: http://dx.doi.org/10.1371/journal.pone.0041659.
29. Jin P, Zhao Y, Ngalame Y, Panelli M, Nagorsen D, et al. (2004) Selection and validation of endogenous reference genes using a high throughput approach. BMC Genomics 5: 55. Available: http://www.biomedcentral.com/1471-2164/5/55.
30. Chang C-W, Cheng W-C, Chen C-R, Shu W-Y, Tsai M-L, et al. (2011) Identification of human housekeeping genes and tissue-selective genes by microarray meta-analysis. PLoS One 6: e22859. Available: http://www.pubmedcentral.nih.gov/articlerender.fcgi?artid = 3144958&tool = pmcentrez&rendertype = abstract. Accessed 15 August 2013.
31. Eisenberg E, Levanon EY (2013) Human housekeeping genes, revisited. Trends Genet: 1–6. Available: http://www.ncbi.nlm.nih.gov/pubmed/23810203. Accessed 6 August 2013.
32. Thorrez L, Van Deun K, Tranchevent L-C, Van Lommel L, Engelen K, et al. (2008) Using ribosomal protein genes as reference: a tale of caution. PLoS One 3: e1854. Available: http://www.pubmedcentral.nih.gov/articlerender.fcgi?artid = 2267211&tool = pmcentrez&rendertype = abstract. Accessed 20 March 2013.
33. Chen M, Xiao J, Zhang Z, Liu J, Wu J, et al. (2013) Identification of human HK genes and gene expression regulation study in cancer from transcriptomics data analysis. PLoS One 8: e54082. Available: http://www.pubmedcentral.nih.gov/articlerender.fcgi?artid = 3561342&tool = pmcentrez&rendertype = abstract. Accessed 7 October 2013.
34. Risso D, Schwartz K, Sherlock G, Dudoit S (2011) GC-content normalization for RNA-Seq data. BMC Bioinformatics 12: 480. Available: http://www.pubmedcentral.nih.gov/articlerender.fcgi?artid = 3315510&tool = pmcentrez&rendertype = abstract. Accessed 22 September 2013.
35. He L, Isselbacher KJ, Wands JR, Goodman HM, Shih C, et al. (1984) Establishment and characterization of a new human hepatocellular carcinoma cell line. In Vitro 20: 493–504. Available: http://www.ncbi.nlm.nih.gov/pubmed/6086498. Accessed 10 December 2013.
36. Oefinger PE, Bronson DL, Dreesman GR (1981) Induction of hepatitis B surface antigen in human hepatoma-derived cell lines. J Gen Virol 53: 105–113. Available: http://www.ncbi.nlm.nih.gov/pubmed/6268737. Accessed 10 December 2013.

37. Zimonjic DB, Zhou X, Lee J-S, Ullmannova-Benson V, Tripathi V, et al. (2009) Acquired genetic and functional alterations associated with transforming growth factor beta type I resistance in Hep3B human hepatocellular carcinoma cell line. J Cell Mol Med 13: 3985–3992. Available: http://www.ncbi.nlm.nih.gov/pubmed/19426152. Accessed 10 December 2013.

PUBLICATIONS

1: **Ersahin T**, Ozturk M, **Cetin-Atalay R**. Molecular Biology of Liver Cancer. Encyclopedia of Molecular Cell Biology and Molecular Medicine (EMCBMM), 3rd Edition, Edited by Robert A. Meyers, John Wiley & Sons, 2014. (In publication)

2: **Ersahin T**, Carkacioglu L, Can T, Konu O, Atalay V, **Cetin-Atalay R**. Identification of novel reference genes based on MeSH categories. PLoS One. 2014 Mar 28;9(3):e93341. doi: 10.1371/journal.pone.0093341.

3: Arslan S, **Ersahin T**, **Cetin-Atalay R**, Gunduz-Demir C. Attributed relational graphs for cell nucleus segmentation in fluorescence microscopy images. IEEE Trans Med Imaging. 2013 Jun;32(6):1121-31. doi: 10.1109/TMI.2013.2255309.

4: Keskin F, Suhre A, Kose K, **Ersahin T**, Cetin AE, **Cetin-Atalay R**. Image classification of human carcinoma cells using complex wavelet-based covariance descriptors. PLoS One. 2013;8(1):e52807. doi: 10.1371/journal.pone.0052807.

5: Isik Z, **Ersahin T**, Atalay V, Aykanat C, **Cetin-Atalay R**. A signal transduction score flow algorithm for cyclic cellular pathway analysis, which combines transcriptome and ChIP-seq data. Mol Biosyst. 2012 Oct 30;8(12):3224-31. doi: 10.1039/c2mb25215e.

6: Ligons DL, Tuncer C, Linowes BA, Akcay IM, Kurtulus S, Deniz E, Atasever Arslan B, Cevik SI, Keller HR, Luckey MA, Feigenbaum L, Möröy T, **Ersahin T**, **Atalay R**, Erman B, Park JH. CD8 lineage-specific regulation of interleukin-7 receptor expression by the transcriptional repressor Gfi1. J Biol Chem. 2012 Oct 5;287(41):34386-99. doi: 10.1074/jbc.M112.378687.

7: Buontempo F, **Ersahin T**, Missiroli S, Senturk S, Etro D, Ozturk M, Capitani S, **Cetin-Atalay R**, Neri ML. Inhibition of Akt signaling in hepatoma cells induces apoptotic cell death independent of Akt activation status. Invest New Drugs. 2011 Dec;29(6):1303-13. doi: 10.1007/s10637-010-9486-3.